The Morphology and Dynamics of the Lower Lambert Glacier and Amery Ice Shelf System.

by

Kim A. Krebs, BSc (Honours) JCUNQ

Submitted in fulfilment of the requirements for the degree of

Master of Science

University of Tasmania [IASOS]

(January, 1997)

This thesis contains no material which has been accepted for the award of any other degree or diploma by the University or any other institution, except by way of background information and duly acknowledged in the Thesis, and to the best of my knowledge and belief no material previously published or written by another person except where due acknowledgment is made in the text of the Thesis.

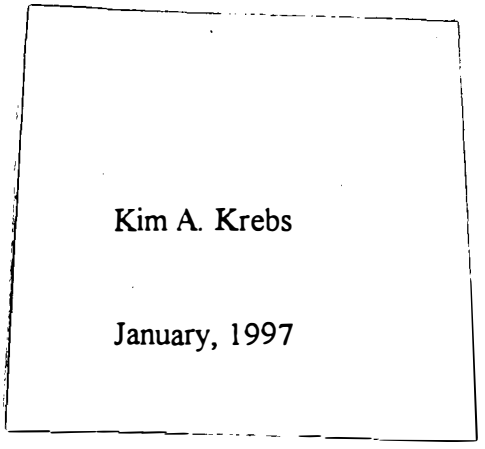

Kim A. Krebs

January, 1997

Abstract

The Lambert Glacier and Amery Ice Shelf system is one of the major east Antarctic drainage basins and is the subject of long term and on-going investigation as part of the Australian Antarctic program. In the region of the grounding zone between the glacier stream and the floating ice shelf, snow which accumulated over tens of thousands of square kilometres of the interior ice sheet is funnelled through a relatively narrow area. The way in which the ice in this region flows is influenced by subglacial topography, ice thickness, internal ice flow properties and the nature of the source area of the ice.

The primary aim of this study is to use all available data to describe the morphology and dynamic regime of the lower Lambert Glacier and Amery Ice Shelf, and to provide the best estimate of the present mass balance and spatial distribution of the grounding zone. The available data include radio echo soundings of ice thickness, surface elevation data, ice velocity and surface mass balance measurements from Australian field projects in 1968-1970 and in 1988-1990, satellite imagery, derived products from satellite altimetry and Russian geophysical surveys.

The main region being studied is located between 70° to 72°S and 68° to 72°E. Within this area, five transecting profiles have identified the Lambert Glacier ice stream from both eastern and western plateau ice that also flows into the Lambert graben before entering Prydz Bay via the Amery Ice Shelf. Two of these profiles are situated north of T4 at 71°13'S 69°28'E (Budd *et al.*, 1992), the remaining three are south of T4. The Lambert Glacier ice stream broadens from an average width of 34km to 42km in the area between the profiles south of T4 and the profiles north of T4. Two longitudinal profiles incorporating the eastern and western edges of the drainage system have added to the conclusion that previously determined grounding zone parameters for the Lambert Glacier need to be redefined. The grounding zone is estimated to cover a distance of 220km from an area near T4 (71°39'S) to the Lambert Glacier hinge line near 73°19'S. Total mass flux through the lower Lambert Glacier averages 9.6Gt a^{-1} in the grounding zone and increases marginally to 9.8Gt a^{-1} on the Amery Ice Shelf proper. These figures are comparable with the earlier calculations of Budd *et al.* (1982).

Acknowledgment

Thanks go to my research supervisor Dr Ian Allison (Antarctic CRC) and supervisor Prof. Bill Budd (University of Tasmania) who provided technical advice throughout the thesis. I have appreciated all their experiences in the field of Antarctic sciences and will enjoy working with them in the future.

I also acknowledge all the ANARE expeditioners who took part in the collection of RES data and velocity data used in this research.

Table of Contents

Abstract	iii
Acknowledgment	iv
List of Figures	viii
List of Tables	xiii

Chapter One: Introduction **1**
1.1 Where, what and why Antarctica? 1
1.2 Antarctica's response to climate change 2
1.3 Research objectives and thesis outline 3

Chapter Two: The Lambert Glacier and other ice streams **6**
2.1 Introduction 6
2.2 Geography of the region 8
2.2.1 Bedrock topography 8
2.2.2 Climate 10
2.3 A review of the studies on the Lambert Glacier 11
2.4 Studies on other outlet glaciers and ice streams of Antarctic 18
2.4.1 Ice streams of the Ross Ice Shelf area 18
2.4.2 Other Antarctic glaciers and ice streams 22

Chapter Three: The Amery and other ice shelves **25**
3.1 Introduction 25
3.2 Amery Ice Shelf 26
3.2.1 Morphology 26
3.2.2 Changes to the calving front 28
3.2.3 Snow accumulation and surface climate 29
3.2.4 Surface elevation, surface slope and ice thickness 31
3.2.5 Internal structure 33
3.2.6 Dynamics and mass budget 34
3.3 Other ice shelves 39
3.3.1 The Ross Ice Shelf 39
3.3.2 Ice shelves on the eastern and southern Weddell Sea 44

Chapter Four: Morphology of the lower Lambert Glacier and Amery Ice Shelf system **48**
4.1 Introduction 48
4.2 Ice streams and flow lines 48
4.2.1 Upper Amery/ Lower Lambert Glacier 49
4.2.2 Confluence and hinge zone 49
4.2.3 Tributary ice streams 53
4.2.4 Lower Lambert Glacier flow lines 55
4.3 Ice thickness and surface elevation 59
4.3.1 Longitudinal profiles of the Lambert Glacier into the region of the grounding zone 65
4.3.2 Basal melt lakes 74
4.3.3 Transverse profiles 77
4.3.3.1 Profile #1 77
4.3.3.2 Profile #2 80
4.3.3.3 Profile #3 82
4.3.3.4 Profile #4 84
4.3.3.5 Profile #5 86
4.3.4 Upper Lambert system 89
4.3.5 Total system 90
4.4 The grounding zone of the Lambert Glacier and Amery Ice Shelf system 98

Chapter Five: Dynamics of the Lambert ice stream and Amery Ice Shelf system **101**
5.1 Introduction 101
5.2 Velocity and mass flux across the lower Lambert ice stream and Amery Ice Shelf 101
5.2.1 Velocity data 101
5.2.2 Mass flux data 105
5.2.3 Smoothed cross section profiles of velocity and mass flux 111
5.3 Longitudinal profiles of velocity and driving stress along the Lambert ice stream 116
5.3.1 Introduction 116
5.3.1.1 Surface and basal melt rates 118
5.3.2 Data 119
5.3.3 Extrapolation with assumption of continuity 121
5.3.3.1 Driving stress 122
5.3.3.2 Surface mass balance 125
5.3.3.3 Velocity 128
5.3.4 Discussion 132

Chapter Six: Mass flux 133
6.1 Introduction 133
6.2 Mass budget 133
6.3 Discussion 139

Chapter Seven: Conclusion 140

Appendices 145

References 154

List of Figures

2.1 The Lambert Glacier and Amery Ice Shelf. 7

2.2 Map illustrating ice free regions of the Prince Charles Mountains. 9

2.3 Selected radial profiles of the surface of the Antarctic ice sheet . 13

2.4 The Ross Ice Shelf and ice streams A-E. 19

2.5 Cross section LL' through ice streams A, B and C. 20

2.6 The location of the Rutford Ice Stream and the Filchner-Ronne Ice Shelf. 23

3.1 The over snow traverse route from Mawson over to the Amery Ice Shelf covered in 1963-64. 27

3.2 Changes in the ice front of the Amery Ice Shelf. 29

3.3 Annual net accumulation contours on the Amery Ice Shelf. 30

3.4 Surface and basal ice profile of the Amery Ice Shelf along a longitudinal profile. 33

3.5 Measured velocity profiles across the Amery Ice Shelf through G1 and G3 and shown as a function of the distance which is perpendicular to the flow direction. 37

3.6 Map of the Amery Ice Shelf showing surface features positioned by satellite altimetry, together with features identified from imagery and ground survey. 39

3.7 Three images surrounding the behaviour of the ice in the region of Siple Coast. 43

3.8 Schematic outline of major ice streams feeding the ice shelves in the eastern and western Weddell Sea. 44

4.1 Flow lines for the Lambert Glacier as interpreted from satellite images. 50

4.2 Flow lines for the southern limits of the Lambert Glacier grounding zone. 51

4.3 Tributary glacier flow lines. 54

4.4 Tributary glacier source and flow lines for the Lambert ice stream. 56

4.5 Tributary ice streams identified in the Lambert Glacier confluence area. 57

4.6 RES flight paths over the northern Prince Charles Mountains. 61

4.7 RES flight paths over the lower Lambert Glacier and Amery Ice Shelf. 62

4.8 1988-1989 RES flight paths. 63

4.9 Map of all flight paths used in this study. 64

4.10 Eastern and western longitudinal profiles of the Lambert ice stream. 67

4.11 Elevation for hydrostatic equilibrium against measured surface elevation for the eastern longitudinal profile. 71

4.12 Elevation for hydrostatic equilibrium against measured surface elevation for the western longitudinal profile. 73

4.13 Flight 03 (1988) basal profile between 150-350km. 75

4.14 Sketch of 'basal melt lakes' derived from Figure 4.13. 75

4.15 Measured surface elevation and surface elevation for hydrostatic equilibrium for Profile #1. 78

4.16 Cross section of ice thickness and interpolated surface elevation for Profile #1. 78

4.17 Measured surface elevation and surface elevation for hydrostatic equilibrium for Profile #2. 81

4.18 Cross section of ice thickness and interpolated surface elevation for Profile #2. 81

4.19 Measured surface elevation and surface elevation for hydrostatic equilibrium for Profile #3. 83

4.20 Cross section of ice thickness and interpolated surface elevation for Profile #3. 83

4.21 Measured surface elevation and surface elevation for hydrostatic equilibrium for Profile #4. 85

4.22 Cross section of ice thickness and interpolated surface elevation for Profile #4. 85

4.23 Measured surface elevation and surface elevation for hydrostatic equilibrium for Profile #5. 87

4.24 Cross section of ice thickness and interpolated surface elevation for Profile #5. 87

4.25 Profile from Flight 03 (1988) through the southern Prince Charles Mountains. 89

4.26 The interior ice sheet transect from the Amery Ice Shelf front to Dome Argus. 91

4.27 Ice thickness contour map for the lower Lambert Glacier. 94

4.28 Specific ice thickness contours plus Lambert ice stream flow lines. 95

4.29 Ice thickness, ice stream width and surface elevation for the Lambert ice stream. 97

4.30 The Lambert Glacier grounding zone. 99

5.1 Velocity vectors over the northern reaches of the grounding zone. 102

5.2a Longitudinal profile of average velocities from the lower Lambert Glacier transects. 103

5.2b Velocity curves for Profiles #1 to #5 104

5.3 Flux rate per width of Profiles #1 to #5. 110

5.4 Velocity, ice thickness and mass flux across Profile #1. 111

5.5 Velocity, ice thickness and mass flux across Profile #2 112

5.6 Velocity, ice thickness and mass flux across Profile #3 113

5.7 Velocity, ice thickness and mass flux across Profile #4 114

5.8 Velocity, ice thickness and mass flux across Profile #5 115

5.9 Eastern and western longitudinal profiles comparing ice thickness and basal shear. 120

5.10 Basal shear to normal stress ratio. 123

5.11 Centre line velocities, ice stream width, surface slope and side stress. 124

5.12 Elevation for hydrostatic equilibrium, normal stress and basal shear for the eastern longitudinal profile. 126

5.13 Surface mass balance observations and estimations. 127

5.14 Ice velocity contour map. 130

5.15 Summary profile comparing velocity, surface mass balance and normal stress along the eastern longitudinal profile. 131

6.1 Comparison between mass flux across the entire profile and the flux from the Lambert ice stream only. 134

6.2 Percentage contribution of tributary glaciers towards the total profile mass flux. 135

6.3 Mass flux, ice stream width, velocity and ice thickness from G1 to A.79. 139

Appendix A Thematic Mapper image of the Lambert Glacier confluence region and southern limits of the grounding zone. 146

Appendix C Illustration of profiles and points from RES surveys used to define the Lambert Glacier and Amery Ice Shelf dynamics. 149

List of Tables

1.1 The generalised time scale of climatic events for high southern latitudes. 2

2.1 A comparison of mass balance and accumulation rates between results from McIntyre (1985) and Allison (1979). 15

3.1 Measured parameters on the Amery Ice Shelf. 28

3.2 Calculations of divergence of flow lines. 35

3.3 Apparent advance of ice edges and apparent advance rates in the eastern and southern Weddell Sea. 46

3.4 Quantitative estimates of the ice edge velocities in the eastern and southern Weddell Sea. 47

4.1 Ice and water densities for hydrostatic equilibrium. 70

5.1 Summary of mass flux across each profile. 107

5.2 Ice thickness, velocity and mass flux values for Profile #1. 107

5.3 Ice thickness, velocity and mass flux values for Profile #2 108

5.4 Ice thickness, velocity and mass flux values for Profile #3 108

5.5 Ice thickness, velocity and mass flux values for Profile #4 109

5.6 Ice thickness, velocity and mass flux values for Profile #5. 109

5.7 Driving stresses on the western side of the study area. 121

5.8 Driving stresses on the eastern side of the study area. 121

5.9 Summary of driving stress values from G1 to A.79. 125

6.1 Summary of ice dynamics for LGBT to G1. 136

6.2 Surface and basal mass balance between the referenced profiles. 137

Appendix B List of cartographic maps, satellite images and aerial photographs used in this study. 147

Appendix D Selected velocity vectors used and related to the study area. 150

for Jill

Chapter One

Introduction

1.1 Where, what and why Antarctica?

Antarctica is approximately 14 million square kilometres in size (4500 km in diameter) with only 0.3% (42,000 sq km) ice free (Fox and Cooper, 1994). The main ice free regions are the TransAntarctic Mountains and Ellsworth Mountains of West Antarctica and the Prince Charles Mountains of East Antarctica. These mountain ranges support mountain or alpine-type glaciers in the order of ten kilometres in length that behave out-of-phase with the larger outlet glaciers during climatic changes brought about by glacials and inter-glacials (Chinn, 1980; Denton and Hughes, 1981; Krebs, 1996). The outlet glaciers and ice streams, which sometimes flow through these mountain ranges, are major drainage systems hundreds of kilometres in length that channel the continental ice sheet towards the coast, in effect transporting the ice from an area of accumulation to an area of ablation (Sugden and John, 1976). Nearer to the coastline, the ice streams flow into ice shelves before calving off as ice bergs or melting at the ice shelf base (Walton, 1987). The extent of sea ice surrounding this polar continent varies from 3.5×10^6 km^2 (minimum) to 19×10^6 km^2(maximum) (Gloersen *et al.*, 1992). The maximum sea ice extent occurs during September-October (Gloersen *et al.*, 1992).

Antarctic glaciers have been fluctuating in response to climatic changes over an estimated 35 million year history (Oerlemans and Hoogendoorn, 1989). To this date, there are still no definitive estimations of the continent's total accumulation, of the ice loss from outflow and melt or of the balance between these, the mass budget. Closer

study of all the drainage systems individually and then collectively will enhance this understanding as data quality and quantity continues to improve.

1.2 Antarctica's response to climate change

The Antarctic continent is our planet's principal heat sink for the global climate system (Phillpot, 1985). Temperature trends derived from ice cores from deep boreholes in Antarctica indicate that around 18 000 years BP the temperature was much cooler. This has been identified as the Last Glacial Maximum by Denton *et al.* (1981). Information gathered from geological, palaeontological and climatic studies, has indicated that Antarctica has evolved from a series of glaciations which have fluctuated in response to climatic changes over an estimated 35 million year history (Sugden and John, 1976; Oerlemans and Hoogendoorn, 1989). It is now generally accepted that the cause of these global climatic changes is primarily related to variations in the Earth's orbit and distance from the Sun (the Milankovitch theory). Table 1.1 is a generalised time scale by Phillpot (1985) of climatic events in the high southern latitudes. The Antarctic ice sheet has a pivitol role in global climate patterns and has a significant role in the Milankovitch theory.

Year × 10^6 BP	Climatic Event
37	Sharp drop in surface ocean temperature (4 - 5 ^{o} C).
26	Glaciers reach sea-level in Ross Sea.
15 - 5	Pronounced drop in surface ocean temperatures.
	Rapid build-up of ice in Greater Antarctica.
	Valley-carving state in TransAntarctic Mountains (Taylor V).
5.5 - 3	Antarctic Polar Front shifts 300 km northward.
	Ross Ice Shelf expands to edge of continental shelf.
4.7 - 4.3	Substantial build-up of ice in polar regions. Possible glacial surge.
4.25 - 3.95	Marked warming of surface ocean temperatures (8-10 ^{o} C).
	Possible melting of the ice sheet in Lesser Antarctica and marine invasion of Wright Valley.
3.95 - 3.35	Lengthy and marked cooling.
3.35 - 0.7	Fluctuations in ocean surface temperatures (period: 170 000 years)
3.5 - 2.7	Spill over of ice from Greater Antarctica (Taylor IV)
2.1 - 1.6	(Taylor III)
1.6/1.2 - >49 K	(Taylor II)
34.8 K - 9.49 K	(Taylor (I)
0.7 - present	Wider fluctuations in ocean surface temperatures (periods: 110 000 years)

Table 1.1 The generalised time scale of climatic events for high southern latitudes. After Frakes (1978) modified by Phillpot (1985) pg 37.

1.3 Research objectives and thesis outline

The work presented in this thesis provides new data on one of Antarctica's major drainage systems. It identifies the ice types, their dynamics and mass flux for the lower Lambert Glacier and Amery Ice Shelf as well as providing a redefinition for the boundary between these two ice types. The geomorphology and physical nature of this glacial system, which drains about one-fifth or ~870,000 km^2 of the East Antarctic ice sheet (Hambrey and Dowdeswell, 1994; Herzfeld *et al.*, 1993), forms the focus of the research.

The Lambert Glacier drainage basin extends as far south as 80^0 to an elevation of 4000 m above sea level (asl) (Swithinbank, 1988; Drewry et al, 1982). This large drainage network flows through a 70 km wide trough around the grounding zone (Allison, 1979). The total system includes a continental ice sheet, ice streams and an ice shelf. These three ice mass types are typical across the entire continent with the differences being only in the extent and hence dominance of each ice mass type and the surrounding system.

Continental ice is slow moving ice, in the order of 5 - 50 ma^{-1}, that is typically frozen to the subglacial topography. Small amounts of basal melt can also occur in some regions. The ice accumulates under extreme conditions of minimal snowfall, typically in the order of 50 $gm^2 a^{-1}$ (5 cm a^{-1} water equivalent) (Sharp, 1988). In general, movement of the ice body is by internal deformation (Paterson, 1994). The profile of an ice sheet surface in Antarctica can be affected by the topography of the bedrock or by any change in the accumulation rate within the catchment area (Colbeck, 1980). Sharp (1988) defines an ice sheet as an area which has a very large, thick sheet of glacial ice covering an area greater than 50,000 km^2. This volume of ice submerges the subglacial topography while flowing outward in all directions towards the coast. As the slope towards the coast increases, the rate of flow increases. This slope increase is reflected in the ice velocity which may increase from a few metres a year in the continental interior to anywhere from one hundred to over one thousand metres per

year at the coast (Hooper, 1991). For the purpose of this study, discussion will concentrate on the lower region of the Lambert Glacier and Amery Ice Shelf.

The second ice mass type in the region of the Lambert Glacier and Amery Ice Shelf system includes ice streams, or outlet glaciers. As the draining glacier nears the coast, or perhaps as it overrides a geothermal "hot spot", basal melt may occur and in some cases make a hydraulic connection to the sea which can reduce the effective normal stress on the bed and increase the basal velocity of the ice further, which also increases the total speed. The velocity of outlet glaciers can often range from tens of metres to several hundred metres per annum (Sharp, 1988). This faster flowing ice drains from a dome, or other body of ice, that is within the catchment area of the drainage basin. It is essentially only partially grounded ice, with some basal sliding apparent across various regions in flow. Streams of ice flow through the ice sheet, not unlike rivers, with a respectably high velocity of 50 - 500 ma^{-1}. The ice streams can also be identified as outlet glaciers which flow through a valley as they drain ice away from an ice sheet or ice cap (Sharp, 1988).

The third ice mass in this study region is that of ice shelves. Moving with a velocity that increases towards the seaward edge, ice shelves are almost completely floating bodies of ice that thin rapidly towards the seaward edge as their velocity increases. In Antarctica, ice mass loss is primarily through the calving of icebergs off the coastline. In many instances, the glacier will enter a bay and form a floating and confined ice shelf. Ice shelves are distinctive in that they are not basally fixed, but rather they are floating bodies of ice. Because there is no basal drag associated with ice shelves, the flow of ice into the open ocean increases as the confines of the bay broadens. As the ice shelf velocity increases, the thickness of the body of ice decreases to maintain mass continuity. Ice shelves typically flow up to 1500 ma^{-1} at their leading edge (Paterson, 1994).

The transition zone, or grounding line, is defined by Paterson (1994) as "the region in which the deformation pattern changes from the shear characteristics of an ice sheet

frozen to its bed to the longitudinal stretching typical of a floating ice shelf' (p311-12). As a transition zone divides an ice shelf from an ice sheet, the "accurate determination of the grounding line position is necessary not only for predicting likely ice-sheet and ice-shelf responses to changes in climate, but also for understanding internal ice physics in this transitional area" (Uratsuka *et al.*, 1996 p103).

Until now, the transition zone of the Lambert Glacier and Amery Ice Shelf system has been defined by a single point (Budd, 1966). In order to more fully comprehend the morphology and dynamics of this drainage system, a clear definition of the grounding line is sought. This has been achieved through radio-echo-sounding (RES) data, velocity measurements, satellite and aerial photograph interpretation. These findings will assist in future research surrounding the modelling of Antarctica as it responds to climatic variations.

This thesis entails seven chapters as follows after this introduction. Chapter Two covers a review of previous studies and field work conducted on the Lambert Glacier as well as an overview of other similar scale drainage systems in Antarctica. Chapter Three presents a summary of past studies on the Amery Ice Shelf, including comparative studies on other Antarctic ice shelves. Chapter Four gives a presentation of the morphological results for the lower Lambert Glacier and Amery Ice Shelf system. Chapter Five presents the results for the study of the dynamics of the Lambert ice stream and Amery Ice Shelf system. Chapter Six assesses the mass flux of the drainage system and Chapter Seven presents the conclusions derived from this study.

Chapter Two

The Lambert Glacier and Other Ice Streams

2.1 Introduction

The Lambert Glacier basin area and the Amery Ice Shelf combine to create a dynamic and important area of the eastern Antarctic continent. Draining 10.9% of East Antarctica, the Lambert Glacier is reported to be the worlds largest glacier (Swithinbank, 1988; Drewry *et al.*, 1982). Glaciers and ice sheets have a delayed response to climatic parameters such as those in Table 1.1 (p2), and hence their fluctuation can be used to identify such past events as varying sea levels and climatic conditions (Andrews, 1975). Similarly, interaction between climate change and the dynamics of ice streams can provide information such as mass balance, velocity and strain rates, to assist in modelling glacier activity (and the Antarctic ice sheet) and thus provide tools for identifying environmental variation.

The Lambert Glacier basin has a 1 million square kilometre drainage area (Figure 2.1). The lower part of this system consists of several ice streams that flow through the Southern Prince Charles Mountains, namely the Fisher, Geysen, Collins, Mellor, West Lambert, and the Lambert Glaciers. These tributary glaciers merge together to form the Lambert Glacier proper at approximately 73° South, where the glacier flows between the Mawson Escarpment to the east, and the Prince Charles Mountains to the west. The Mawson Escarpment has several local alpine-type glaciers which may behave in the same out-of-phase manner as the Northern Prince Charles Mountains alpine-type glaciers (Krebs, 1992). North of 71° South, the Charybdis and Scylla Glaciers flow directly into the Amery Ice Shelf, after flowing through the Northern Prince Charles Mountains (Figure 2.2).

To examine the ice masses of the Lambert Glacier and their response to climate change, this study incorporates an area that includes the entire drainage basin and the ice shelf downstream. More specifically, the area of study concentrates around the areas where the ice stream begins to float, and includes the redefinition of the Lambert Glacier grounding zone. What follows is a review of previous work completed in the Lambert Glacier region and a summary of what is currently

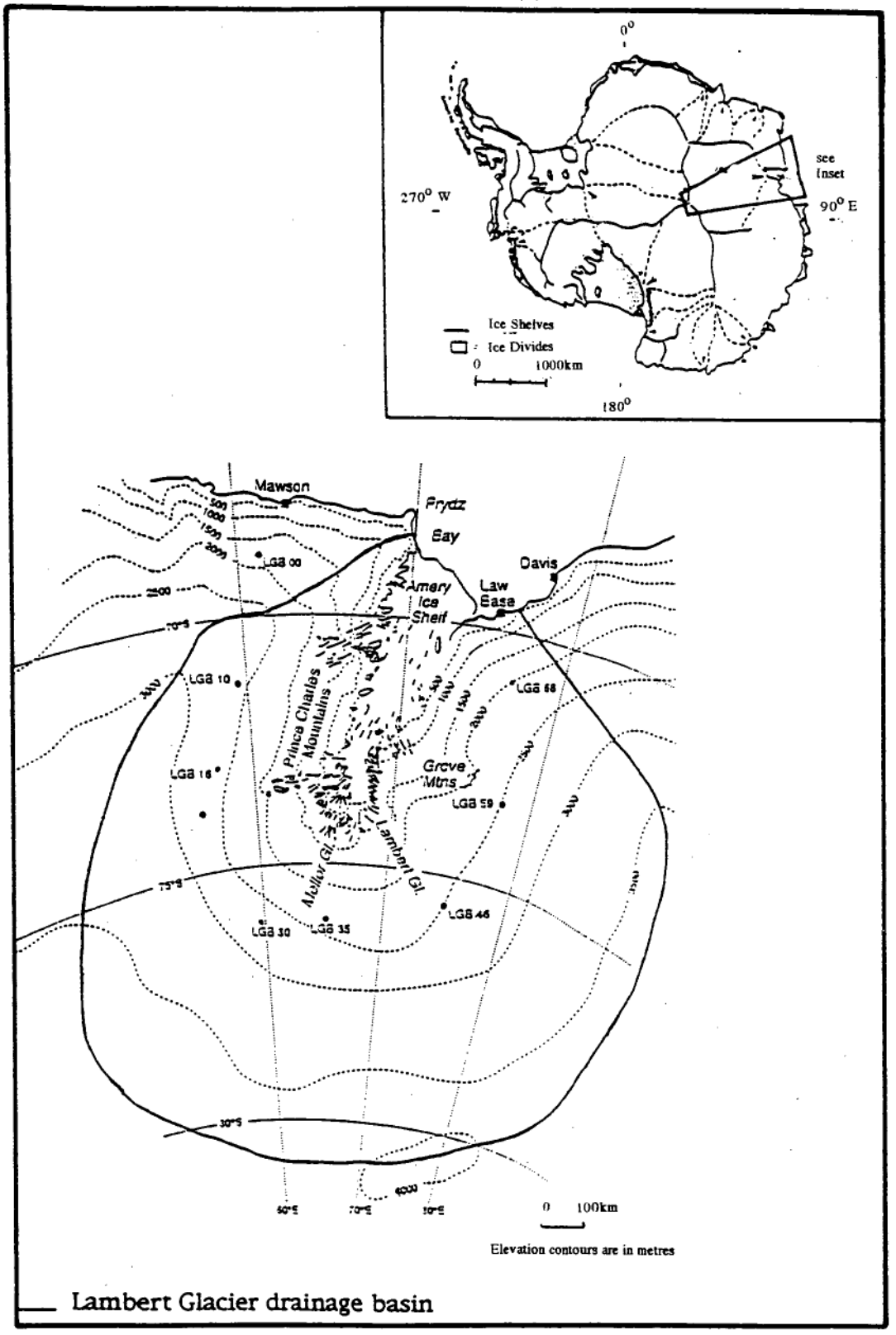

Figure 2.1. Incorporating grounded plateau ice, ice streams and an ice shelf, the Lambert Glacier drainage basin flows from an elevation of 4000m asl to sea level passing through the Prince Charles Mountains. The LGB locations are situated on the Lambert Glacier Basin traverse route (Higham, 1994). The inset map (after Mabin, 1991) illustrates the location of this drainage system in relation to other Antarctic drainage systems.

known of the region. It is followed by an overview of the work done on other ice streams and outlet glaciers of Antarctica.

2.2 Geography of the Region

2.2.1 Bedrock Topography

The Lambert Glacier flows through a large area of ice free outcrops named the Prince Charles Mountains. In the north west the Athos, Porthos and Aramis Ranges have elevations upward of 2000 m asl: for example Mount Bechervaise 2362 m, Crohn Massif 2438 m and Mount Bucher 2527 m. At the south western end of the Prince Charles Mountains, the exposed bedrock elevations are up to 3335 m asl (Mt. Menzies). Mawson Escarpment, in the south east of this system, is the largest single ice free outcrop in the Prince Charles Mountains (Figure 2.2) at approximately 130km by 35km in area. Outcrops in this region are generally massif mountains and nunataks along the Lambert valley eg Clemence Massif and Fisher Massif. The Prince Charles Mountain system is not a single range, but rather it is a group of nunataks and mountain massifs that are separated by up to 50 kilometres by the outlet glaciers that drain the east Antarctic ice sheet (Bardin, 1977). On the eastern edge of the Lambert Glacier system the Mawson Escarpment dominates the valley at 1000 to 1500 m asl, or 600 to 800 m above the surface of the Lambert Glacier.

South of the Fisher and Geysen Glaciers, toward the upper reaches of the Lambert Glacier, are several other mountains called the Concord Mountains (comprising Mounts Rubin, Ruker, Newton etc). Further south into the Lambert Glacier catchment area there are no mountains or massifs exposed as ice free outcrops with the exception of Komsomolískiy Peak at 74° 30'S. The drainage system then continues south towards the IGY Valley and Gamburtsev Subglacial Mountains.

Across the exposed surfaces of the mountain massifs of the Prince Charles Mountains, dissected or periglacial relief is common. There are also widespread erosion-denudation (preglacial) landscapes apparent in this area, and to a lesser extent, low-hill (glacial) relief. The preglacial landscape is the type of terrain which is termed an 'old planate surface' and has been uplifted by preglacial tectonic activity (Tingey, 1991).

The Lambert Glacier region contains both an area of steady block uplift that has resulted in the Prince Charles Mountains, and a block of subsidence through which the Lambert Glacier flows. Voronov (1964) identified the Lambert Glacier depression and its upstream continuation (the IGY Valley) to be "a huge graben in the central part of a horst" (p261). The Lambert Glacier and all of its tributaries therefore flow through fault valleys. Morgan and Budd (1975), using RES data, identified the 1000 m bedrock contour between Mount Twigg and Mawson Escarpment. Approximately 90 km north of this contour, Morgan and Budd (1975) identified their deepest sounding, situated in the middle of Lambert Glacier, with 2500 m of ice below the 500 m asl surface ice elevation.

2.2.2 Climate

The climate of Antarctica today is influenced by three major geographic regions: the waters of the Southern Ocean, the variable sea ice cover, and the continental ice sheet (Phillpot, 1985). Over central East Antarctica there is a definite sinking of upper level air that is balanced by near surface outflow due to inversion and katabatic winds. Concluding from these results, on the high East Antarctic plateau, stratospherically derived air is the dominant weather source (Whillans and Bindschadler, 1988). Over West Antarctica, Whillans and Bindschadler (1988) have concluded that horizontal air advection through the troposphere is the more dominant source for air mass exchange. On a more local scale, proximity to the coast is the variable that has the most influence on near-coastal environments.

From automatic weather station recordings between 100° and 140° East, Allison *et al.* (1993) established that mean surface wind speeds reached their maximum with proximity to the coast, but not actually at the coastline. They also established that in this area there are interrelationships between surface temperature, pressure and wind in relation to the topography of the ice sheet. Goodwin *et al.* (1993) noted that across the western slopes of the Lambert Glacier basin, in Eastern Kemp Land, snow accumulation rates are significantly lower than at other coastal areas of East Antarctica, such as Wilkes Land. The low rates of accumulation, less than 280 kg m^{-2} a^{-1} (typically 150 kg m^{-2} a^{-1}) are due to the low atmospheric moisture transport regime and the lack of penetration inland and to higher elevations of the coastal cyclonic systems (Goodwin *et al.*, 1993). Accumulation on the coastal slopes of Eastern Kemp

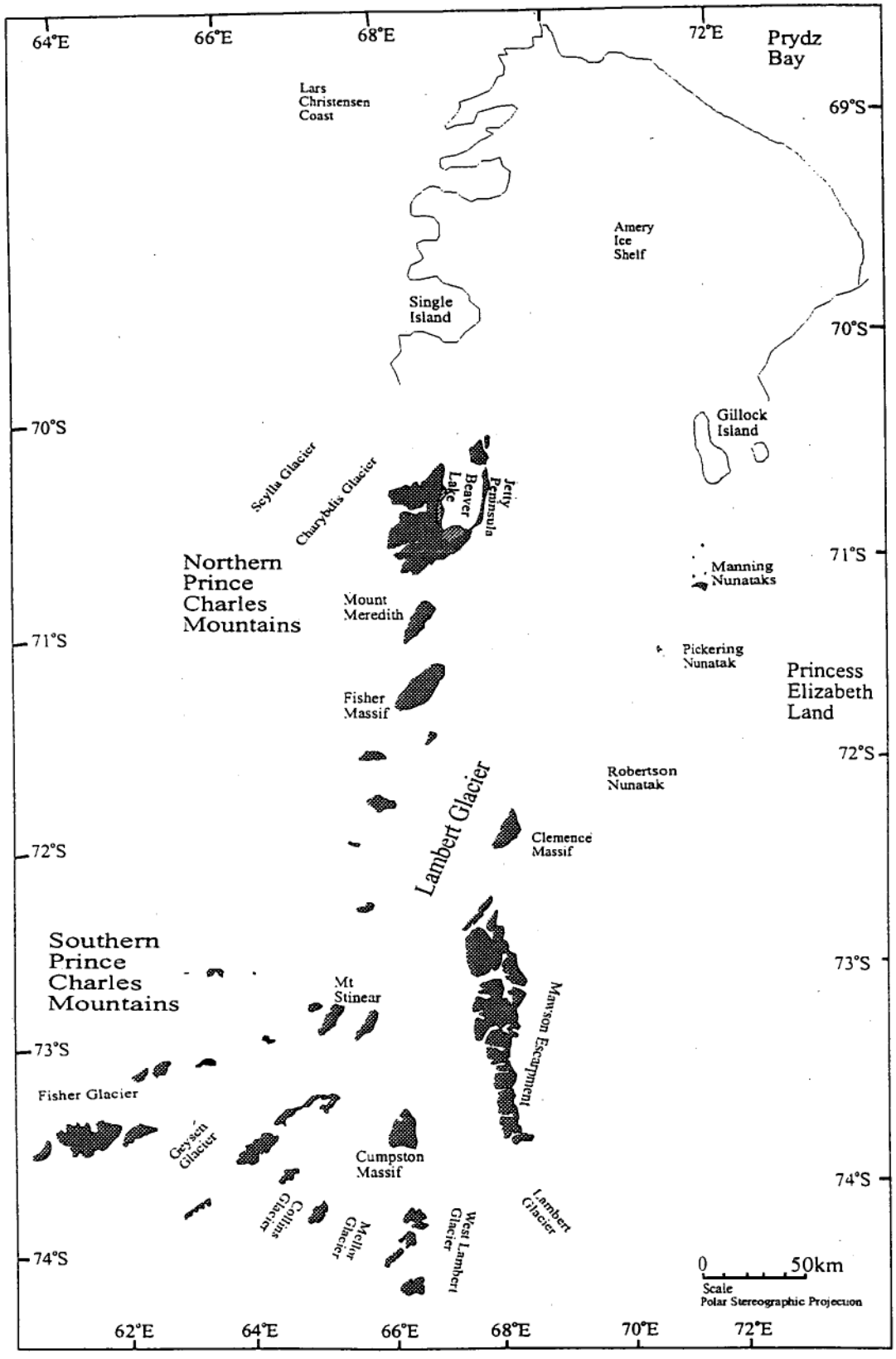

Figure 2.2 Map of the ice free regions of the Prince Charles Mountains. Mawson Escarpment and other massifs and nunataks surrounding the Lambert Glacier and Amery Ice Shelf.

Land is mainly due to the redistribution of snow that results from diverging surface winds throughout the western Lambert Glacier basin (Giovinetto *et al.*, 1992).

The temperature distribution within the drainage basin varies from approximately -12°C mean annual temperature in the coastal regions to an annual mean temperature of -60°C: at 4000m asl inland. The lowest recorded surface temperature of -89°C was recorded at the Russian Station Vostok within the Australian Antarctic Territory (Hooper, 1991).

2.3 A Review of the studies on the Lambert Glacier

McLeod (1967) showed, as part of the Australian National Antarctic Research Expeditions (ANARE) glaciology program, that the drainage of Enderby, Mac.Robertson and Kemp Lands was dominated by the Lambert Glacier system. This called for a more detailed expedition into the heart of the Lambert Glacier drainage system.

Initial findings were concentrated on the Fisher Glacier in the Southern Prince Charles Mountains. This glacier originates from the ice sheet west of 60°E (longitude) at an elevation of 2000 m asl plus (McLeod, 1967). It was identified as the most prominent and clearly defined tributary to the Lambert Glacier system. Fisher Glacier has several minor tributaries, and it was thought that the main tributary was the Geysen Glacier (McLeod, 1967). Based on the conclusions discussed in Chapter Four, the present author suggests that the Geysen Glacier may be an independent ice stream. At the Fisher Glacier's confluence with the Lambert Glacier, the glacier's elevation was noted to have fallen 1560m in 200 km. Intense deformation of the ice in this area of convergence between Fisher, Lambert and Mellor Glaciers was also noted (McLeod, 1967).

McLeod's (1967) report noted that the majority of ice was drained from the ice sheet to the west into the Lambert Glacier system as opposed to the less contributive east. Trail (1964), in a study of the ice free areas of the north and south Prince Charles Mountains, found lateral moraines on the mountain outcrops that suggested thicker ice conditions existed in the past.

Bardin (1977), in a study of the glacial geomorphology of the Lambert Glacier and its surrounding mountains, described the ice surface elevation as rising to the south and also rising very steeply towards the west and east of the Lambert Glacier and Amery Ice Shelf region. The ice stream flows through a valley that reaches 100 km in width, as it cuts through the Prince Charles Mountains, extending even further south into the IGY Valley; making a total length of over 700 km. By Bardin's definition, the Lambert Glacier is a large intermontane depression and the tributary glaciers, being of a smaller scale, are valley or mountain-valley glaciers.

A longitudinal profile from the Pole of Inaccessibility through the IGY Valley, Lambert Glacier and the Amery Ice Shelf assisted in identifying the zone of transition from grounded ice to floating ice (Figure 2.3). The Lambert Glacier merges into the Amery Ice Shelf, as estimated by Morgan and Budd (1975), at approximately the 90 m elevation contour line estimated at 1200km from the Pole of Inaccessibility (Figure 2.3). The absolute elevation of the glacier surface in this region of the grounding zone varies from 40-50 m at the northern floating ice edge of the transition zone to 70-80 m on the more southern portion (Bardin, 1977). A large area of surface crevassing occurs on the Lambert Glacier, around the confluence zone at approximately 1000km from Pole of Inaccessibility. This coincides with the area where the surface slope changes from ~1650m asl to ~250 m asl with a gradient of approximately 8.75×10^{-3}.

Morgan and Budd (1975) reported on results from the Lambert Glacier obtained with a 100 MHz radio-echo sounder flown over 20 000 km^2 in the region of the ice streams. Their data enabled more accurate descriptions of the region. The deep subglacial trench at the confluence of Fisher, Mellor and Lambert Glaciers contains ice which is 2500 m thick. With a low surface slope and high ice velocity about the area of convergence, Morgan and Budd suggested that this could be indicative of an area of basal melting.

Morgan and Budd (1975) indicated that the smooth, flat, uniform surface of the lower Lambert Glacier could be overlying considerable amounts of melt water at the base of the glacier. The elevation pattern across the drainage system begins with the convex plateau inland which then leads onto a zone of steep slope between 2000 and 1000 m asl. Once past the area of confluence, the surface of the ice is very uniform below 500 m asl before merging with the Amery Ice Shelf at approximately 90 m asl. The zone of steep slopes was identified by Morgan and

Budd (1975) as the region of maximum basal shear stress and the transition zone from an area of flow with low or no sliding to one of high sliding and reduced basal shear stress.

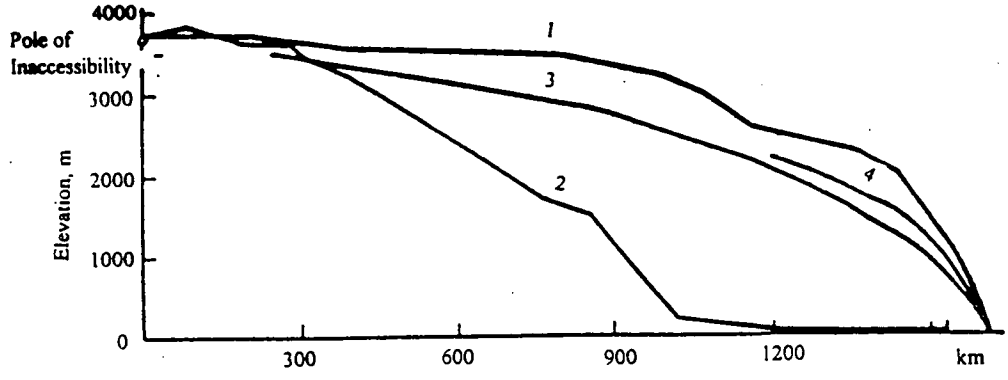

Radial profiles of the surface of the Antarctic ice sheet.
Legend: 1 - Pole of Inaccessibility - Molodezhnaya
2 - Pole of Inaccessibility-IGY Valley-Lambert Glacier-Amery Ice Shelf
3 - profile of an axially symmetric ice sheet (after P.A. Shumskiy)
4 - average elliptic profile, marginal part (after I.A. Suyetova)

Figure 2.3. The four profiles illustrate the appearance of predominantly grounded plateau ice from the pole of Inaccessibility to the coast. Profile 2 is of the Lambert Glacier drainage line, and therefore includes continental ice, ice streams and ice shelf ice mass types. From: Bardin (1977)

Because of the large size of the contribution of the Lambert Glacier and Amery Ice Shelf drainage system to the total ice sheet balance, calculating the mass balance of the overall east Antarctic ice sheet is very much dependant on the accuracy in measuring the mass flux in this system. Accurately estimating the mass budget of the Lambert Glacier system is difficult owing, primarily, to the logistics required to carry out adequate measurements. For example; physical access is limited due to the distances and climatic parameters. Satellite imagery, for remote sensing observations, is also restricted due to orbital limitations that do not allow for complete Antarctic coverage.

Earlier attempts to estimate the balance and input of the Lambert Glacier and Amery Ice Shelf area have included work by Mellor (1959, 1964), Giovinetto (1964, 1970) and Budd *et al.* (1967). Allison (1979) calculated the mass flux into the head of the Lambert Glacier system from measured velocity and ice thickness data. From this, and estimates of the mass accumulation in the interior basin, it was suggested that the whole Lambert Glacier basin has a positive mass balance. The total mass flux of the interior basin was estimated at 60 Gta^{-1} while the total mass flux across the 2000 m contour was 30 Giga tonnes per annum; and a budget excess over the interior basin area of 30 Gta^{-1}. Mass discharge measured near the grounding zone was 11 Gta^{-1} while another 7 Gta^{-1} was lost within the Lambert Glacier streams due to surface ablation and basal melt thus giving an overall mass excess for this section of 12 Gta^{-1}.

The loss of mass within the Lambert Glacier system comes from a net ablation area of 332 000 km^2 as based on Landsat data interpretation (Allison, 1979). Much of the Lambert Glacier stream system is an area of ablation with melt streams and lakes appearing on the surface of the glacier during the austral summer. The loss, due to evaporation, is unlikely to be in excess of 0.15m water per annum. It is important to note that the summer melt may actually be a form of mass redistribution and not mass loss (Budd *et al.*, 1967). At the same time, mass loss by basal melt can not be discounted as a contribution to mass redistribution (Budd, 1970). The idea of the existence of large scale basal melt particularly at the area of confluence has fuelled the theory that the Lambert Glacier has the potential to surge (Budd and McInnes, 1979) as Wellman (1982) hypothesised about the Fisher Glacier.

The largest uncertainty in these budget estimates is the snow accumulation in the interior. With lack of data for the centre of the drainage basin (75-80° South), a variety of accumulation results have been hypothesised. Low values for net accumulation (less than 100 kg m^{-2} a^{-1}) at the stations measured by Allison (1979) suggested that the 100 kg m^{-2} a^{-1} accumulation isopleth used by Kotlyakov *et al.* (1974) was actually further north than had been originally plotted.

McIntyre (1985) proposed a re-assessment of the mass balance of the Lambert Glacier drainage basin based on interpretation of Landsat imagery and a reassessment of the area of the drainage from the *SPRI Atlas* (Drewry, 1983). The recalculated area of the drainage basin was 902 000 km^2 (17% less than Allison). McIntyre also interpreted dark areas on Landsat images, centred at 76°15'S 68°

18'E and approximately 200km southeast of Mawson Escarpment, as being regions of bare ice, and hence net ablation. The total extent of the area of ablation was thus 56 000 km^2 (22 800 km^2 greater than Allison). Table 2.1 is a comparison between Allison's (1979) interpretation and those of McIntyre (1985). McIntyre concluded that the lower reaches of the ice stream are in balance and that the upper reaches are not as significantly out of balance as previously thought. In explaining the expansive area of the blue ice identified in satellite imagery, McIntyre reported that this area was a region with steep slopes and prone to deflation from the strong katabatic winds.

Re-calculation of the mass balance of Lambert Glacier on the basis of the revised area and accumulation rates (Bracketed values are those of Allison (1979).)

	Interior drainage basin	Lambert Glacier system	Total drainage basin
Inflow ($Gt\ a^{-1}$)	- (-)	30 (30)	- (-)
Gain in basin ($Gt\ a^{-1}$)	32 (60)	-7 (-7)	25 (53)
Outflow ($Gt\ a^{-1}$)	30 (30)	11 (11)	11 (11)
Budget ($Gt\ a^{-1}$)	+2 (+30)	+12 (+12)	+14 (+42)
Budget limits ($Gt\ a^{-1}$)	-11, +16 (+3, +79)	-4.5, +28 (-4.5, +28)	0, +25 (+9, +89)
Area (thousand km^3)	902 (1090)	62 (62)	964 (1152)
Mean annual surface level change ($m\ a^{-1}$ water)	+0.002 (+0.03)	+0.19 (+0.19)	+0.015 (+0.04)
Surface change limits ($m\ a^{-1}$ water)	-0.014, 0.016 (+0.003, +0.07)	-0.07, +0.45 (-0.07, +0.45)	0, 0.024 (+0.01, +0)

Table 2.1. A comparison between results from McIntyre (1985) and Allison (1979). From: McIntyre (1985)

Allison *et al.* (1985) disputed McIntyre's interpretation of ablation areas from satellite images. The redefinition of the ablation zone by McIntyre (1985) highlights the issue of the potential misinterpretation of satellite imagery. For example: tonal differences in a single spectral band do not necessarily differentiate between hard winter snow glaze and blue ice on satellite images (Allison *et al.* 1985). As an example, in areas 500 km south of the Lambert Glacier, there are patches of older snow that have recrystallised and as such have lowered the surface albedo, making the surface appear darker in satellite imagery (Swithinbank, 1988). Surfaces that appear brighter would then be newer snow which would have more interstitial air making for a lighter reflection. An alternative theory is that the subtle slope changes in the area have differing reflections on the surface and as such would produce different albedo responses to the solar illumination.

This discussion by Swithinbank (1988) repeats the Allison *et al.* (1985) refutation of McIntyre's (1985) interpretation of the satellite data that led to the conclusion that there may be a greater area of ablation than previously thought. The ANARE series of oversnow traverses into the interior of the Lambert basin (1989/90 - 1994/95) clearly showed that there was no large areas of net ablation in the region (Allison, pers. comm. 1996). Using McIntyre's new and more accurate definition of the area of the drainage basin Allison *et al.* (1985) concluded that the mass input to the system is 50 Gta^{-1} and the outflow is 30 Gta^{-1}.

The stability of the Lambert Glacier has also been questioned. Hambrey and Dowdeswell (1993) have proposed that either the Lambert Glacier is out of equilibrium and prone to surging or it is presently in a steady-state. They recognise that the most dominant feature (as seen on satellite imagery) is the longitudinal foliation. Longitudinal foliation in glaciers is generally parallel to the medial moraine and as such can be used as an indication for the flow patterns within portions of the ice stream (Sharp, 1988: Hambrey and Dowdeswell, 1993). The Lambert Glacier system has eight major flow units (Hambrey and Dowdeswell, 1993) that are visible right along the ice stream up to close to the coastal edge of the Amery Ice Shelf. Because the coastal area is blanketed by new and localised accumulation the flow lines are then obscured. Due to a lack of folds in surface flow features, Hambrey and Dowdeswell (1993) concluded that the Lambert Glacier has been in a steady-state flow regime since the end of the Pleistocene Epoch (0.01-1.6 Ma).

Recent changes in the position of the grounding line of the Lambert Glacier have been hypothesised after analysis of satellite altimeter data. Herzfeld *et al.* (1993) applied "kriging" to some selected satellite data. Kriging is a method of estimating spatially distributed values from limited known points (Swan and Sandilands, 1995). It is a method that allows for limitations in spatial data to be interpolated after the removal of data that can be attributable to random noise or inconclusive data (Myers, 1985). Using this method, new elevation maps of the region based on a 3 km grid were created from Seasat data (1978) and Geosat ERM (1987-1989) data. Using the break at the 100m contour interval as the approximation for the grounding line, Herzfeld *et al.* (1993) concluded that the grounding line has advanced between 100 m and 400 m each year between 1978 and 1987-1989.

Lingle *et al.* (1993) also studied recent elevation changes on the Lambert Glacier using orbital crossover analysis of satellite radar altimetry data. Geosat ERM (1987-1989) data and Seasat (1978) data were analysed from 72°6' to 70°24' South. Lingle *et al.* (1993) made several conclusions, the main ones being that the mean rate of increase in the surface height on the lower Lambert Glacier (between the two study dates) was 30 $\pm$10 mm yr^{-1}. The modelled mean rate of increase as a result of orbit adjusted crossover was 70 $\pm$ 10 mm yr^{-1}. This then combines to a 20-80 mm yr^{-1} surface height increase across the lower Lambert Glacier. Satellite radar altimetry data used to calculate surface elevation variation was calibrated from sea ice measurements and was intermittently affected by seasonal effects on ice surface temperature that impacts on the depth of radar penetration.

In summary, the Lambert Glacier is 90 km wide in its lower reaches and approximately 400 km long (Giovinetto and Bentley, 1985; McIntyre, 1985). Studies to date indicate that about the grounding zone, the ice is approximately 800 m thick (Budd *et al.*, 1982) and the glacier is believed to have a positive mass balance (Allison *et al.*, 1985). The conclusion of Lingle *et al.* (1993) and Herzfeld *et al.* (1993) based on the late spring 1986 through to late winter 1989 Geosat ERM data and late winter 1978 Seasat data are that the grounding line is advancing and that the glacier is possibly surging like Ice Stream B from the Ross Ice shelf area (Shabtaie *et al.*, 1988). That is, it may be currently thinning upstream and thickening downstream, or it may be flowing fast while remaining in balance. These conclusions were related to an increasing elevation on the lower Lambert Glacier as a result of a positive net mass balance

across the entire catchment area (Allison, 1979; Allison *et al.*, 1985) with a mean thickening rate of up to 210 ± 290 mm yr^{-1} in ice equivalent (Allison, 1979).

2.4 Studies on Other Outlet Glaciers and Ice Streams of Antarctica

2.4.1 Ice streams of the Ross Ice Shelf Area

The Ross Ice Shelf is an ice shelf which is fed by ice streams off the east and west polar plateaus and through the TransAntarctic Mountains via mountain glaciers, outlet glaciers and ice streams. Studies have been carried out on the major ice streams in this area over many years since their initial identification in the 1960's. The objective in each case has been to geographically map the glaciers and their drainage basins, identify flow structures and surface features, as well as to estimate the mass flux of the vast volume of ice involved in each drainage system and to determine the dynamic behaviour of the systems, and their potential for change.

This research is aimed at relating ice mass dynamics with climate change over both long and short time scales. The predominant ice streams in West Antarctica draining into the Ross Ice Shelf are Ice Streams A, B, D and E (Figure 2.4). The lesser ice streams are C and F. The Ross ice streams drain 95% of the part of the West Antarctic ice sheet which exits via the Ross Ice Shelf (Shabtaie *et al.*, 1988).

Ice Streams A and B both appear to be in a state of negative mass balance while the inactive Ice Stream C is in a state of strong positive mass balance (Shabtaie *et al.*, 1985; Whillans and Bindschadler, 1988). Ice Stream A has main tributaries in the Reedy Glacier and Horlick Ice Stream set within 1000 m and deeper troughs that converge downstream into a single trough (Shabtaie and Bentley, 1988). It has recently been suggested that Ice Stream A is actually two ice streams (A1 and A2) and that they flow over different subglacial troughs (Shabtaie and Bentley, 1988). Ice Stream A is discharging more ice than it is accumulating in its catchment area and is thinning at a rate of 0.08 ± 0.03 m a^{-1} (Shabtaie *et al.*, 1988).

Ice Stream B comprises two separate ice streams, B1 and B2 (Figure 2.5). Ice stream B1 has a deep trough inland which shoals markedly nearer to the grounding

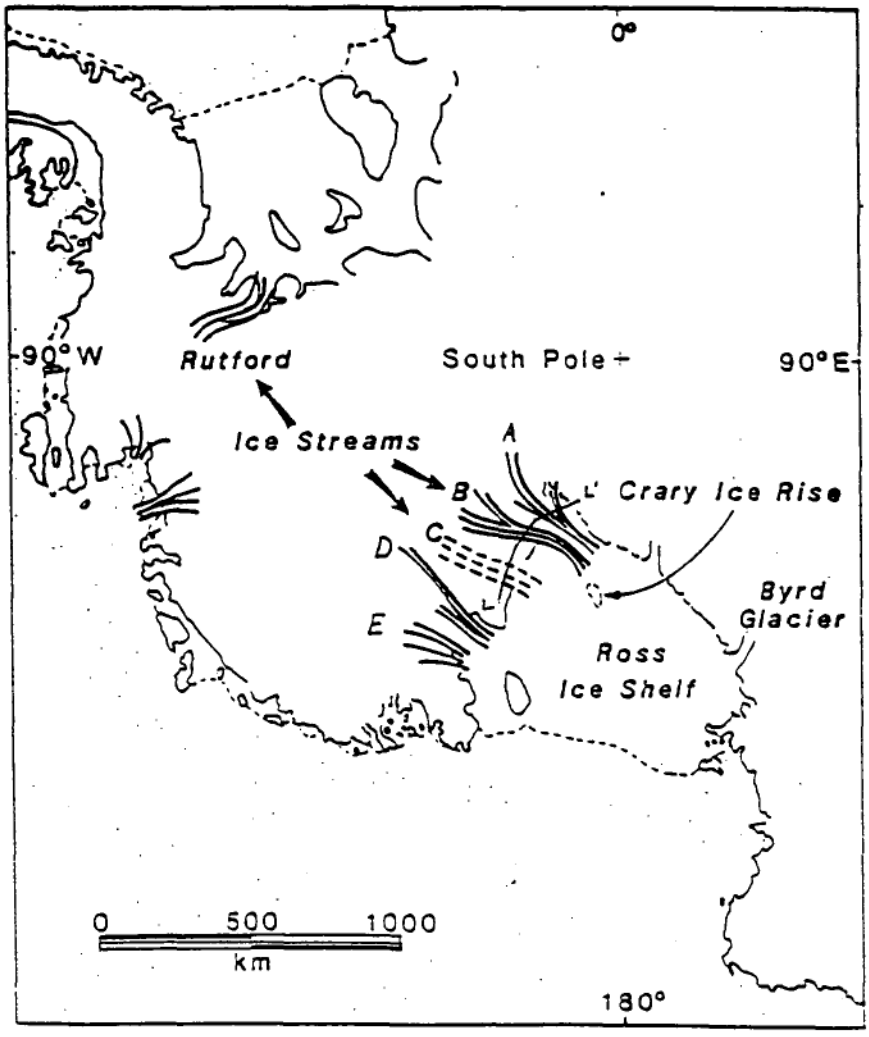

Figure 2.4. The Ross Ice Shelf and major ice streams A-E. From: Whillans and Bindschadler (1988)

line, while B2 is 1000 m thinner than B1 and has a relatively constant trough depth throughout (Shabtaie and Bentley, 1988). At the head of B1 the ice thickness is greater than 2000 metres thus demonstrating the existence of a deep subglacial trough (Shabtaie and Bentley, 1988). The ice ridge between B1 and B2 is unstable and appears to be contributing to the overall mass of Ice Stream B. There is also lateral movement between Ridge AB and Ice Stream B (Shabtaie and Bentley, 1988).

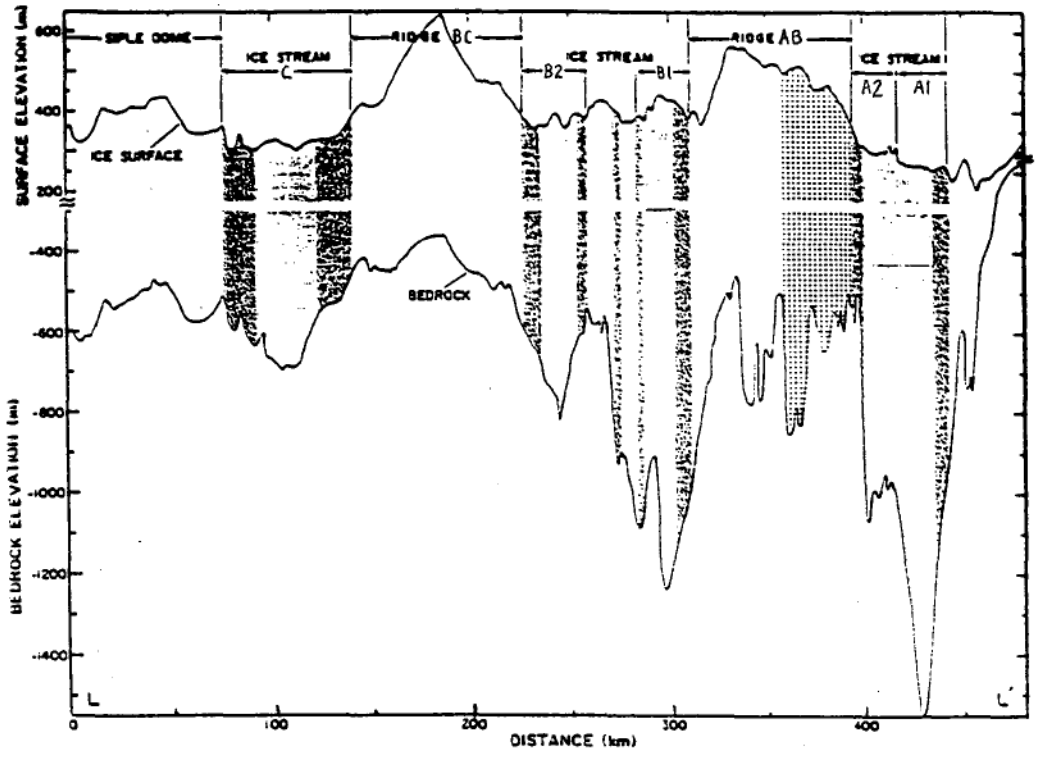

Figure 2.5. Cross section LL'. The heavy shading is marginal shear zones of the ice stream; light shading is the main glacier body. The surface and bedrock elevations (solid lines) were interpolated data from flight lines. From: Shabtaie and Bentley (1988)

Shabtaie *et al.* (1988) have noted a slight thinning in the catchment area, while there is a much faster rate of thinning in the region of the confluence of B1 and B2. Thickening of the ice stream occurs in the main glacier body, decreasing with distance from the confluence.

B1 is thinning at a rate of 1.3 m a^{-1}, decreasing in thickness twice as quickly as B2 (Shabtaie *et al.*, 1988). Generally, both ice stream B1 and B2 are sliding due to the existence of basal melting (Whillans and Bindschadler, 1988). The ice stream is 'breaking up' with rafts in the up-stream ice. Down-stream of the B1 and B2 confluence Ice Stream B has an ice rise ("ice rise a") that is now moving at the same rate as the glacier at 460 m a^{-1} (Shabtaie *et al.*, 1988). Shabtaie *et al.* (1988) believe that if "ice rise a" was stationary in the recent past and has only just begun to flow (by no longer being pinned), it may have had the potential to exert pressures up-stream that could slow up the ice velocities there. If the ice rise has become unpinned only recently, ice velocities upstream may not have fully adjusted

as a result. Shabtaie *et al.* (1988) use this situation as a possible point of reference for the potential surging nature of Ice Stream B. They noted that just down-stream of the confluence, the net flux of B1 is strongly positive, while B2 net flux is strongly negative. This makes the area in a state of net balance while up-stream of the confluence, both B1 and B2 carry about the same mass. The flow of Ice Stream B is perpendicular to the elevation contour and parallel to crevasse margins. In the upper reaches of Ice Stream B where the crevasse margins are diagonal to elevation contours, defining the catchment area becomes more difficult (Whillans and Bindschadler, 1988).

Ice Stream C has surface features which are poorly correlated to ice thickness (Shabtaie and Bentley, 1988). The glacial bed elevation is relatively constant at between 600-900 m below sea level (like B2) (Whillans and Bindschadler, 1988). There are several subglacial irregularities and local subglacial rises that may be contributing to the stagnant nature of Ice Stream C (Whillans and Bindschadler, 1988). This ice stream and its catchment area are thickening at a rate of 0.12 ± 0.02 m a^{-1} (Shabtaie *et al.*, 1988) which is also reflected in the output which is thirty-seven times less than the mass influx. The gross imbalance in the mass flux of the ice stream may also be helping to cause a reversed hydraulic potential gradient (Shabtaie and Bentley, 1988) which may eventually lead to the reactivation of Ice Stream C (Hughes, 1970). The stream now flows at 10 ma^{-1} in both the catchment area and at the grounding line, and although there are no surface crevasses apparent, there are buried crevasses which suggest past activity (Bentley *et al.*, 1987).

Overall, across the ice streams of the Ross Ice Shelf area in West Antarctic, there is a negative net balance rate for both the ice streams and their catchment areas (Shabtaie and Bentley, 1987). Inland of the grounding zone there are ten deep underlying troughs. By the time the main ice flows into and along the ice streams towards the coast, in the vicinity of the grounding line only four deep troughs remain to underlie ice streams A, B1, B2 and C (Shabtaie and Bentley, 1988). The troughs are deeper nearer to the TransAntarctic Mountains but these shoal out far more quickly and although there is no step in either the bed or surface topography as seen in other glaciers (McIntyre, 1985) this may be due to the greater impermanence of these features in comparison to the outlet glaciers which have fixed rock wall boundaries (Shabtaie and Bentley, 1988).

2.4.2 Other Antarctic Glaciers and Ice Streams

The Jutulstraumen Ice stream in Dronning Maud Land is 50 km wide at its and 250 km long (Gjessing, 1970). Gjessing (1970) also noted that at the area of maximum ice thickness, 1560 m, the surface velocity is 390 m yr^{-1} giving a mass transport of the ice stream of 27.4 × 10^9 tonnes per year (Gjessing, 1970). The ice stream begins on the plateau at 3000 m asl at Kronprinsesses Märtha Kyst. It is bounded to the east by the mountain massifs Sverdrupfjella and to the west by Borga and Ahlmannryggen massifs. Jutulstraumen Ice Stream flows into the Fimbulisen Ice Shelf.

Pine Island Glacier on the Walgreen Coast of West Marie Byrd Land, flows to the east of the Hudson Mountains in West Antarctica. This glacier has a drainage basin of 214,000 ± 20,000 km^2, with a total input into the system of 86 ± 30 Gta^{-1} and a mass flux at the ice front of 25 ± 6 Gta^{-1} (Crabtree and Doake, 1982). The average accumulation rate for the drainage area is 0.40±0.1Mg m^{-2} a^{-1} (Bull, 1971; Giovinetto, 1964). Crabtree and Doake (1982) therefore suggest that based on a minimum input at the ice front of 56 Gta^{-1} (using an average thickness 0.5 km and width 26km) the drainage basin is most probably building up. This compares to the Lambert Glacier (Allison, 1979) and the Shirase Glacier (Shimizu *et al.*, 1978), with an input that is 1.5 to 3 times greater than the output. The Pine Island Glacier is a good example of a glacier that is capable of rapid retreat. This is due mainly to the absence of a buttressing ice shelf. Instead, Pine Island Glacier is grounded on a bedrock sill 1200 -1300 m below sea level, which can influence the position of the grounding line. The ice front has an average velocity (over 2 years of observation) of 2.1 ± 0.2 km a^{-1} (Crabtree and Doake, 1982).

Another ice stream is the Rutford Ice Stream, which flows between the Ellsworth Mountains to the west and Fletcher Promontory to the east in Ellsworth Land, West Antarctica (Figure 2.6). In some areas of the Rutford Ice Stream, the ice thickness is in excess of 2000 m with the deepest bedrock at 1580 m below sea level (Stephenson and Doake, 1982). The drainage basin is 40 500 ± 4 000 square kilometres and the 30 km wide glacier has a mass flux at the grounding line of 18.5 ± 2.0 Gta^{-1} (Crabtree and Doake, 1982). Along the longitudinal line of the ice stream, the surface velocity has been recorded at between 360-400 ma^{-1} (Frolich and Doake, 1988). Two distinct flow regimes within this ice stream have been described by Frolich and Doake (1988): a marginal zone where side wall shear dominates the flow, and the central zone where basal friction dominates.

The majority of shear deformation occurs across a 10 km wide boundary on either side of the glacier. Within the more central 10 km band of the ice stream body, the lateral shear stress is zero (Frolich and Doake, 1988). Therefore Frolich and Doake (1988) concluded that the strain across the glacier edge does not impede mid-glacier flow rates.

The grounding line of the Rutford Ice Stream was identified by Stephenson and Doake (1982) to within 2 km accuracy. This was done by using hydrostatic tiltmeters to locate floating and grounded ice. Based on modelling, Stephenson and Doake (1982) found that the basal melt rate was 1.8 ma^{-1} based on the small surface gradient of about 1.8×10^{-3} and implied basal strain rates of 3×10^{-3} a^{-1} in the area of the grounding zone. The accumulation rate on the Rutford Ice Stream

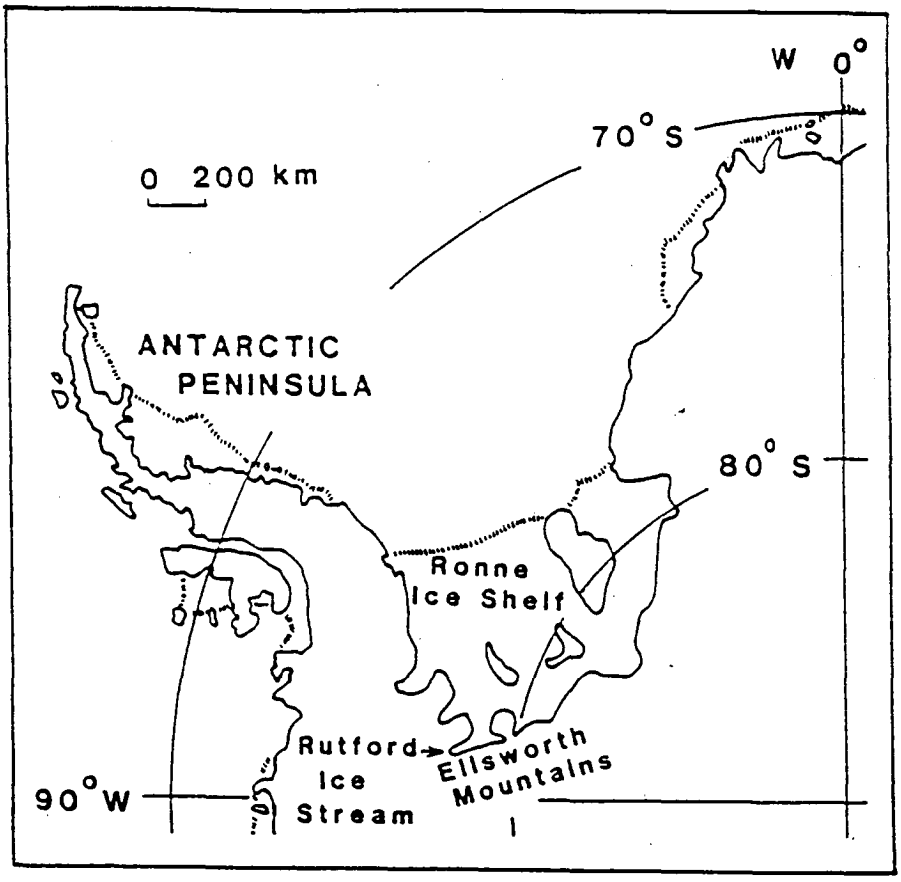

Figure 2.6. The location of the Rutford Ice Stream and the Filchner-Ronne Ice Shelf. From Frolich and Doake (1988) pg 11.

was approximately 0.30 Mg m^{-2} a^{-1} (Stephenson and Doake, 1988). The location of the grounding line is considered to be very sensitive to small changes in ice thickness (Stephenson and Doake, 1988) that result from climatic change - be it global climate change or local climate change brought on by major calving events.

Within the dynamic systems of such landscapes as ice sheets, ice streams and ice shelves, the region which is least understood is the area about the grounding line, the boundary between the floating ice shelf and the grounded ice (Weertman, 1976; MacAyeal *et al.*, 1986).

Chapter Three

The Amery and Other Ice Shelves

3.1 Introduction

Ice shelves were a mystery to early explorers: they were a bleak, barren and silent world. Although they are relatively flat, ice shelves are often fractured by bands of crevasses while the surface may be furrowed with small scale wind-formed ridges called sastrugi from several centimetres to metres in size (Hooper, 1991). Ice shelves are floating ice. Although typically anchored to land on one to three sides, the ice flows horizontally through coastal embayments and occasionally over shallow bed elevations not unlike islands beneath the ice (MacAyeal and Thomas, 1986). They may be fed by the seaward flow of ice streams and outlet glaciers into the ice shelves and tend to thin with distance from the grounding line due to spreading under their own weight and possibly from bottom melting as well, although basal freezing can also take place (Weertman, 1957; Swithinbank and Zumberge, 1965). The two most important boundaries on ice shelves are the hinge or grounding line, where continental ice begins to float, and the ice front, where the ice shelves calve forming ice bergs (Sharp, 1988).

Ice shelves are constantly being added to by ice from the inland ice sheet, local accumulation and in some areas, basal freezing. They are also constantly loosing ice by the calving of icebergs and from sub-ice shelf melting. Thus they play an important role in the process of mass discharge, or ablation, for the Antarctic continent. If this accumulation and ablation ratio remains equal, then the ice shelf will be stable. Any observations of variation in the balance between the loss or gain of the ice shelf will provide data on the net budget of the system and its response to the climatic and physical environment. The velocity of ice movement, ice thickness, density and both surface and basal mass exchanges are important variables for understanding ice shelf behaviour. This is important if one considers that ice shelves comprise 44% of the Antarctic coastline (Drewry, 1988) and drain approximately 60% of the Antarctic ice sheet (Markov *et al.*, 1968).

This chapter discusses results from some of the major studies on the Amery Ice shelf, the behaviour of ice shelves in general, and an overview of some comparable ice shelves in Antarctica. The morphology, accumulation and ablation studies, dynamics and mass budget are discussed. Paterson (1994) states that an ice shelf is controlled largely by the flow of ice streams, and as such, it is necessary to gain an understanding of the drainage system dynamics. Because ice streams and outlet glaciers continue to exist within ice shelves as fast moving ice, the ice is retarded by drag and shear stress from the confining embayments all the way to the calving front of the ice shelf (Paterson, 1994). Hence the Amery Ice Shelf, and other ice shelves, need to be studied in detail to fully comprehend the implications of ice morphology and dynamics.

3.2 Amery Ice Shelf

3.2.1 Morphology

The Amery Ice Shelf in Prydz Bay, drains part of the East Antarctic ice sheet predominantly via the Lambert Glacier system, and other smaller tributaries such as the Charybdis and Scylla Glaciers. The area of the ice shelf is 3-4 $\times$ 10^4 km^2 (Budd, 1966; Budd *et al.*, 1967; Drewry *et al.*, 1982) and the Amery Ice Shelf drains 1.3 $\times$ 10^6 km^2 of the East Antarctic ice sheet, 70% of which is part of the Lambert Glacier and its drainage basin (Giovinetto and Bentley, 1985). The location of the grounding line was proposed by Budd *et al.* (1982) to be around the 100 m asl contour. Between this area and the ice front, only the more southern portions of the ice shelf are near any significant ice free regions. These are the northern Prince Charles Mountains on the western side of the system. Most of the terrain parallelling the boundaries of the Amery Ice Shelf to the east and west is the ice covered plateau. Aerial photography and satellite imagery for the area has allowed the western and eastern limits of the ice shelf to be mapped. Interpreting the information from these images is a continuing process.

The width of the ice shelf varies from 200 km at the ice edge to 100 km across the ice at T4 276 km from the front in 1968 (Budd *et al.*, 1982) (Figure 3.1). Measured parameters of the Amery Ice Shelf are shown in Table 3.1. Budd *et al.* (1982) recorded elevations ranging from 45 m at the edge, 71 m at G2, 117 km from the front, to 100 m at T4. The velocity of the ice at G2 is about 800 m $\pm$100 m yr^{-1}

compared to 410 ±50 m yr^{-1} at T4. The accumulation rates for these two points range from 33 cm^{-2} yr^{-1} to 10.5 cm^{-2} yr^{-1} for G2 and T4 respectively, while the 10m firn temperatures varied from -20.9°C for the former and -23.5°C for the latter. From Budd *et al.* (1982) the ice thickness ranged from ~300 m at the edge, to ~430 m at G1 66 km from the front, and ~800 m at G3.

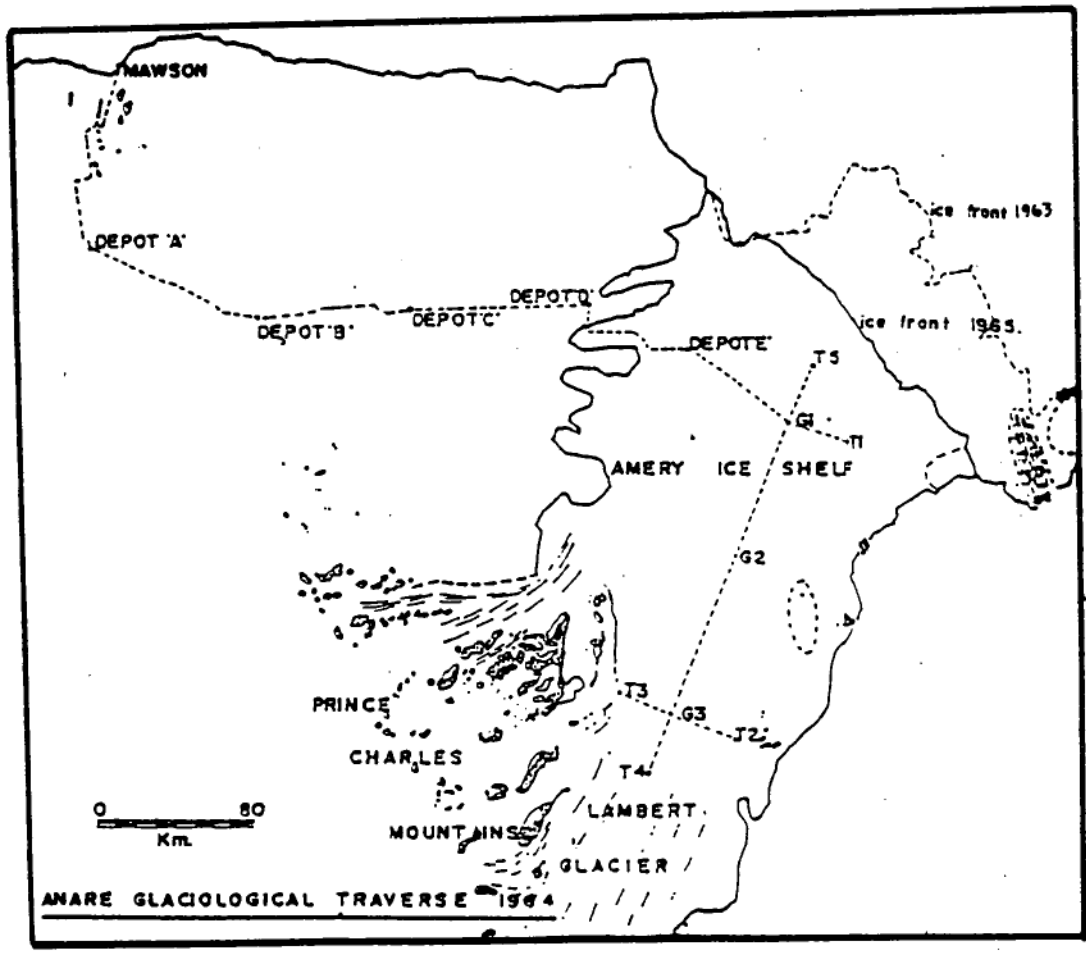

Figure 3.1 The over snow traverse route from Mawson to and over the Amery Ice Shelf completed in 1963-64. Accumulation stakes were installed at 3 km intervals along the route. Strain grids were established at Depot E, G1, G2 and G3. From Budd (1966).

Station	Distance from ice front (km)	Surface Elevation (m asl)	Ice Thickness (m)	Velocity (m a^{-1})
Edge	0	45	~300	~1200
T5	34	54	375	980
G1	66	63	430	800
G2	147	71	700	800
G3	244	88	~800	410
T4	276	100	850	410

Table 3.1 Measured parameters on the Amery Ice Shelf. From Budd *et al.*(1982).

3.2.2 Changes to the calving Front

Studies on the Amery Ice Shelf have been reported by Budd (1965, 1966), Mellor and McKinnon (1960), Law (1966), Budd *et al.* (1967); Wakahama and Budd (1976) and Budd *et al.* (1982). After initial observations, work concentrated on determining the dynamics of the Amery Ice Shelf. Documented changes in the position of the ice front led to the conclusion that the Amery Ice Shelf is not a system in a complete state of balance, because the position of the front seems to fluctuate over an interval of some 40 years (Budd, 1966). This does not exclude the interior shelf region from being in balance.

Because large icebergs may be periodically calving off the Amery Ice Shelf, the ice shelf is not entirely in a state of steady balance. Between 1963 and 1965 a major calving event occurred across the ice front (Figure 3.2). The ice front retreated by approximately 60 km and the ice shelf lost about one fifth of its area. Budd (1966) described how the ice front gradually advances and spreads out with increasing speed until a major calving event occurs such as in 1963. He postulated that these occur every 40-50 years. The ice shelf then again enters a pattern of advancing, spreading and calving. A regular pattern of changes supports of the idea that this change in morphology is related to increasing ocean stress on the advancing front until calving occurs. This type of regime with approximately periodic calving could exist with a steady state flow and thickness morphology behind the calving line.

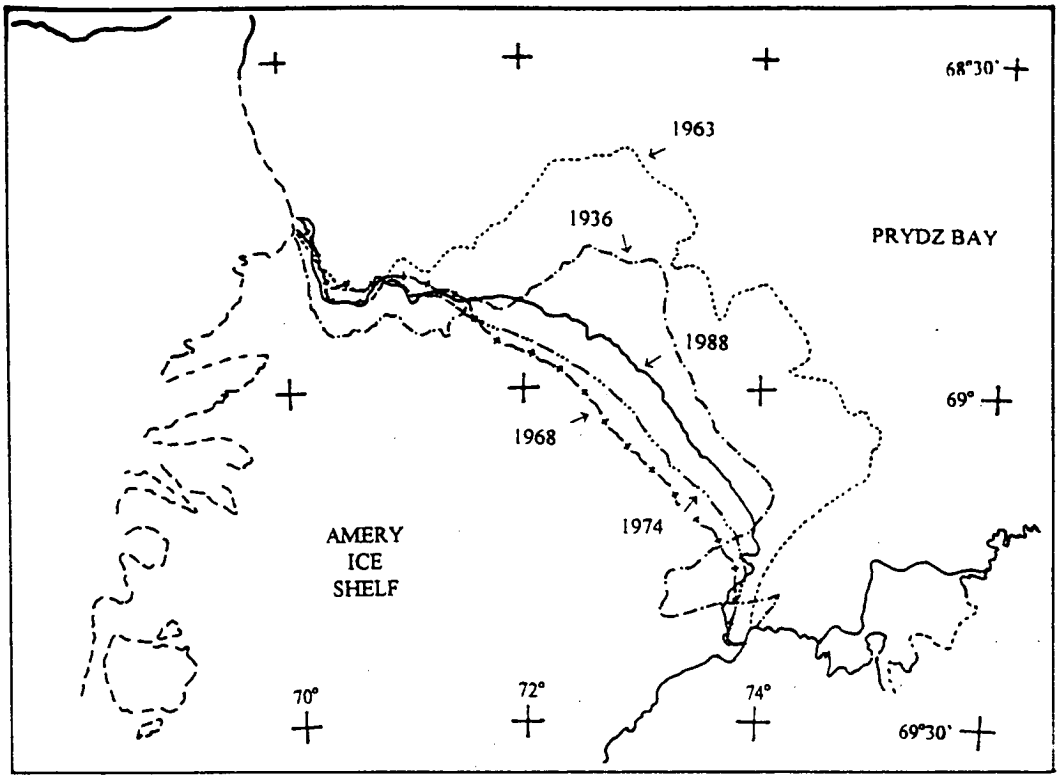

The position of the Amery Ice Shelf front plotted by different expeditions is shown as follows:

1936 Lars Christensen Expedition
1963 ANARE
1968 ANARE
1974 after Robertson
1988 after Robertson

Figure 3.2. Changes in the ice front of the Amery Ice Shelf. After: Budd (1966) and Robertson (1993)

3.2.3 Snow accumulation and surface climate

Along the Amery Ice Shelf, the accumulation rate decreases approximately uniformly from 40 g cm^{-2} per year near to the ice front to zero on the Lambert Glacier (Figure 3.3), where the surface of the area is predominantly blue ice (Budd, 1966).This is due to the local effects of coastal precipitation initiated by maritime air masses that diminish in intensity with distance from the coast. Budd *et al.* (1982) reported additional accumulation measurements made in 1968-1970. Snow accumulation varied

from 1.2ma^{-1} (~0.45 ma^{-1} water equivalent) near the ice front to 0 ma^{-1} (zero) on the Lambert Glacier 300 km inland. There is also evidence of a very small topographic influence to the accumulation. A recent ANARE expedition onto the Amery Ice Shelf has remeasured the 1968 optical levelling traverse line and was able to find some original marker stakes from which a 27 year accumulation profile from the ice shelf will be ascertained (I. Allison pers. com., 1996).

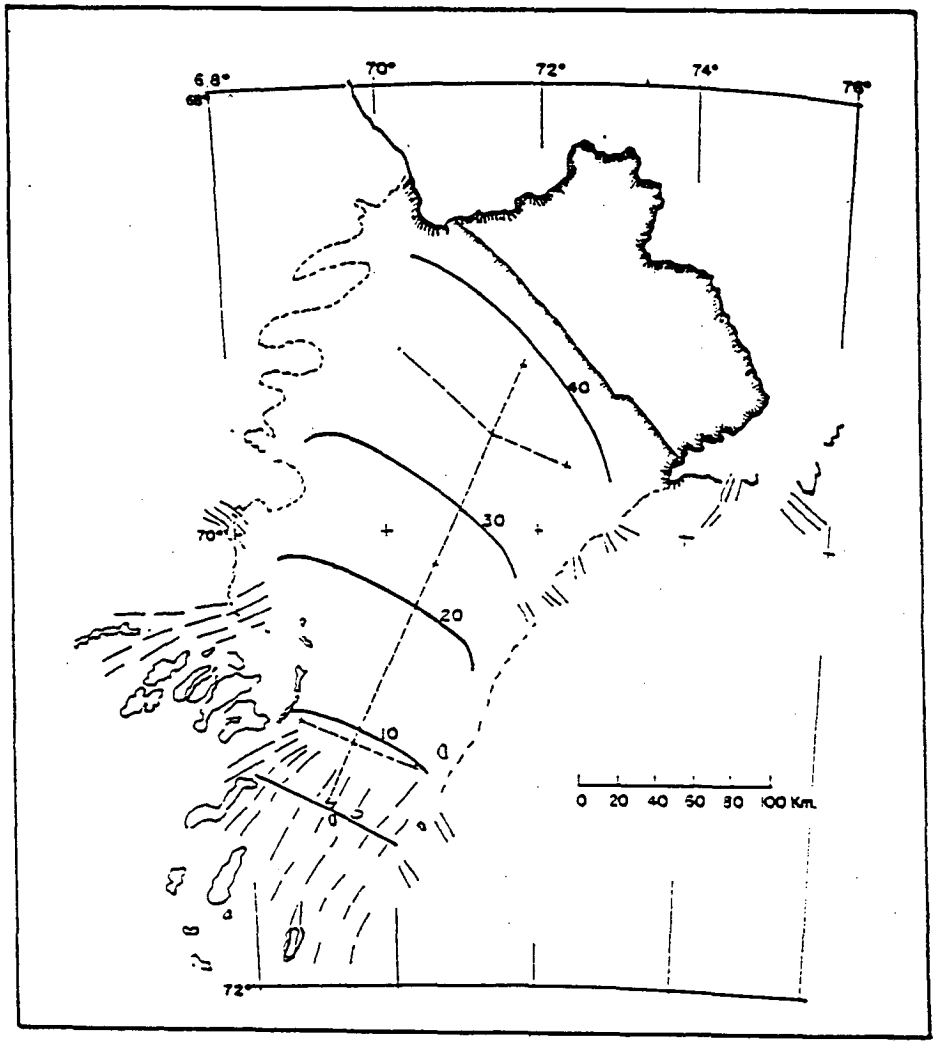

Figure 3.3. Annual net accumulation contours in g cm^{-2}yr^{-1}. From: Budd (1966)

On the western side of the ice shelf small sastrugi are oriented 200° from true north, while on the eastern side the sastrugi are oriented 160° (Budd, 1966). The sastrugi are an indication of the predominant wind directions, which in the case of the Amery Ice Shelf are relatively light winds. Budd (1966) stated that these winds essentially blow longitudinally down the ice shelf. Budd (1966) reported that the average density of the annual surface layer was 350 kg m^{-2} a^{-1} over the total thickness of the shelf, measured from ice cores, while at 6 m depth the average density was 490 kg m^{-2} a^{-1}. At G1, the ice density averaged over a 313m deep core drilled in 1968 was 854 kg m^{-2} a^{-1} (Budd *et al.*, 1982).

Accumulation and snow/ice density rates are determined in part by air temperature. Annual mean air temperatures were estimated by Budd (1966) from temperature profiles measured in the top 10 m of the ice (in 1962, 1963 and 1964). The results showed that temperature decreases slightly with distance from the coast, from -21° C at G1 to -23° C at G3. At the ice front, the average temperature was -11° C. The average temperatures experienced at the coastally located Australian Antarctic station Mawson is comparable to the ice front average (P. Dawson, pers. comm. 1992).

3.2.4 Surface elevation, surface slope and ice thickness

The surface of the Amery Ice Shelf is relatively flat, averaging 1.8×10^{-4} at the ice front, to 2×10^{-4} at G3 (see Figure 3.1 for location). The gradient of the surface then rises quite rapidly to 3.75×10^{-4} at the region identified as the transition zone between the Lambert Glacier and the Amery Ice Shelf by Budd *et al.* (1982). The central area of the ice shelf is typically smooth and featureless. Some long tension crevasses, which run parallel to the ice front, are found about the region of G1 (Budd, 1966). In the area nearer to the grounding line of the Lambert Glacier, undulations across the surface were observed during the over snow traverse of the area as the slope of the ice began to rise from G3 to T4 (Budd, 1966). Towards the boundary region of the ice shelf, the slope increases to over 3.75×10^{-4} (Budd *et al.*, 1982). This compares to 6×10^{-4} of the eastern side of the Ross Ice Shelf near "Little America" (Crary and Chapman, 1963). In Budd's (1966) calculations, the assumption was made that the Amery and Ross Ice Shelves were similar in morphology. These authors hence assumed that the density distribution of the Ross and Amery Ice Shelves are similar;

This was necessary at the time due to the lack of ice thickness data over the Amery Ice Shelf. This is discussed further in section 3.2.6.

Accurate elevation data were gathered from optical levelling along the centre-line and cross lines in 1968. Ice thickness was measured along the same route with a radio echo sounder. The levelling data had an error of ±10 mm over a scale of kilometres and an error of ±0.5 m over the "whole net" (Budd *et al.*, 1982). This "whole net" is the area from Sandefjord Bay to Beaver Lake and over the ice cliffs of the ice front. Except towards the centre of the ice shelf where a slight rise is apparent, the surface is relatively flat, but does slope noticeably downward from the Lambert Glacier south of T4 at approximately 100 m elevation to 45 m at the ice front, a distance of roughly 300 km. Thus the average slope of the Amery Ice Shelf is approximately $1.8. \times 10^{-4}$ (Budd *et al.*, 1982). On a small scale, between 1-5 km, it is the surface and basal fluctuations which are predominant and appear to be related. Over a larger scale, the region is of a relatively uniform thickness. Around the grounding line of the Lambert Glacier, a slight thickening occurs once the ice is fully floating. The ice then gradually thins towards the ice front due to the forward spreading of the ice shelf within its lateral boundaries. Near the ice front the elevation to thickness ratio is 0.160; near T4 the ratio is 0.113 (Budd *et al.*, 1982). The variation in ratios is due to changes in the average density of the column of ice which increases as the accumulation rate decrease with distance from open water. At G1 the elevation to thickness ratio is 0.142, but the average ice density is 854 kg m^{-2} a^{-1} (Budd *et al.*, 1982).

The grounded-floating transition between the Lambert Glacier and the Amery Ice Shelf was reported by Budd *et al.* (1982) to be 3 km south of T4 occurring at a localised maximum on the surface slope. This is where the surface rises from 88 m to 100 m asl in just 19 km with small change in ice thickness (which is generally around 800 m in this area). In the vicinity of this grounding- floating transition zone there is an ablation area with a high density "blue ice" surface (Budd *et al.*, 1982). Slight groundings occur along the ice shelf and are reflected across the surface as many small-scale undulations with wavelengths that are several times the ice thickness. These grounding spots have been postulated by Budd *et al.* (1982) to possibly have a minor affect on the flow of the ice shelf. These would only have very minor impacts, otherwise there would be significant surface slope deviations reflecting these slightly grounded zones. It has been noted by Bentley (1987) that for grounded ice, the

maximum slope typically occurs at the area of maximum driving stress. This will be elaborated on below.

3.2.5 Internal structure

A profile of the Amery Ice Shelf's internal structure was derived from work on a 310m ice-core from a bore hole at G1 which was analysed for $^{18}O/^{16}O$ oxygen isotope ratios. The measured profile indicated that glacial ice from the Lambert Glacier basin occurred or was apparent at G1 between a depth of 70-270 m (Morgan, 1972). Below 270m, the ice is of an oceanic origin, having frozen onto the bottom of the shelf, and above 70m it has originated from local snow accumulation (Figure 3.4). Temperature profiles were also measured in the borehole and a close match was obtained between the observed temperature-depth profile and that modelled assuming a basal-ice growth rate of 0.6 m a^{-1} (Budd *et al.*, 1982).

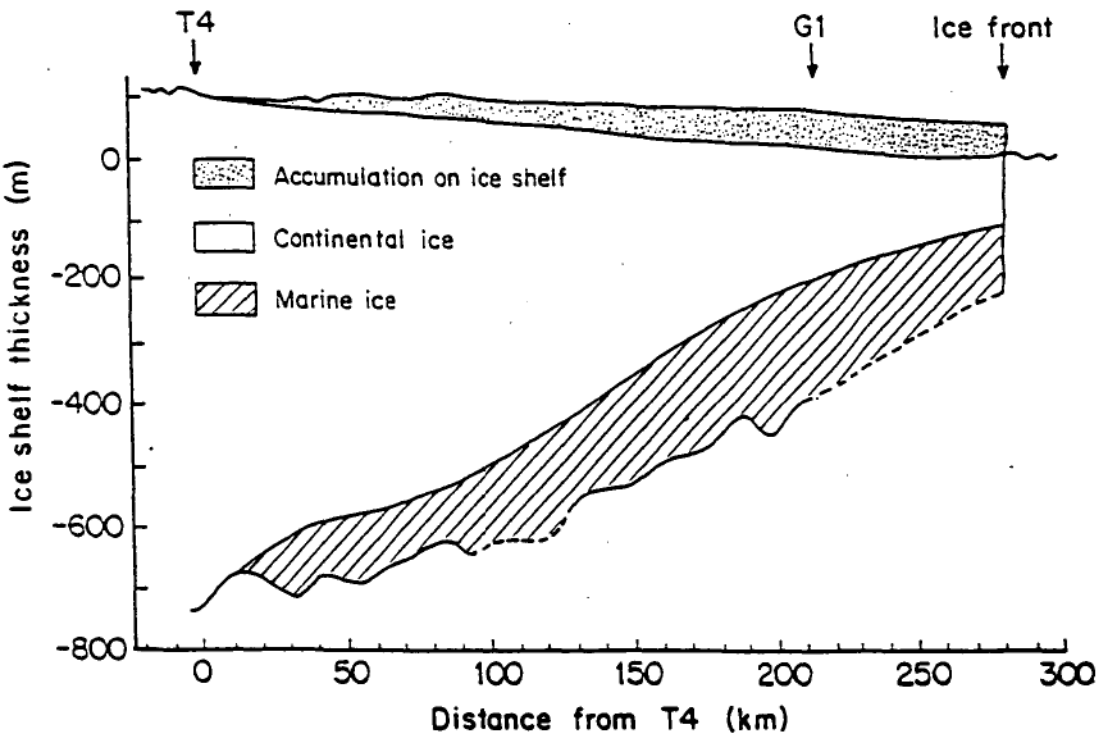

Figure 3.4. Surface and basal ice profile of the Amery Ice Shelf along a longitudinal profile. From: Budd *et al.* (1982) modified by Hellmer *et al.* (1992)

The ice flow and basal melt regimes that determine the internal structure of the Amery Ice Shelf are illustrated by particle paths (Budd *et al.*, 1982). Particle paths are determined by the surface elevation and accumulation rate (which in turn provide the surface and horizontal mass flux). At the base of the ice the difference between basal particle paths and the measured base has enabled the delineation of the basal growth and/or melt rate. Results of Budd *et al.* (1982) showed a substantial basal melt rate just after the ice began floating. The basal growth was obtained to beyond G1. The accumulated basal ice increased to a maximum thickness of approximately 200 m near G1. This occurred where the depth of the base ice was about 400 m. Further north, toward the ice front, Budd *et al.* (1982) concluded that the increasing influence of the rate of strain thinning would reduce the ice thickness of the marine ice to about 100 m. Overall, along the ice shelf it is the strain and advection rates which are more important than the surface or basal accumulation rates in determining the thickness profile of the ice shelf. Once the ice is floating, the basal growth is approximately balanced by strain induced thinning, this is particularly related to the initial 50 km of the ice shelf. Closer to the ice front Budd *et al.* (1982) noted that the basal ice slope becomes steeper which, together with the higher velocity rates, causes horizontal advection to roughly balance the large strain-rate thinning.

3.2.6 Dynamics and mass budget

Ice movement data on the Amery Ice Shelf which were available up until 1982 included a longitudinal profile (Figure 3.4) and two cross profiles. One cross profile is through G1, near the ice front, and the other profile intersects G3 between Beaver Lake and Manning Nunataks. The movement of the ice was obtained by comparing tellurometer and theodolite surveys in 1968 with a repeat measurement in 1969-70 (Budd *et al.*, 1982).

The velocity results that were gathered prior to 1963 (pre-calving) showed the ice front existing at that time was advancing at approximately 1500 m yr^{-1} (Landon-Smith, 1964). The general velocity pattern is one that increases towards the ice front. Down the centre of the ice shelf, the velocities ranged from 0.8 km per year at G1, 0.50 km yr^{-1} (G2) and 0.41 km yr^{-1} (G3). The strain rates (Table 3.2) were 0.8×10^{-3} yr^{-1}, 0.05×10^{-3} yr^{-1} and 0.15×10^{-3} yr^{-1} for G1, G2 and G3 respectively (Budd, 1966).

Position	Transverse Strain-Rate	Velocity	Ice shelf Width	Divergence Angle
	ε_θ	v	d	$\theta = \delta\varepsilon_{/\theta}$
	a^{-1}	km a^{-1}	km	u
G1	0.8×10^{-3}	0.80	160	$0.16 = 9°$
G2	0.05×10^{-3}	0.50	140	$0.014 = 0.7°$
G3	0.15×10^{-3}	0.41	110	$0.04 = 2.3°$

Table 3.2 Calculation of divergence of flow lines. From Budd (1966)

One of the most important features of ice shelves is their overall movement. The flow of the ice shelf is governed by a number of features including the ice thickness, the surface slope, the width and resistance of the sides (Paterson, 1994). The rate of movement is also dependent on the volume of ice that has flow which is relatively uninhibited by grounding obstructions. Sections of the ice shelf that are pinned, either due to the physical embayment of the shelf or by the ice riding over basal shoals, will slow down the flow or creep of the ice shelf.

If the sides of the bay or inlet that confine the ice shelf are not parallel, then the flow lines of the ice shelf will not be parallel (Paterson, 1994). Ice rises and regions of pronounced ice thickness change, generally in the region of merging ice streams and the ice shelf, will also influence the direction of flow of the ice shelf. This impact on the flow pattern of the ice shelf is termed *divergence* or *convergence* of flow (Paterson, 1994). One other concept that has been used to describe ice shelf dynamics is *back force*. This is the pressure that is provided by elements opposing the spread of the ice shelf, and is reflected upstream as opposite pressure, or back force opposing the gravitational driving stress. These forces do not include the pressure of the ocean at the ice front, but rather it includes ice rises and other 'shear stress' inducing features. Thomas and MacAyeal (1982) have shown for the Ross Ice Shelf that the back force (which is force per unit width divided by thickness) varies from 40 kPa at the ice front to 200 - 300 kPa near the grounding line.

Van der Veen and Oerlemans (1987) have concluded, from longitudinal and transverse strain rates based on steady state uniform density ice shelf profiles, that an ice shelf responds to mass balance changes more rapidly than an ice sheet. Calculations for the strain rates about the Lambert Glacier/Amery Ice Shelf transition zone have been difficult to accurately ascertain due to the apparently smooth transition between

difficult to accurately ascertain due to the apparently smooth transition between grounded and floating ice. This transition zone is also the region where the stress and velocity distributions are changing from those typical of grounded ice to those of an ice shelf (Paterson 1994).

At G3 however, Budd (1966) found the strain-rate to be small and suggested that the velocity is due almost entirely to the large scale surface slope and ice thickness gradient. Near the centre of the Amery Ice Shelf the effects of shear across the ice shelf were considered negligible in contributing to the creep of the ice (Budd, 1966). Sharp (1988) comments that if the creep rate is proportional to depth, then ice movement must decrease inland from the ice front. Budd (1966) showed that the typical decrease of strain rate going inland observed on large ice shelves is due to the dominance of the transverse strain rate and effect on the side.

From the G1 ice core analysis combined with the other data, Wakahama and Budd (1976) estimated the average freezing rate of sea water at the bottom of the ice shelf to be about $0.5ma^{-1}$. This rate of basal growth is expected to influence the thickness and ice dynamics further upstream.

Based on data collected in the winter of 1968 and the summer seasons of 1970-71, Budd *et al.* (1982) explored further aspects of the Amery Ice Shelf. This program primarily included ice core drilling and over snow traverse surveys which collected data on ice movement, optical levelling, ice thickness soundings and snow accumulation. Results derived from G1 by Budd *et al.* (1982) suggested that a significant rate of growth exists at the base of the ice shelf, especially inland where the ice thickness is greater than 450 m such as in the vicinity of G3. Towards the ice front, the high strain thinning is balanced by horizontal ice advection. Surface slope and ice velocities were suggested to result from gravity induced strain on confined floating ice while simultaneously creating high restraining shear stress zones along the sides of the ice shelf (Budd *et al.*, 1982).

The dynamics of the Amery Ice Shelf has also been examined by considering the variation of velocity of the ice across the ice shelf and along the centre line (Budd *et al.*, 1982). Based on the profiles through G1 and G3, velocity variations along the ice shelf and across the ice shelf were used to compute strain rates. These strain rates were of particular interest where the transition occurs between fast flowing ice and the

velocity data, it was calculated by Budd *et al.* (1982) that the shear strain rates near the ice shelf sides were large and the longitudinal strain rates are relatively small but increase towards the centre line and ice front. Through the Amery Ice Shelf project, Budd *et al.* (1982) were able to calculate the maximum strain thinning near the ice front to be 1.6 % a^{-1}.

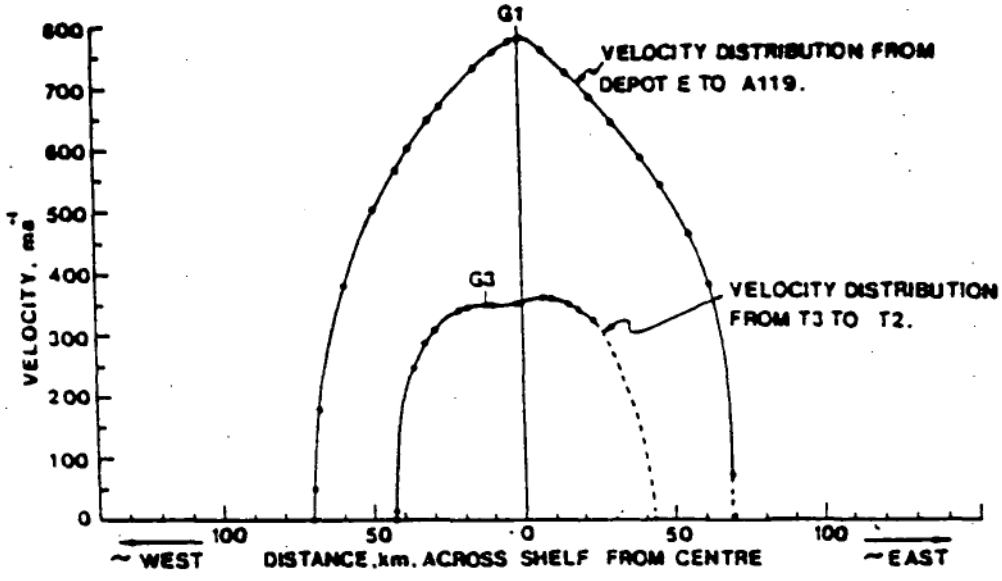

Figure 3.5. Measured velocity profiles across the ice shelf through G1 and G3 are shown as a function of distance perpendicular to the flow direction. From Budd *et al.* (1982)

In the late 1980's, perhaps as an indirect result from Allison's (1979) study on the Lambert Glacier or the extensive project review by Budd *et al.* (1982), the Amery Ice Shelf was being looked at for morphological changes as an early sign of climatic change (Partington *et al.*, 1987). The regions most likely to be responsive indicators of climate change are the shear zones and the area about the grounding line. As mentioned above, shear zones are the boundaries of separately recognisable regions of flow, or flow bands, within the body of ice. When there is a fluctuation in the mass balance (within the drainage basin) it is more than likely to appear as movement in the shear zones, flow band thickness and velocity (Partington *et al.*, 1987).

balance (within the drainage basin) it is more than likely to appear as movement in the shear zones, flow band thickness and velocity (Partington *et al.*, 1987).

Because the surface slope across the grounding line may become less steep in order to reduce basal shear stress, the grounding line of the Lambert Glacier onto the Amery Ice Shelf could be easy to identify if a sharp change in surface gradient occurs. The horizontal position of the grounding line is possibly the most sensitive region of the system to thickness changes both in the ice sheet and the ice shelf. As the Amery Ice Shelf has a relatively narrow ice front (250 km) outlet width, draining one of Antarctica's largest drainage basins, it seems probable that the Amery Ice Shelf is a sensitive indicator to mass balance changes further inland (Partington *et al.*, 1987). Budd *et al.* (1982) and Partington *et al.* (1987) have proposed a location for this grounding line, but as discussed in the following chapters, the predominant grounding line for the Lambert Glacier is believed by this author to exist further south.

With a mass flux across the ice front of approximately 2.7×10^{13} kg yr^{-1} ±35% (Budd, 1967; Allison, 1979), and an ice front velocity in the order of 1.2 km a^{-1} (Budd, 1967; Allison, 1979) the Lambert Glacier and Amery Ice Shelf system is unquestionably a substantial one. As a comparison, Ice Stream B has a ratio of width to depth of 30 (Paterson, 1994). The Lambert Glacier has a mean width (40 km):depth (1050m) ratio of 38 (after Allison, 1979). A typical valley glacier has a ratio of 6 (Paterson, 1994). This indicates how side drag can be important to the flow of ice streams. Although the main body of the ice stream may be mostly afloat, the sides experience resistance and inhibit flow. The bed and side drags in valley glaciers are often treated relatively simply by use of a valley cross section shape factor, but for ice streams the relative base and side drag are not well known (Paterson, 1994).

Partington *et al.* (1987) mapped the Amery Ice Shelf surface features by satellite altimetry. The most important result was that the altimetry has revealed grounded regions beneath the ice shelf (Figure 3.6). These grounded areas can then be used as markers for variations in the ice shelf such as ice thickness, surface elevation and mass flux, velocity and shear rates. As the glaciers, ice streams, ice shelves and ice sheets respond to varying sea levels and climatic regimes, their interactions with grounded zones will vary. Attempting to more clearly identify the Lambert Glacier/Amery Ice Shelf grounding line and transition zone is the primary intention of this research and will be expanded on in the ensuing chapters.

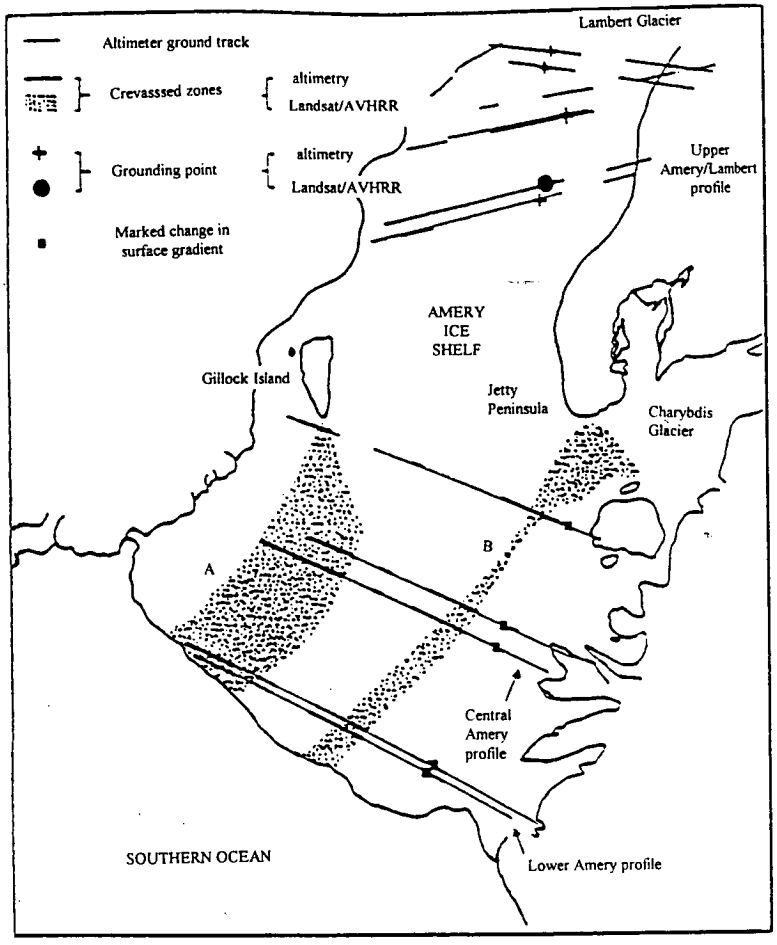

Figure 3.6. Map of the Amery Ice Shelf showing surface features positioned by satellite altimetry, together with features identified from imagery and ground survey (Budd *et al.*, 1982). From: Partington *et al.* (1987)

3.3 Other Ice Shelves

3.3.1 The Ross Ice Shelf

The Ross Ice Shelf is one of the largest ice shelves in Antarctica, encompassing an area of about 500 000 km^2. Laying between East and West Antarctica, the Ross Ice Shelf has the extensive TransAntarctic Mountains to its west, buffering the ice shelf from the store of the continental ice sheet. Numerous outlet glaciers flow through this mountain range onto the ice shelf. On the opposite side to the TransAntarctic Mountains, the main ice streams draining into this ice shelf originate from the central region of West Antarctica interior to the Siple Coast. Of these ice streams the major

Mountains, the main ice streams draining into this ice shelf originate from the central region of West Antarctica interior to the Siple Coast. Of these ice streams the major ones are Ice Stream A, B1, B2, C, D and E. Ice Stream F is a minor contributor to polar plateau drainage via the Ross Ice Shelf. Numerous studies have been undertaken to examine the nature of the Ross Ice Shelf and have been used here as the main comparison for discussing the dynamics of the Amery Ice Shelf. Ice Stream B appears to be most similar to the Lambert Glacier and is also examined more closely in this section.

A map drawn with 20 m contour intervals (Bentley *et al.*, 1979) reveals a detailed network of ice thickness patterns and dynamics on the Ross Ice Shelf. This reflects the complexities involved with this and any ice shelf. Important features identified across the Ross Ice Shelf were associated with the region around the grounding zone of the ice streams that flow into the ice shelf. Some of the features identified by Bentley *et al.* (1979) include regionally steep gradients of 10 m km^{-1} in free floating ice, the presence of highly contorted contours which are suggestive of large scale variability, and the existence of two distinctive step-like changes in the ice thickness. This and other results were used by Bentley *et al.* (1979) to suggest that the Ross Ice Shelf is not in a state of dynamic equilibrium and that the ice shelf may be prone to rapid changes in areas of transient dynamics across the ice shelf.

The delineation of flow bands across the ice shelf has shown a constant and regular flow from the main East Antarctic outlet glaciers to the calving front. Smaller mountain glaciers, at the same time, show distinct patterns of discontinuous flow banding which Bentley *et al.* (1979) suggest as an indication of a variable meso-climate in the vicinity of the Trans Antarctic mountain glaciers within the last 1000 years. The alpine-type glaciers of this area also show an out-of-phase behaviour in relation to the activity of the larger outlet glaciers and ice streams (Chinn, 1991). This is also apparent in the alpine-type glaciers of the Northern Prince Charles Mountains (Krebs, 1992).

Strong radio-echo sounding reflections nearer the ice front indicate the possibility of bottom melting of the Ross Ice Shelf saline ice; ice that has been previously frozen to the under-side of the shelf. Not necessarily coinciding with the behaviour of the ice self bottom, the visibility of rifts (or apparent rifts) show two distinct lateral bands of ice. The Ross Ice Shelf is not just a flat ice shelf. Bentley *et al.* (1979) found the

D) and with the outlet glaciers (Byrd and Nimrod Glaciers being the most important, the former being the largest in regards to ice flux).

The velocity of movement in the Ross Ice Shelf was examined by Jacobs *et al.* (1986) following the ice front advance between 1962-1985. The average velocity across a transect of the ice shelf was estimated at 840 ma^{-1}; lower velocities occurred on the eastern side of the Ross Island part of the ice shelf at an average 325 ma^{-1} and the maximum velocities were recorded around the central and western areas at 1040 ma^{-1}. West of longitude 178°E, the ice front was identified by Jacobs *et al.* (1986) to be at its most northerly extent in its observed 145 year history, with no major calving event for at least 75 years (this is on the western end of the ice shelf). The central ice front is currently at its most southern extent, but it has the most rapid advance rate for the ice shelf. This central zone is also a major calving area, specifically around the central ice front. The most notable recent calving occurred from the eastern part of the front with the iceberg labelled B9. In October of 1987 this iceberg, 154 × 35 km in size, calved away from the Ross Ice Shelf; its centre was then at 77°55' South 164°55' West. This major calving event allowed for the specific analysis of ocean currents as the course of B9 was tracked by Landsat imagery (Jacobs, 1992). Having a more complete knowledge of ice shelf mass balance requires an accurate understanding of calving rates and approximate volumes of mass output. The central area of the ice front is now known to overlay the warmest ocean currents that flow into the sub ice shelf cavity (Jacobs *et al.*, 1979; Pillsbury and Jacobs, 1985). This body of water is also warmer than the water which flows under the Filchner-Ronne Ice Shelf. With a basal melting rate near the ice front of the Ross Ice shelf of approximately 3 ma^{-1}, basal melting is almost equal to calving events in maintaining the ice shelf mass balance (Jacobs *et al.*, 1986).

The input of ice into the Ross Ice Shelf drainage basin has been estimated by Zotikov (1974) at 300 $km^3 a^{-1}$, at 327 $km^3 a^{-1}$ by Doake (1985) and by Bentley (1985) to be approximately 248 ±40 $km^3 a^{-1}$. The ice output has been estimated at 148 $km^3 a^{-1}$ (Jacobs *et al.*, 1986), 150 $km^3 a^{-1}$ (Doake, 1985) and 173 ±17 $km^3 a^{-1}$ (Bentley, 1985). At the ice front, the surface accumulation is about 0.25 ma^{-1}, with a thinning rate of approximately 0.35 ma^{-1} (Thomas *et al.*, 1984). Therefore Jacobs *et al.* (1986), using a thickness gradient of 4 m per kilometre, estimated the basal melting rate at 3.26 ma^{-1}. This compares to 0.6 ma^{-1} (Crary and Chapman, 1963) and 3.2 ma^{-1} (Kohnen, 1982). The location of Ross Ice Shelf front appears to have remained relatively stationary

(apart from the continual forward advance) due to the infrequency of major calving events. This has had the effect of increasing the role of basal melting as opposed to iceberg calving in the attrition of the ice shelf (Jacobs *et al.*, 1986). It is important to note that basal melting has the effect of weakening the ice, and as such, increasing its susceptibility to fracturing along pre-existing faults or crevasses. This can then influence the timing of calving events (Jacobs *et al.*, 1986). Jacobs *et al.* (1992) have also emphasised the importance of basal melt and refreezing processes in an ice shelf's mass budget.

During an 11 year period (January 1974 to December 1984) the grounding line of the Ross Ice Shelf appeared to have retreated approximately 300 m (Thomas *et al.*, 1988). This was concluded from measurements along an 8 km stake network extending from the ice sheet, across the grounding line, and on to the floating ice shelf (Figure 3.7). This retreat is caused by net thinning of the ice shelf. With less ice thickness, the ice shelf floats across a larger area. This means the grounding line retreats southward. A possible cause for thinning is due to the decrease in the discharge of Ice Stream C, which is slowly thickening upstream (Thomas *et al.*, 1988). One theory is that during active periods of the ice stream, the grounding line advances into "ice plains" (Thomas *et al.*, 1988). These ice plains eventually block the mouth of the ice stream, which can no longer push the lobes of ice out to sea. As such the ice stream begins to slow down its flow and grow thicker upstream. The fluctuation or alternation between advancing and retreating ice streams has direct implications on the dynamics of the ice shelf. Similar impacts on ice dynamics have arisen from the theory by Budd (1966) that drag between ice shelves and their sides or grounded ice rises has a major affect on ice streams flowing into ice shelves.

The term "ice plain" is the same as referring to a glacier ice shelf transition zone; the region where the glacier is changing its morphology from a continental ice stream to a floating ice shelf. The ice plain that separates Ice Stream B from the Ross Ice Shelf is 200km long (Alley and Whillans, 1991). The Lambert Glacier ice plain is believed to be longer than this and is discussed in the body of this research. For a sharp grounded to floating ice boundary it is thought that the transition zone typically extends no more than ten ice thicknesses long (Paterson, 1994). The ice streams of Siple Coast, however, are effectively zones of transition between inland ice and ice shelves because of the low surface slope, low basal shear and minimal vertical shear.

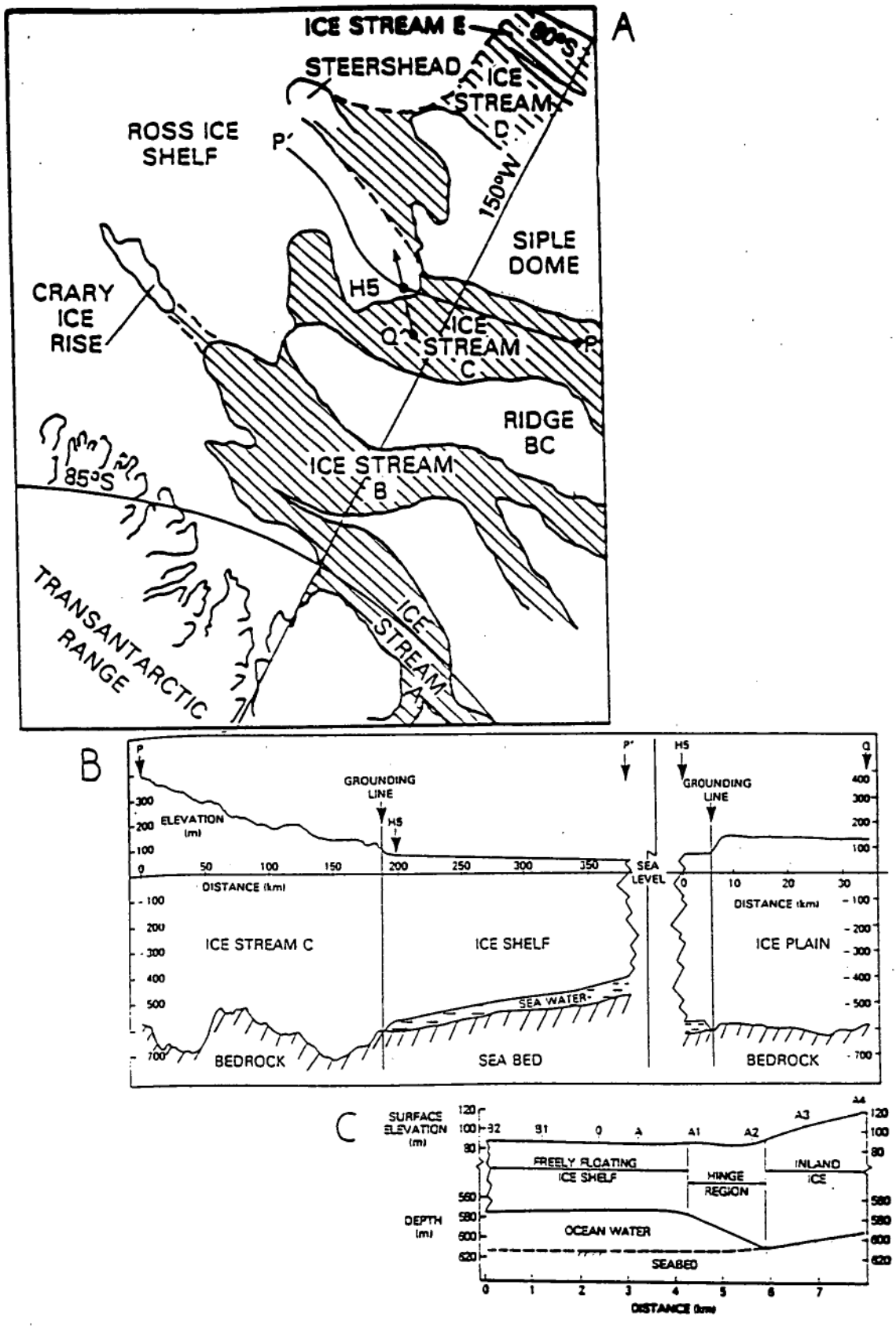

Figure 3.7 A- The Siple Coast showing ice streams A, B, C, D and E. The location of H-5, and the positions of ice thickness profiles, P to P' and H-5 to Q shown in figures B and C. From: Thomas *et al.* (1988)

3.3.2 Ice Shelves on the Eastern and Southern Weddell Sea

Fluctuation in the ice fronts of some of the major ice shelves along the eastern and southern Weddell Sea have been studied and are briefly outlined below. Figure 3.8 provides the location for some of the ice shelves discussed. The main ice shelves in this area are the Brunt, Riiser-Larsen, Ekström and Filchner-Ronne.

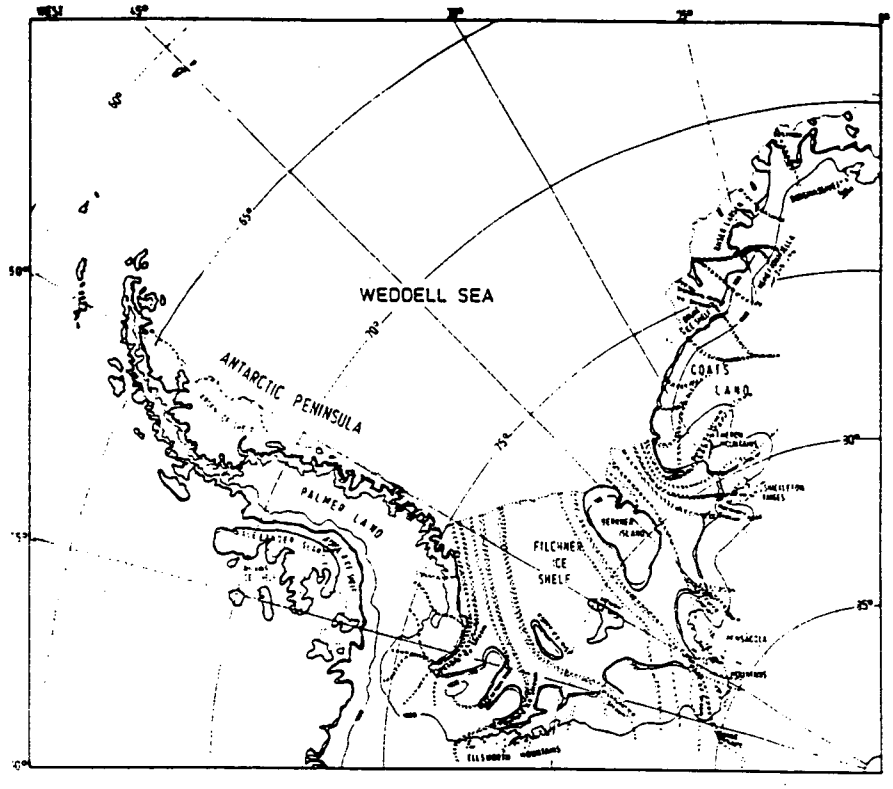

Figure 3.8. Schematic outline of major ice streams feeding the ice shelves in the eastern and southern Weddell Sea (after Hughes, 1977). Also shown is the 0m isobath and the 200 and 1000m elevations on the ice surface. From: Lange and Kohnen (1985)

Parts of the Brunt Ice Shelf have an apparently steady velocity at the ice front, of 2000 m a^{-1} (Lange and Thomas, 1985). On the western side of the ice shelf, near the Dawson-Lambton Ice Stream, the velocity is around 500 ma^{-1}. Along the eastern end, within the Stancomb-Wills Ice Stream, the velocity is about 1300 ma^{-1} (Simmons, 1986). By comparison, the more southern portion of the Riiser-Larsen Ice Shelf (between 73-74°S) has an apparent velocity rate of 1600 ma^{-1} (Lange and Thomas, 1985).

Further east again, lies the Ekström Ice Shelf. Most of this area is moving slowly at approximately 150 ma^{-1}, possibly by being close to an equilibrium between the supply and calving rate of the ice (Lange and Kohnen, 1985). With an average ice thickness of up to 900 m (Thyssen and Grosfeld, 1988), the edge of the Ekström Ice Shelf 27°W to 37°W (the Luitpold Coast region) has an almost equal supply and calving rate as the ice has a virtually uninhibited flow directly into the Weddell Sea.

The Filchner-Ronne Ice Shelf has two apparently different moving portions on either side of the large inlet at 42°W (Lange and Kohnen, 1985). The advance rate along the eastern reaches is of the order of 1000 to 1100 ma^{-1} and moving towards the north-east. Across the western side, the velocity calculated by Lange and Kohnen (1985) was estimated at 1200 ma^{-1} and moving to the north-west. Berkner Island separates these two flowing masses of ice. With an ice front velocity of 1050-1070 ma^{-1} and with a heading of 55°, Kohnen (1982) calculated a bottom melting rate for the Filchner-Ronne Ice shelf of approximately 3.2 ma^{-1} - this was at 20 km south-west of the ice front. The ice thickness is approximately 450 m around the central region (Thyssen, 1986; Lange and MacAyeal, 1986; Thyssen, 1988; Swithinbank *et al.*, 1988).

The Larsen Ice Shelf, on the eastern side of the Antarctic Peninsula, is the most northerly situated major ice shelf in Antarctica, and as such may be more sensitive than other ice streams and ice shelves in responding to global climate patterns. The ice shelf was studied by Ridley *et al.* (1989) using satellite altimetry data. This ice shelf incorporates 500 km of the Wilkes Coast. The eastern edge of the ice shelf has many separate grounding zones, such as the Gipps Ice Rise and Robertson Island. The overall ice surface is irregular and broken due to rifts, stagnant ice, undulations and glacier tongues. The northern ice shelf is typically low lying and generally not above 38 m asl; the central area ranges mostly between 30- 45 m asl (the total range is 80 m to less then 30 m asl at the ice edge).

Across the Riiser-Larsen Ice Shelf, the northern part of the ice shelf (between 72-73°S), until relatively recently, has been thought of as near equilibrium (Gjessing and Wold, 1981). Remote sensing interpretation has indicated to the contrary, with the recent and quite sudden deterioration of the Larsen Ice shelf, thought to be attributable to climatic warming (Vaughan and Lachlan-Cope, 1995). In January 1995, 4,200 km^2 of the Larsen Ice Shelf calved away (Rott *et al.*, 1996), and the ice shelf proceeded to steadily retreat beyond its critical limit until a new equilibrium was obtained. This trend

of major calving events and ice shelf re-equalising has also been noted across the entire Antarctic Peninsula (Vaughan and Doake, 1996) and with the Pine Island Bay (Jenkins *et al.*, 1994).

Along the ice edge of the eastern and southern Weddell Sea, the ice shelves fronts have advanced at a rate of between 3740 ma^{-1} (70°41'S 9°03'W) and 509 ma^{-1} (77°26'S 48°06'W) (Table 3.3). Velocities range from 150 ma^{-1} at the Ekström Ice Shelf to 1700 ma^{-1} plus along the Filchner-Ronne Ice Shelf (Table 3.4). There has been a general advance of all the West Antarctic ice shelves between 6° and 61°W since 1956, except the glaciated Luitpold Coast and northern Riiser-Larsen Ice Shelf which are near to their equilibrium (Lange and Kohnen, 1985). The most active is the Filchner-Ronne Ice Shelf. This might be a reflection of general behaviour which sees long ice shelves advance for many years before major calving events occur (Lange and Kohnen, 1985).

Location (Lat.S)	*(Long.W)*	*Period*	*Azimuth (degree)*	*Ice Advance (m)*	*Apparent ($m\ a^{-1}$)*
70°40'	9°03'	1983-84	329	3740	3740
73°25'	20°20'	1980-84	260	6480	1620
74°43'	24°48'	1983-84	271	5300	5300
77°46'	36°31'	1983-84	32	1230	1230
77°19'	40°40'	1980-84	26	4260	1065
77°42'	42°30'	1980-84	323	5093	1273
77°26'	48°06'	1980-84	49	2037	509
77°23'	48°30'	1980-84	42	3148	787
76°52'	51°08'	1980-84	58	4300	1075
76°49'	51°23'	1980-84	25	5186	1296
76°24'	52°24'	1980-84	57	5741	1435
75°35'	58°09'	1980-84	39	6945	1736
74°14'	59°39'	1980-84	47	5649	1412
74°54'	60°48'	1980-84	43	3704	926

Table 3.3. Apparent advance of ice edges and apparent advance rates in the eastern and southern Weddell Sea. From: Lange and Kohnen (1985)

Region	*Location*		*Velocity*	*Azimuth*	*Method*
	Lat.S	*Long.W*	*ma^{-1}*	*degree*	
Ekström Ice Shelf	70°36'	8°17'	150	10°27'	doppler satellite
	70°36'	8°21' (Neumayer St)	153	3°20'	
Brunt Ice Shelf	75°30'	26°40' (Halley St)	750	272°	doppler satellite
	74°25'	22°20'	1300	314°	astronomical
	75°10'	24°40'	1500	309°	
	75°30'	26°40' (Halley St)	272	272°	
	75°30'	26°40' (Halley St)	712-756 ?		ERTS-images
Filchner Ice Shelf	77°42'	38°04' (Belgrano St)	1400	27°	doppler satellite
	77°01'	50°08' (Filchner St)	1059	58°08'	doppler satellite
	77°44'	36°31' (Shackleton St)	1024	32°	doppler satellite
	77°59'	36°10' (Shackleton St)	1242	?	astronomical
	77°59'	38°44' (Belgrano St)	1460	?	
	77°39'	41°02' (Ellsworth St)	1762	?	
Filchner Ice Shelf	77°59'	37°10' (Shackleton St)	644	?	ERTS-images
	77°59'	38°44' (Belgrano St)	721	?	
	77°39'	41°02' (Ellsworth St)	1194	?	
	75°	60°	1224-1938		

Table 3.4. Quantitative estimates of the ice edge velocities in the eastern and southern Weddell Sea. From: Lange and Kohnen (1985)

Chapter Four

Morphology of the Lower Lambert Glacier and Amery Ice Shelf System.

4.1 Introduction

In this chapter the morphology of the lower Lambert Glacier and Amery Ice Shelf system is examined. Based on satellite image interpretation, the independent ice streams and flow lines that make the Lambert Glacier are identified. The study area encompasses the region from the Southern Prince Charles Mountains, south of the Lambert-Fisher Glacier confluence, through to the Amery Ice Shelf front. After establishing the sources of the ice that flows through the Lambert Glacier and Amery Ice Shelf system, ice thickness and surface elevation profiles were created. This has been done using data from Radio Echo Sounding (RES) surveys in 1988-1989 and 1989-1990. Five transverse profiles across the lower Lambert Glacier and Amery Ice Shelf and two longitudinal profiles have been created from the Radio Echo Sounding data, and form the basis for the discussion below. The transverse sections are titled Profile #1 to Profile #5 moving north and the longitudinal profiles are titled east or west pertaining to the side of the drainage system. Chapter Four also uses interpretation of satellite imagery and RES data to redefine the grounding zone of the world's fourth largest ice drainage system.

4.2 Ice Streams and Flow Lines

The flow lines of the lower Lambert Glacier and Amery Ice Shelf were derived totally from Landsat satellite imagery. Features identified on the Landsat multi Spectral Scanner (MSS) and Thematic Mapper (TM) images (Appendix A and Appendix B) were projected onto the polar stereo-graphic maps used here. The satellite images provided a very good basis for interpretation of the ice surface features. Where distinct flow lines were not visible, a continuous line was drawn in the same direction as the known orientation of the apparent ice flow lines. The poor quality of some of the satellite images has meant a loss of clarity in the details of the flow lines, and aerial photography would improve surface interpretations. However, only oblique aerial images are available for the lower reaches of the

grounding zone, and these are not very useful in mapping surface features. Hence the flow lines established can only be considered as a guide to the direction of flow unless confirmed by ice movement measurements.

4.2.1 Upper Amery/ Lower Lambert Glacier

Figure 4.1 is an illustration of the flow lines of the lower Lambert Glacier and Amery Ice Shelf around the area of the five profiles between 70°S and 72°S (Appendix C). From these interpreted flow lines, the Lambert Glacier ice stream between Profile #1 to #3 has an average width of 34 km. By Profile #4 the width of the Lambert Glacier ice stream has expanded 8 km to 42 km and this is maintained through Profile #5.

In the region of the lower Lambert Glacier and Amery Ice Shelf, the ice mass which is draining the hinterland meets with grounded ice draining from east and west of the system. Within this area, the close proximity of the Northern Prince Charles Mountains may also be influencing the behaviour of the ice. The broadening of the Lambert Glacier ice stream coincides with a transition from restricted to free-floating ice.

4.2.2 Confluence and Hinge Zone

Figure 4.2 has been derived from two Thematic Mapper images (AUSLIG, 1995) specifically processed to show the Mawson Escarpment. For the purposes of this study, they also provide valuable information regarding the geomorphology around the southern limits of the study area and the southern reaches of the Lambert Glacier grounding zone. The resolution of these images has enabled clear delineation of flow lines and surface features. Flow direction is towards the top of the page. Note that this illustration is not at the same scale as Figure 4.1. In order to more clearly discern the flow lines and their origins, a scale approximately twice that of the one used in the northern limits of the Lambert Glacier grounding zone has been used. The regional location map (Appendix C) will orientate the reader as to the location of Figure 4.2.

The dashed line in Figure 4.2 is a clearly identifiable topographic surface feature. In the Thematic Mapper (TM) image the feature appears as an apparent step in

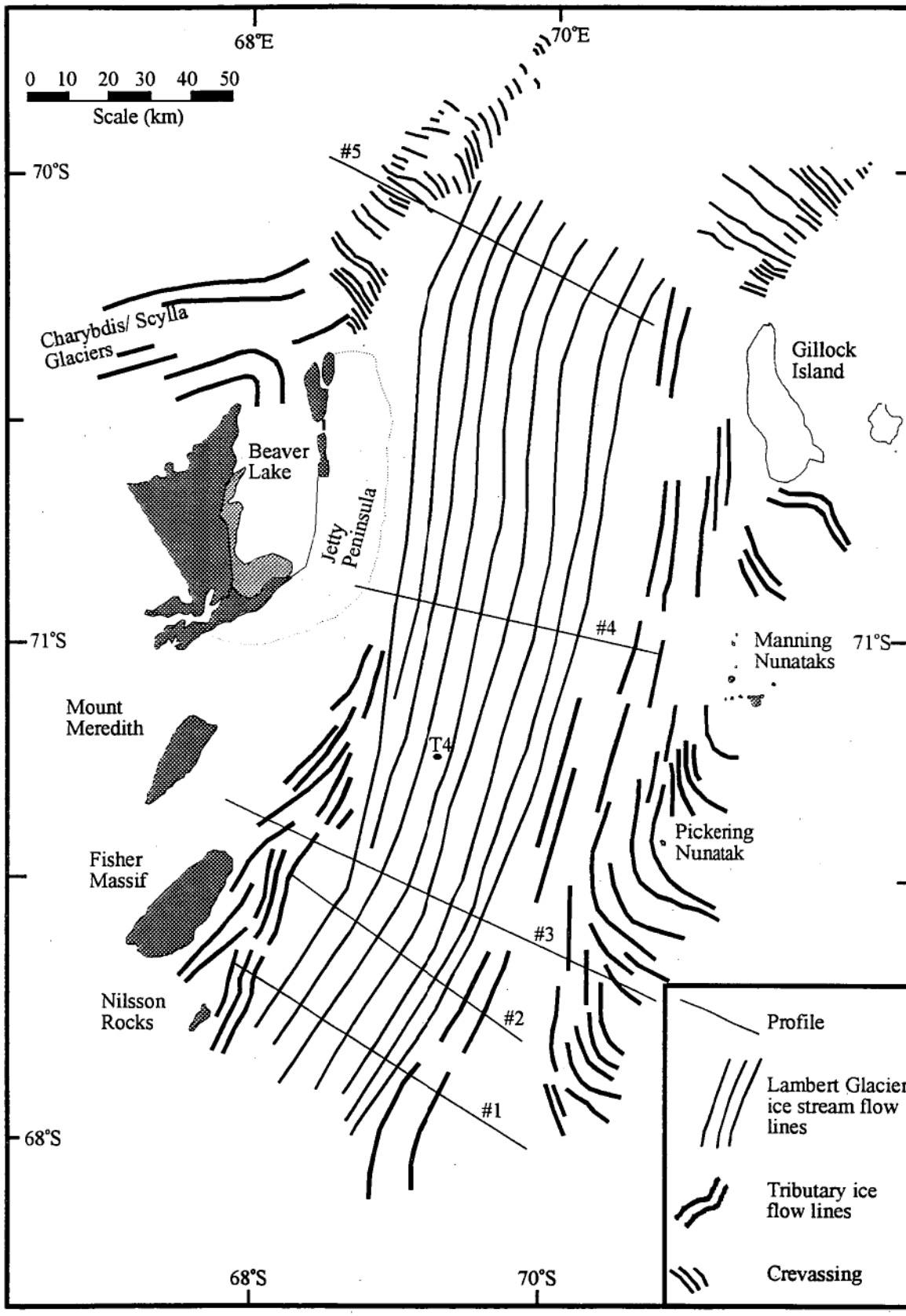

Figure 4.1. Flow lines for the lower Lambert Glacier and Amery Ice Shelf as interpreted from satellite imagery. Based on a polar stereographic projection.(see Appendix B).

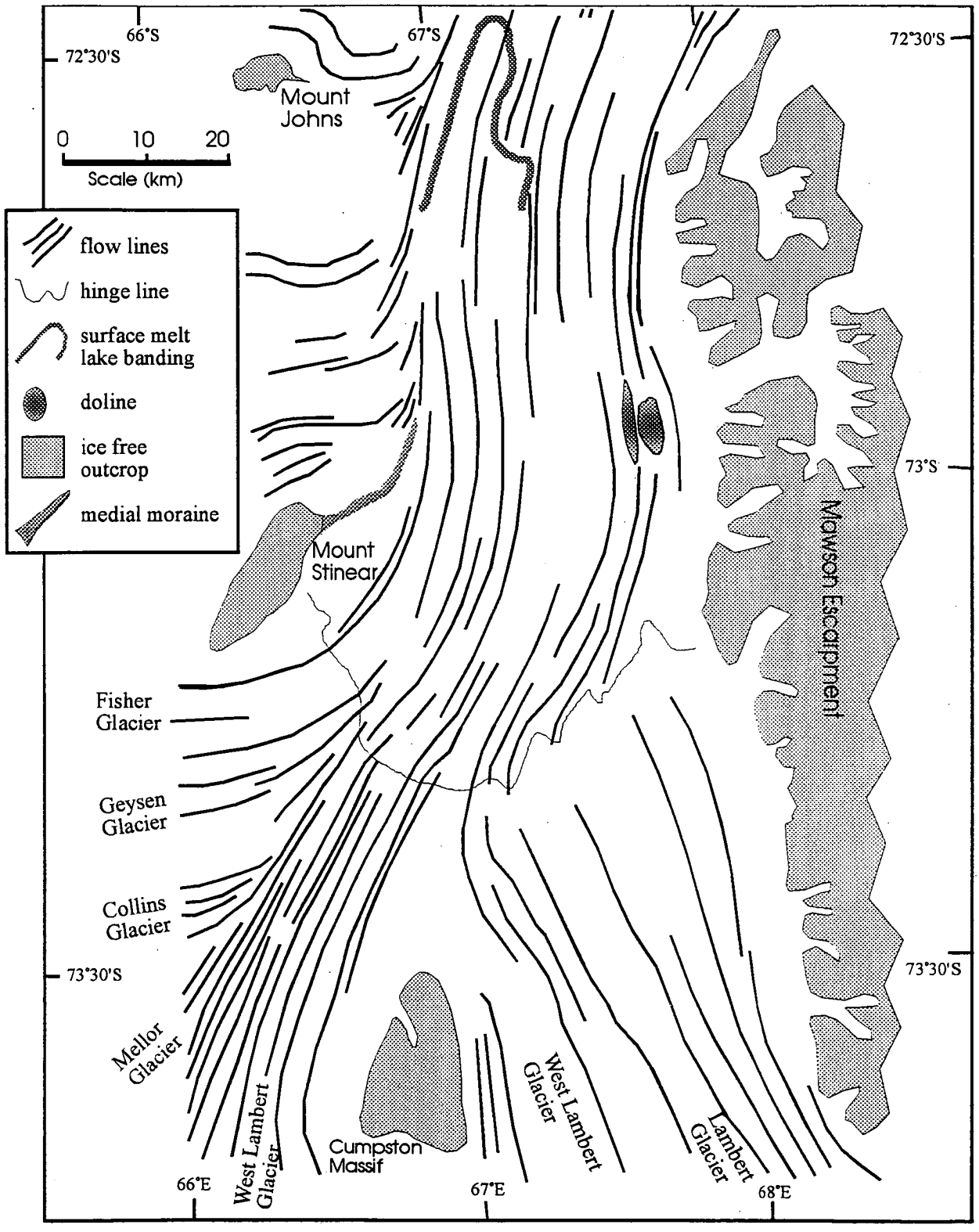

Figure 4.2. Flow lines derived from TM images for the southern limits of the Lambert Glacier grounding zone. Also illustrated is a band of melt lakes (double dashed lines), the hinge line (dashed line) of the Lambert Glacier drainage system and ice dolines. This area is also known as the 'convergence zone' of all the tributary glaciers into the Lambert Glacier system. (Polar stereographic projection.)

surface elevation. This coincides with a general region of rapid surface elevation change as discussed later in this Chapter. This feature, indicated by the dashed line, coincides with the location of the Lambert Glacier hinge line and hence the southern-most extent of the grounding zone, which is 255 km from T4. (T4 is a station from the work of Budd *et al.*, 1982, which partially defines the Lambert Glacier grounding zone) The hinge line is particularly evident in the eastern longitudinal profile that traces the flow of the Lambert Glacier ice stream in a southerly direction upstream and is discussed later.

Bentley (1987) located the Lambert Glacier grounding zone 180 km from T4, in an area characterised by a belt of surface melt lakes (the double dashed line in Figure 4.2). This surface feature is most noticeable on the western side of the Lambert Glacier drainage system, and can be observed in the western longitudinal profile discussed later. It was difficult to differentiate between the possibility of the grounding zone commencing 180 km from T4 (Bentley, 1987) or at a distance of 255 km as is clearly evident on the eastern side of the drainage system. This band of melt lakes also runs in the same direction as the flow lines of the Lambert Glacier.

The network of surface melt lakes, situated east of the Lambert Glacier and Amery Ice Shelf drainage systems centre line, appears in the satellite images to be a morphological 'dividing line' between Lambert Glacier ice and ice originating from the grounded ice to the east (Appendix A). The MSS images indicate, by tracing the path of the flow lines, that in the area of Clemence Massif grounded ice and ice that originates east of the Lambert Glacier tributary (south of Mawson Escarpment) flows in a manner identifiable with at least partial grounding and hence variable basal shear stresses. This occurs as the ice from Princess Elizabeth land enters the Lambert Glacier and Amery Ice Shelf system and into the northern limits of the Lambert Glacier grounding zone. This area of surface unconformity can be likened to Swithinbank's (1988) concept of 'ice rumples'.

Dolines are surface features that represent an area of slumping. This slumping is not restricted to glacial environments and is often found in other terrestrial environments such as karst regions. Slumping occurs where the topography beneath the slump is a hollow or water filled depression and unable to support the weight of the overlying material, in this case the glacier. Mellor and McKinnon (1960) suggested that in the case of glaciated terrains, ice dolines are caused by meltwater drainage into zones of weakness due to crevassing. There are dolines in the

between the band of surface melt lakes and the Lambert Glacier hinge line west of the Mawson Escarpment: these are features of outlet glaciers that typically exist primarily on floating ice. These ice doline surface features appear to be in an area of apparent surface snow net accumulation as interpreted from satellite imagery; the TM image from March 1995 (Appendix A) shows a summer snowline interpreted here as the Lambert Glacier's equilibrium line. This 'surface accumulation' zone is used to differentiate between an area of deposition/redeposition and 'blue ice'. West of the central melt lake band, and south of the melt streams opposite Mount Johns, the ice surface is 'blue ice' ablation zone. North and east of the surface melt lake band the appearance of the glacier surface suggests accumulation. It is this author's opinion that any accumulation in this region is most likely redeposition of snow rather than new snow deposition. Surface mass balance on the Lambert Glacier and Amery Ice Shelf system is illustrated in Chapter Five.

4.2.3 Tributary Ice Streams

The tributary glaciers of the Lambert Glacier are (from west to east) the Fisher Glacier, the Geysen Glacier, the Collins Glacier, the Mellor Glacier, the West Lambert Glacier and the Lambert Glacier. Although the West Lambert Glacier can be interpreted as of separate origin to the Lambert Glacier, recent results from the Lambert Glacier Basin Traverse (LGBT) suggest they are parts of the same stream (I. Allison, pers. comm., 1995). The two branches of the West Lambert Glacier diverge around Cumpston Massif before entering the confluence zone. Figure 4.3 shows the contribution of the six tributary glaciers to the Lambert Glacier ice stream.

Through the identification of the tributary ice streams it has been possible to continue the work done by Allison (1979) in the southern reaches of the Southern Prince Charles Mountains. Allison established ice movement stations and was able to estimate the mass flux of the ice moving through his defined Lambert Glacier boundary. These results are referred to in this study as A.79. In conjunction with the work done by Higham (1994) and Allison (1979) this research has been able to identify specific information on the morphology and dynamics of the Lambert Glacier and Amery Ice Shelf between these two areas of work and link it with the work of Budd *et al.* (1982) near the Amery Ice Shelf calving front. These results are discussed in conjunction with the mass flux and mass budget of the Lambert Glacier in Chapter Five.

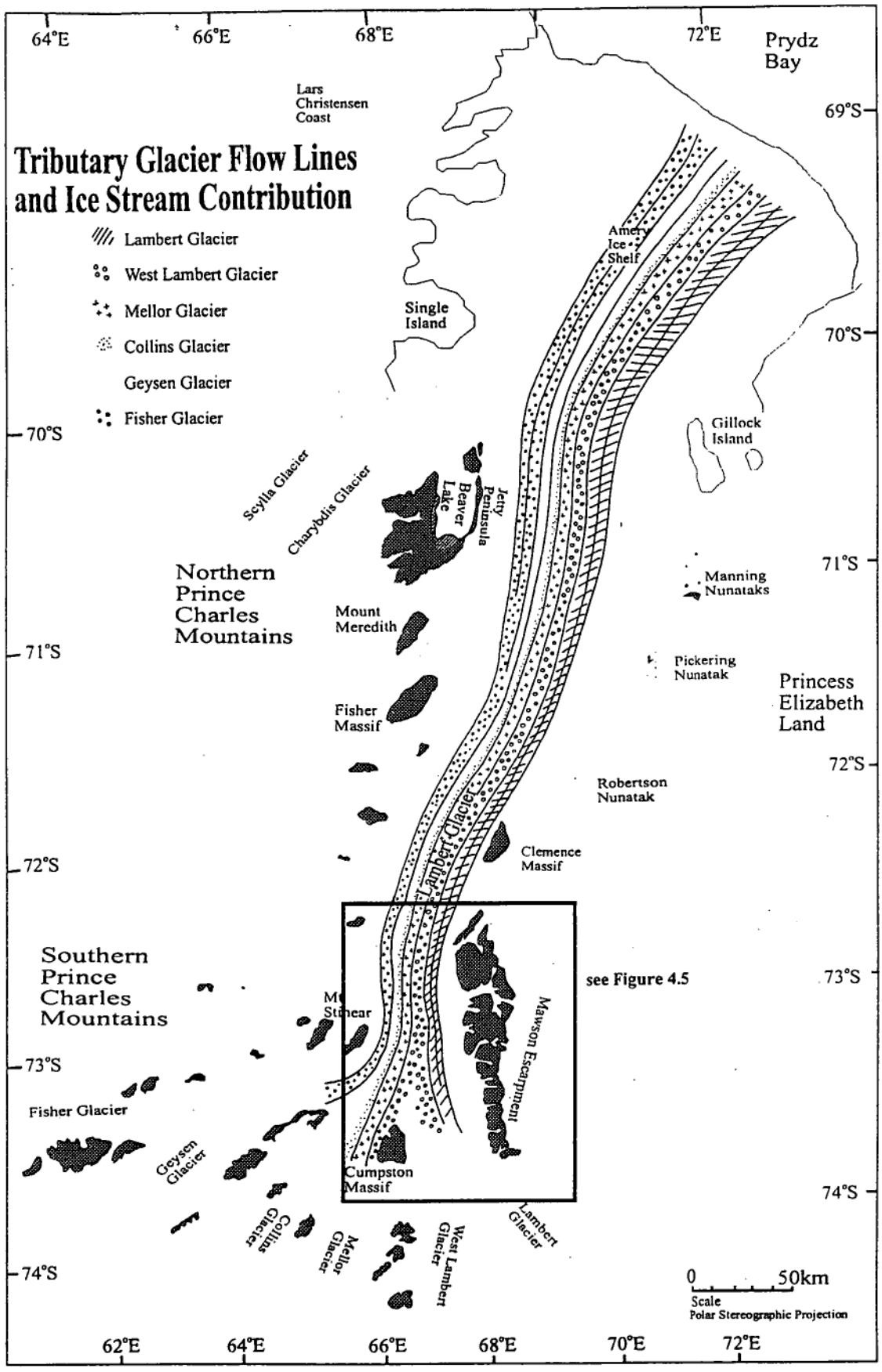

Figure 4.3. **The lower Lambert Glacier tributary flow lines and tributary ice streams identified. Figure 4.5 is an enlarged view of the confluence area as inferred from satellite images interpretation.**

4.2.4 Lower Lambert Glacier Flow Lines

Landsat Multi-Spectral Scanner and Thematic Mapper images of the Lambert Glacier and Amery Ice Shelf (Appendix B) have been interpreted to establish an image of the surface ice flow lines (Figure 4.4). The ice that is attributable to the six tributary glaciers has been identified and illustrated in Figure 4.5. The hatched flow lines represent the Mellor and Lambert ice streams and were used in the analysis of the Lambert Glacier stream dynamics. The West Lambert Glacier was included as part of the Lambert ice stream in this work.

The Lambert Glacier merges to a single ice stream at the confluence region (Figure 4.3) between Mawson Escarpment (east) and Mount Stinear (west). Prior to this, the tributary glaciers flow through the Southern Prince Charles Mountains. At 73° South the ice stream is approximately 25 km wide (Figure 4.4). Flowing north, the Lambert Glacier ice stream predominantly occupies the eastern side of the drainage system. By Profile #1 the total Lambert Glacier is 37 km wide, 40% of this width originating from the upstream Lambert and West Lambert Glaciers, 20% from the Mellor Glacier, 7% the Collins Glacier and 17% from each of the Geysen and Fisher Glaciers.

Across Profile #3, between Mount Meredith and the eastern grounded ice sheet, the Lambert Glacier is 35 km wide. Despite a slight decrease in ice stream width percentage contribution from each of the tributary ice streams remains constant. Seventy kilometres north, at Profile #4, the ice stream is 45 km wide. The Lambert and West Lambert Glaciers contribute 42% to the overall ice stream width; the Mellor 16%; the Collins 7%; the Geysen Glacier 18%; and the Fisher Glacier 18%. By Profile #5 the Lambert Glacier is 54 km wide. The Lambert and West Lambert Glacier contribute 44%, Mellor 15%, Collins 6%, Geysen 15% and Fisher Glacier 20%. Throughout the five main transects of the study, the percentage contribution from all the tributary glaciers to the width of the total system remains approximately constant. Near G1, the Lambert Glacier ice stream within the Amery Ice Shelf is approximately 66 km wide.

In the vicinity of Profile #5 the Lambert Glacier veers noticeably to the east. This bend in the flow coincides with the grounded point 20 km east of Single Island (discussed later in this chapter). This grounded zone appears to divert the direction of flow. This is evident in the change of direction evident in the surface features of this region. In this area the Scylla and Charybdis Glaciers, which drain the

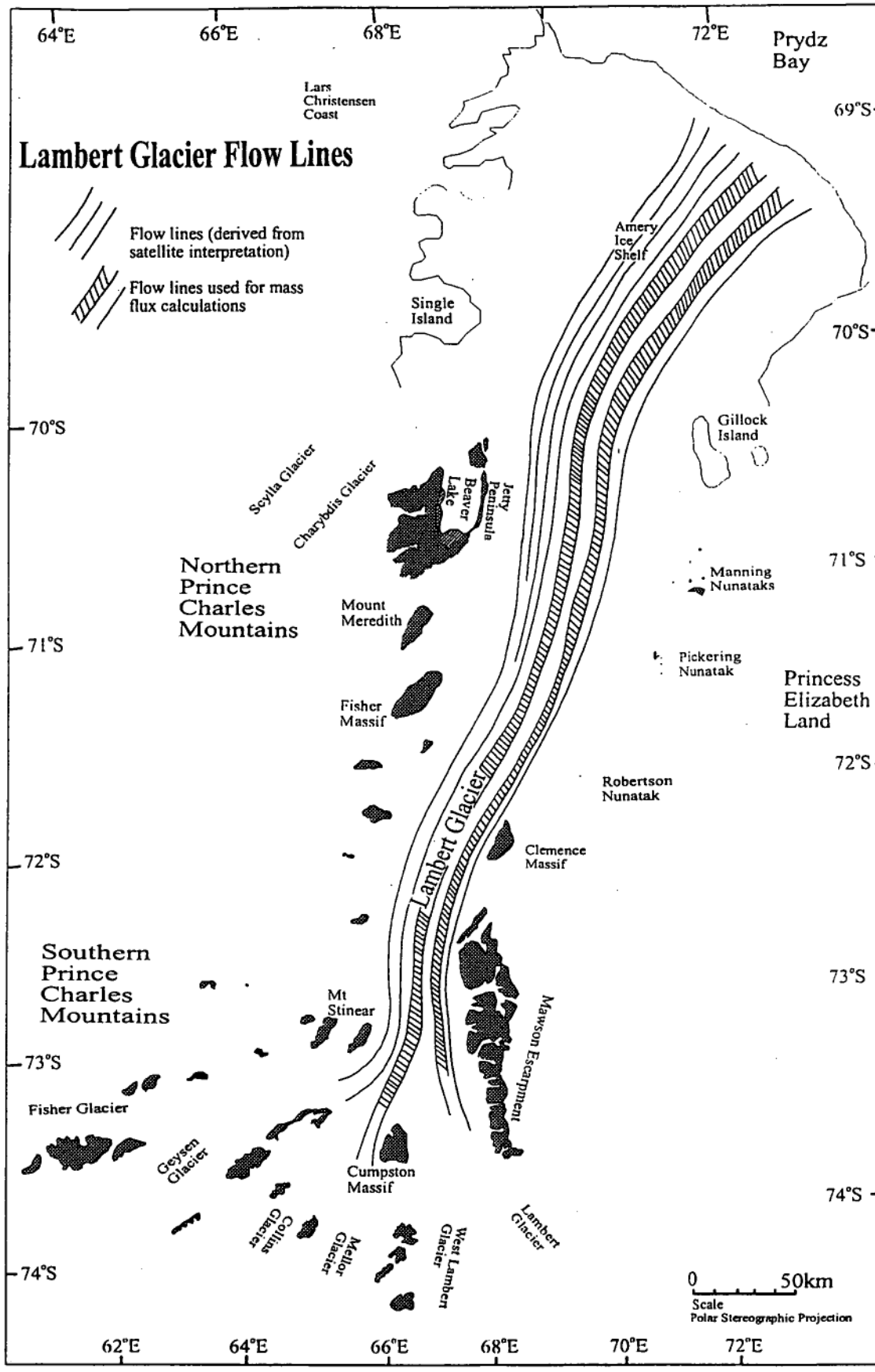

Figure 4.4 The lower Lambert Glacier flow lines derived from satellite image interpretation(TM and MSS). The hatched lines are within the Mellor and Lambert ice streams. It is this area that is the basis for ice dynamics calculations discussed in Chapters Five and Six.

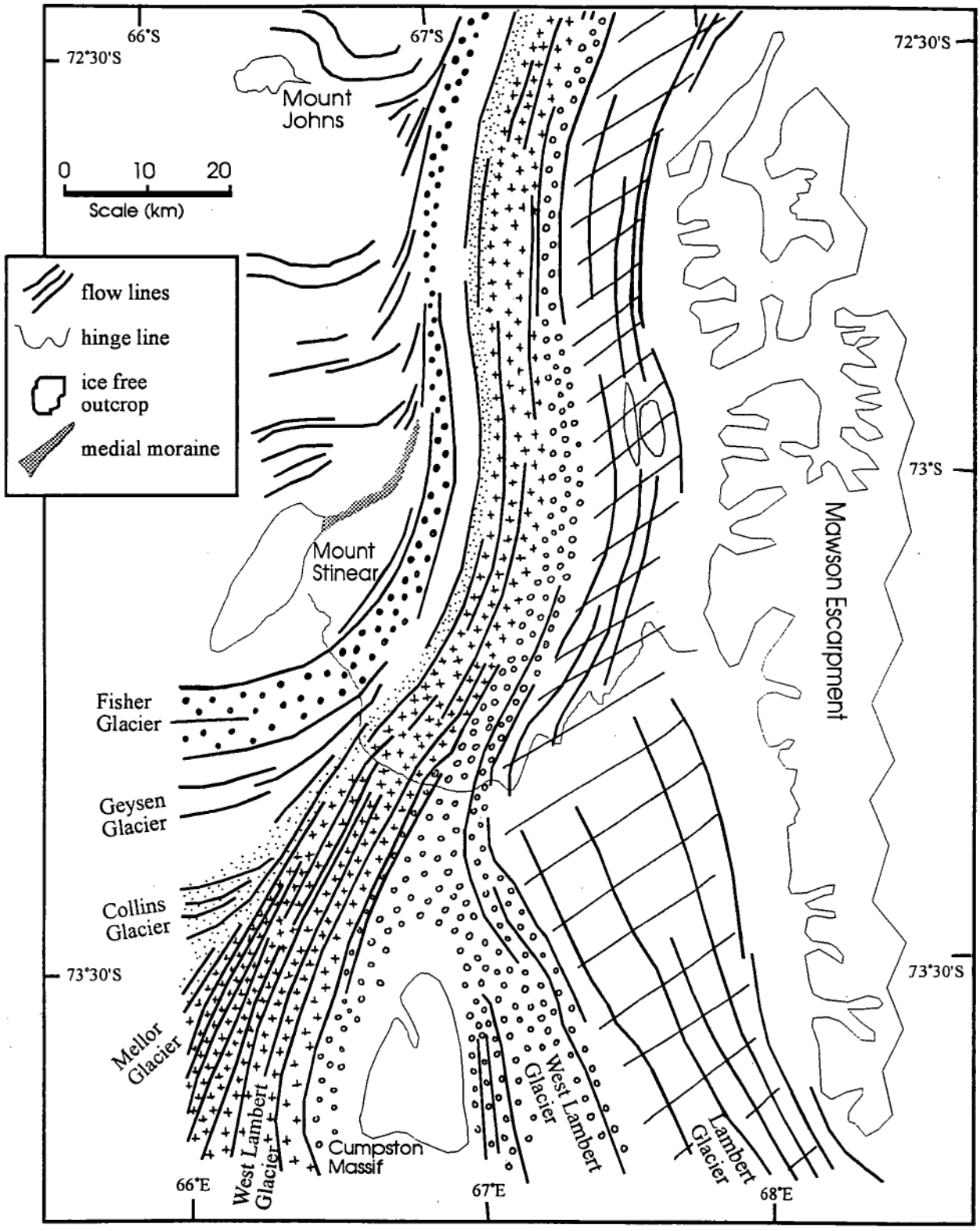

Figure 4.5. An enlarged view of the confluence region of the Lambert Glacier in Figure 4.3. The patterns used here to differentiate the tributary ice streams are the same as Figure 4.3. The Lambert Glacier constitutes 40% of the ice stream area north of the confluence, the Mellor 20%, Collins 7% and both the Geysen and Fisher Glaciers contribute 17% towards the Lambert Glacier ice stream.

grounded ice from the west through the Northern Prince Charles Mountains, also converge with the Lambert Glacier.

The location of ice surface features apparent in Appendix A, has been used as a basis for discerning the tributary glacier flow lines. As discussed earlier, two dolines on the Lambert Glacier are the type of glacial feature that are often associated with floating ice. Bands of surface melt lakes coincide with two major ice characteristics. The flow line between the Mellor Glacier and West Lambert Glacier corresponds with a melt lake band. Another band of melt lakes exists on the flow line boundary between the Fisher Glacier and western tributary ice. These areas of surface melt lakes exist east of Mount Johns and extend over the Fisher, Geysen, Collins and Mellor Glaciers. Surface melt lakes are believed to be the result of basal disturbances and can indicate zones of grounded ice within predominantly floating bodies of ice (Sharp, 1988). The pattern of surface melt lakes has features in common with ice thickness; this will be discussed further below. The location of these surface melt lakes is approximately 180 km from T4 and may have been used by Bentley (1987) in his definition by satellite interpretation of the Lambert Glacier grounding zone.

From figures in Appendix A and referred to in Appendix B, stagnant ice on the periphery of the Lambert Glacier is clearly visible. The eastern side of the Lambert Glacier ice is flowing at a slower rate than the rest of the ice mass. This differentiation is apparent when viewing the alpine-type glaciers on Mawson Escarpment. Terminal moraines are clearly visible on Lambert Glacier ice. This ice must not be flowing at any rate comparable to the main body if these small moraines are still intact. Based on the work of Krebs (1992) on the alpine-type glaciers of the Northern Prince Charles Mountains, these alpine-type glaciers would now be at their maximum extent and retreating. Time series observations of the terminal moraine disruption would indicate the flow rate of the lateral Lambert Glacier in this area.

Appendix A also shows the heavily crevassed zone and apparent marked elevation change discussed earlier as the Lambert Glacier hinge line. In Figure 4.2 the hinge line is marked as a single dashed line. The radio echo sounding data collected in this area is poor in quality due to crevassing. The calculations discussed in Chapter Five show this hinge line to be a significant boundary in the Lambert Glacier drainage system. South of this line the ice is grounded but flowing with some basal sliding probably due to the presence of a thin sheet of subglacial water and/or till.

4.3 Ice Thickness and Surface Elevation

Budd *et al.* (1982) estimated that the point where the Lambert Glacier reached hydrostatic equilibrium was "about 3 km south of T4 where a maximum in the surface slope occurs" (p 38). This was based on a longitudinal ice thickness profile interpreted by Budd *et al.* T4 is situated at 71°13' South 69°28' East at approximately the 100 m surface elevation. As revealed in the discussion later in the chapter, the northern limit (seaward extent) of the Lambert Glacier grounding zone is proposed to be further south of T4. What follows below is this author's interpretation of the 1988-89 and 1989-90 RES data that has contributed to the redefinition of the Lambert Glacier grounding zone.

A total of twenty aerial sorties carrying RES equipment have provided over 5000 km of ice thickness data. These flights have provided data over three general regions: the Scylla and Charybdis Glaciers of the Northern Prince Charles Mountains (Figure 4.6); the region about the lower reaches of the Lambert Glacier (Figure 4.7); and a wider regional survey which includes the seaward edge of the Amery Ice Shelf between the Australian Antarctic stations of Mawson and Davis and the Lambert Glacier stream south into the Southern Prince Charles Mountains to the tributaries and confluence area (Figure 4.8).

Ice thickness measurements were made with the Australian National Antarctic Research Expeditions (ANARE) 100 MHz radio echo sounding radar. This instrument has a resolution of 10 m. Bottom echo was not always obtained especially over areas of heavy crevassing where much of the radar energy was scattered. Where ice thickness data were missing from this data series, further information pertaining to the depth of the ice was estimated from the work of Thost *et al.* (1995) and Pozdeev (1991).

The region under study is primarily located between 70 to 72°S, 68 to 72°E (Figure 4.9). Within this area five sections across the lower Lambert Glacier and Amery Ice Shelf system have been derived from the RES data. This data series was collected between the austral summers of 1988-89 and 1989-90. The cross sections were used to distinguish the Lambert Glacier ice stream from the grounded ice sheet to the east and west. Two longitudinal profiles along the eastern and western sides of the Lambert Glacier and Amery Ice Shelf to 74°S, and a sixth transect through the Southern Prince Charles Mountains were also studied

in the region. The area between 72°S and 69°30'S includes that portion of the Lambert Glacier system which separates floating and grounded ice.

The horizontal position, and therefore the accuracy of all the RES flights is dependent on navigational precision. The 1988-1989 flights in the area of the Amery Ice Shelf used pseudo-range GPS (with 'selective availability' disabled) although because of a limited GPS satellite constellation, GPS navigation was not always available. This, on average, provided accuracy to within 30 m, with data being recorded manually every minute. Some of these flights (eg. travel between Mawson and Davis, incorporating flights across the northern edge of the Amery Ice Shelf) were navigated from a combination of 'dead reckoning', identifying geomorphological features located on MSS images coupled with some GPS data. This provided an accuracy measure, in the horizontal, from a few hundred metres to a kilometre. These data were logged manually at 1-2 minute intervals. All 1989-1990 RES flights had GPS logged automatically every 10 seconds ('selective availability' activated) with an accuracy in horizontal positioning in the order of 100 m.

One flight, Flight 03 1988-89, covered longitudinal sections along the western and eastern sides of the Lambert Glacier stream. The longitudinal profiles cover an area from 70°20' South 71°5' East to 73°53' South 67°32' East over a distance of 440 km (Appendix C). Because the limited GPS satellite constellations available at the time, navigation was done by a combination of dead reckoning and with reference to visible features, including surface ice features identifiable on Landsat imagery. The flight followed the flow lines of the eastern limits of the Lambert Glacier ice stream commencing 165 km from the Amery Ice Shelf calving front to 605 km south and up the Lambert Glacier. The most northern reach of the profile begins 20 km south of G2 70°10' South 70°52' East (Budd *et al.*, 1982). The transect never got closer than 5 km to Mawson Escarpment.

A second longitudinal profile along the western side of the system has been derived from the data collected from the return path of Flight 03 in 1988-1989. This transect travels downstream along the Lambert Glacier. Starting at 73°12'S 66°14'E this profile begins by transecting the Fisher Glacier, a major tributary into the Lambert Glacier and Amery Ice Shelf system. The profile is 300 km in length and for the purposes of this study, discussion of the profile concludes where the transect begins to rise onto Jetty Peninsula at 70°49'S 68°33'E.

It has been necessary in this study to interpolate surface elevation. During many of

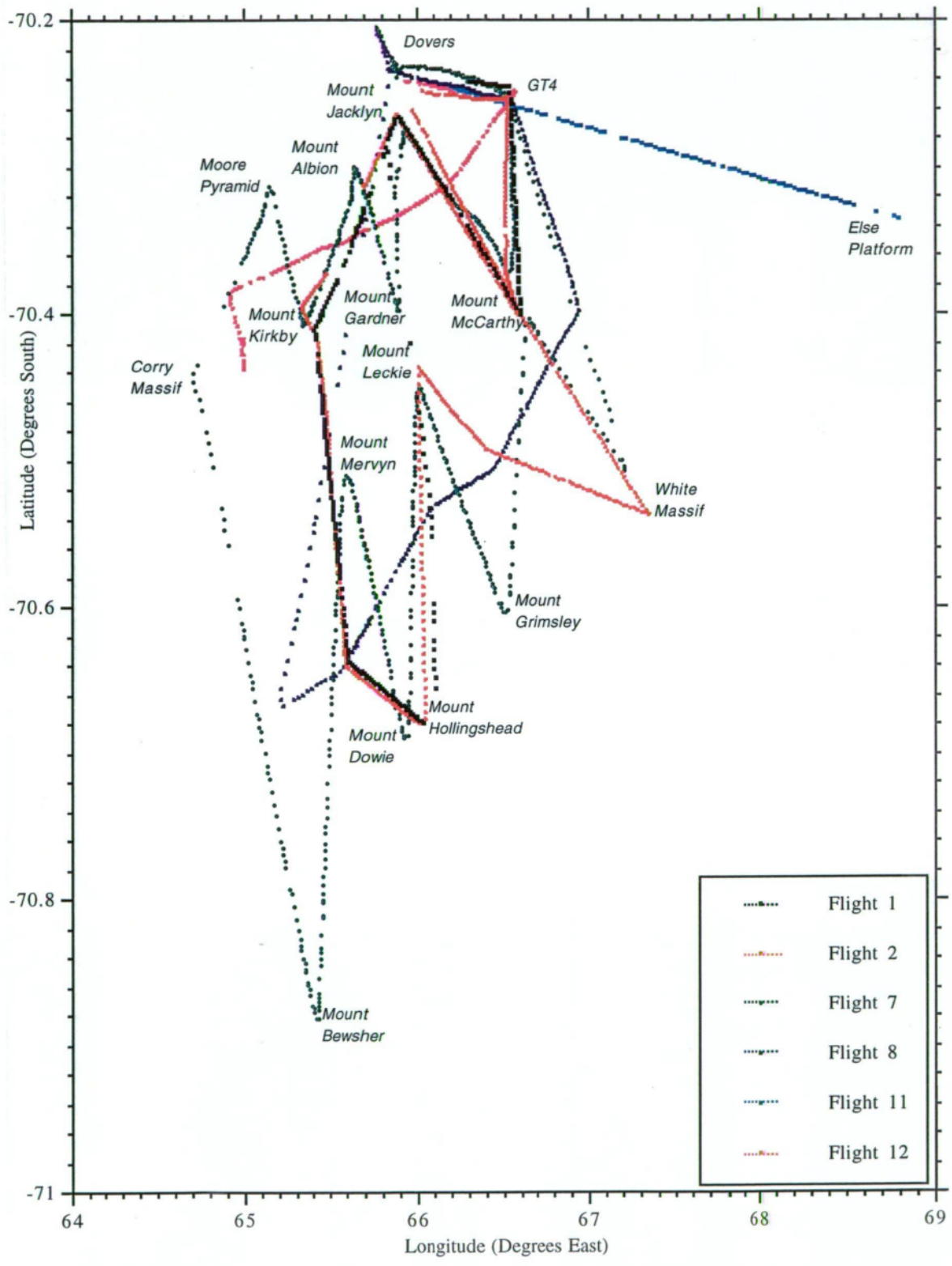

Figure 4.6. Schematic representation of Radio Echo Sounding flights over the Northern Prince Charles Mountain. This schematic map is plotted at a rectangular latitude/longitude projection.

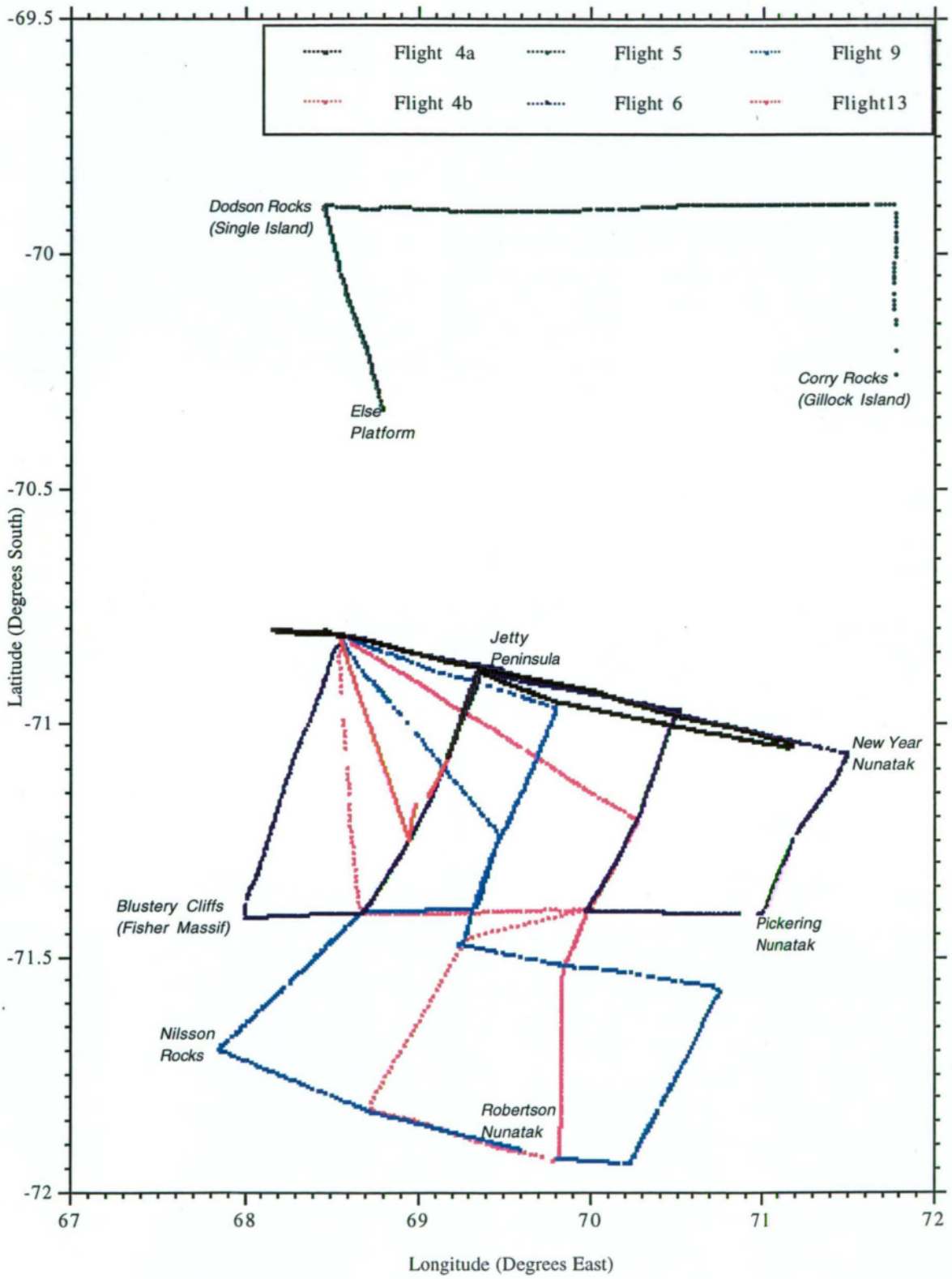

Figure 4.7. Schematic representation of Radio Echo Sounding flights from 1989 -1990 in the lower Lambert Glacier and Amery Ice Shelf region.

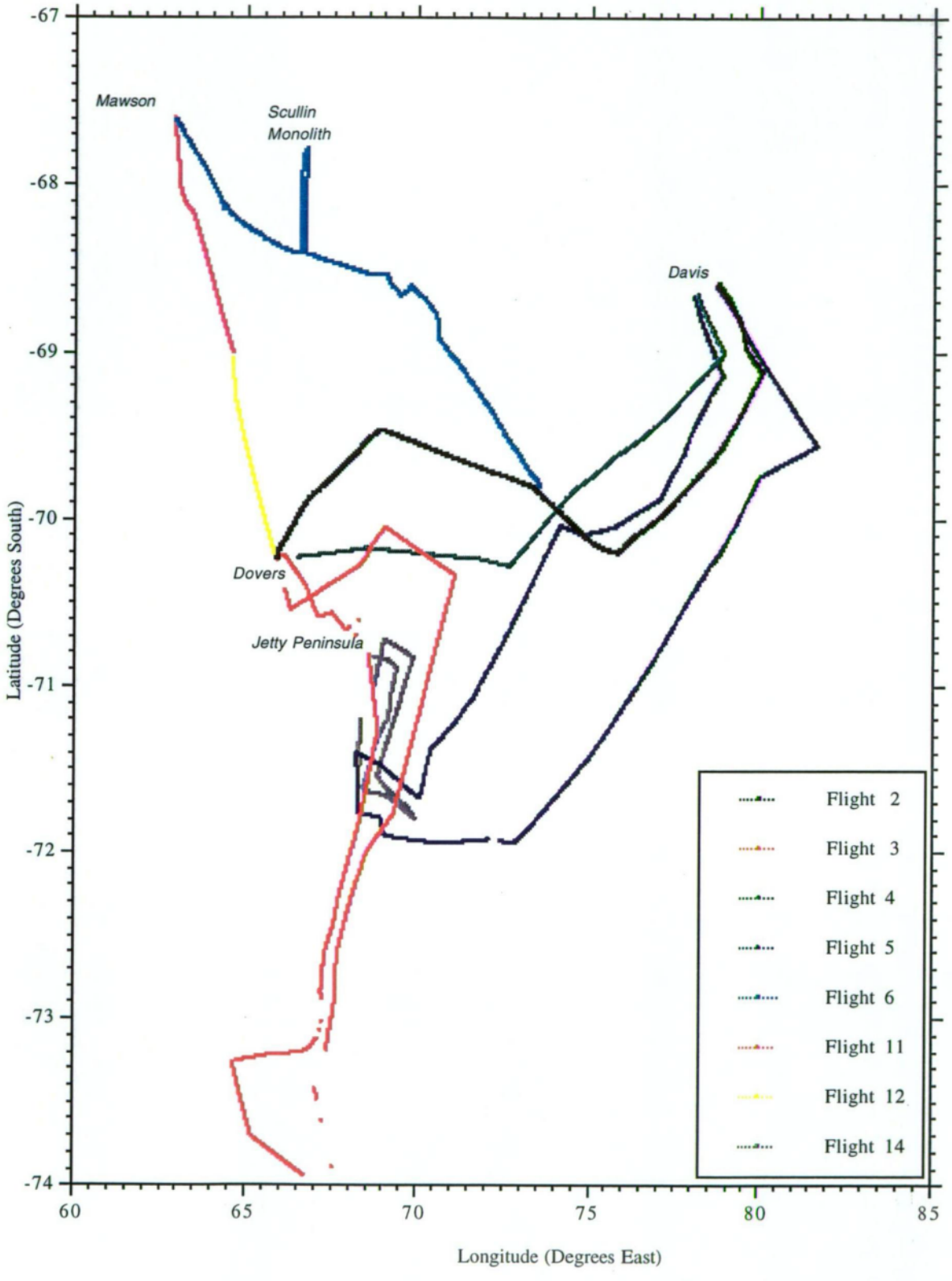

Figure 4.8. Schematic representation of 1988-1989 Radio Echo Sounding flights between the Australian bases Mawson and Davis (across the northern edge of the Amery Ice Shelf) and along the Lambert Glacier to 74^{o} South.

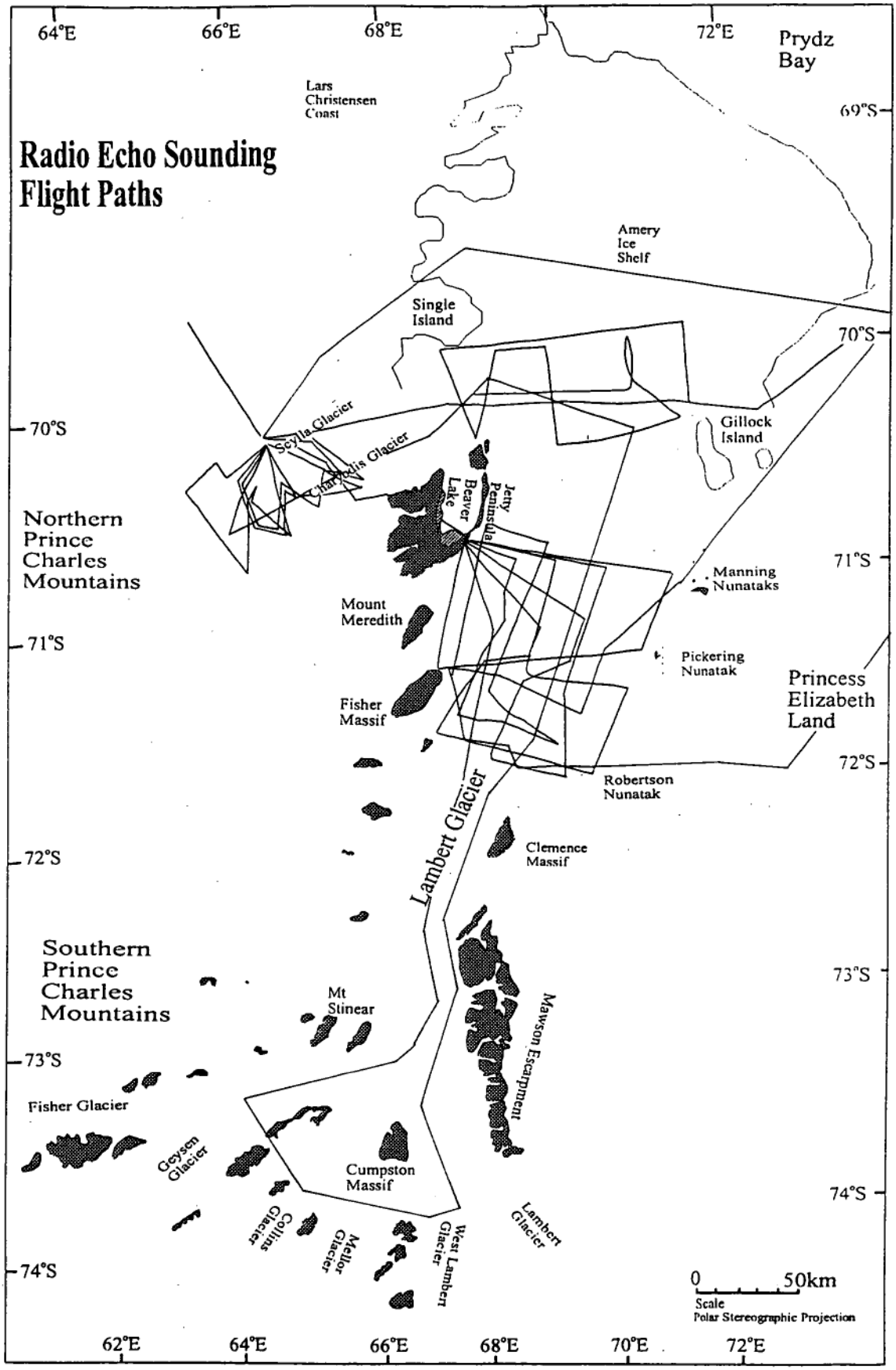

Figure 4.9. **This map is an illustration of the radio echo sounding surveys conducted during 1988-89 and 1989-90 (by the Australian National Antarctic Research Expeditions - ANARE) that have provided the basis for this study on the morphology and dynamics of the lower Lambert Glacier and Amery Ice Shelf system. Figures 4.6, 4.7 and 4.8 are specific flight maps that identify each flight path in more detail.**

the flights the aircraft-surface distance can be obtained from the radar data, but because the barometric altimeter failed, aircraft height and hence surface elevation cannot be obtained directly. Instead, the flight lines were superimposed on Russian 1:200,000 topographic maps derived from photogrammetry and some Australian ground survey points (1968-1969 optical levelling and 1988-1990 GPS). Over the Amery Ice Shelf, surface elevations were derived from the radar data, assuming that the aircraft flew a straight elevation path between overflights of successive known ground points. Because of the sparsity of ground-truthed surface elevation points and the unknown control for the Russian photogrammetry, the error in elevation data presented in the figures is estimated at ±20 m or more.

Surface characteristics of the Lambert Glacier, as with any other polar glacier or ice stream, are a reflection of basal topography, ice dynamics and ice type. As will be discussed below, the Lambert Glacier in part of the study area, shows a marked narrowing downstream coinciding with a reduction in ice velocity and basal shear. This is being used to suggest that portions of the ice mass are grounded. The majority of the ice mass within the study area is, however, predominantly floating ice.

Smoothed profiles of ice thickness have been obtained from the Radio Echo Sounding data with spot elevations extrapolated from Russian maps and Australian spot data points (Appendix B). Surface elevations from these sources were used to check against the RES data that was collected from the two airborne platforms (a DeHavilland Twin Otter fixed-wing aircraft and an Aerospatiale Squirrel helicopter) at different intervals over the two austral summers. As discussed above, the error in surface elevation is ±20 m where no spot elevation is known.

In the following discussion, all directions are based on true north. Unless otherwise stated, distances cited in relation to the profiles are measured from west to east across the ice. All elevations are measured with reference to the mean sea level, or geoid. There is, however, some uncertainty in the reference geoid and sea level in this region (W. Budd pers. comm. 1996).

4.3.1 Longitudinal Profiles of the Lambert Glacier into the region of the Grounding Zone

Figure 4.10 begins just south of the most easterly measurement of Profile #5. Distances are relative to T4, and positive to the south. At T4, the surface elevation

from the RES data is 55 m asl. Between T4 and where the transect crosses Profile #4 (40 km north of T4) the surface elevation rises to 61 m asl. This equates to a 1 metre rise in surface elevation every 13 km. From Profile #4 to a line perpendicular across the Amery Ice Shelf at T4 (Budd *et al.*, 1982), the surface slope remains at 1 m per 13 km.

From Profile #4 to Profile #3 the surface elevation rises 5 m in 65 km (1 m in 13 km or 7.7×10^{-5}). Between Profile #3 and Profile #2 there is a change in slope and surface elevation rises 66 m asl to 82 m asl over 19 km (8.3×10^{-4}). The surface elevation rises further to 94 m asl along the 24 km separating Profile #2 and Profile #1 (1 m in 2 km or 5×10^{-4}). The ice surface then levels to a gradient of 1 metre rise over each 4.5 km for the next 55 km (2.2×10^{-5}).

One hundred and fifty kilometres upstream, west of the northern tip of Mawson Escarpment, the surface height is 126 m asl (72°27' S 67°51' E). Between this point and Profile #1 there is a 32 m increase in elevation over 80 kilometres (1 m in 2.5 km or 4×10^{-4}). Bentley (1987) proposed that the grounding zone of the Lambert Glacier was located 180 km south of T4. The gradient of the surface slope between T4 and Bentley's site is 1 m rise per 20 km. Between 180 kilometres and 230 km along the profile, the surface elevation increases more steeply with a further 46 m rise (equating to 1 m in 1.1 km or 9.2×10^{-4}).

Over a distance of 30 km, between 230 km and 260 km, the surface elevation rises 226 metres (1 m in 0.12 km or 7.5×10^{-3}). This is a gradient of nearly one metre rise in surface height for every one hundred and twenty horizontal metres. The remaining 54 km of the profile rises to 940 m asl (1×10^{-2}). The last 80 km of the transect is across the grounded ice of the Lambert Glacier. The elevation at the southern reaches of the grounding zone is 380 m asl. This steep elevation rise begins at approximately 250 km from T4.

Ice thickness for this eastern-side longitudinal profile (Figure 4.10a) is considered to have an inaccuracy in its measurements in the order of ±20 metres. The radio echo sounding data that has been used showed excellent return pulses up until 220 km along the profile where heavy surface crevassing contributed to the loss of signal. From 120 km north of T4 to Profile #4, a distance of 80 km, the ice thickness ranged from 716 m to 814 m. Both the surface elevation and ice thickness generally increase uniformly along this section. A minimum ice thickness

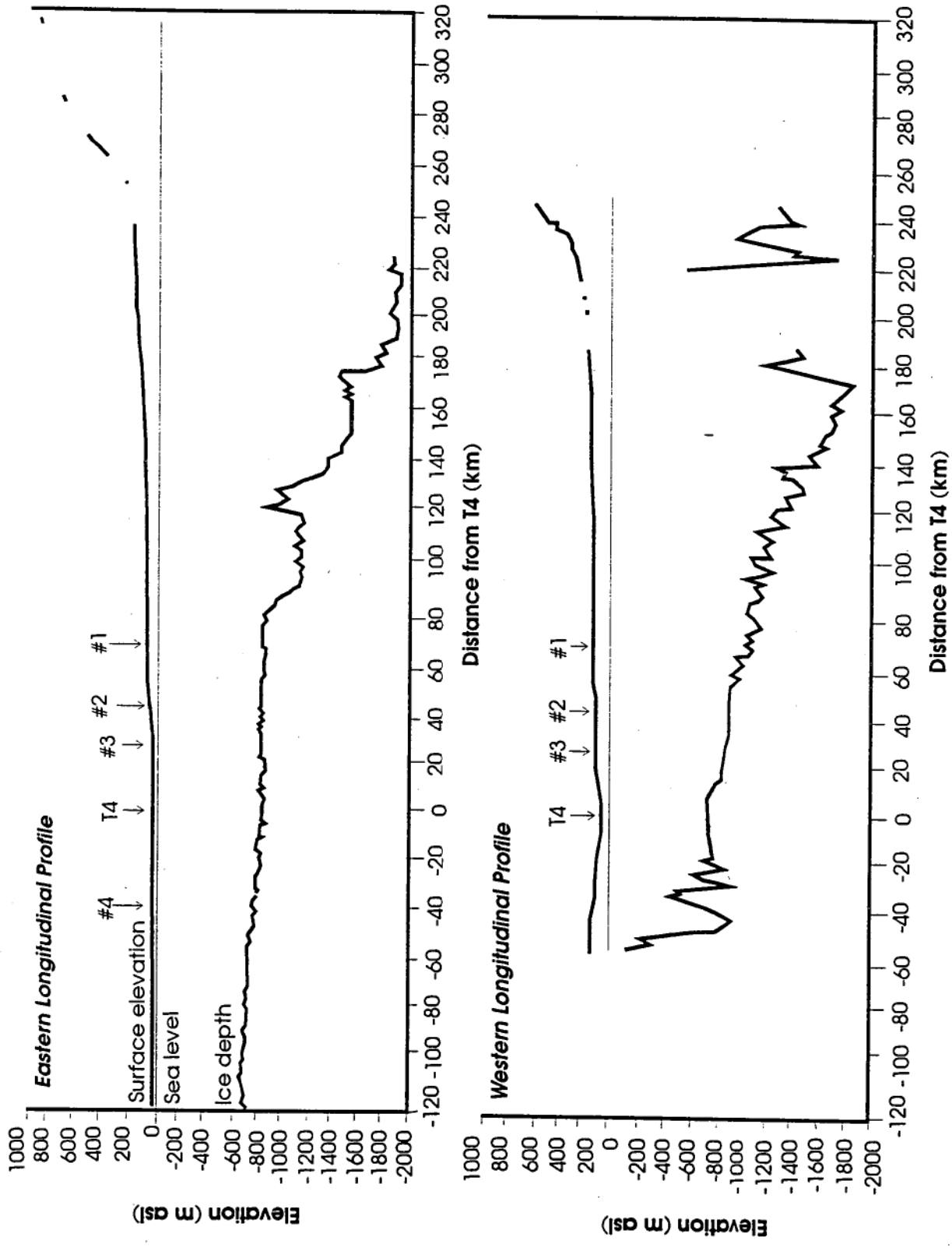

Figure 4.10. Eastern (a) and western (b) longitudinal profiles of the Lambert Glacier ice stream. Distances are relative to transverse cross section through T4 (A406) Budd *et al.* (1982). Positive distances are upstream of T4, negative are downstream.

of 650 m occurs 105 km north of T4. If the ice were floating, and had a density of 900 kg m^{-3}, the average ice thickness would be 730 m ±20 m. The maximum ice thickness of 880 m ±20 m, near T4, indicates the ice (in profile) is thinning at the base the closer to Profile #4 (and the ice edge).

Between the section on the profile that is perpendicular to T4 and Profile #3 (30 km south of T4) the ice thickness is relatively uniform. The ice thickness in this area varies from 864 m to 880 m, and given the estimate of error involved with these measurements, it can be considered as uniform. Further upstream (and therefore south of T4), the ice shows short sections of over deepening. For example, 60 to 65 km south of T4 the ice thickness increases 50 m which is 6 percent of its overall thickness between Profile #3 and Profile #1.

Seventy kilometres south of T4, the thickness of the ice rapidly increases to an average of 1375 m ±20 m. From the data, the ice surface in this area is relatively constant at 100 m ±20 m asl. At 120 km along the profile, the ice thickness within 2 km, decreases from 1292 m thick to 948 m with almost no change in surface elevation. Within a further 8 km the ice again begins to thicken. This suggests the ice is at least partially grounded in the vicinity of Profile #1 (discussed further in sections 4.3.4 and 4.3.6).

Coinciding with the area north of Mawson Escarpment, 150 km south of T4 and located at 72°27'S 67°51'E, the profile of the ice maintains a thickness of approximately 1620 m ±20 m for 20 km with a surface elevation of 126 m ±20 m asl. This could be indicative of a basal melt lake. The ice then thins by nearly 100 m over a distance of 3 km (172 to 175 km south of T4 along the profile). Within this section of the profile, the surface elevation steadily increases the further south of T4. Approximately 180 km from T4 is the area identified by Bentley (1987) as the grounding line.

Sounded ice thickness reaches a maximum of 2200 m 213 km south of T4. Here the surface elevation is 188 m asl. Beyond this point on the eastern-side longitudinal profile along the Lambert Glacier, the ice no longer thickens, but rather the surface elevation rises from approximately 255 km south of T4. Two-hundred and twenty kilometres south of T4 the return echo became weak and intermittent due to surface crevassing and signal disruption. By 265 km south of T4 the base of the ice is at 1122 m below sea level and the surface elevation is 480 m asl.

Figure 4.10b shows the longitudinal profile on the western side of the stream. Distances discussed below are measured from T4 and discussed as if heading northward, that is, moving towards the coast. The initial 70 km (250 to 180 km south of T4) of this profile has intermittent RES data, and only an inaccurate ice thickness profile exists. The ice thickness 250 km from T4 is 1850 m ±20 m before thinning to 1290 m ±20 m 12 km further north along the profile. The surface elevations fall from 550 m ±20 m to 320 m ±20 m respectively. This is in the vicinity of this author's proposed Lambert Glacier grounding zone discussed for the eastern longitudinal profile. The thinner ice also coincides with a change in surface slope; from a gradient of 19 m per kilometre upstream to 2.7 m per kilometre downstream. The ice then thickens rapidly to 1960 m within 7 km, only to again thin to 824 m within 5 km (220 km from T4). The signal from the Radio Echo Sounder was lost until 180 km from T4. This rapid thinning of the ice can be explained as an isolated outcrop. Assuming that the overlying ice surface is a reflection of basal topography, the thinning of the ice may be the edge of the over deepening of the graben into which the Lambert Glacier and tributaries converge.

Where data were recovered the ice thickness is 1611 m: it than rapidly over deepens to 1967 m over a distance of 6 km, heading north, about 180 km from T4. This area of ice thickening occurs in the vicinity of Bentley's (1987) grounding zone for the Lambert Glacier. Given the appearance of the western profile of the Lambert Glacier and Amery Ice Shelf system, this could suggest a possible start of the grounding zone for the western side of the drainage system.

From 180 km south of T4, the thickness of the ice steadily decreases with intermittent thinning and thickening on a very small scale. By 140 km from T4 the ice has thinned to 1470 m, and for another 140 km essentially maintains a steadily decreasing thickness until at a point perpendicular to T4 where the ice thickness is 790 m. At the intersection of Profile #1, the ice thickness is 1156 m, by Profile #2 the ice is 1022 m thick. At the intersection of Profile #3 and this longitudinal profile downstream, the thickness of the ice is 968 m.

The basal profile of the ice from 45 km to 10 km south of T4 along the western profile, (south of Profile #2 to half way between Profile #3 and T4) has a uniform ice depth. This area underlies a region of clearly visible blue ice and high surface melt lake activity (as seen on the satellite imagery of the region). North of the zone perpendicular to T4, the thickness of the ice rapidly decreases over the irregular

outcrops of Jetty Peninsula as the flight path deviates off the ice shelf and onto the grounded ice.

The calculation of the surface elevation of the ice that would be necessary for buoyancy or hydrostatic equilibrium is dependent on several factors; the density of the water and the average density of the ice column (which includes the effect of crevassing). Only assumptions can be made about the average ice density which depends on the amount of new snow, wind packed snow, firn and glacial ice in the column. As with the ice, the density of any water underneath this system is also uncertain. The salinity of the water directly effects the buoyancy of the ice. For hydrostatic equilibrium (h*), the ratio of surface elevation to ice thickness is given by:

$$h^*/Z = (\rho_w - \rho_i)/\rho_w \qquad \text{(Equation 4.1)}$$

where h* is the surface elevation of the ice, Z is the thickness of the ice column, ρi is the mean density of the vertical ice column and ρ_w is the mean density of the subglacial water. Varying ice (ρ_i) and water (ρ_w) densities will change the results discussed below. Table 4.1 shows typical h*/Z ratios for different combinations of mean ice and water densities. Note that there can be a strong vertical density gradient in the ice. Figure 4.11 compares all the surface elevations along the eastern

		h*/Z		
ρ_i	880	900	910	916
ρ_w				
1000	0.12	0.10	0.09	0.084
1026	0.14	0.123	0.113	0.107
1033	0.148	0.129	0.120	0.113

		Z/h*		
ρ_i	880	900	910	916
ρ_w				
1000	8.33	10.00	11.11	11.90
1026	7.33	8.34	9.08	9.59
1033	6.98	8.01	8.61	7.77

Table 4.1 Various values for ice and water densities that contribute to the calculation for surface elevation for hydrostatic equilibrium (h*) ($kg^{-1}m^{-3}$).

longitudinal profile with the elevations required for an elevation to thickness ratio of 0.1; that is for hydrostatic equilibrium of a free-floating ice shelf with a mean density of 900 kg m^{-3} overlying water of density 1000 kg m^{-3}. At T4, a density ratio of 0.113 was used by Budd (1982) to calculate the location of the grounding line. This author has assumed, based on an apparent blue ice surface south of T4, that the mean ice density is 900 kg m-3 and that the water under the floating ice is strongly influenced by basal melting and thus it is assumed that the mean density of the water column south of T4 is 1000 kg m^{-3}.

The surface elevation south of T4, as already stated, has been interpolated from single spot elevations derived predominantly from Russian topographic maps. On Figure 4.11 the straight lines connecting these points are used to illustrate surface elevation along the entire eastern-side longitudinal profile along the Lambert Glacier and its ice stream within the Amery Ice Shelf. As a result of this interpolation many surface features, such as small scale undulations, go unnoticed and therefore are not shown.

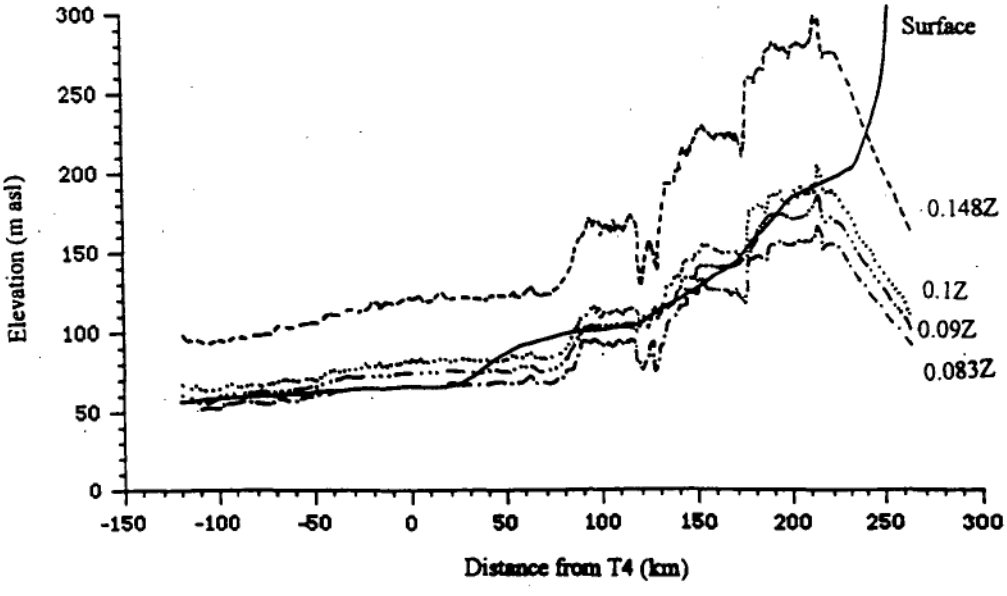

Figure 4.11. Profile for the Eastern Longitudinal transect following, as near as possible, the flow lines of the Lambert Glacier in an upstream direction. The solid line is the surface elevation while the dashed lines are the elevation for hydrostatic equilibrium (based on a range of h*/Z). Surface elevations is not illustrated beyond 250 km south of T4.

Horizontal positioning errors may also contribute to deviations from the profile assumed for hydrostatic balance. For example, there are some incidences of inaccurate navigation during Flight 03 (1988-89). This appears in Figure 4.11 as spot elevations that are correct but the location of the point do not coincide with the surface elevations from the Russian and Australian maps or the calculated hydrostatic equilibrium elevation line.

However, the relationship between surface elevation and ice thickness indicates that the majority of the ice along this longitudinal profile may be floating or close to floating. From 46 km to 88 km south of T4, where Profiles #2 and #1 intersect the longitudinal transect and the area immediately south, the ice cannot be considered as truly floating. The ratio is still too low to suggest that the ice mass is completely grounded. Similarly between 119 km and 133 km, the nature of the ice is indicative of neither floating nor grounding. Along the profile at 174 km south of T4 the ice again displays a small rise in the surface to thickness ratio though it only marginally exceeds the value of 0.1 used to delineate floating from grounded ice (Figure 4.11).

Based on these hydrostatic equilibrium calculations the ice 222 km inland of T4 appears grounded. The deviation between surface elevation for buoyancy and the observed surface elevation north of the region 220 km from T4 is suggested by this author to be "sticky spots". This assumption is based on ice morphology discussed later in section 4.3.3. Both north and south of these sticky spots, the ice body is at least partially floating.

One observation that can be made from the relationship of surface elevation for hydrostatic equilibrium to that of observed surface elevation is that each sticky spot coincides with regions of surface slope change. A relationship that can be seen between hydrostatic equilibrium and ice thickness is the high correlation of sticky spots to regions of relatively rapid thickness change.

Figure 4.10b is a longitudinal transect showing surface elevation, mean sea level and ice thickness along the western side of the Lambert Glacier stream and thus showing portions of the Fisher Glacier. At the southern limits of the profile, the surface elevation is approximately 560 m asl. Over the next 15 km moving north towards T4, the surface height of the ice decreases to 288 m asl. This is a slope gradient of 19 m per kilometre. Between 225 km and 180 km from T4, the surface elevation falls 123 m at a slope of 2.7 m per kilometre. The 180 km mark on

Figure 4.10 coincides approximately with Bentley's (1987) definition of the grounding zone.

Between 180 km and 57 km south of T4, from the Bentley grounding line to Profile #1, the surface elevation decreases from 165 m to 111 m, at a gradient of 0.5 m per kilometre. A surface rise can be depicted in Figure 4.12 between these two points, but as no corresponding surface feature can be identified in satellite imagery or aerial photographs, and as the rise is 20 m above the average slope gradient, it is believed to be an error in the data.

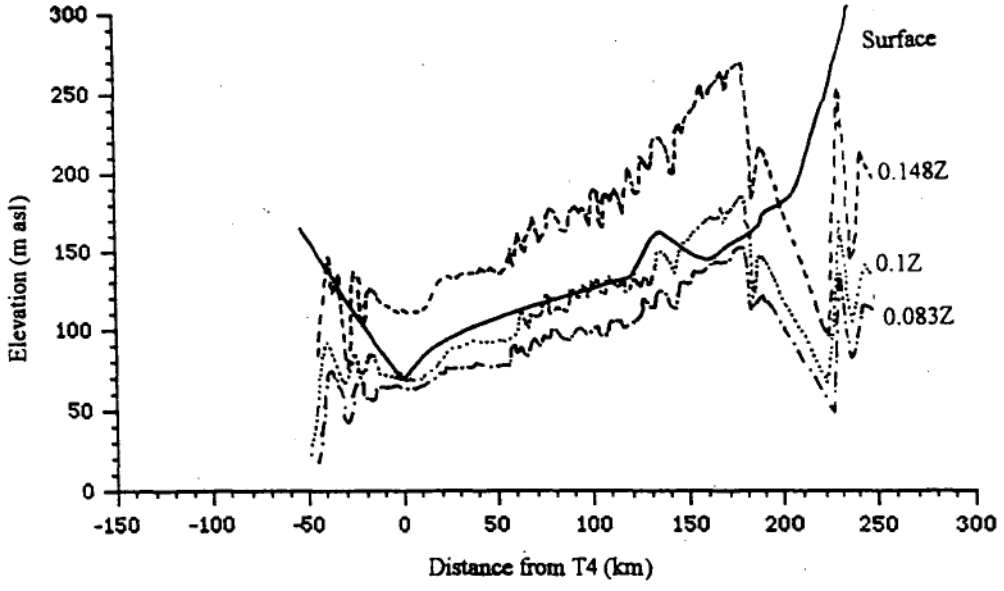

Figure 4.12. Profile for the Western Longitudinal transect of the Lambert Glacier ice stream following the flow lines downstream. The solid line represents the surface elevation while the dashed lines are the interpolated surface elevation for hydrostatic equilibrium based on various fractions of ice thickness (Z) as shown.

From Profile #1 to Profile #2, the surface gradient is 0.4 m per kilometre and the elevation drops 10 m. Over the 18 km between Profile #2 from #3, the surface decreases its elevation by 8 m at a gradient, again, of 0.4 m per kilometre. Perpendicular to T4, at a distance of 0 km along the longitudinal profile downstream on the Lambert Glacier ice stream, the glacier's surface elevation is 70 m asl. The gradient between this point and Profile #3 is 0.8 m per kilometre. An increase in surface slope can be attributed to the region in line with T4 being a

zone of convergence between the ice mass of the Lambert Glacier ice stream, and the major westerly grounded ice tributary in particular the contribution of ice flowing between Mount Meredith and Fisher Massif. This region is also the start of a rapid surface elevation increase onto Jetty Peninsula as the flight path tracks off the Amery Ice Shelf.

The variation in buoyancy of the ice mass in the longitudinal profile moving downstream along the Lambert Glacier and Amery Ice Shelf system is illustrated in Figure 4.12. Studying this profile from south to north, the right hand side of the profile shows only the Fisher Glacier until 180 km south of T4, ie for a distance of approximately 65 km. Available information on ice thickness and surface elevation suggests that the ice mass is grounded. For a further 30 km towards T4 the ice is floating. From 150 km to 60 km south of T4, the ice can be interpreted as marginally afloat. As discussed earlier, this possibly suggests an extensive area of basal water. In the area north of the T4 intersect, the ice is floating where the tributary of western plateau ice flows from between Mount Meredith and Fisher Massif but becomes grounded where the flight path deviates west of the flow line onto the foot of Jetty Peninsula.

Evidence from Figures 4.10, 4.11 and 4.12 suggest that the eastern side of the lower Lambert Glacier and Amery Ice shelf system has a grounding line approximately 250 km south of T4. In comparison, the western side of the drainage systems suggests the grounding line at approximately 180 km south of T4. The topography of the drainage system in this area may be impacting on this variation in grounding line location as the ice draining the polar plateau from the west flows through the Southern Prince Charles Mountains while the ice from Princess Elizabeth land to the east is inhibited by Mawson Escarpment.

4.3.2 Basal Melt Lakes

A continuous Radio Echo Sounding flight (03: 1988-89) traced south along the eastern side of the lower Lambert Glacier drainage system, circled through the Southern Prince Charles Mountains before heading north along a trajectory that essentially passed over the western side of the Lambert Glacier and Amery Ice Shelf system. This flight has been the main source for many of the longitudinal profiles and has formed the basis for many calculations. Some unusual basal features appear approximately 90 km south of T4 along this profile.

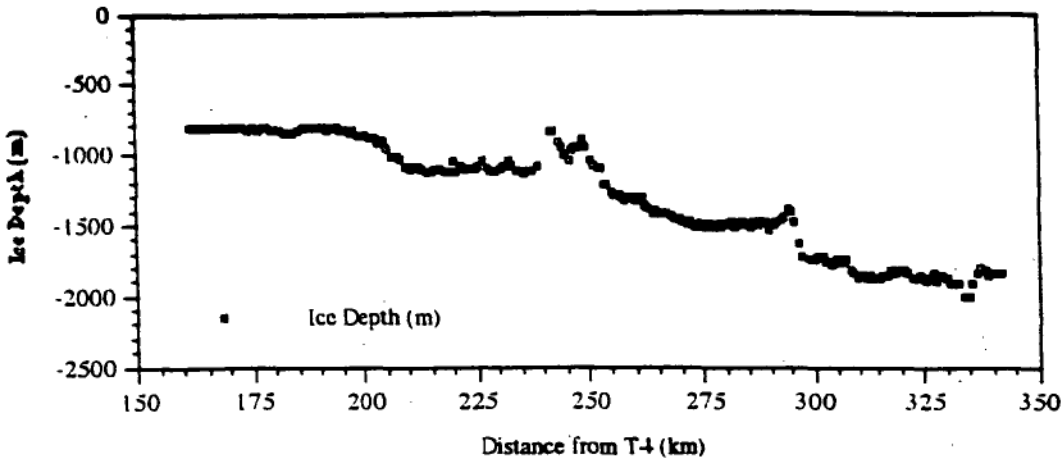

Figure 4.13. The region of Flight 03 (1988) that best illustrates the area of probable basal melt lake activity. This area is located primarily between Profile #1 and the southern limits of the grounding zone for the Lambert Glacier ice stream. Two distinct regions between 260-290 km and between 305-320 km suggest basal melt lakes. Between 210-240 km the basal topography could be interpreted as a past basal melt lake environment.

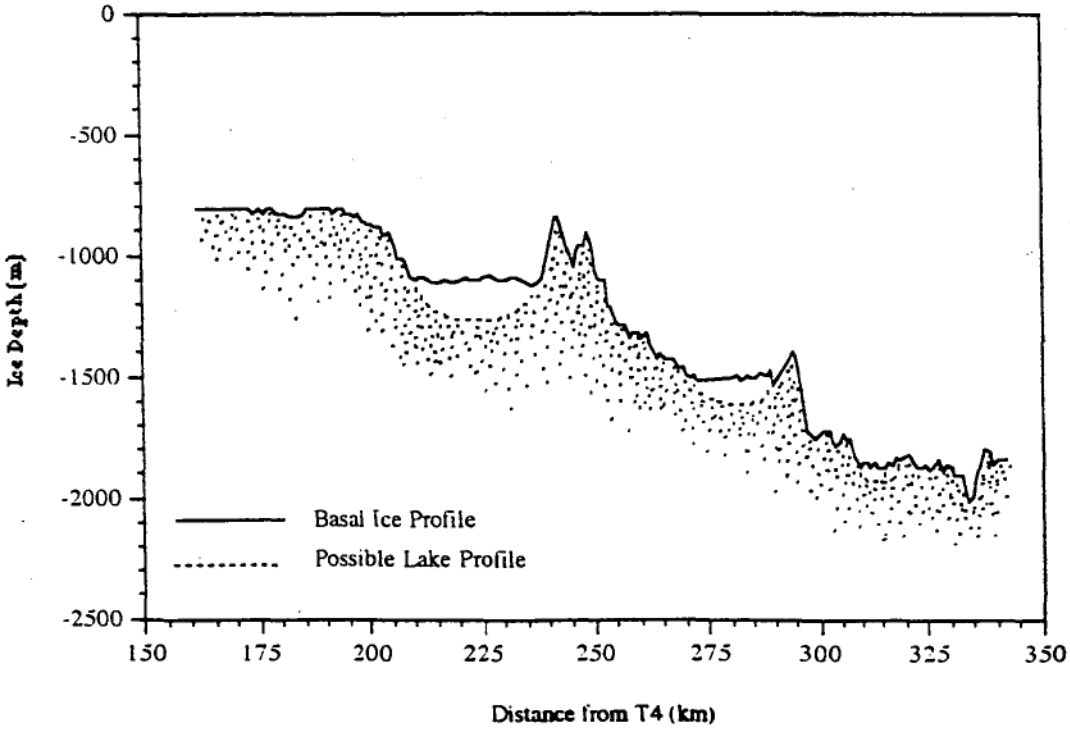

Figure 4.14. Sketch of the basal melt lake region on the eastern side of the Lambert Glacier ice stream in the vicinity of the southern grounding limit. The dashed lines represent a possible scenario for the continuation of the basal topography, with the overlying basal melt lake (solid line).

Figure 4.13 shows a 200 km section of this basal profile. Three separate near horizontal sections can be discerned in this part of the profile. The first is approximately 26 km long, the second is 18 km long and the third and most southern is 12 km long. It is suggested that these near horizontal basal ice profiles are basal melt lakes or the infiltration of channelled marine water from Prydz Bay. These features have two main characteristics: a near horizontal basal profile and steep thinning of the ice at the sides both north and south of each feature, suggesting the existence of containment ridges. This supports the idea that these depressions are water filled. Figure 4.14 is a more conjectural view of the profile. The dashed lines are hypothetical bedrock profiles, assuming the existence of basal water is a viable interpretation.

It should be noted that these basal melt lakes exist within the grounding zone of the Lambert Glacier. Bentley's (1987) definition of the grounding zone, 180 km south of T4, is situated north of these basal features. This author's definition of the grounding zone is a further 85 km south and will be discussed further at the end of this chapter. Between Bentley's southern grounding zone and this author's, there are two surface ice dolines on the eastern side of the drainage system. These dolines overlay an area that coincides with the third and most southern basal melt lake. As noted above, dolines typically occur over unsupported ice and a slump will exist if there is basal water. This is also in the area of the thickest ice measured during the 1988-89 and 1989-90 RES flights. The still intact terminal moraines from the alpine-type glaciers from Mawson Escarpment, seen in TM images, suggest that the area around the dolines is a very slow moving part of the Lambert Glacier system. As the dolines are surface features reflecting basal ice activity, it is thought that the dolines have slowly moved north/downstream of the thickest ice and are no longer directly above the underlying basal melt lakes.

A final comment on these three basal melt lakes relates to the most northern feature. The basal profile is quite angular in comparison to the other two more southern features. As such, this feature may be an extinct basal melt lake that is no longer water filled. It could also be a remnant feature of a previous ice thickness for the Lambert Glacier therefore reflecting a climatic period when a greater volume of ice moved by basal sliding in this area. Similarly, these basal ice features may reflect an existing series of basal melt lakes. This conclusion can be compared to a similar profile of basal ice near Vostok that has been interpreted as a basal melt lake (Kapitsa *et al.*, 1996). This Lambert basal melt lake is currently 500 km from the open waters of Prydz Bay. This entire area is definitely moving by basal sliding

the open waters of Prydz Bay. This entire area is definitely moving by basal sliding and the dynamics evidence for this conclusion will be discussed further in Chapter Five.

4.3.3 Transverse Profiles

From the total of twenty RES radar flights carried out in the Lambert Glacier and Amery Ice Shelf area (Figure 4.1 and Appendix C), data from eight flights (Flights 03 and 14: 1988-89 and Flights 05, 06, 09, 10, 13: 1989-90) referred to in Figures 4.6-4.8 were used to derive five transverse cross sections across the lower Lambert Glacier and Amery Ice Shelf in the presumed area of the system's northern limit of the grounding zone. As with the longitudinal profiles, the RES data consisted of the ice thickness measurements that were manually scaled from a film record at approximately every 500 metres. Surface elevations were derived from spot heights and aircraft height as with the longitudinal profiles. Horizontal position was measured by GPS navigation which was almost always available, and logged either manually every minute (1988 - 1989 flights) or digitally every ten seconds (1989 - 1990 flights).

Five transverse sections were defined across the ice shelf and glacier, orthogonal to the ice flow. Data from nearby RES flights (which were not themselves always orthogonal to the flow) were linearly projected onto these to give idealised sections across the ice mass. These ice thickness co-ordinates were plotted against the 1977 series R-42, S-42 and R-43 Russian topographic maps at a scale of 1:200,000 which were based on photogrammetry. Estimations of surface elevation (above sea level) were determined along the flight profiles from these maps.

The accuracy is dependent, in the case of surface elevation, on the estimation of height from interpolation with Russian maps (which in turn have their own inherent errors due to poor ground control). Instruments used to gauge ice thickness suggest data accuracy is ±5 m. Due to the RES data not always being available in a direction perpendicular to the flow lines, and as such the data had to be interpolated to fit the transects, the spatial accuracy is expected to be within ±5 km.

4.3.3.1 Profile #1

Extending 85.5 km, from 71°38'S 68°E to 72°4'S 70°E, elevations along Profile #1 range from 800 m asl on the edge of the ice sheet east into the Lambert Glacier

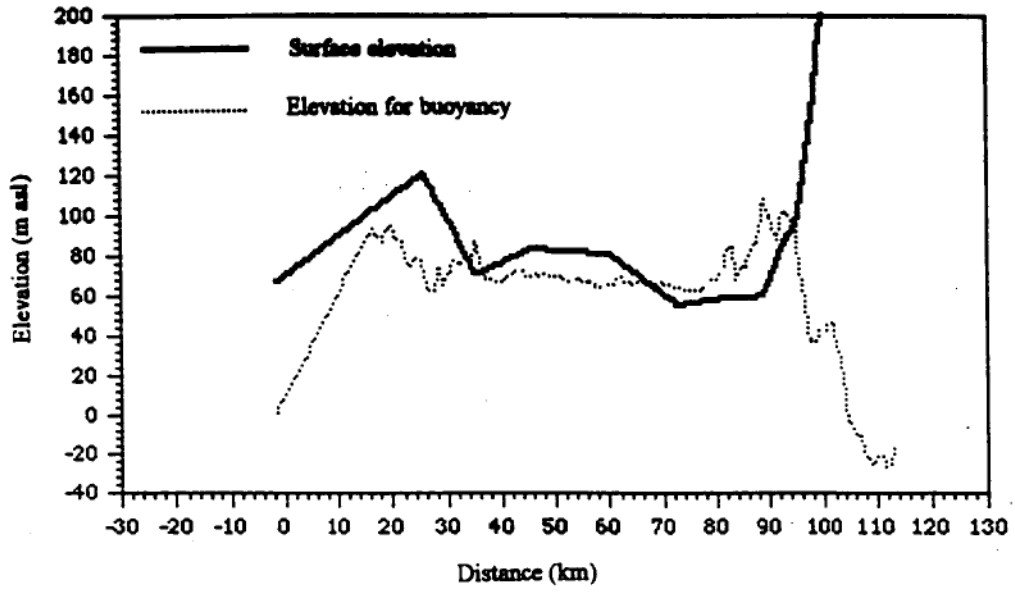

Figure 4.15. The relationship between the interpolated surface elevation (solid line) and the calculation of hydrostatic equilibrium and ice buoyancy derived from 0.1Z (dashed line) for Profile #1.

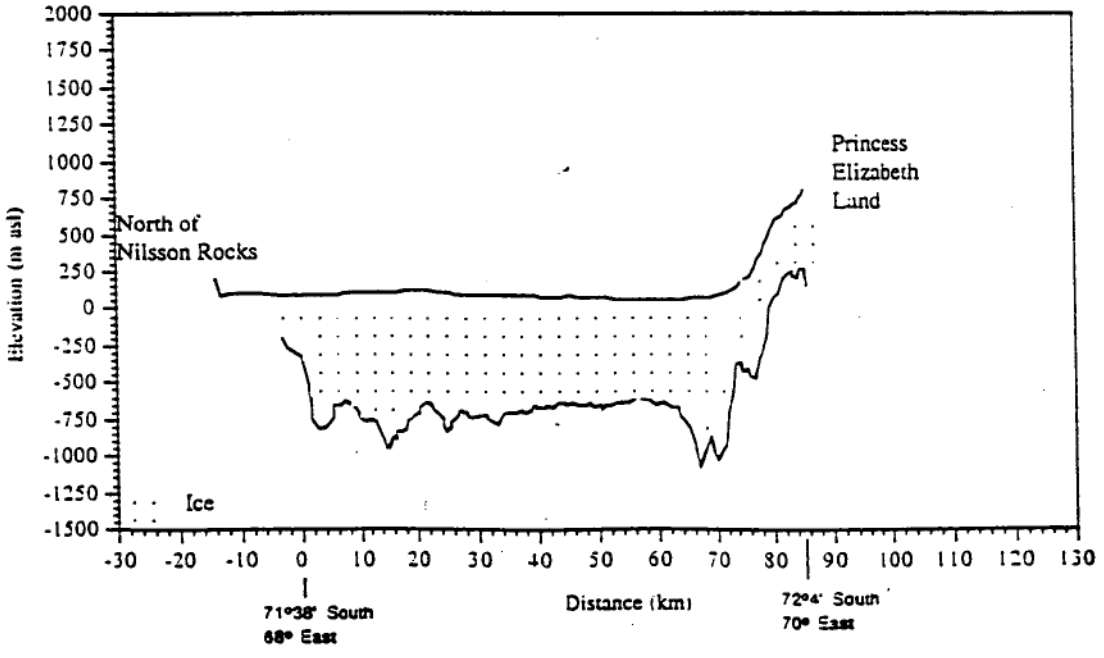

Figure 4.16. Cross section of ice thickness and interpolated surface elevation for Profile #1.

drainage system and then across to the western ice sheet at 90 m asl. This profile concludes east of Fisher Massif and to the north of Nilsson Rocks (Appendix C).

Figure 4.15 indicates that the eastern side of the ice shelf has a lower mean elevation of about 50 metres above sea level compared to the western side which averages 70 m asl. Within the core of ice originating from the main Lambert Glacier ice stream (14 to 47 km along the profile shown in Figure 4.15) the surface reaches an elevation of 100 m asl, again on the most western side while the eastern transect that is not the Lambert Glacier has a 60 m asl maximum. The average elevation across the transect is 80 m asl. As the profile extends up into the grounded ice to the east beyond Robertson Nunatak, the surface elevation increases rapidly to 600 m asl over 20 km. The ice on the higher western side of the drainage system appears as a distinctive area of 'blue ice' typical of an ablation area.

The quantity and quality of the RES data for this transect of the Amery Ice Shelf and its internal ice streams have provided some valuable detail on the ice thickness distribution over the area (Figure 4.16). As with surface elevation, the ice thickness data quality is variable with an accuracy of ±20 m. The average ice thickness across this entire profile is 750 m while the average ice thickness in the core of the Lambert ice stream is 850 m.

On the western side of the profile the ice thickness has a minimum of 214 m where the bedrock rises as part of the western extension of Nilsson Rocks. This shallow feature only occurs over a small area and the ice becomes 900 m thick within 4 km further towards the east. While the bulk of the ice is relatively uniform in thickness, there are two significantly thicker regions at either side of the transect. The western maximum ice thickness is 1070 m the eastern maximum (68 km along the profile) is 1140 m. Between these two maxima the ice thickness is 770 m ±60 m with a trend in thinning eastward before thickening considerably at the foot of the easterly grounded ice from Princess Elizabeth Land. In this region, the ice thickness decreases from 1140 m to 500 m over 20 km. The ice of the Lambert ice stream is deeper on its western margin compared to the east. The maximum western depth is 1070 m, while the eastern maximum is 800 m.

Figure 4.15 compares the surface elevation along Profile #1 with the elevation required for hydrostatic equilibrium of a free floating ice shelf (0.1Z) with a mean ice density of 900 kg m^{-3} which can be used as a reference even though the density

ratio may be expected to have considerable variation. The surface elevation cannot be below the level for buoyancy (as for 70-95 km) which means the density ratio (0.1Z) is too high there. However the density ratio can vary with ice thickness associated with the variation in mean column density. The ratio for isostasy used for calculations across this profile equal 0.1Z for buoyancy, and when this hydrostatic buoyancy line is interpreted between 34 km and 88 km across Profile #1, the ice mass appears to be floating. The region between 12 kilometres and 34 km is not so clearly buoyant. These conclusions are within the errors of the measured elevations and include the uncertainty in the mean ice density and mean water density. This "sticky" area is coincidental with the area of higher surface elevation and encompasses an area of both westerly grounded ice sheet and that of the Lambert Glacier ice stream.

The average column density of ice can be expected to range from 880 kg m^{-3} to 916 kg m^{-3} depending primarily on the amount of firn or crevassing on the upper surface. Similarly the density of basal water, whether it is fresh or marine, can range from 1000 kg m^{-3} to 1033 kg m^{-3}(see Table 4.1). The calculation for surface elevation of ice buoyancy is then based on the average stated above (Equation 4.1).

4.3.3.2 Profile #2

Profile #2 traverses a distance of 68.5 km from 71°27'S 68°28'E to 71°50'S 70°E. The profile of the Lambert Glacier system is 24 km north of Profile #1. This profile covers an area from the lower reaches of the easterly grounded ice across to the westerly grounded ice sheet, finishing north east of Fisher Massif (Appendix C).

The surface elevation trend across the profile, although essentially uniform, does suggest that the western perimeter is higher than the eastern (Figure 4.18). Reaching a maximum of 90 m asl, this higher elevated surface corresponds with the drainage system of the polar plateau as well as the proximity to Fisher Massif and the grounded ice that is flowing through this region. Towards the eastern side of the profile, the surface elevation rises significantly over only a small distance. This coincides with the grounded ice of Princess Elizabeth Land and the Amery Ice Shelf's inland coastal margin. Prior to this surface elevation rise, the minimum height across the profile is 60 m asl which lasts for 20 km along the transect.

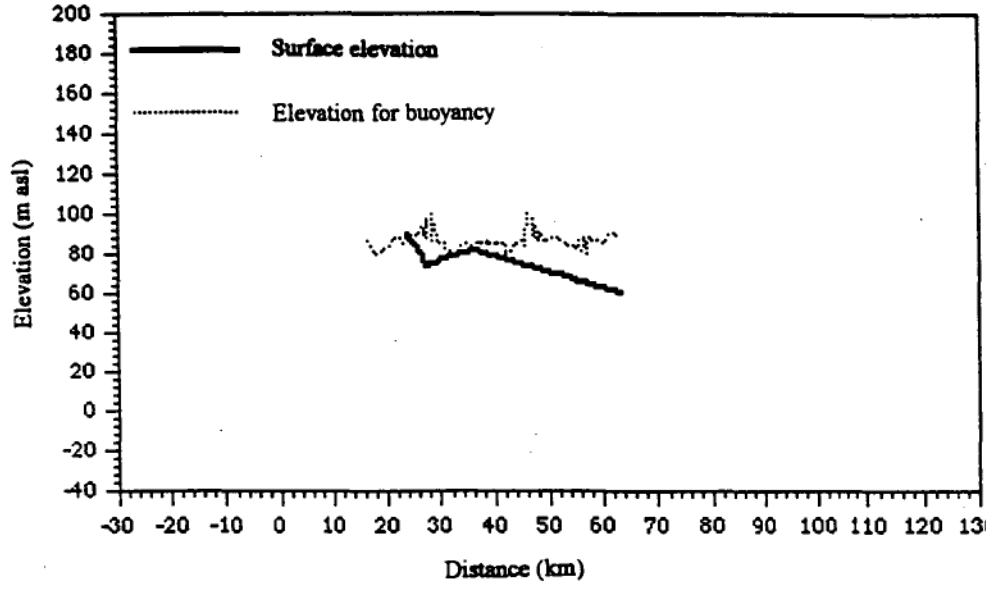

Figure 4.17. Interpolated surface elevation (solid line) compared to a calculation of ice buoyancy (0.1Z) and hydrostatic equilibrium (dashed line) for Profile #2.

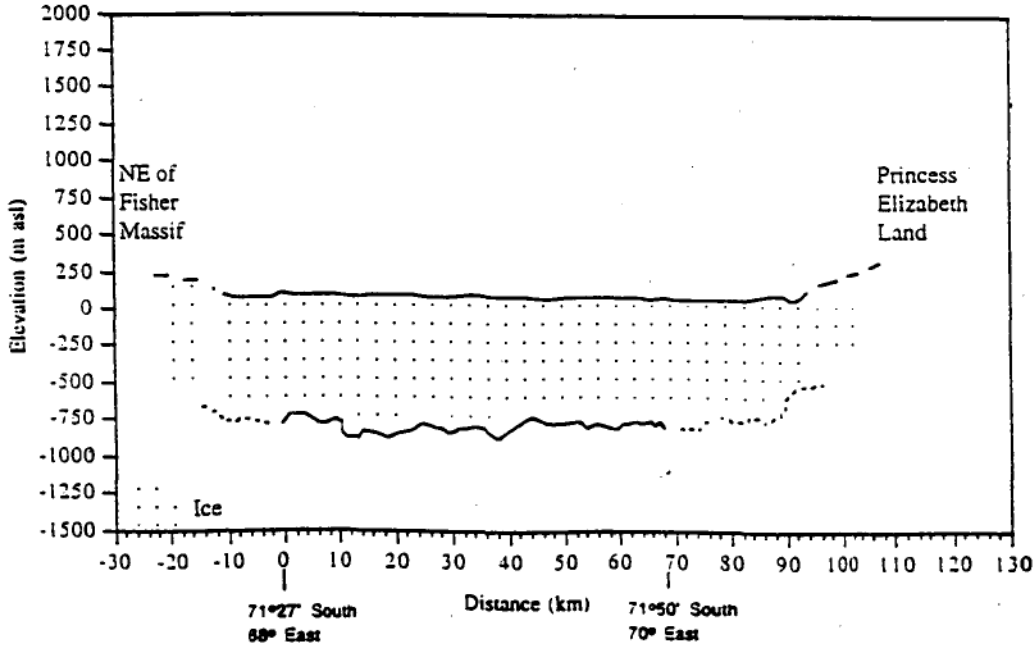

Figure 4.18. Cross section with ice thickness and interpolated surface elevation for Profile #2. Dashed lines represent a proposed basal ice profile due to a lack of data for the lateral portions of the lower Lambert Glacier and Amery Ice shelf in this site.

Figure 4.18 shows the relationship between surface elevation (m asl) and ice thickness. As with all the cross section analyses, this is a profile of the base of the ice shelf or glacier and not necessarily bedrock elevation or topography. Across Profile #2 the thickness of the ice is relatively uniform. At its thickest, the ice measures 1000 m, the thinnest ice along the profile is 830 m. There is an average thickness of 900 m for the entire profile. The area encompassing the Lambert Glacier ice stream between 12 km and 4 km across the profile is the only portion of the cross section that remains consistently thicker in cross section, averaging 945 m. The grounded ice contributions from the west and east are comparable as they both show a similar ice thickness. North east of Fisher Massif the ice is typically 865 m thick. Across the eastern reaches of the profile the ice from Princess Elizabeth Land is similar in thickness, averaging 870 m.

The ice towards Fisher Massif is progressively more grounded in a westerly direction (Figure 4.17). From the radio echo sounding data, the isostasy computations, based on an ice density of 900 kg m^{-3} and water density of 1000 kg m^{-3}, indicates that across Profile #2 the ice mass is typically floating. The buoyant ice is located towards the eastern reaches of the cross section. This compares to the western side of the Lambert Glacier and Amery Ice Shelf drainage system which, based on hydrostatic buoyancy, appears to be grounded.

4.3.3.3 Profile #3

Profile #3 is the longest transverse profile measured in this area of the Lambert Glacier grounding zone. With a length of 119 km from 71°17'S 68°28'E to 71°46'S 71°E this transect incorporates the eastern grounded ice of Princess Elizabeth Land across to the westerly grounded ice to the north of Fisher Massif and east of Mount Meredith (Appendix C). The Lambert ice stream is 42 km wide and is situated between 36 km and 70 km along the profile.

Westward from approximately 12 km, the surface elevation rises 200 m within 1 km (Figure 4.20). This is the western edge of the ice shelf, north of Fisher Massif. Between this point along the profile over to the edge of the Lambert Glacier ice stream, another 24 km along the transect, the surface elevation gradually descends from 95 m asl to 80 m asl. Within the flow lines of the ice stream, the surface continues to descend eastward from 85 m asl to 65 m asl over 34 km. The lowest surface elevation for Profile #3 occurs 80 km along the profile, with an elevation

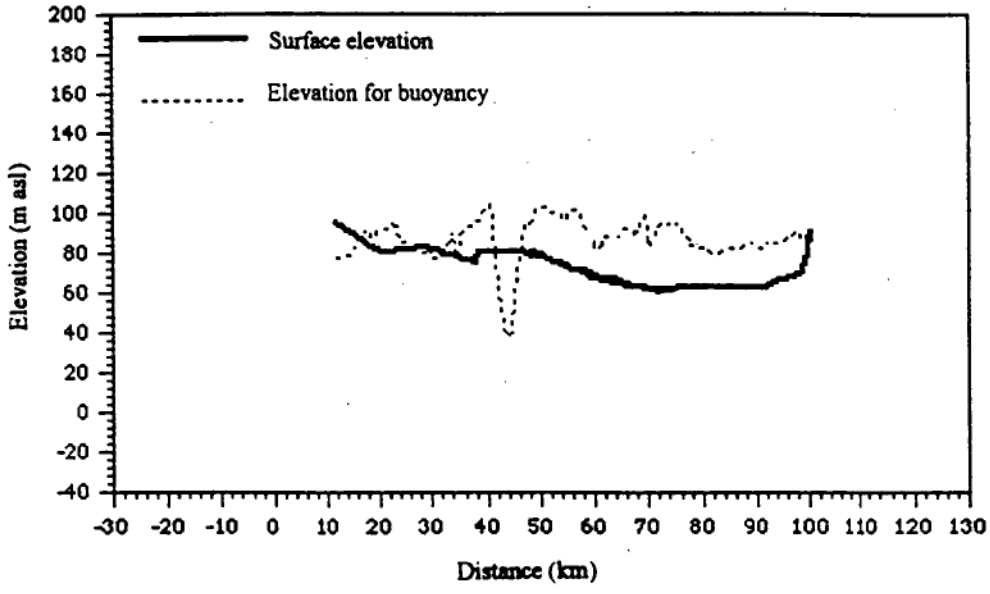

Figure 4.19. Comparison between interpolated surface elevation (solid line) and 0.123Z as a measure of elevation accuracy as well as ice buoyancy for Profile #3.

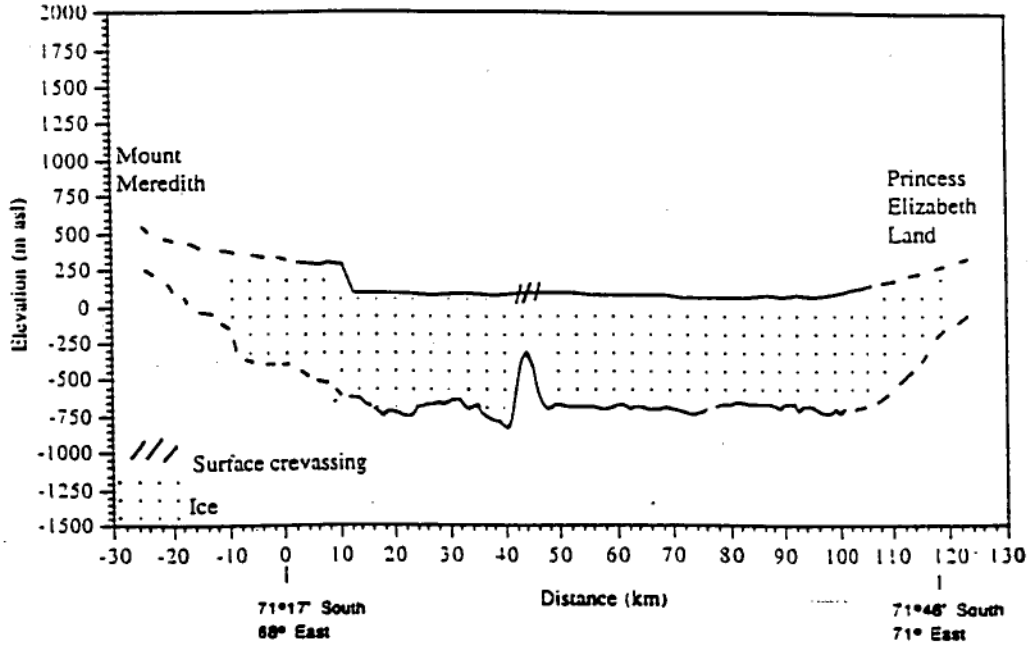

Figure 4.20. Cross section of ice thickness and interpolated surface elevation for Profile #3. The region of rapid ice thinning is overlain by an area of surface crevassing in the location of distinct blue ice.

of 60 m asl. Further east of this area of lowest surface elevation, the surface steadily rises up the steep sided Amery Ice Shelf coastal boundary (found 100 kilometres along the profile).

Forty to forty-four kilometres along the transect, an area of surface crevassing exists within the same region as a small rise in the surface elevation. This distinctive surface feature is located within the defined flow lines of the Lambert Glacier ice stream and also delineates the eastward extent of the blue ice observed on satellite images and aerial photographs.

As shown in Figure 4.20 the average ice thickness is 770 m. Along the region where grounded ice from the west flows into the system the ice thickness ranges from 630 m near Mount Meredith to 650 m in the area of the Lambert Glacier ice stream. As stated above, the region between 36 km and 70 km is the contribution defined by flow-lines originating from the Lambert Glacier. The average ice thickness in this region is 800 m. Between 42 km and 46 km along the profile, there is rapid thinning of the ice from 920 m to 380 m within 4 km (heading west) before increasing to a thickness of 700 m within a further 2 km. This feature suggests a single outcrop protruding into the ice in the same area that surface crevassing has been identified. No other region of rapid ice thinning in the ice stream is evident along this transect. Ice originating from the easterly grounded ice averages a thickness of 760 m. For the most part, it can be seen that the ice thickness maintains a regular 10 m thinner profile east of this subglacial outcrop towards the Princess Elizabeth Land coast.

As mentioned above, east of the localised ice thinning area, the ice is in the order of eight per cent thinner than across the region west of the protrusion (Figure 4.20). On the basis of hydrostatic equilibrium calculations, the region of rapid thinning is a point of grounded ice that also corresponds to a slight rise in the surface elevation. West of this isolated grounding, the ice surface elevation is only just above the fraction 0.123Z for hydrostatic equilibrium (Figure 4.19). This density ratio is calculated assuming ice density is 880 kg m^{-3} and water density is 1033 kg m^{-3}. East of the grounded ice, the profile exhibits a definite floating nature until the rise onto the eastern grounded ice sheet begins at 100 km.

4.3.3.4 Profile #4

This transect from 70°50'25"S 69°E to 71°S 71°E is 75 km long and is situated very near to the G3 transect of Budd *et al.* (1982). The profile encompasses the

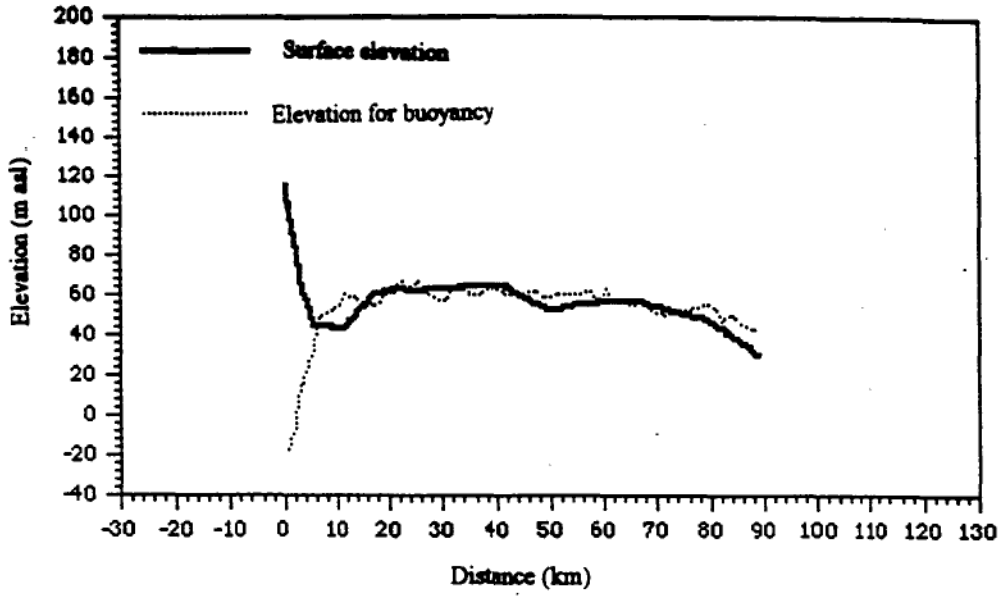

Figure 4.21. Interpolated surface elevation (solid line) in comparison with 0.148Z (dashed line) used as an indicator of ice buoyancy and hydrostatic equilibrium for Profile #4.

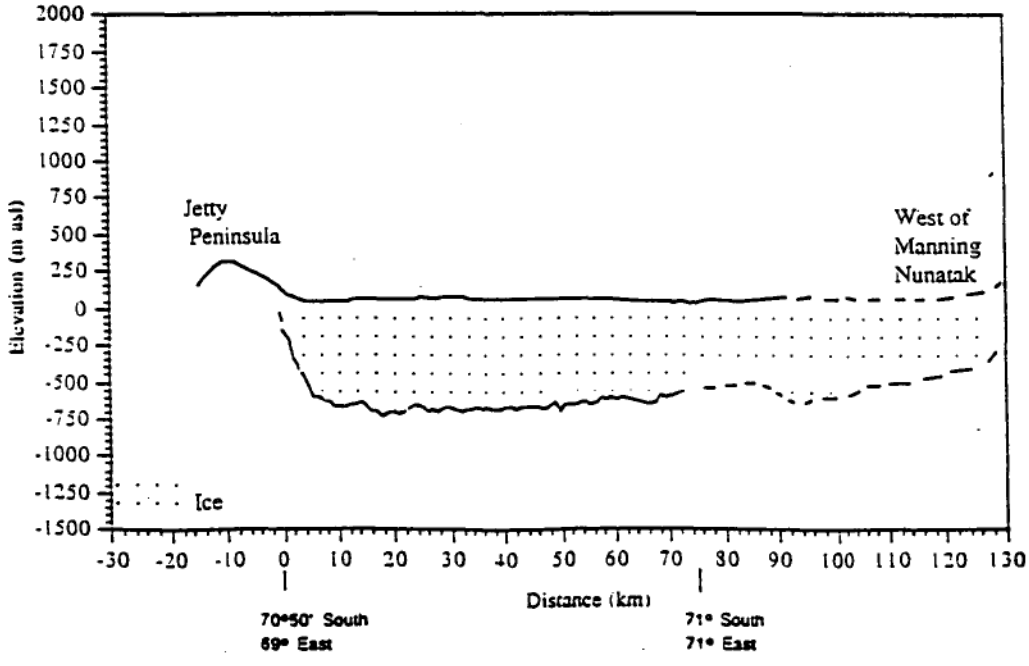

Figure 4.22. Cross section with ice thickness and surface elevation of Profile #4. Dashed line represents assumed basal profile due to lack of RES data.

area between Jetty Peninsula to within 20 km of New Year Nunatak (Appendix C). Due to the proximity of this profile to that which was derived by Budd *et al.* (1982), the comparisons between the two interpretations will be discussed in the following chapter.

The surface elevation of Profile #4 is relatively uniform (within measurement error). Figure 4.21 includes Jetty Peninsula which is on the eastern side of Beaver Lake. Beaver Lake is 250 km from the open water coastline and is known to be tidal (Bardin, 1986). The surface elevation of the Lambert Glacier ranges from 65 m asl on the westerly side to 55 m asl towards the east. The minimum height along the profile is 33 m asl (±5 m). This smaller error in this region is due to the more extensive GPS, optical levelling, and radar altimeter measurements, as opposed to the elevations up glacier which were derived from Soviet maps with an error of ±20 m.

Figure 4.22 is an ice thickness profile from Jetty Peninsula to within 20 km of Manning Nunataks (incorporating New Year Nunatak). At the beginning of the profile, the ice is 270 m thick, and reaches a maximum thickness of 770 m by 17 km along the profile, and maintains a regular thickness for almost 40 km before gradually thinning towards the eastern grounded ice sheet and Manning Nunataks. The average ice thickness for the entire cross section is 680 m.

By Profile #4, the width of the contribution from the main Lambert ice stream has widened considerably from the typical 32 km for cross sections 1, 2 and 3 to 42 km. This core ice stream has an average ice thickness of 755 m. The Lambert Glacier ice is progressively thinning, and gradually widening within the Amery Ice Shelf. From the ratio between surface elevation and ice thickness (Figure 4.21) 4 km eastwards along the profile marks the area that appears free floating ice. This assumption is based primarily on the relationship between the measured surface elevation and the averaged apparent elevation for hydrostatic equilibrium (0.148Z). The surface elevation being greater than the calculated elevation for buoyancy. This gives a very good fit to the observed surface elevation and could be a result of the lower ice density (880 kg m^{-3}) because of the presence of firn on the ice surface and very little high density marine basal ice.

4.3.3.5 Profile #5

This cross section is 87.5 km long from 69°53'S 69°E to 70°16'30"S 71°E between Single Island across to Corry Rocks on Gillock Island. Flow lines observed on

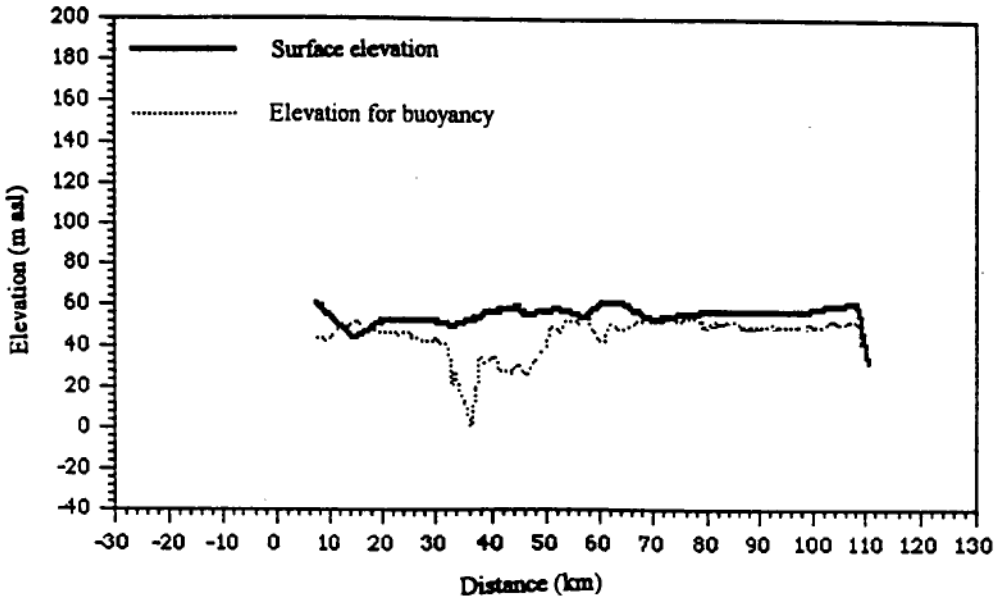

Figure 4.23. Interpolated surface elevation (solid line) in comparison with 0.118Z (dashed line) for Profile #5. The "sticky point" is evident in the large disparity between 30 km and 50 km along the profile.

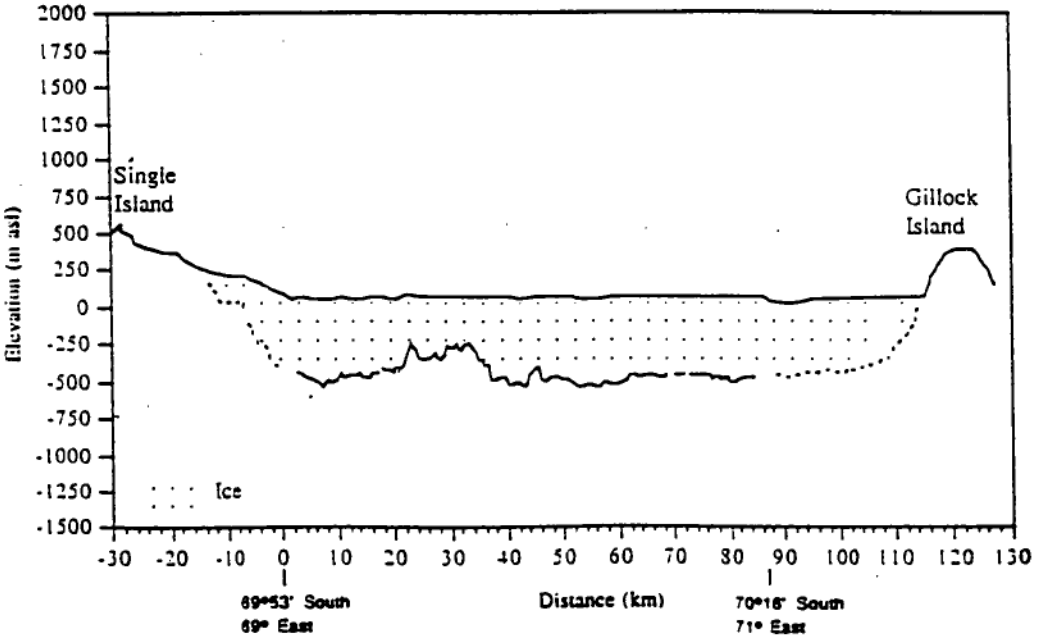

Figure 4.24. Cross section of Profile #5 between Single Island and Gillock Island. The ice from on the west of the cross section is from the Charybdis and Scylla Glaciers while the Lambert Glacier ice stream is between the "sticky point" and eastward for 42 km.

satellite imagery show that some of the ice originates from the Scylla and Charybdis Glaciers (flowing through the Northern Prince Charles Mountains) as well as from the Lambert stream and the east and west grounded ice (Appendix C). Profile #5 is 90 km north of Profile #4.

Across this transect, surface elevation remains relatively constant (Figure 4.24) at 40 to 65 m asl ± 5 m. The inclusion of Corry Rocks and Single Island in the figure is done to illustrate that this relatively uniform profile continues for the entire width of the cross section and hence the entire width of the drainage system in this area. There is an area of heavy crevassing 20 to 36 km across the profile that is not repeated elsewhere in the cross section. The 15 m apparent surface elevation drop at 86 km along the profile is not reflected as any feature observable on the satellite imagery and may be due to inaccuracy in the elevation data.

The core Lambert ice stream lies between 39 km and 81 km across the profile and from Figure 4.24 it can be seen that the ice thickness reflects three separate ice masses. Between 0 km and 20 km from the western end of the transect, the average ice thickness is 490 m. From 36 km across to the end of the ice thickness measurements another drainage channel can be identified, with the possibility of a minor third channel existing from about 80 km eastward towards Gillock Island just before the ice thickness data stops. The average ice thickness here is 545 m. The ice streams corresponding to these three potential drainage channels are the Scylla/Charybdis Glaciers, the Lambert ice stream and the eastern grounded ice sheet respectively. The average ice thickness for the Lambert ice stream is 550 m.

Of significance is the area between 20 km and 40 km across the profile (Figure 4.23). Here the ice thins to 300 m and corresponds to an area of extensive surface crevassing. The average thickness within this 20 km region of the transect is 340 m, 200 m thinner than the ice flowing east or west (Figure 4.24). This could be the northward extension of Jetty Peninsula or an isolated grounding point. It also underlays the initial point of convergence between the Northern Prince Charles Mountain drainage ice stream and the Lambert Glacier drainage system which the crevassing may also be reflecting.

West of the grounded region, the ice mass is floating until closer proximity to Single Island grounds the ice. The Lambert ice stream is floating with the possibility of a separate and minor grounding point or "sticky patch" at 45 km along the profile. This could be associated with the grounded region to the west

which marks the divide between the Scylla/Charybdis Glaciers and the Lambert Glacier ice flowing into Prydz Bay through the Amery Ice Shelf.

4.3.4 Upper Lambert System

RES data from Flight 03 (1988-89) of the upper parts of the Lambert Glacier and Amery Ice Shelf transition are used to examine some of different ice streams that combine to form the Lambert Glacier and Amery Ice Shelf system (Figure 4.25). This cross section from the Mellor Glacier to Geysen Glacier shows ice that is fully grounded. Further south of this profile Allison (1979) established stations to measure velocity. The closest velocity station to the area covered in Figure 4.25 was GL 10 at 74°4'13"S 68°23'20"E at an elevation of 1462 m asl, ice thickness of 1950 m and with a velocity of 230.5 ma^{-1} (Allison, 1979).

Figure 4.25 shows a 120 km transect within the Southern Prince Charles Mountains from 73°56' S 66°43' E to 73°14' S 65°3' E and is a view from west to east. The surface elevation ranges from 720 m asl within the centre of the Mellor Glacier to 1020 m asl on the ice that lies between Mount Bird and the ridge separating Mount Ruker (south) and Mount Rubin (north). The surface elevation of Mellor and Collins Glaciers is nearly 200 m lower than the ice over the Geysen Glacier.

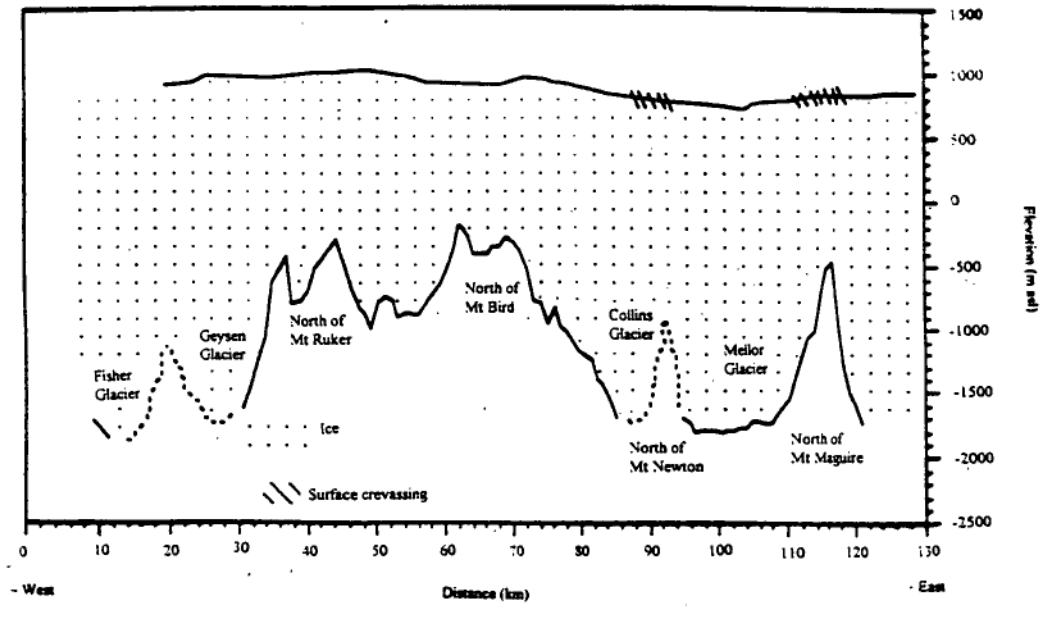

Figure 4.25. Profile derived from Flight 03 through the southern Prince Charles Mountains. Surface crevassing coincides with areas of ice thinning. The ice in this region is grounded and although north of Allison's (1979) velocity stations, is assumed to be moving at similar velocities of the order of tens of metres per year.

The section shows four significant drainage channels. A fifth channel would be the one containing the Fisher Glacier. The average thickness (over a distance of more than several times that of the ice depth) for the Mellor Glacier is 2500 m; Collins Glacier has been interpreted as being marginally deeper at 2550 m based on a slightly higher surface elevation. North of Mount Bird, the average thickness of the ice is 1180 m, while the average thickness of the ice north of Mount Ruker is 1200 m. In between these two ice free outcrops is thicker ice whose average thickness is 1770 m. The thickness of Geysen Glacier is in the order of 2770 m.

The relationship between surface elevation and ice thickness shows that this entire region is grounded ice. From this profile it has been possible to identify subglacial outcrops. As seen in Profiles #5 and #3, surface crevassing directly relates to rapid thinning of the ice mass. Based on this, the ice between 12 km and 18 km north of Mount Maguire has an intense region of surface crevassing which appears on the Landsat images of the Southern Prince Charles Mountains. Underlying this area it is assumed that an outcrop exists where the thickness of the ice rapidly changes from 2580 m to 1286 m. Approximately 35 km along the profile, the radio echo sounding signal was lost for a distance of 10 km, over a region of surface crevassing. On the basis of the association of surface crevassing with rapid ice thinning, it has been assumed that the outcrop that divides the Mellor Glacier from Collins Glacier is located here. The same principle was used to find the divide between the Geysen and Fisher Glaciers.

4.3.5 Total System

Based on the analysis of the eastern and western longitudinal profiles discussed in section 4.3.2, a conclusion can be made as to the location of the grounding zone (Figure 4.26). An area of rapid elevation descent, combined with a high incidence of crevassing is typical of a glaciers hinge line (Sharp, 1988). For the Lambert Glacier, this feature appears very near to the 400 m asl contour at the head of the confluence area of the Fisher, Geysen, Mellor and Lambert Glaciers (Appendix A). Further upstream of the 400 m contour interval there is continental ice that is fully grounded but possibly sliding due to the existence of subglacial melting. This 400 m contour is shown in Figure 4.26 (the eastern longitudinal profile) at 250 km from T4. In Figure 4.11 (the western longitudinal profile) it is apparent in the sudden large disparity between derived hydrostatic surface elevation (0.1Z) and the field data for surface elevation again at 250 km from T4.

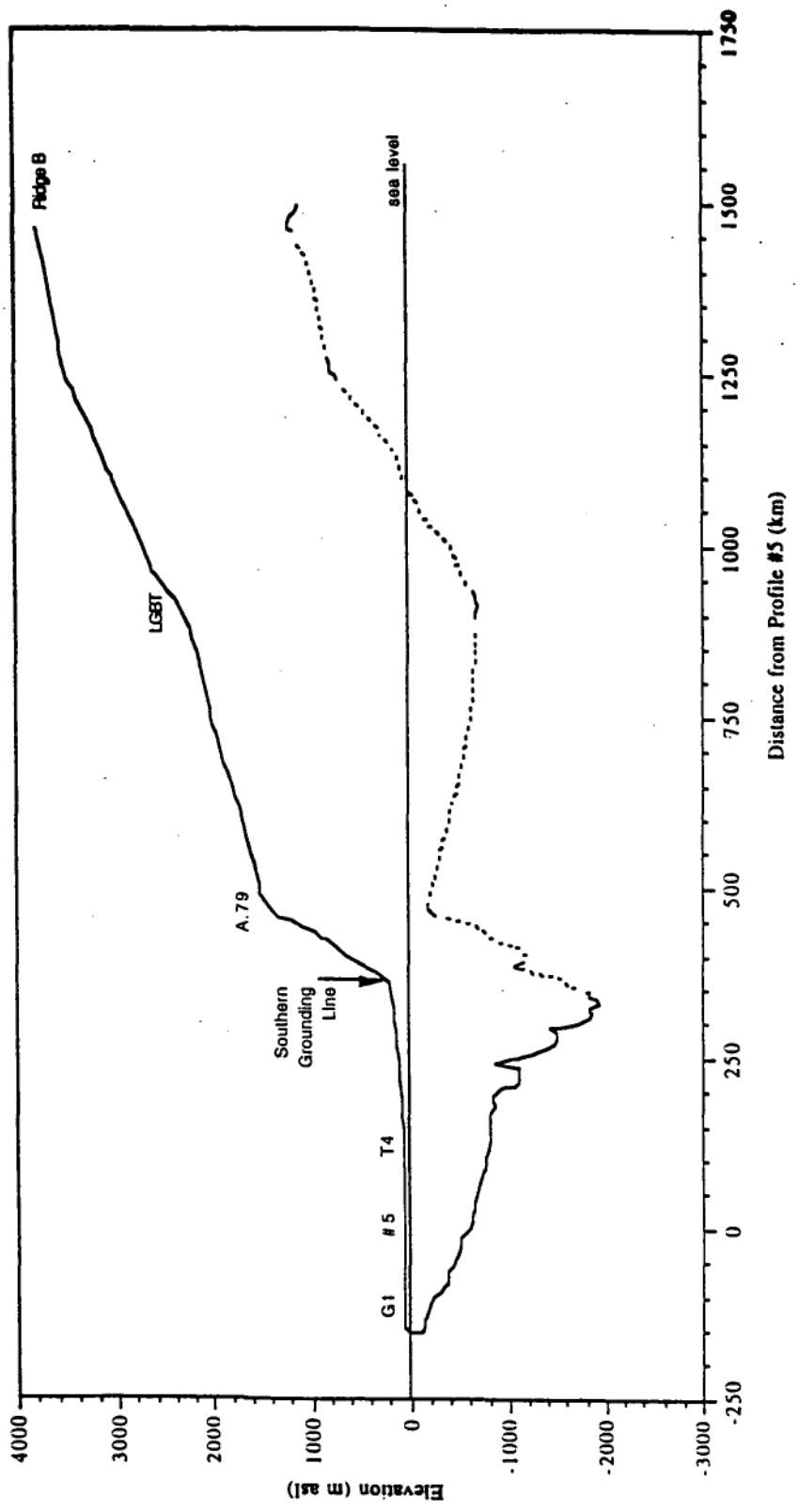

Figure 4.26 The interior ice sheet: transect from the Amery Ice Shelf front to Ridge B based on work by this author, Budd *et al.* (1982), Allison (1979), Higham (1994) and Drewry (1983).

The western longitudinal profile is more difficult to interpret owing to the flight path. As the profile descends Fisher Glacier, it does not enter the confluence region directly, but rather moves over the western edge of the graben close to Mount Stinear and therefore not providing Lambert Glacier ice thickness measurements. With this point in mind, the hinge line can be identified from the comparison between 0.1Z and surface elevation in Figure 4.12. Here the hinge line lies between 180 km and 250 km from T4. Due to the high incidence of signal drop-out from the radio echo sounding radar, and the existence of extensive crevassing in the same area, the transition zone between partial floating and the clear fully grounded region is assumed to lay within this 180 km to 250 km sector.

On the north-westerly reaches of the grounding zone, where the ice begins to float as the Amery Ice Shelf proper, it can be seen that the Lambert Glacier ice stream appears at least partially grounded until approximately 42 kilometres from T4 (Figure 4.11). In this western longitudinal profile, the region about the grounding zone is not consistently distinctive. Because the flight path is closer to the westerly grounded ice sheet, the indication is that the grounding zone exists up to T4 after which the track deviates and ascends Jetty Peninsula.

Extensive data analysis to determine the spatial distribution of the entire grounding zone of the Lambert Glacier has it existing, on average, between 71°39'S (~65 km south of T4) and 73°19'S, a total distance of 180 km. In this region an extensive surface melt lake system exists. These melt lakes are tens of kilometres in length. Towards T4, and during early summer, the melt lakes are predominantly quite shallow; only 20 cm deep from field observations (I. Allison, pers. comm. 1993). These types of ablation features may, however, become deeper with the ensuing summer season, or may become deeper further south. As discussed in Chapter One, ablation or net loss in Antarctica is primarily through ice berg calving away from the coast. Surface melt lakes exist in ablation zones and include the liquid stage in evaporation. Typically, ablation in Antarctica is by sublimation where the ice evaporates directly from a solid state to a vapour state. Surface melt lakes are seasonal and reach a maximum extent during the brief peak period of the Antarctic summer.

From the combination of ice thickness and surface elevations of the eastern and western longitudinal profiles, it would appear that the graben into which the Lambert Glacier system drains is deeper on its western side. Where the ice flows from the western grounded ice sheet into the drainage system, ice thickness varies

between the deeper grounded ice and the thinner floating ice mass. Coinciding with this deeper western profile is the extensive number of ice free outcrops of the northern and southern Prince Charles Mountains. A possible explanation for this thicker ice, between 20 km and 57 km along the western profile (Figure 4.11), is the mass flux flowing from the western grounded ice sheet and entering the Lambert Glacier system between Fisher Massif and Mount Meredith. In this area, the surface elevation rises from 90 m asl on the Lambert Glacier to over 700 m asl by the southern flank of Fisher Massif over a distance of 65 km; that is a surface gradient of 11.2 m per kilometre or 9.4×10^{-3} (Krebs, Figure 6.1a, 1992). This is a similar gradient to that around the Lambert Glacier hinge line were the tributary glaciers merge in the confluence zone opposite Mawson Escarpment.

The eastern longitudinal profile shows two distinct input depressions that coincide with the region between Mawson Escarpment and Clemence Massif and between Clemence Massif and Pickering Nunatak. A possible barb, or sediment trap, can be identified on this eastern profile 80 km from T4. This flattened region immediately south may be a sediment trap that arises from the changing nature of the ice mass from grounded to floating. The appearance of the overlying surface topography was mentioned in the discussion of the transverse profiles in the lower Lambert Glacier and Amery Ice Shelf area in section 4.3.4.

The more detailed information regarding ice thickness covers an area from Profile #5 to nearly 400 km south. As stated above, the major crevassing beyond the hinge line has meant that little RES data exists beyond 73° South. Two major flight paths cover this stretch of the lower Lambert Glacier. The flight along the eastern side of the drainage system and the return path on the western edge of the drainage system, coupled with all the other RES flights around 70° to 72° South have been used to create an ice thickness contour map of the lower Lambert Glacier drainage system (Figure 4.27).

Several features can be seen in this map. The thickest ice, 2000 m deep with a surface elevation of 180 m ± 20 m, is found on the eastern side of the confluence. By Clemence Massif, 100 km north, the ice is 1200 m thick. In the vicinity of Profile #3 the ice averages a thickness of 800 m with a surface elevation of 70 m ± 20 m. Underlying this ice, six independent channels of deeper ice, which are oriented in the direction of flow, are evident. With more detailed RES data upstream, this feature would be expected to appear further upstream than at Profile #3. This channelling pattern has been observed in the Ross Ice Streams

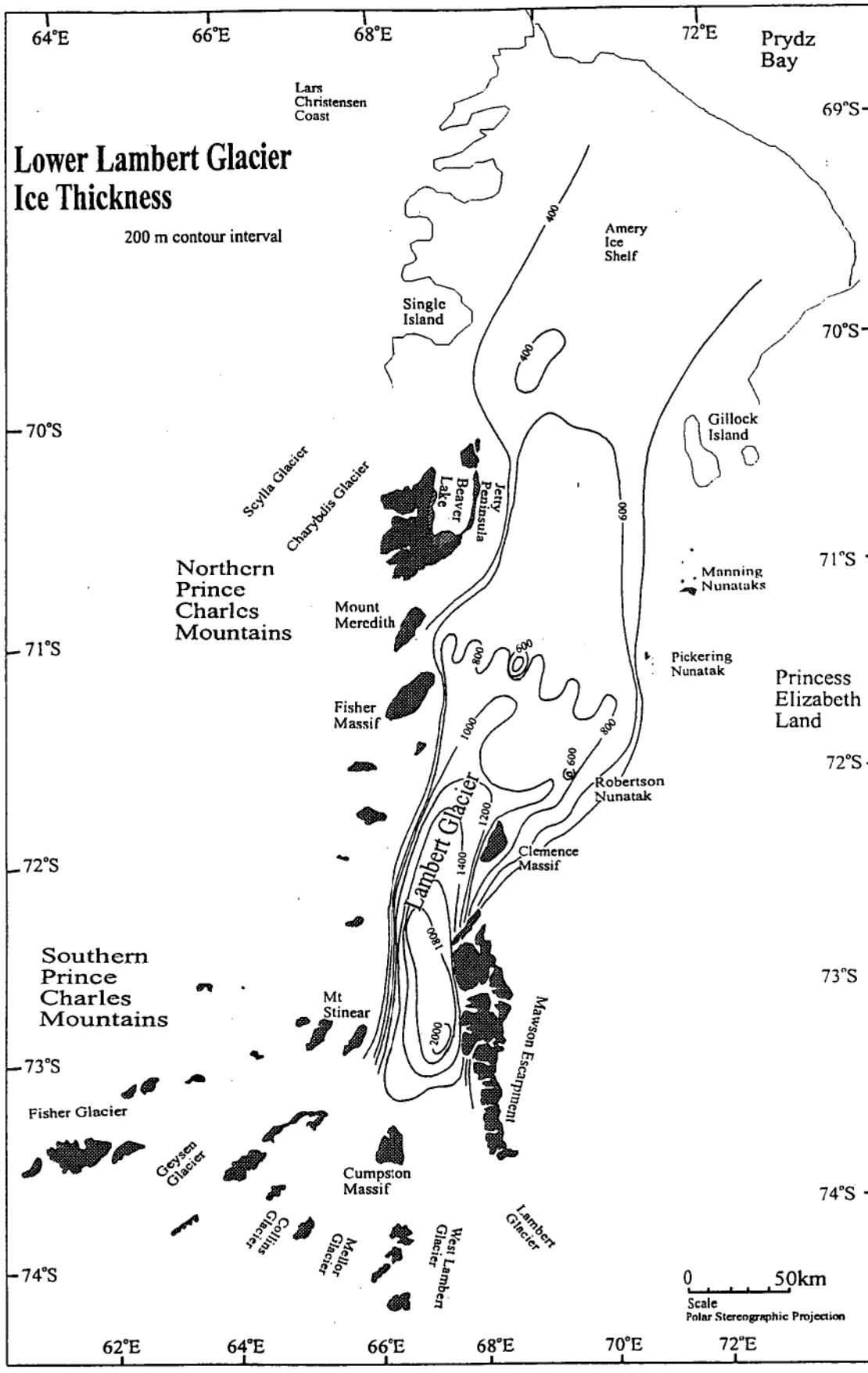

Figure 4.27. Ice thickness contour map of the lower Lambert Glacier and Amery Ice Shelf system based on RES data. The isolated grounded ice in the vicinity of Profile #3 (between Fisher Massif and Pickering Nunatak) is clearly visible as is the depression between Mawson Escarpment and Mount Stinear (the confluence region for the Lambert Glacier and its tributary glaciers).

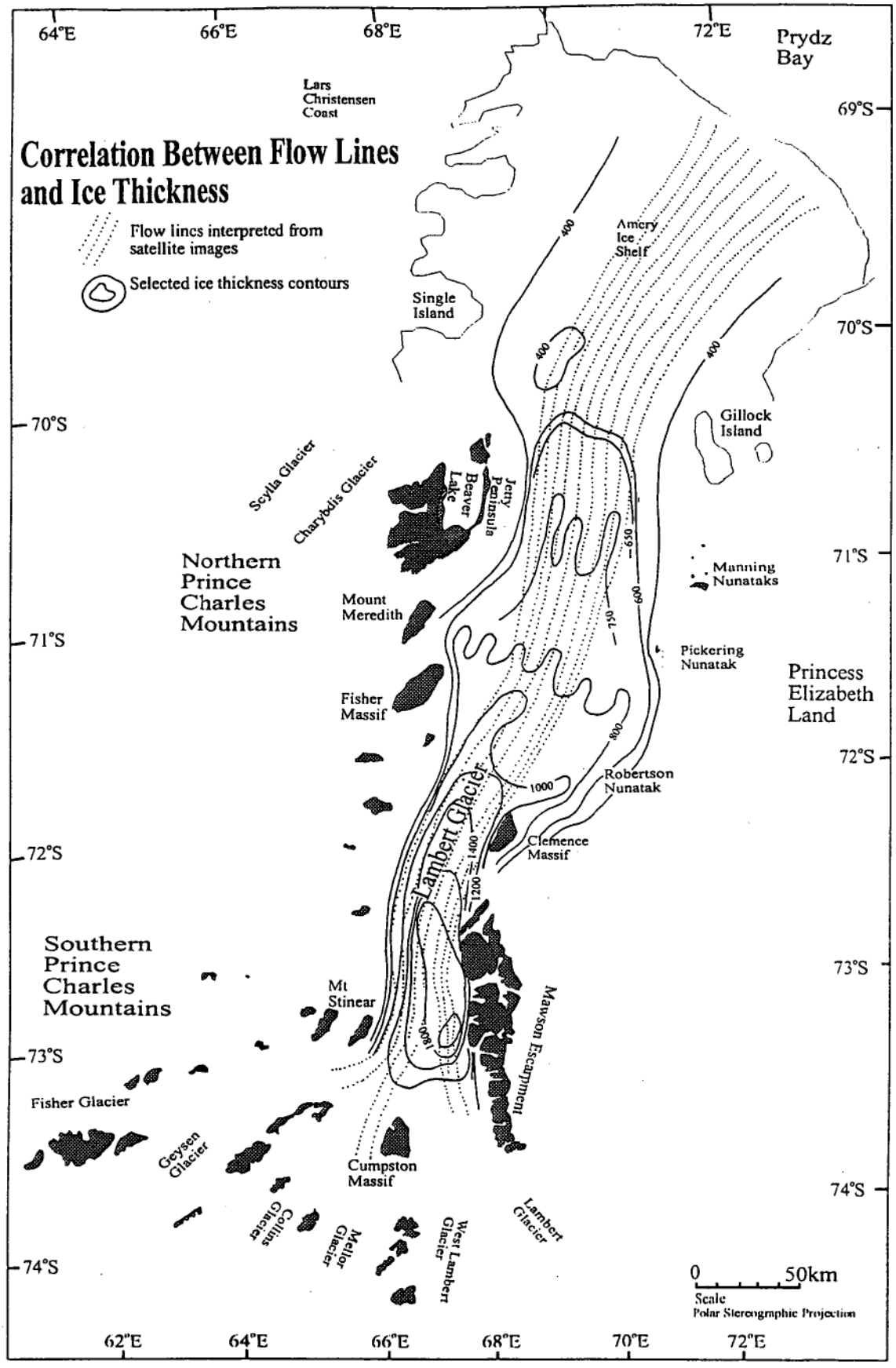

Figure 4.28. The combination of selective ice thickness contours and the Lambert Glacier flow lines establishes a trend about the morphology of the Lambert graben and the Lambert Glacier. Ice channelling primarily from the Fisher, Mellor and Lambert Glaciers are still evident as far north as Jetty Peninsula and Manning Nunataks. Between Fisher Massif and Clemence Massif, the bend in the flow lines coincides with a variation in ice thickness.

(Shabtaie and Bentley, 1988; Stephenson and Doake, 1982). If specific ice thickness contours are overlain with the flow lines of the Lambert Glacier (Figure 4.28) then between Jetty Peninsula and Manning Nunataks three distinct channels are still visible. The western channel can be traced back via satellite interpretation to the Fisher and Geysen Glaciers. The central channel has been traced upstream to the Mellor Glacier with some input from the smaller Collins Glacier. The eastern channel corresponds with the Lambert and West Lambert Glaciers.

The grounded point of ice on Profile #3 can be linked with a change in the preferred direction of flow within the ice stream, where the ice rapidly thins to 300 m. Beyond this grounded point, the Fisher and Geysen Glacier contributions widen. The second grounding point at Profile #5 similarly appears to divert the flow of the Lambert Glacier ice stream and also marks the boundary between the Scylla/Charybdis and Lambert Glaciers. This grounding point east of Single Island may be a continuation of Jetty Peninsula. The continual crevassing between Else Platform and the grounding zone may also be due to the merging of the Northern Prince Charles Mountains drainage and Southern Prince Charles Mountains drainage system.

Ice thickness data to be discussed in Chapter Five are taken from the eastern side of the Lambert Glacier system. This is so that a consistency in data can be maintained. That is, the various interpolations have been predominantly related to the Mellor and Lambert tributary glaciers which are in part measured by the eastern longitudinal profile. It is also believed that due to navigational difficulties during the field data collection, that the western longitudinal profile may have drifted too far westward in places. This is especially of concern around the hinge line. What the western longitudinal profile does indicate is that the ice on the western side of the lower Lambert Glacier drainage system is of the order of 200 m thicker than the ice on the eastern side. This could be due to the western plateau draining with a steep surface gradient into the graben and consequently resulting in a form of overburden. The western plateau ice flows into the drainage system more perpendicularly to the direction of the Lambert Glacier flow, but the eastern plateau ice enters the graben at a more oblique angle. Due to Mawson Escarpment the ice originating from Princess Elizabeth Land does not flow into the graben until north of Clemence Massif.

Figure 4.29 shows ice thickness, surface elevation and ice stream width. The graph incorporates point data from G1 to Profile #1 as well as point data from Point A to

D. This graph also contains information about the activity of the ice which has been derived from the Mellor and Lambert Glacier. Ice stream width measurements halt at Point D due to lack of T M satellite image data but point data at A.79 and LGB have been included from Allison (1979) and Higham (1994). Figures 4.28 and 4.29 show that ice stream width increases steadily the further north the observation is taken from Profile #2.

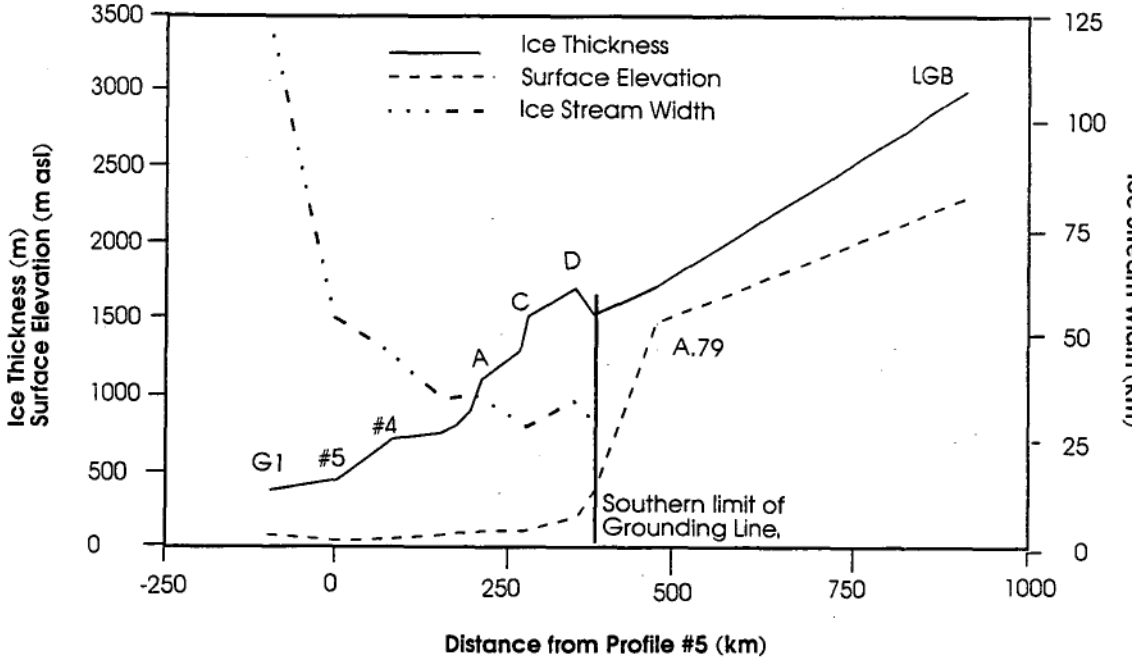

Figure 4.29. Ice thickness, ice stream width and surface elevation for the Lambert Glacier based on average values from the Lambert and Mellor ice streams. LGBT values are from Allison (pers. com., 1995). The A.79 values have been averaged from the stations 10, 8 and 7 (after Allison, 1979). G1 is derived from the work done by Budd *et al.* (1982). Profile #5 is 120 km north of T4.

The relationship between surface elevation and ice thickness is also shown in Figure 4.29. Where the surface elevation drops quickly between the A.79 transect

and Point D (between 350 km and 450 km from Profile #5) the ice thickness also begins to decrease though at a much slower rate and shows a delayed response to this slope change. Further RES information through the Southern Prince Charles Mountains may assist in better outlining the ice morphology around the confluence. The area of the confluence (around Point D) shows the ice thickening before rapidly thinning as the ice stream widens beyond Profile #2. The change at approximately 375 km from Profile #5 is interpreted as the Southern Grounding Line or the hinge line.

4.4 The Grounding Zone of the Lambert Glacier and Amery Ice Shelf System

Surface elevation trends in both the longitudinal profiles and the five cross sections show that the western side of the Lambert Glacier and Amery Ice Shelf system has a typically higher western elevation than on the east. Especially in the area of Profiles #1 to #3, this higher surface elevation coincides with a large prevailing area of blue ice. This area of distinct ablation is apparent in satellite images.

Coinciding with a higher western surface elevation is greater ice thickness on the western side of the system. As discussed above, this deeper ice could be attributable to the occurrence of the ice free outcrops and consequential subglacial valleys that are formed between the Northern Prince Charles Mountains. This allows for a greater volume of ice to pass into the Lambert Glacier and Amery Ice Shelf system.

The pattern displayed in the analysis of the buoyancy of each profile has shown a trend towards greater buoyancy the further northward the profile extends. This agrees with previous work by Budd *et al.* (1982), Partington *et al.*(1987), Hambrey (1991) and Hellmer *et al.* (1992). The body of ice, especially the ice specific to the Lambert Glacier ice stream, is more readily definable as floating on the eastward side on all the five profiles analysed in this chapter. Between Profile #3 and Profile #4, the Lambert Glacier ice stream expands from an average width of 34 km to 42 km. There is only one major "sticky point" in the ice at Profile #3. Across Profiles #2 and #1 there are grounded and floating ice across each transect. By Profile #4 there is no more evidence of grounded ice as the glacier flows as a floating body of ice in the Amery Ice Shelf along the eastern portions of the ice

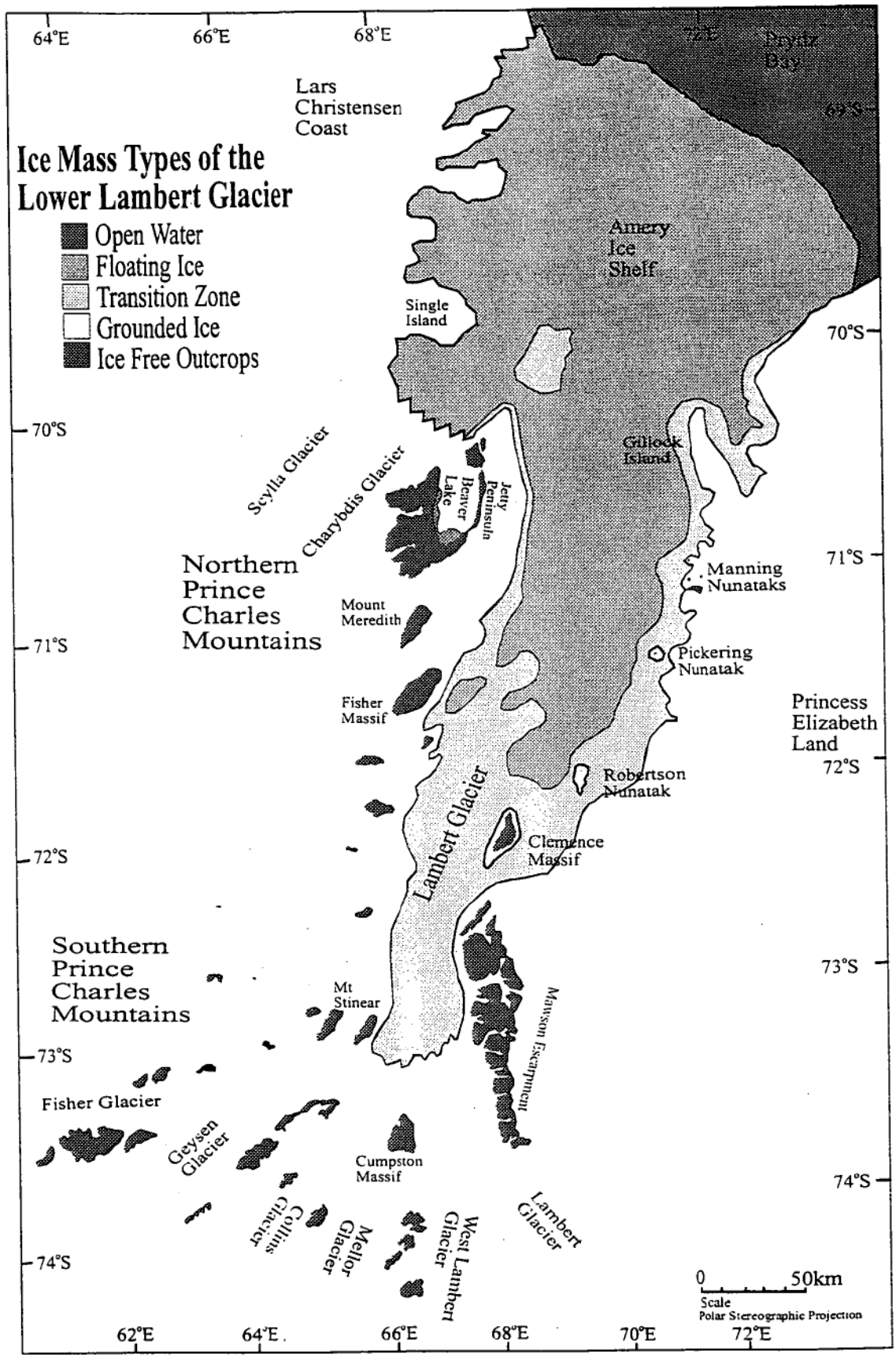

Figure 4.30. The redefined boundaries of the ice mass types of the Lambert Glacier and Amery Ice Shelf system. This map is based on satellite image interpretation, driving stress calculations and basal ice profiles.

shelf out into Prydz Bay. Across Profile #5 the ice is disrupted by a grounded zone where the Scylla/ Charybdis Glacier flows into the Amery Ice Shelf.

This chapter has discussed the morphology of the lower Lambert Glacier and Amery Ice Shelf system. Flow lines and tributary ice stream interpretation has been based on the available satellite imagery (Appendix A and B). This has been combined to identify the Lambert Glacier ice from tributary and other grounded ice sources as the system undergoes a transition from ice stream to ice shelf. RES data have only partially contributed to the definition of the lateral parameters of the grounding zone of the lower Lambert glacier. The limitations on the spatial extent of the RES flights conducted has meant that the eastern side of the drainage system was defined essentially from geomorphological interpretation from Landsat MSS images (after Swithinbank, 1988). The break of slope 'line' was identified as the boundary between grounded and floating ice coupled with a rapid change in direction of the flow lines draining a portion of Princess Elizabeth land into the lower Lambert Glacier and Amery Ice Shelf system. The Lambert Glacier grounding zone is proposed to exist between 72° South and 73°30' South, 255 km from T4, where the surface elevation begins to rise southwards at a gradient of 100 m per kilometre. (Figure 4.30)

A grounding zone is a broad region where an ice mass starts to partially float. Where grounding occurs over a large isolated area, the ice may begin to dome in shape, and form an ice rise, which creates independent flow patterns (Paterson, 1994). Ice rumples are regions of surface undulations that move with an ice shelf due to grounding zones which are not impacting on the entire ice stream at the same location (Paterson, 1994). Within the zone of transition from grounded to floating ice, the behaviour or dynamics of the ice changes from a regime of basal shear to a friction-less base and longitudinal stress gradients. Some of these dynamics are discussed further in Chapter Five.

Although grounding zones are often thought of as transitional areas only a few times the length of the ice thickness, they are not usually sharply defined lines. The low surface slope of the Lambert Glacier and small driving stresses coupled with the appearance of the ice stream flow lines suggest that the Lambert Glacier grounding zone is a large area of the Lambert Glacier and Amery Ice Shelf system.

Chapter Five

Dynamics of the Lambert ice stream and Amery Ice Shelf System

5.1 Introduction

This chapter is a discussion on the dynamics of the lower Lambert Glacier and Amery Ice Shelf system based on the conclusions and results derived primarily from Chapter Four. Satellite imagery has provided detailed surface characteristics over the area for the interpretation of the ground based data. Radio Echo Sounding (RES) data have highlighted ice thickness patterns that have led to the redefined Lambert Glacier grounding zone. The results from the ice surface velocity data are now coupled with the results from the ice thickness profiles in this chapter to examine the mass fluxes and the ice dynamics. The combination of this thickness and surface feature information including net accumulation will allow mass flux and driving stresses of the ice to be calculated and used in the further verification of the parameters for the grounding zone of the Lambert Glacier and Amery Ice Shelf system. All calculations have been made initially under the assumption that the Lambert Glacier is a system in equilibrium. The results of the computed horizontal fluxes and surface net accumulation allow estimates to be made of the net rate of thickness change or implied basal melt rates. Combined, these calculations reinforce the redefined grounding zone described in Chapter Four. The net mass budget will be discussed further in Chapter Six.

5.2 Velocity and mass flux across the lower Lambert ice stream and Amery Ice Shelf.

5.2.1 Velocity Data.

During the austral summers of 1988-89 to 1989-90 ice movement was measured by differential carrier-phase GPS survey in the area predominantly covered by the

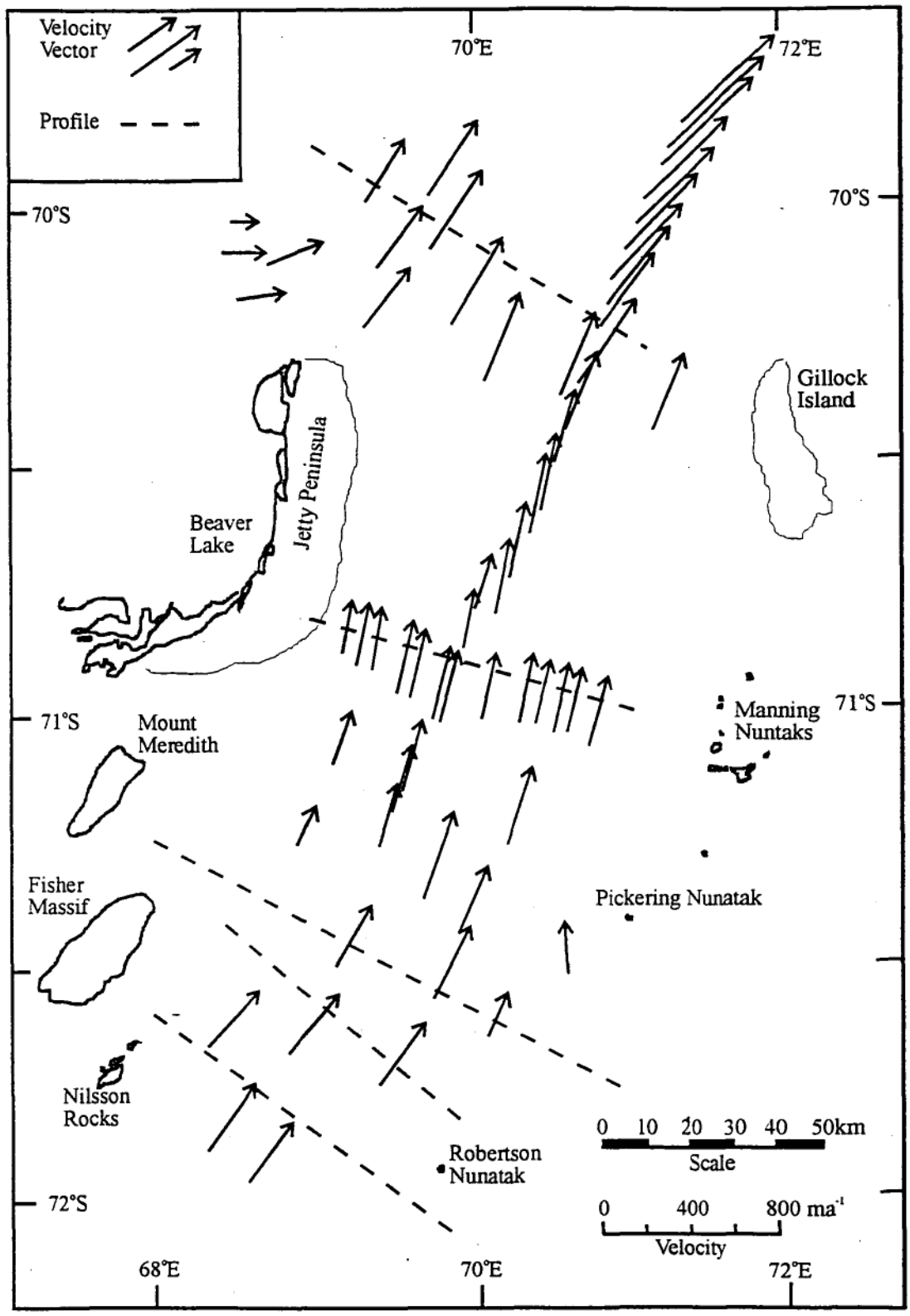

Figure 5.1. Velocity vectors used to determine the dynamics of the Lambert Glacier ice stream and the Amery Ice Shelf in the region of the northern reaches of the grounding zone. Profile #1 is at the bottom of the page and Profile #5 (and north) is towards the top of the page. These velocity vectors are from Table 5.1 in Appendix D)

RES flights. Earlier data on ice movement were also available from the Amery Ice Shelf Project of 1968 to 1970 (Budd *et al.*, 1982). The 1968-69 data were obtained from theodolite and electronic distance measuring (EDM) traverses (Appendix D). These measurements extended over an area 69° South to 72° South. Velocity was measured by return visits to stakes that had been fixed in their initial location and remeasured. Using the velocity measurements from Budd *et al.* (1982) and those collected during the 1988-89 austral summer, a smoothed velocity profile was interpolated to coincide with each of the ice thickness cross sections of Chapter Four (Figure 5.1).

Figure 5.2a and Figure 5.2b present summary illustrations of the ice movement down the lower Lambert Glacier and Amery Ice Shelf system. Profiles #1 to #5 are all centred with relation to the "centre line" positions corresponding to A129 (or G3; Budd *et al.*, 1982) and hence centred relative to each other. Included in Figure 5.2b is the velocity profile derived by Budd *et al.* (1982) from T2 to T3 via G3. As stated in the previous chapter, this G3 cross section very nearly is overlain by Profile #4. The slight discrepancy between the two velocity profiles is possibly due to varying methodology in interpolation used by this author and Budd *et al.* (1982).

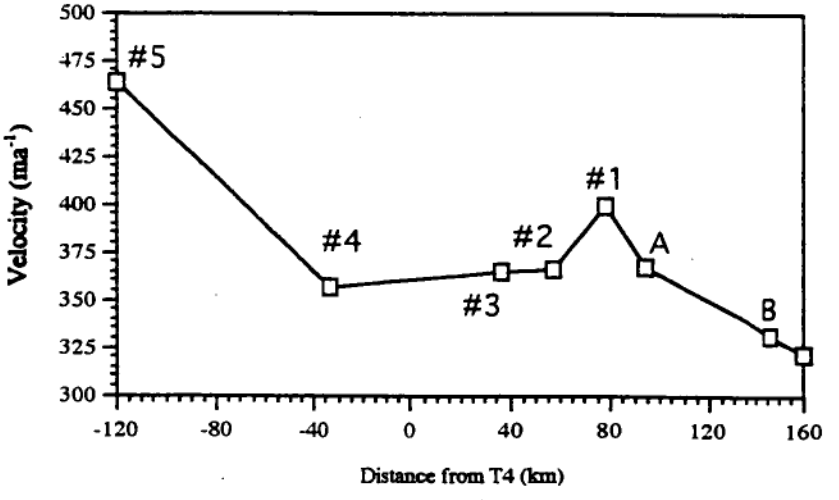

Figure 5.2a Longitudinal profile of velocity based on the average surface ice movement rate (calculated from the carrier-phase GPS surveys in 1988-89 and 1990-91) of each cross section on the lower Lambert Glacier and Amery Ice Shelf based on Figure 5.2b.

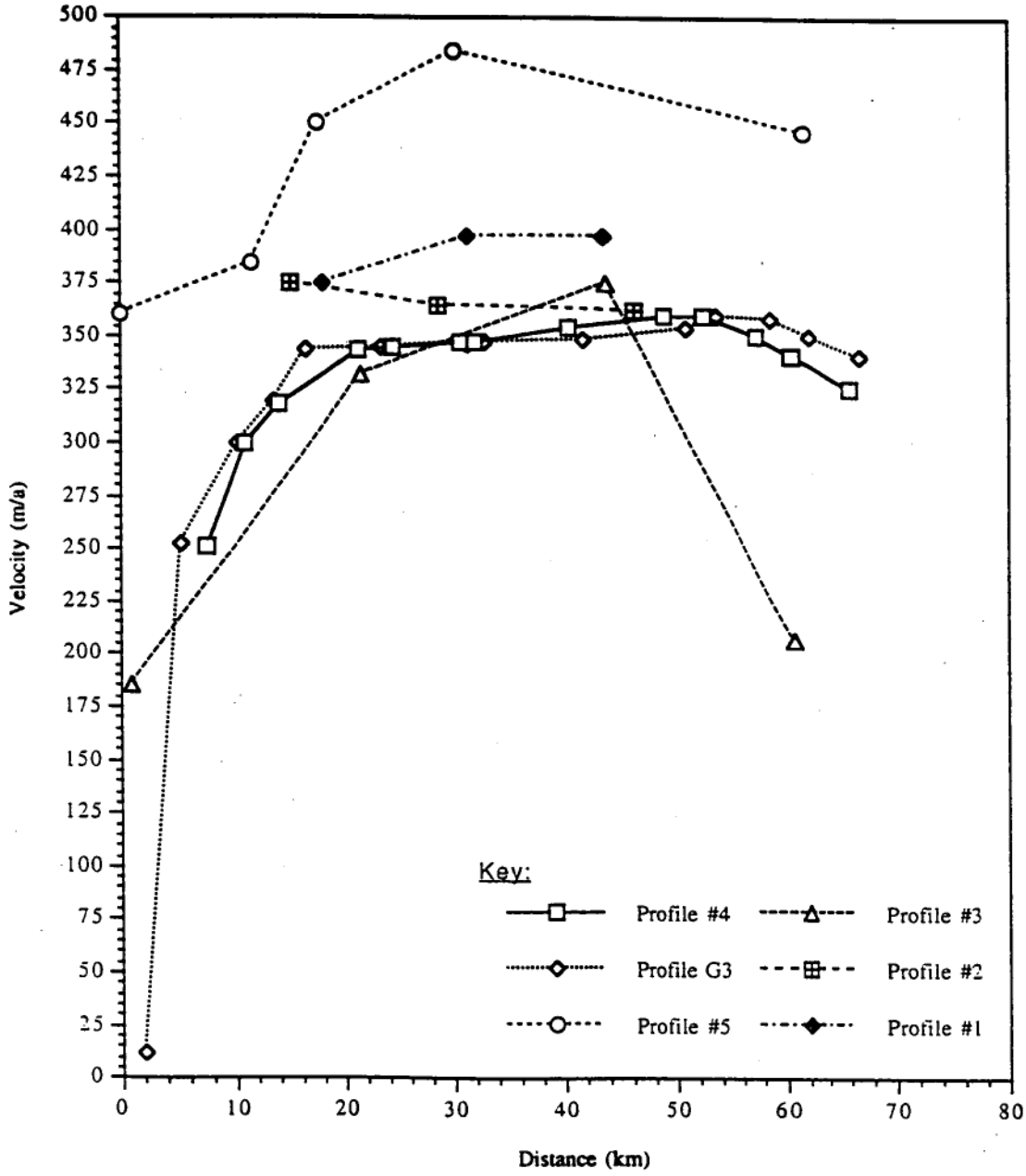

Figure 5.2b. A comparison of cross section velocity curves between Profiles #1 to #5. These velocity profiles are the measured values and are in turn compared to the results of Budd *et al.* (1982) across G3. All these profiles have been centred to match the G3 profile.

The velocities across Profile #1 averages 397 ma^{-1} and this is the second fastest flowing transect. Twenty-seven kilometres north, at Profile #2, the rate of ice movement has slowed by nearly 50 ma^{-1}. By the third profile another 15 km north, the rate of ice surface velocity has reduced even further. At Profile #4 the velocity of the ice passing through the transect has begun to increase, though not reaching the rate of flow passing through Profile #1 and #2. Profile #5 as would be expected, has the highest velocity of ice movement of all the profiles. Even the ice entering the system from the Charybdis and Scylla Glaciers is flowing more rapidly than the previous four profiles of Lambert Glacier ice. This suggests that despite the "sticky spot" located in Profile #5, the remaining ice is probably free-floating.

5.2.2 Mass Flux Data

The discussion in Section 5.2.3 about the velocity across the five transects is accompanied by five illustrations, one for each profile. These graphs (Figures 5.4 to 5.8) also illustrate ice thickness and mass flux per unit width. Ice thickness across the transects was discussed in Chapter Four. Mass flux has been derived from estimated ice densities, ice thickness, velocity and cross section distance. Ice densities have been assumed from the following argument. The mass budget summary will be presented in Chapter Six.

Based on satellite image interpretation, 'blue ice' can be visually separated from areas on the drainage system that are possible accumulation zones. As pure ice has a density of 917 kgm^{-3} (Paterson, 1994) it will be assumed that the ice at profile #1 is 900 kgm^{-3}. In the area of Profile #1, half the transect is within a zone of 'blue ice'. The work of Budd *et al.* (1982) at G1 produced an ice density at G1 of 854 kgm^{-3}. In this study, Profile #5 will be considered as being in a very similar environment, so for the purpose of these mass flux calculations, Profile #5 has an ice density of 850 kgm^{-3}. Because Profile #1 and Profile #2 are close together and share a visibly similar surface environment, the ice density at Profile #2 is assumed to be 900 kgm^{-3}. Profile #3 is further north and appears as an area of both 'blue ice'

and surface accumulation. In maintaining a form of continuity between the assumed densities at Profile #1 and Profile #5, the average density at Profile #3 is estimated at 890 kgm^{-3}. Profile #4 is assumed to have an average density of 870 kgm^{-3}.

The estimation of mass flux has been limited to the region of the five profiles because they are transects with velocity and thickness data measured orthogonal to the direction of flow, as with the G1 profile of Budd *et al* (1982). Given that the results discussed earlier indicate that these five transects are either part of the Amery Ice Shelf and floating or show extensive basal sliding, the depth averaged velocity is assumed to be equal to the measured surface velocity.

Mass flux rate (Q) is given by:

$$Q = \int \rho v z dy \qquad \text{(Equation 5.1)}$$

Where ρ is the average column density of the ice, v is the average column velocity, z is ice thickness and y is the distance orthogonal to the flow of the ice.

Table 5.1 is a summary of the mass flux calculations for Profiles #1 to #5. In tables 5.2 to 5.6, the mass fluxes across Profiles #1 to #5 are presented. These tables are derived from measured ice thickness points, extrapolated orthogonal to the direction of ice flow and from various radio echo sounding data. The velocity data are interpolated between measured movement stations. Across the 84 kilometres of Profile #1, the total mass flux is 22.7 Gta^{-1} and for that part of the section defined as the Lambert ice stream the mass flux is 11.0 Gta 01 ±15% (Table 5.2). The average flux per unit width is 0.27 Gta^{-1} per kilometre. Profile #2 has a mass flux of 20.4 Gta^{-1} over 68 km (Table 5.3). The Lambert ice stream has a mass flux per kilometre of 11.3 ± 15%. The average mass flux for this section is 0.3 Gta^{-1} for its 119 km measured profile (Table 5.4). The total mass flux of Profile #3 is 16.1 Giga-tonnes per annum ± 15%. The average mass flux per unit width for Profile #4 is 0.19 Gta^{-1}. The 75 kilometre profile has a total mass flux of 14.7 Giga-tonnes per annum ± 15% (Table 5.5). The fifth cross section has measurements extending

	Q	$Q_{per\ unit\ width}$	$Q_{Lambert\ Glacier}$
	(Gt a^{-1})	*(Gt $a^{-1}km^{-1}$)*	*(Gt a^{-1})*
Profile #1	22.7	0.27	11.04
Profile #2	20.4	0.30	11.3
Profile #3	16.1	0.15	8.5
Profile #4	14.7	0.19	9.85
Profile #5	13.9	0.19	9.89

Table 5.1. Summary table of the mass flux across each profile, the Lambert Glacier and the average mass flux per unit width. This data is expanded in Tables 5.2 to 5.6.

Profile #1 Distance (km)	Ice Thickness (m)	Surface Velocity (ma^{-1})	Mass Flux per unit width (Gt km^{-1} a^{-1})	Total Mass Flux for segment (Gt a^{-1})
0	214	200		
4	893	293	0.12	0.19
6	750	333	0.23	0.16
11	875	375	0.26	1.29
14	***1071***	***387***	***0.33***	***1.00***
19	***875***	***393***	***0.34***	***1.71***
24	***893***	***400***	***0.32***	***1.58***
30	***786***	***400***	***0.30***	***1.81***
34	***821***	***400***	***0.29***	***1.16***
40	***820***	***398***	***0.29***	***1.77***
47	***786***	***398***	***0.29***	***2.01***
50	750	400	0.28	0.83
53	694	402	0.26	0.78
57	714	407	0.26	1.03
64	821	410	0.28	1.98
67	1143	415	0.36	1.09
68	964	415	0.39	0.39
70	1125	405	0.39	0.77
72	500	407	0.30	0.59
74	536	393	0.19	0.37
76	714	387	0.22	0.44
78	446	360	0.19	0.39
82	428	275	0.12	0.50
84	500	200	0.10	0.20
		Average	**0.27**	
			TOTAL	**22.65**
			Total for Lambert ice stream	**11.04**

Table 5.2. Based on a density of 900 kgm^{-3}, calculations for the mass flux across Profile #1 are presented. Ice thickness is from Figure 4.18, and velocity is taken as the mean between segments based on a smoothed velocity curve. Bold and italic numbers are for values within the Lambert ice stream.

Profile #2 Distance (km)	Ice Thickness (m)	Surface Velocity (ma^{-1})	Mass Flux per unit width ($Gt\ km^{-1}\ a^{-1}$)	Total Mass Flux for segment ($Gt\ a^{-1}$)
0	885	350		
3	827	363	0.27	0.82
7	885	369	0.28	1.13
12.5	***980***	***375***	***0.31***	***1.72***
15	***923***	***373***	***0.32***	***0.80***
20	***1000***	***368***	***0.32***	***1.60***
27	***923***	***365***	***0.32***	***2.22***
32	***1000***	***365***	***0.32***	***1.58***
38	***942***	***365***	***0.32***	***1.91***
43	***846***	***365***	***0.29***	***1.47***
48	884	368	0.29	1.43
54	865	369	0.29	1.74
5705	884	369	0.29	1.02
64	846	368	0.29	1.86
68	865	358	0.28	1.12
		Average	**0.30**	
			TOTAL	**20.42**
			Total for Lambert ice stream	**11.30**

Table 5.3. Based on a density of 900 kgm^{-3}, calculations for the mass flux across Profile #2 is presented. Ice thickness is from Figure 4.20, and velocity is taken as the mean between segments based on a smoothed velocity curve. Bold and italic numbers are for values within the Lambert ice stream.

Profile #3 Distance (km)	Ice Thickness (m)	Surface Velocity (ma^{-1})	Mass Flux per unit width ($Gt\ km^{-1}\ a^{-1}$)	Total Mass Flux for segment ($Gt\ a^{-1}$)
0	634	28		
5	692	40	0.02	0.10
10	865	50	0.03	0.16
15	730	69	0.04	0.21
20	807	110	0.06	0.31
25	769	167	0.10	0.49
30	730	208	0.13	0.63
36	***827***	***250***	***0.16***	***0.95***
40	***923***	***275***	***0.20***	***0.82***
44	***384***	***300***	***0.17***	***0.67***
46	***692***	***311***	***0.15***	***0.29***
50	***826***	***340***	***0.22***	***0.88***
56	***807***	***364***	***0.26***	***1.53***
62	***769***	***375***	***0.26***	***1.55***
69	***769***	***375***	***0.26***	***1.80***
75	807	353	0.26	1.53
80	769	311	0.23	1.16
86	750	234	0.18	1.11
91	730	161	0.13	0.65
96	827	120	0.10	0.49
100	807	100	0.08	0.32
109	634	70	0.05	0.49
		Average	**0.15**	
			TOTAL	**16.13**
			Total for Lambert ice stream	**8.50**

Table 5.4. Based on a density of 890 kgm^{-3}, calculations for the mass flux across Profile #3 is presented. Ice thickness is from Figure 4.22, and velocity is taken as the mean between segment based on a smoothed velocity curve. Bold and italic numbers are for values within the Lambert ice stream.

Profile #4 Distance (km)	Ice Thickness (m)	Surface Velocity (ma^{-1})	Mass Flux per unit width (Gt km^{-1} a^{-1})	Total Mass Flux for segment (Gt a^{-1})
0	270	12		
5	615	200	0.04	0.20
9	730	280	0.14	0.56
13	730	309	0.19	0.75
15	***730***	***330***	***0.20***	***0.41***
17	***769***	***335***	***0.22***	***0.43***
24	***730***	***345***	***0.22***	***1.55***
30	***770***	***350***	***0.23***	***1.36***
36	***770***	***353***	***0.24***	***1.41***
43	***770***	***359***	***0.24***	***1.67***
50	***750***	***362***	***0.24***	***1.67***
56	***692***	***352***	***0.22***	***1.34***
64	692	330	0.21	1.64
70	596	295	0.18	1.05
75	596	245	0.14	0.70
		Average	**0.19**	
			TOTAL	**14.75**
			Total for Lambert ice stream	**9.85**

Table 5.5. Based on a density of 870 kgm^{-3}, calculations for the mass flux across Profile #4 is presented. Ice thickness is taken from Figure 4.24, and velocity is taken as the mean between segments based on a smoothed velocity curve. Bold and italic numbers are for values within the Lambert ice stream.

Profile #5 Distance (km)	Ice Thickness (m)	Surface Velocity (ma^{-1})	Mass Flux per unit width (Gt km^{-1} a^{-1})	Total Mass Flux for segment (Gt a^{-1})
0	423	230		
6	577	325	0.12	0.71
10	500	335	0.15	0.60
15	500	358	0.15	0.74
20	461	366	0.15	0.74
23	346			
28	307			
33	307			
36	500	481	0.08	0.25
39	***577***	***481***	***0.22***	***0.66***
41	***580***	***481***	***0.24***	***0.47***
44	***461***	***484***	***0.21***	***0.64***
51	***576***	***487***	***0.21***	***1.50***
58	***576***	***481***	***0.24***	***1.66***
64	***557***	***475***	***0.23***	***1.38***
71	***519***	***465***	***0.21***	***1.50***
77	***538***	***453***	***0.21***	***1.24***
81	***576***	***431***	***0.21***	***0.84***
86	519	411	0.20	0.98
		Average	**0.19**	
			TOTAL	**13.90**
			Total for Lambert ice stream	**9.89**

Table 5.6. Based on a density of 850 kgm^{-3}, calculations for the mass flux across Profile #5 is presented. Ice thickness is from Figure 4.26, and velocity is taken as the mean between segments based on a smoothed velocity curve. (Between 23 km and 33 km, no surface velocity measurements were collected. Owing to the apparent grounding of the ice in this region, no calculations for mass flux rate were attempted). Bold and italic numbers are for values within the Lambert ice stream.

over a total length of 86 km. The total mass flux is 13.9 Giga-tonnes per annum with the maximum flux within the Lambert ice stream being 9.9 Gta^{-1} and with the average flux across the transect of 0.19 Giga-tonnes per annum. Figure 5.3 graphs the results from the Tables 5.2 to 5.6.

In all the mass flux calculations for the entire cross section, only in Profile #1 did the maximum flux per unit width occur outside of the defined Lambert Glacier ice stream. In Profile #2, the maximum flux was in the central flow region. In Profile #3 the maximum flux occurred on the eastern extreme of the ice stream. The maximum flux of Profile #4 is three-quarters of the way across the Lambert Glacier ice stream, in an eastward direction. In Profile #5, the maximum flux occurs west of the central flow of the Lambert Glacier ice stream. Profile #1 has a maximum flux coincidental with the deepest ice at the easterly grounded ice sheet confluence with the Amery Ice Shelf and Lambert Glacier System.

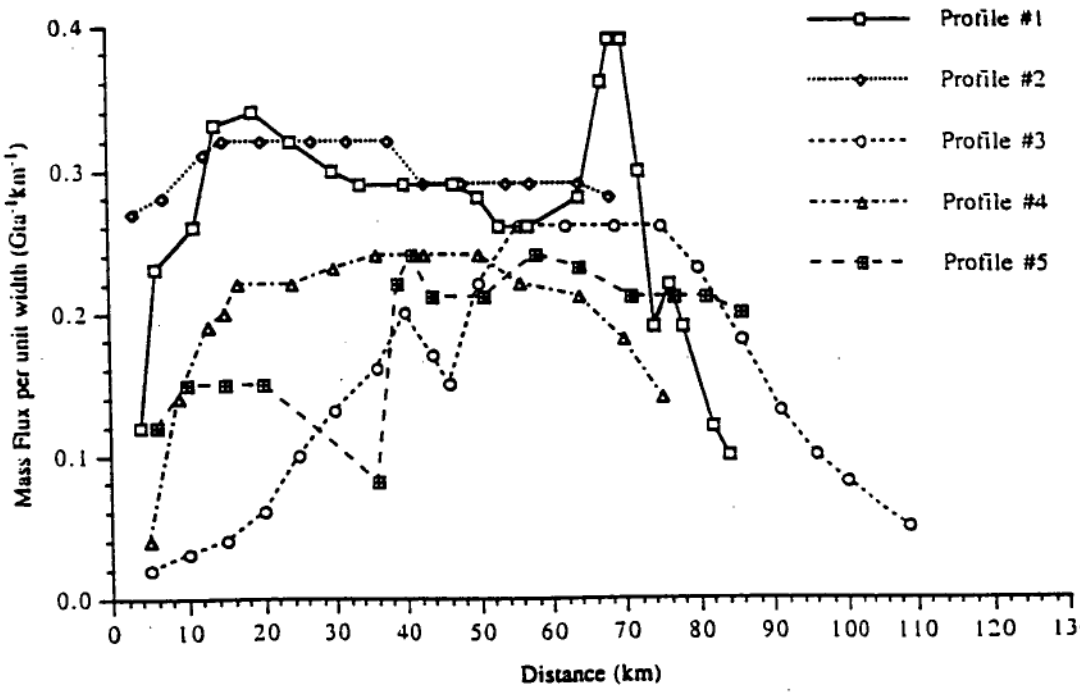

Figure 5.3. Flux rate per unit width of Profiles #1 to #5. This comparison graph has been produced from data with a weighted mean of three applied to the calculations of mass flux per unit width (7 km). The graph is viewed west to east.

5.2.3. Smoothed cross section profiles of velocity and mass flux

Profile #1

The cross section for Profile #1 (Figure 5.4) indicates faster flowing ice towards the eastern edge of the ice mass. This is where the ice is deeper and the surface elevation is slightly lower, along the perimeter of the glacial trough and the easterly grounded ice sheet contribution. The ice is flowing at approximately 425 ma^{-1}, while the Lambert Glacier ice stream is moving at 397 ma^{-1}. This relationship between ice velocity and ice thickness is consistent with the calculations of surface

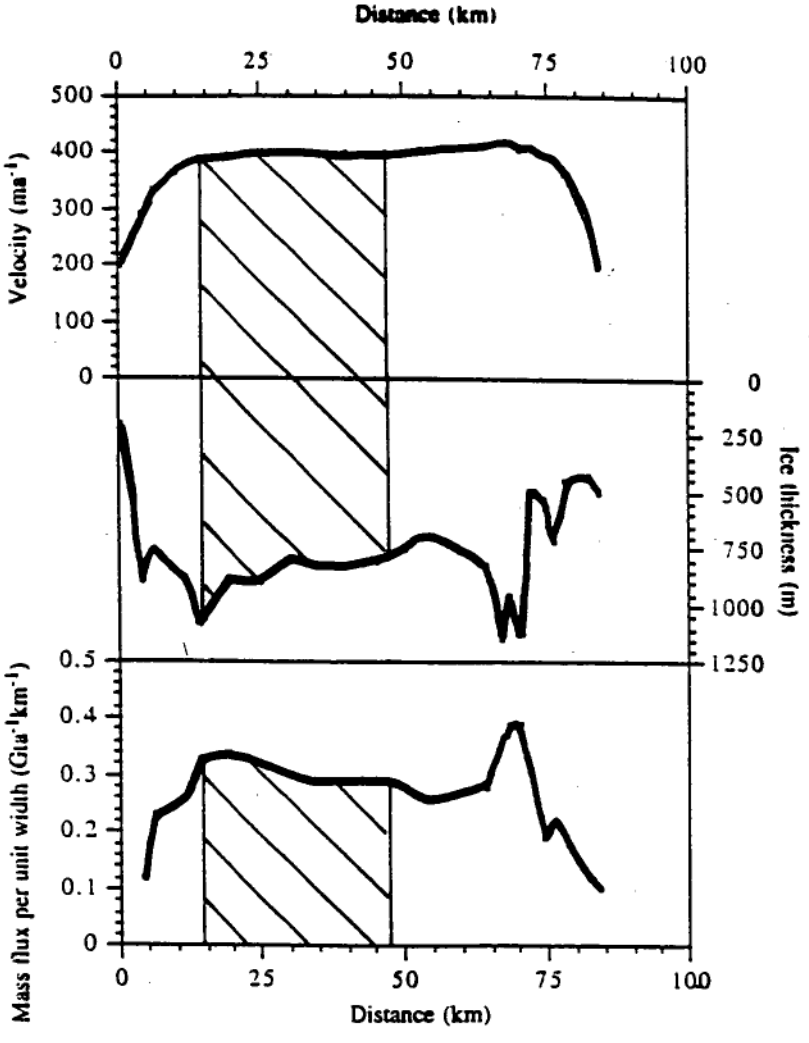

Figure 5.4. Velocity curve, ice thickness profile and mass flux graphs for Profile #1. The Lambert Glacier ice stream is situated between 14 km and 47 km along the transect.

elevation for hydrostatic equilibrium discussed in Chapter Four. This suggests that across Profile #1 there is predominantly a floating ice mass and not a grounded glacier or ice stream.

Profile #2

Within the defined flow of the Lambert Glacier ice stream across Profile #2, the velocity has been interpolated (Figure 5.5) and indicates that faster flowing ice is towards the western margin of this profile. This coincides with the deeper ice and larger ice thickness and higher surface elevation discussed on Chapter Four.

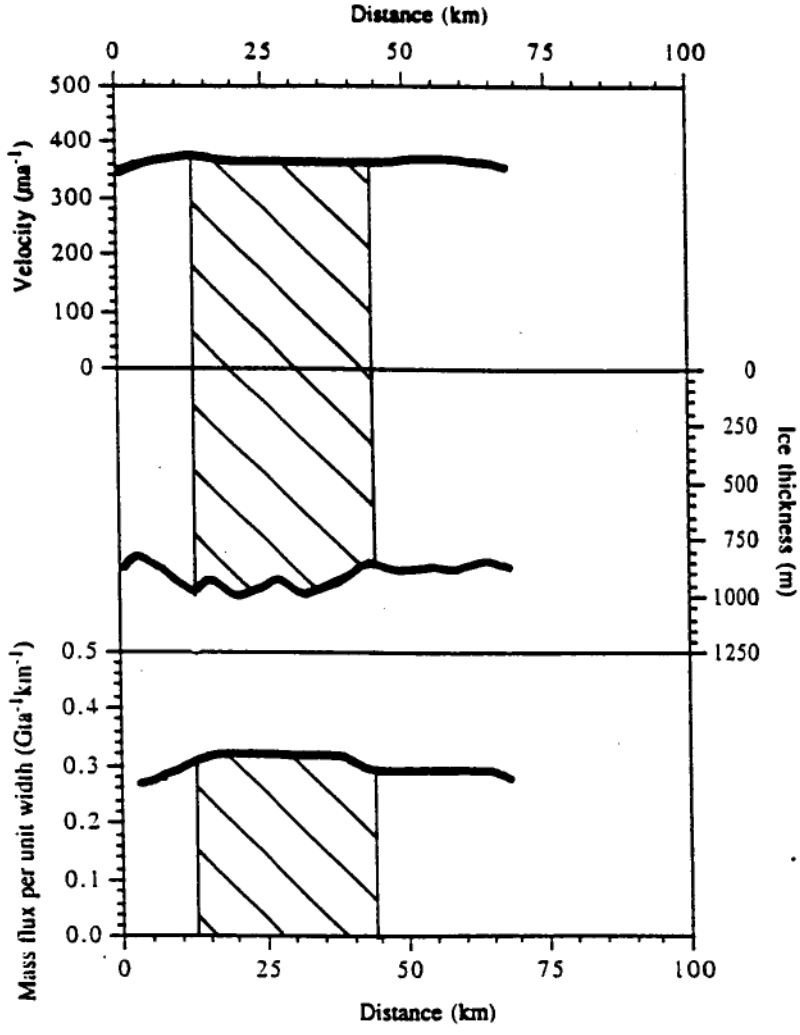

Figure 5.5. Velocity curve, ice thickness and mass flux graphs for Profile #2. The Lambert Glacier ice stream is situated between 12 km and 44 km along the transect.

Reaching a maximum velocity of 375 ma^{-1} on the most westerly edge of the transect, the flow of the ice then rapidly decelerates towards Fisher Massif due to the profile now covering grounded ice. Along the eastern region of the cross section, the velocity curve shows a peak velocity of 369 ma^{-1}, fifty-seven kilometres along the profile where the thickness is 880m. This is in the same region as the central flow line for the easterly grounded ice stream. The relative uniformity across the velocity profile is also seen in the surface elevation, ice thickness and surface elevation for hydrostatic equilibrium for this transect.

Profile #3

From interpolating known velocity measurements in the area of Profile #3, a maximum flow rate of 375 ma^{-1} was found 70 km along the profile, within the core of the Lambert Glacier, a western minimum velocity of 220 ma^{-1} and an eastern

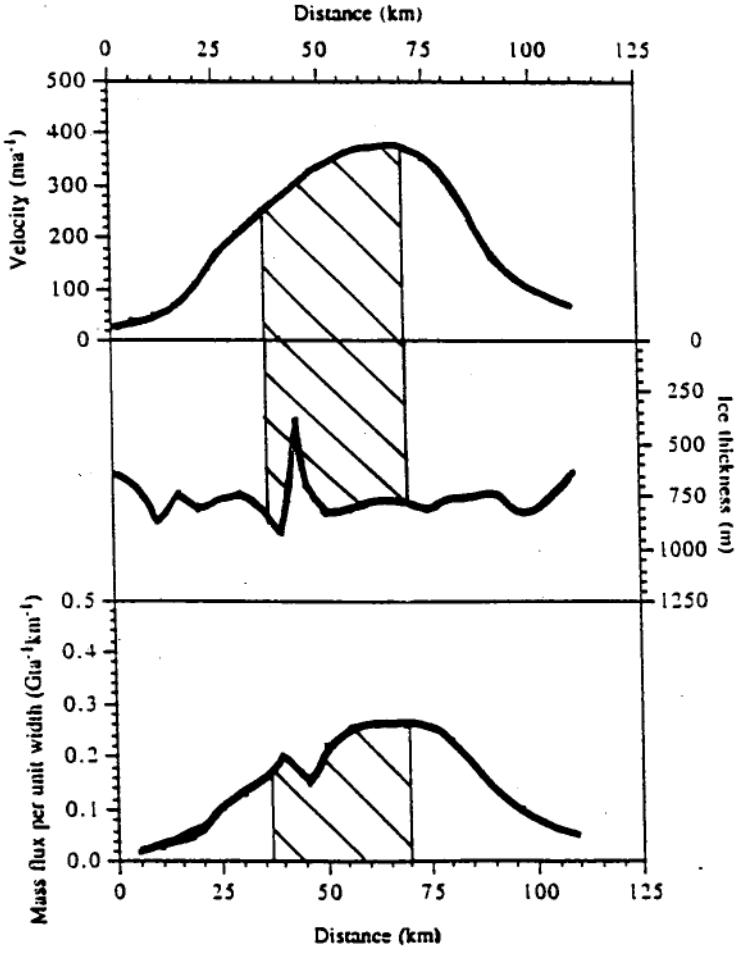

Figure 5.6. Velocity curve, ice thickness and mass flux graphs for Profile #3. The Lambert Glacier ice stream is situated between 36 km and 70 km along the transect. The "grounded" area of ice 40 km along the transect does not appear as a change in velocity based on the interpolation, but is marked with surface crevassing (see Chapter Four).

minimum of 370 ma^{-1} (Figure 5.6). This velocity profile indicates that the average velocity across the area east of the grounding zone is 315 ma^{-1} while west of the thinnest ice the average velocity is 225 ma^{-1}. Beyond the grounded ice towards the west, the ice is flowing at a considerably slower rate.

Profile #4

As with the velocity curve of the third cross section, Figure 5.7 shows a slightly faster area of flowing ice across the easterly margins of Profile #4. The average velocity across the profile is 330 ma^{-1}. From the start of the profile to the western edge of the Lambert Glacier ice stream, the velocity rapidly falls from 310 ma^{-1} to

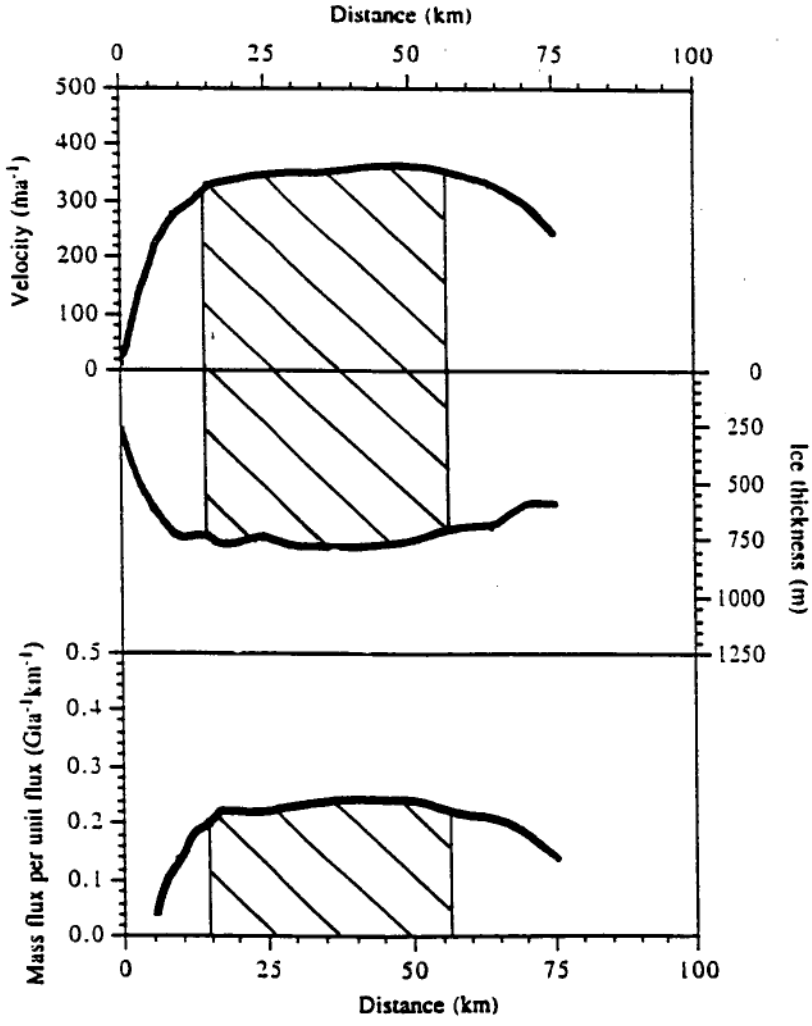

Figure 5.7. Velocity curve, ice thickness and mass flux graphs for Profile #4. The Lambert Glacier ice stream is situated between 14 km and 56 km along the transect. This transverse profile coincides very nearly with the location of the G3 profile (Budd *et al.*, 1982).

12 ma^{-1} within 10 km. The Lambert Glacier ice stream has been identified by its flow lines to be between 14 km to 56 km along the profile. The average velocity for the ice stream is 350 ma^{-1}. For the ice flow that originates from the westerly grounded ice, the velocity averages 285 metres per annum.

Profile #5

Figure 5.8, coupled with the evidence from Chapter Four, indicates that the Lambert ice stream within the Amery Ice Shelf through Profile #5 is floating. The ice in this area is flowing at an average velocity of 475 ma^{-1} with a peak velocity of 487 ma^{-1} just west of the central flow bands. There is a gradual velocity decrease further eastward towards Gillock Island, from 430 ma^{-1} to 340 ma^{-1} over 20 km.

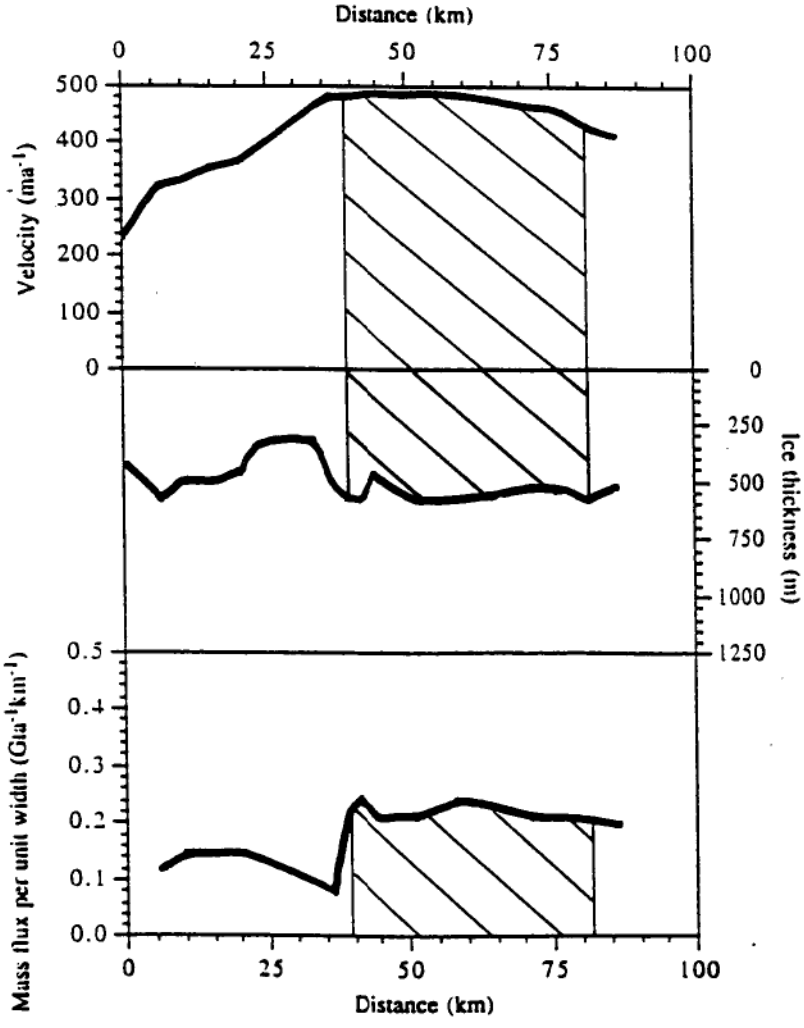

Figure 5.8. Velocity curve, ice thickness and mass flux graphs for Profile #5. The Lambert Glacier ice stream is situated between 39 km and 81 km along the transect.

West of the grounded ice in the 'sticky spot' between 20 km and 40 km, the velocity has been estimated at 353 ma^{-1}, on average. The ice from the Scylla and Charybdis Glaciers may be flowing slower than this based on the measurements 22 km south west where the velocity was measured at 278 ma^{-1} and decreasing a further 50 metres per annum 10 km further upstream.

5.3 Longitudinal Profiles of Velocity and Driving Stresses along the Lambert Ice Stream

5.3.1. Introduction

Stresses are a measure of force per unit area. The down slope driving stress for ice represents the component of the weight of the ice which is parallel to the ice surface plane (Paterson, 1994). This is balanced by basal drag when the assumption is made, in the case of well grounded ice, that there are no down slope (longitudinal) or cross slope (transverse) gradients. The basal shear stress is then assumed to balance or equate to the downslope driving stress and is calculated as:

$$\tau_b = \rho g z \sin\alpha \qquad \text{(Equation 5.2)}$$

Where ρ is ice density, g is acceleration due to gravity, z is ice thickness and α is surface slope.

For a glacier sliding on its base, the ice velocity is partially controlled by the frictional drag at the base. Friction is also a function of the ice basal normal stress which, for a partially floating ice mass, is that component of the column weight not supported by buoyancy. For a glacier of uniform (on average) density ρ_i, thickness z and surface elevation h, overlying water density ρ_w, the excess thickness over hydrostatic balance is given by

$$\frac{\rho_i Z - \rho_w (z-h)}{\rho_i} \qquad \text{(Equation 5.3)}$$

and hence the effective excess normal stress (σ_Z) for the ice on the bed is

$$\sigma_Z = g\,(Z(\rho_i - \rho_w) + h\rho_w) \qquad \text{(Equation 5.4)}$$

For fully floating ice the basal shear effectively becomes zero. In this case, for an ice mass which is bounded at the sides, by bedrock or more slowly flowing ice, the resistance to the downslope driving stress can come from the transverse shear stress across the ice mass to the sides.

From the central region where the ice horizontal velocity is a maximum and the transverse shear stress is zero the shear stress (τ_{xy}) increases approximately linearly with distance (y) towards the sides. In absence of significant longitudinal stress gradients there is then a balance between the downslope driving stress per unit width and the transverse shear stress. That is to say, using the previous notation

$$\tau_{xy} = \rho g \alpha y \qquad \text{(Equation 5.2)}$$

The maximum shear stress occurs near the sides where y = Y(x) giving

$$\tau_y = \rho g \alpha Y \qquad \text{(Equation 5.5)}$$

This relationship was used by Budd *et al.* (1982) to test the flow relation for the ice shelf centre line velocity V given by

$$V/Y = K\,(\rho g \alpha Y)^n \qquad \text{(Equation 5.6)}$$

where n is the index of the power flow law for ice and K is the ice flow parameter appropriate for the iceshelf thickness. Because of the neglect of longitudinal stresses the surface slope (α) and the half width (Y) need to be considered as large scale averages over the floating region.

For the transition region between fully grounded flow (where the basal shear stress dominates the resistance) and fully floating in a confined embayment (where the transverse shear provides resistance) a near floating, partially grounded zone can have a significant fraction of the resistance coming from each of the basal shear stress and the transverse shear stress at the sides. As the ice moves from fully grounded to fully floating the resistance changes from primarily basal shear stress to primarily side drag from the transverse shear stress. This occurs as the effective normal stress above floating (N*) reduces from ρgz to zero. The transition from grounding to floating need not be smooth and patches of grounding and floating may occur over the whole transition region. In this case the effect of longitudinal stress tends to smooth the surface velocities and effectively distribute the resistance to large scale averages over the basal and side regions.

The observations on the Lambert Glacier and Amery Ice Shelf system are used here to examine the manner in which these stresses and the velocity vary from the grounding region to the floating region. The values of the relevant parameters along the ice stream are given in the tables including: surface slope (α), ice thickness (z), cross section half width (Y), downslope or basal shear stress ($\tau_b = \rho g \alpha z$), basal normal stress ($N^* = \rho g \alpha z^*$), side shear stress ($\tau_y = \rho g \alpha Y$) and centre line velocity (v).

5.3.1.1 Surface and basal melt rates

Surface and basal melt rates are another component in the determination of the mass flux in a study area. In order to best interpret the net balance of a glacial drainage system, you need to be able to calculate the rates of accumulation, calving, surface ablation and basal melt. Where basal ice is at the pressure melting point and sliding, the melt rate from frictional drag is derived from

$$M = \tau_b v / L \qquad \text{(Equation 5.7)}$$

Where L is the latent head of ice fusion, V is the average velocity of the ice and τ_b is the basal shear stress. The upper limits for melt rate from frictional drag across each profile is based primarily on available data. Due to the limited velocity measurements, the calculation of melt rate on the entire eastern and western longitudinal profiles is not possible. This discussion then centres exclusively about the northern limits of the Lambert Glacier grounding zone and all melt figures are derived assuming mass continuity between the profiles.

In addition to the basal melt which can come from frictional drag it is also possible for basal melt or ice growth to occur. For this to be appreciable, there needs to be a sufficiently thick water cavity under the ice, well enough connected to the ocean to allow adequate water circulation. At this stage the difference between the ice base depth and the bedrock is not known so the basal melt rate (or ice growth) from ocean processes will be an unknown part of the net mass balance presented here. Nevertheless the derived net mass imbalances along the flowline may provide an indication of possible magnitudes for these basal mass fluxes. In the future if the rate of change of the surface elevation (or ice thickness) can be measured directly, it may be possible to derive with accuracy the basal rates of ice exchange as well.

5.3.2. Data

The slopes used to estimate driving stresses were derived from the Lambert Glacier ice stream and across the transverse profiles and have been averaged over 5 km. The slope used in the longitudinal profile analysis was averaged over 50 km (Figure 5.9). This variation in slope gradient therefore provides differing results when the two final products are compared. Due to the apparent floating ice and high degree of basal sliding in the transverse sections study area, the values for driving stresses are very low. These values still illustrate a trend between the profiles (Table 5.7 and 5.8).

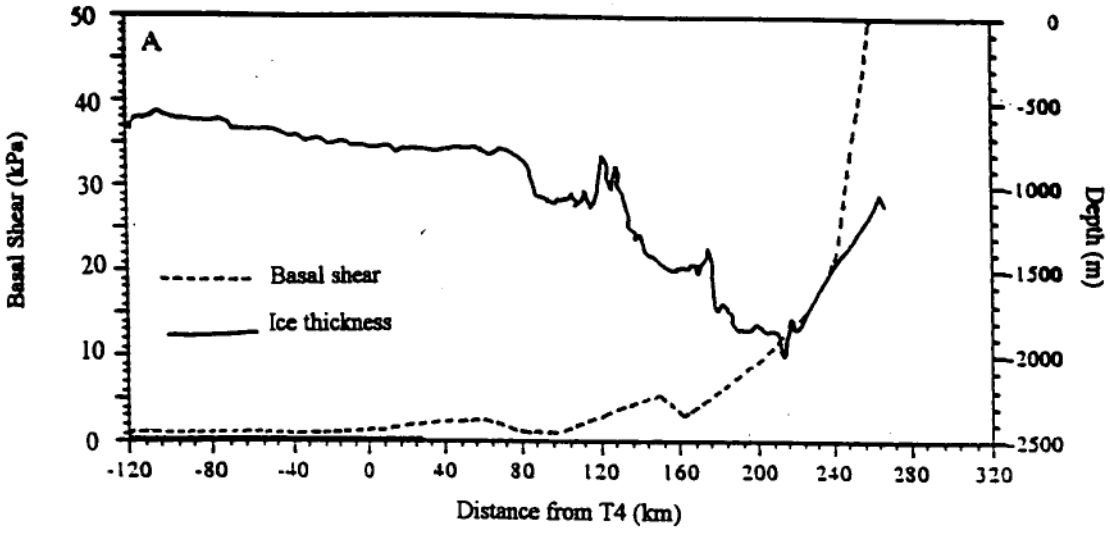

Figure 5.9. Graph A is the eastern longitudinal profile of the Lower Lambert Glacier, comparing the relationship between ice thickness and basal shear stress calculated from the Profiles #1 to #5 and point data A to D.

The low basal shear stress occurring over the transects, shown in part in Tables 5.7 and 5.8, indicates that the resistance on the Lambert Glacier ice stream within the grounding zone may be due to transverse shear stress from the tributary drag from the grounded ice to both the east and west of the drainage system. As such, the grounded sides of the ice shelf may be exerting a transverse shear stress of τ_{xy} onto the ice shelf in a similar way that basal shear applies drag to the ice within the southern reaches of the grounding zone and in around Profile #6 (Chapter Four, Section 4:3.4) within the Southern Prince Charles Mountains.

The calculations for side drag $\tau_{xy} = \rho g \alpha Y$ are given in Table 6.1 and show that the large scale average side drag over the transition grounding zone is comparable with that over the clearly floating ice shelf between Profiles #4 and #5 (T4 and G2). At the same time the central velocities vary only slightly over the transition zone and increase along with the ice shelf width northwards of Profile #3 (G3). This

reinforces the conclusion that over the transition zone the basal drag is relatively small and the ice velocity is governed primarily by the balance between the driving stress and transverse shear stress.

West Profile Intersection	*Distance* *km*	*Slope* *m/ km*	*Mean Velocity* *m/a*	*Mass Flux per unit width* *Gt/a*	*Ice Thickness* *m*	*Basal Shear* *kPa*	*Melt Rate* *kg/m² /a*
Normal to T4	0	0.8	208	0.9	820	0.4	53.6
Profile #3	20	0.4	258	1.4	770	1.3	40.3
Profile #2	32	0.4	375	2.03	900	5.3	59.6
Profile #1	57	0.4	375	2.1	750	2.3	60.6

Table 5.7 Driving stresses and other parameters for the western side of the lower Lambert Glacier and Amery Ice Shelf system. Ice thickness at T4 is after Budd *et al.* (1982), other ice thickness values are the mean across each profile. Distance refers to the number of kilometres between the profiles.

East Profile Intersection	*Distance* *km*	*Slope* *m/ km*	*Mean Velocity* *m/a*	*Mass Flux per unit width* *Gt/a*	*Ice Thickness* *m*	*Basal Shear* *kPa*	*Melt Rate* *kg/m² /a*
Profile #4	-40	0.08	359	0.68	680	1.1	14.8
Normal to T4	0	0.08	340	1.07	820	1.0	94.1
Profile #3	25	0.08	375	1.6	770	5.1	55.2
Profile #2	40	0.8	368	1.4	900	2.0	98.7
Profile #1	69	0.5	398	1.7	750	2.0	62.6

Table 5.8 Driving stresses and other parameters for the dynamics of the eastern side of the lower Lambert Glacier and Amery Ice Shelf system. Ice thickness at T4 is after Budd *et al.* (1982), other ice thickness values are the mean across each profile. Distance refers to the number of kilometres between the profiles.

5.3.3 Extrapolation with assumption of continuity

To estimate the dynamics of the glacier further upstream it has been necessary to assume approximate mass continuity, because of the sparsity of data south of the Lambert Glacier grounding zone. The most southerly ice movement station observed during the 1988-89 and 1989-90 expedition was at 71°38'52" South 68°59'16" East. The next most southerly series of ice movement stations was from the work of Allison (1979) around the southern limits of the Southern Prince Charles Mountains. Between these two data stations the assumption that the ice is behaving in a steady state within uniform parameters is made since no other ice movement studies having being made. Further work in this area will clarify the

conclusions of this assumption. In between these two measured ice movement stations, the drainage of the Lambert Glacier encounters a major topographic disturbance. This appears as a major surface elevation change and a substantial area of surface crevassing, both occurring within a small area just south of the zone of confluence with the Fisher Glacier.

Velocity was linearly interpolated between Profile #1 and A.79 assuming a steady state of equilibrium. This value for velocity was then used in conjunction with the measured ice thicknesses from the RES data and an assumed ice density of 900 kgm^3 to calculate mass flux rate and driving stresses of the grounding zone. Basal melt calculations for this area are difficult to ascertain due to the low quality and quantity of data south of Profile #1. As such, the density of any basal water can not be confidently estimated from hydrostatic equilibrium calculations. However, because the environment of the southern reaches of the grounding zone does not allow for any significant ocean system interchange (that is, it is a closed system) it is expected that lower basal melt rates will occur as opposed to the higher basal melt rates beneath the ice shelf. All calculations for basal melt assume mass continuity between the profiles.

5.3.3.1 Driving Stresses

Based on surface slope measurements over 50 km, the driving stresses within the two longitudinal profiles of the Lambert Glacier and Amery Ice Shelf have been studied. From Figure 5.10 the correlation between grounded and floating ice deviates markedly at approximately 280 km from Profile #5 (150 km from T4). The typical driving stress for an alpine valley glacier is 50 to 150 kPa (100 kPa = 1 bar). A grounded polar ice stream can be expected to have a driving stress between

50 to 200 kPa and typically the basal shear will exceed 100 kPa for grounded ice. Ice shelves have a basal shear much less than 50 kPa (Bentley, 1987) and their dynamics are governed by other stresses as outlines above and will be discussed further later.

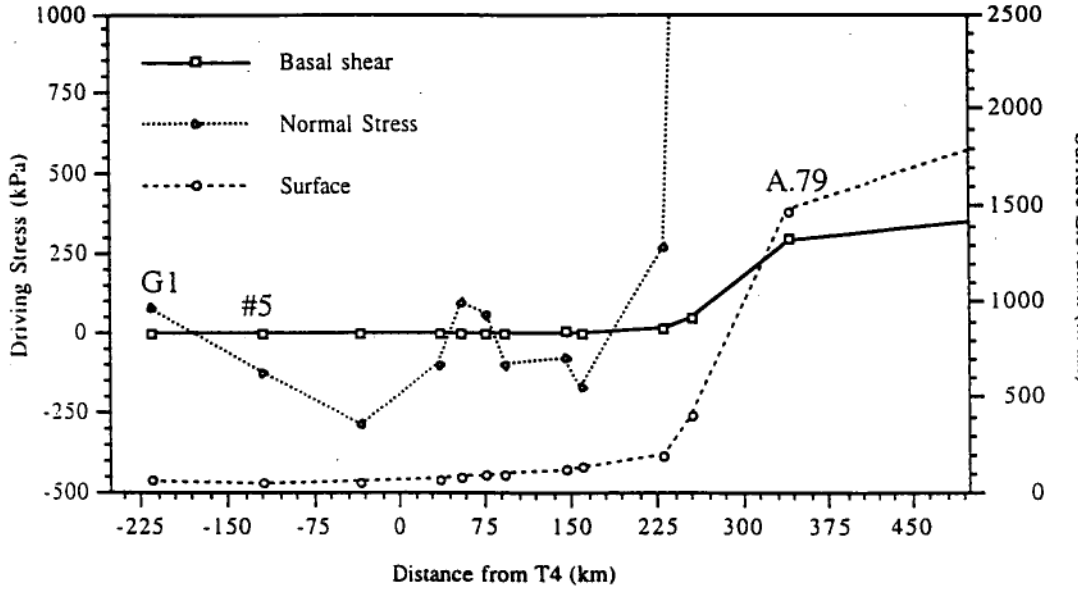

Figure 5.10. Between G1 (Budd *et al.*, 1982) and A.79 (after Allison, 1979) the basal shear stress and normal stress have been plotted. The increase in the vicinity of Profile #3 reflects the pronounced grounding point on the western side of the drainage system in that area.

Figure 5.10 shows basal shear stress and normal stress between G1 and A.79. Figure 5.11 displays the relationship between centre line velocity, ice stream width, surface slope and side stress. To remind the reader, in all these longitudinal studies along the lower Lambert Glacier, the information between Profile #1 and A.79 is predominantly interpolated. More observations need to be conducted in this area and at this stage any deductions are only based on the assumption that glacier activity is in a state of steady equilibrium between the two points of interpolation. The higher incidence of grounded ice on the western side of the system is reflected

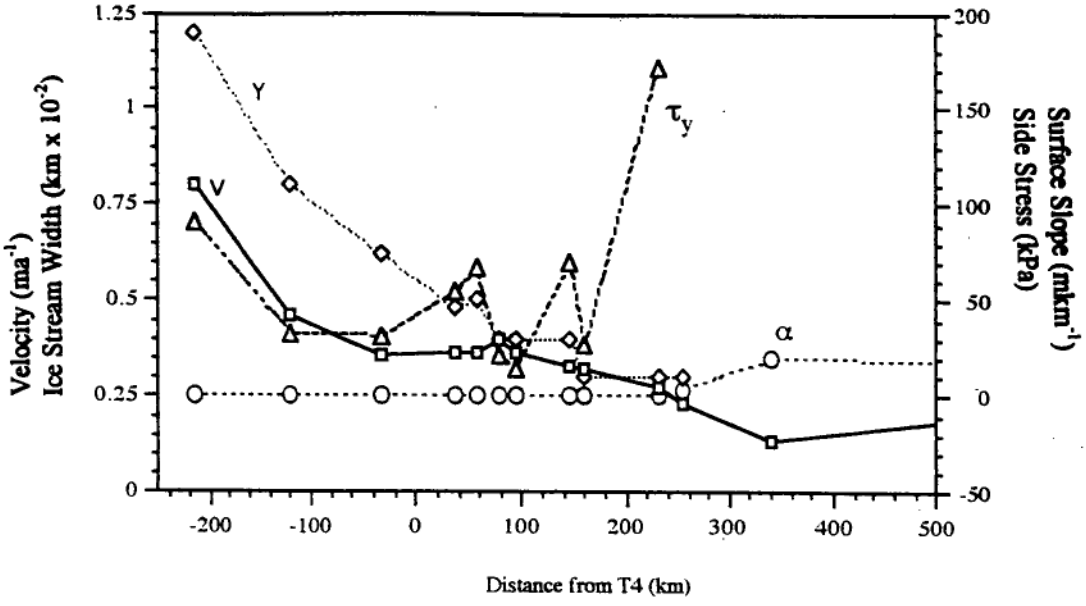

Figure 5.11. A comparison of centre line velocities, ice stream width, surface slope and side stress between G1 (Budd *et al.*, 1982) and A.79 data (after Allison, 1979) with the intervening values calculated by this author from RES data.

in the driving stress calculations, but is not so apparent when the surface slope used in the calculations is averaged over 50 km. This is particularly so around Profile #3 where the grounding point alters the otherwise steady decrease in driving stresses within the grounding zone.

Table 5.9 shows the relationship between velocity, basal shear stress and normal stress and suggests basal shear stress at Point D is 20 kPa. By Point B it has fallen to 5 kPa. Between A.79 and Point D is the southern grounding line of the Lambert Glacier. This appears as a marked reduction in the driving stresses from essentially grounded ice displaying 300 kPa friction of ice against bedrock at A.79 (Allison, 1979) to less than 50 kPa in assumed floating ice.

Distance from T4 (km)	Site	Velocity (ma^{-1})	Basal Shear (kPa)	Normal Stress (kPa)
340	A.79	138	299.9	12,799
230	Point D	272	19.5	274
160	Point C	321	2.6	-167
146	Point B	331	4.6	-78
94	Point A	367	0.8	-98
78	Profile #1	399	1.0	59
57	Profile #2	366	2.1	98
37	Profile #3	364	1.8	-100
-33	Profile #4	356	0.7	-284
-120	Profile #5	463	0.4	-123
-215	G1	800	0.6	83

Table 5.9. Summary of driving stress values from G1 to the A.79 transect.

Figure 5.12 shows this with respect to the relationship between the driving stresses and the surface elevation for buoyancy. The values for basal shear can be seen to drop away rapidly (along with the normal stress) in the area of the southern basal melt lake. This could be seen to support the theory that these basal features are indeed basal melt lakes, especially the central basal melt lake.

5.3.3.2 Surface Mass Balance

Based on work by Allison (1979), Drewry and McIntyre (1986), Giovinetto and Bentley (1985) and Budd *et al.* (1982) a profile of accumulation from a coastal environment to nearly 1000 km inland has been developed (Figure 5.13). Two data sets have been the basis to this profile, accumulation from the Lambert Glacier and Amery Ice Shelf system and accumulation from typical Antarctic coast-to-inland profiles. This has helped to establish a definition of climatic patterns and surface mass balance trends in drainage systems such as here in the Lambert Glacier and Amery Ice Shelf system.

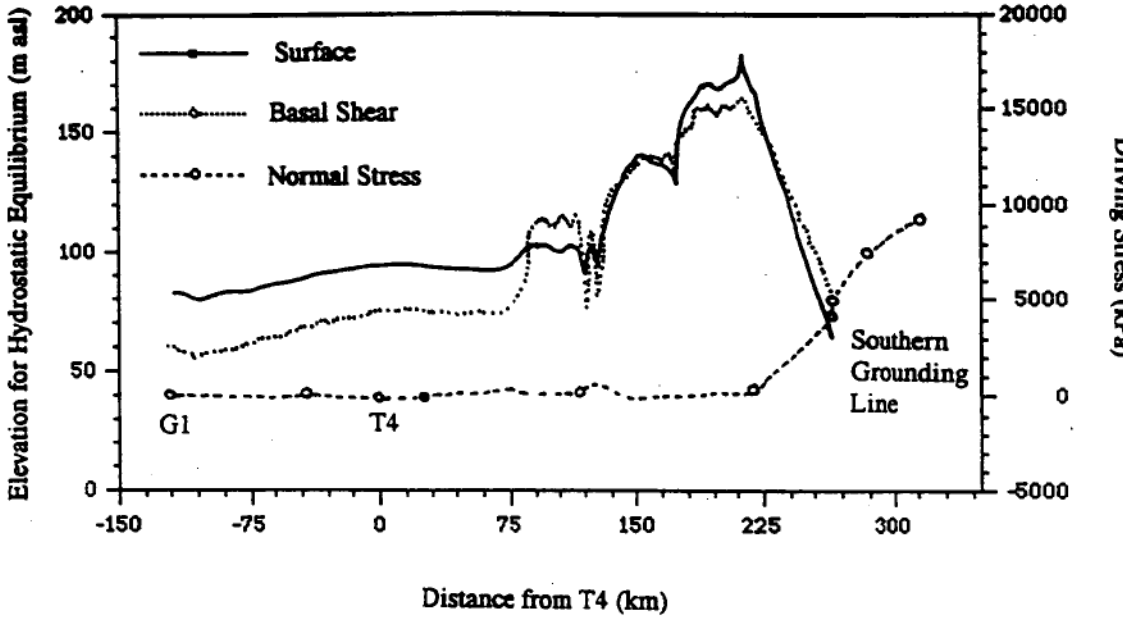

Figure 5.12. A comparison between the hydrostatic equilibrium of the ice (m asl) to that of the normal stress and basal shear rates for the Eastern Longitudinal Profile that closely follows the central flow lines of the Lambert Glacier. Results for the Points A, B, C and D have been interpolated from between Profile #1 and the A.79 transect assuming ρ_i=900 kgm^{-3} and ρ_w= 1026 kgm-3.

The three continental profiles by Allison (1979), Drewry and McIntyre (1986) and Giovinetto and Bentley (1985) show a gradual increase in accumulation rates the lower the elevation and the closer towards the open water of the coastline. Their surface mass balance, in kilograms per square metre per annum water equivalent, ranges from 0 to 220 kgm^{-2}a^{-1}. The profile of accumulation by Budd *et al.* (1982) was collected on the Amery Ice Shelf by the remeasurement of stakes first established in 1963. Where Budd *et al.*'s (1982) accumulation profile finishes at T4, a continuation of the surface mass balance has been calculated from surface

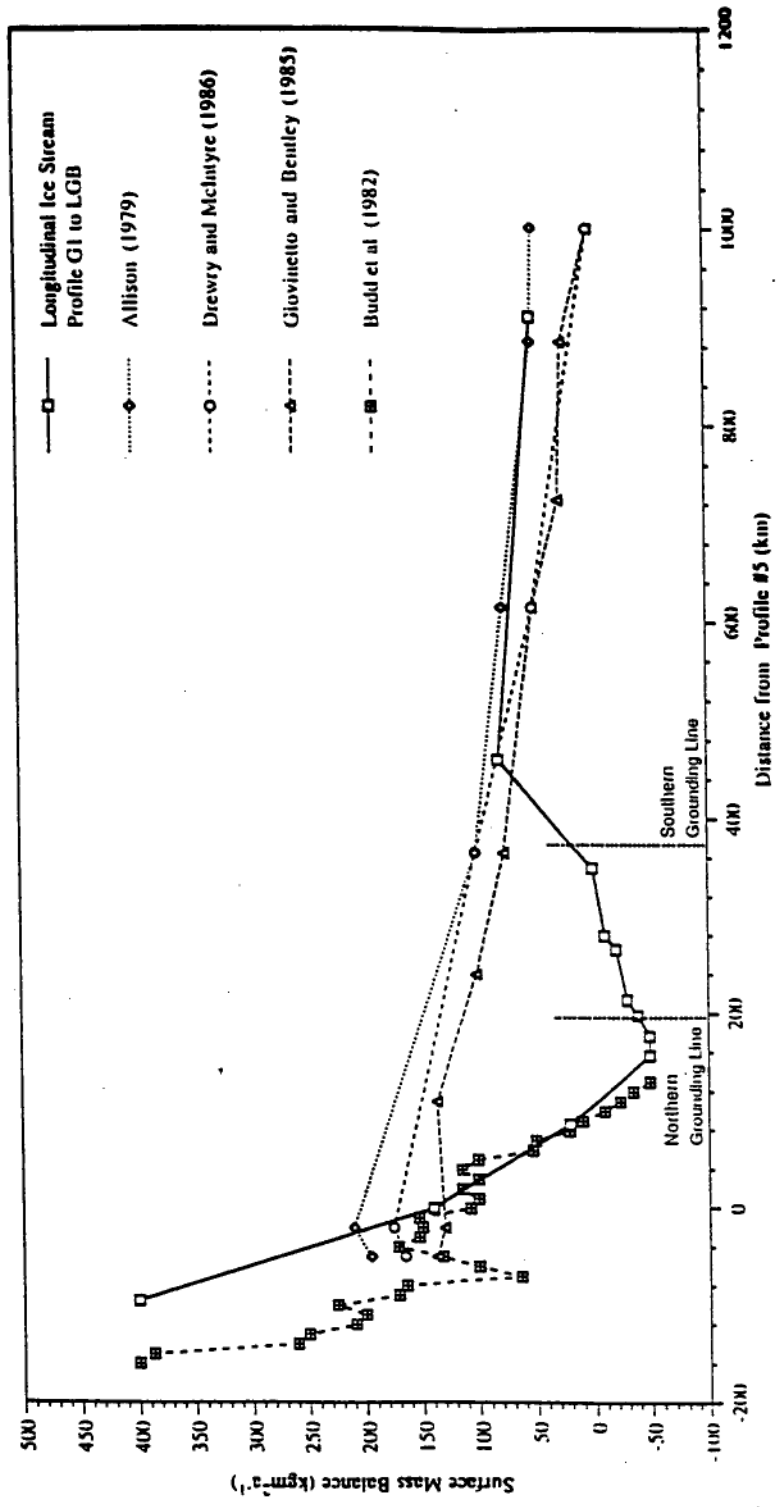

Figure 5.13 A comparison of accumulation observations and estimations. The results from the longitudinal profile (by this author) and those of Budd *et al.* (1982) pertain to the Amery Ice Shelf and lower Lambert Glacier system. The profiles by Allison (1979), Drewry & McIntyre (1986) and Giovinetto & Bentley (1985) are referring only to the surrounding ice sheet and are presented here simply to illustrate the variation in surface mass balance rates across ice shelves/ice streams systems and non ice stream drainage systems.

mass fluxes (based on interpolation) between the profiles and point data to establish a possible accumulation trend. By approximately 100 km from Profile #5 accumulation rates have become ablation rates. This continues for a further 250 km south as deduced by this author from mass flux rates. Visibly, this deduced ablation zone is apparent in the MSS and TM imagery as a 'blue ice' zone, particularly visible on the western side of the drainage system.

From Figure 5.13 (and later in Figure 5.15) the difference between the surface mass balance on a gentle gradient (continental profile) compared to that of a steep gradient (drainage trough) is clearly illustrated. This variation in the pattern of accumulation may be due to the topographic surroundings and elevations inherent with a drainage system. The mountains that form the boundaries of the Lambert Glacier and Amery Ice Shelf drainage system may be inhibiting the rate of accumulation and/or redeposition of snow. This zone of ablation also matches the region defined by this author as the Lambert Glacier grounding zone.

5.3.3.3 Velocity

Figure 5.14 is a contour map of surface ice flow in metres per annum based on the velocity data from the A.79 transect (after Allison, 1979) and the interpolation onto Profile #1 coupled with the velocity of the Amery Ice Shelf repeat surveys. In contrast to the discussion earlier in chapter Five on the transverse velocity profile, this map extends as far south as 74° and north to 69°. This map is included to illustrate the trend in the rate of ice flow in the lower Lambert Glacier and Amery Ice Shelf drainage system.

To the north east of Fisher Massif the grounded point seen in Profile #3 also becomes apparent as a decrease in the ice velocity. Further north of this, the ice is nearing the centre of the Lambert Glacier drainage valley before the rate of ice movement increases. This author attributes this to the input from the western grounded ice sheet between Mount Meredith and Fisher Massif. Coupled with this is information from the Western Longitudinal Profile which indicates grounded ice in the region north east of Fisher Massif, where the basal topography is beginning to rise into Jetty Peninsula. The smoother velocity contours of the eastern side of the drainage system, particularly between Clemence Massif and Gillock Island indicates that the Eastern plateau is not contributing as much mass flux to the Lambert system and the transition from grounded to floating ice is less disturbed.

Around the area bounded by Fisher Massif, Jetty Peninsula, Gillock Island and Clemence Massif, the ice has an average velocity of 300 to 350 ma^{-1}. When the Lambert Glacier begins to move as a free-floating ice mass the velocity increases to 400 ma^{-1}. One exception is along Profile #3 from Mount Meredith to south of Pickering Nunatak where the velocity of the ice decreases. This is due to the influx from the western side of the systems grounded ice through an unnamed glacier between Fisher Massif and Mount Meredith as well as the influence of the nearby Jetty Peninsula.

Between Single Island and Gillock Island, the location of Profile #5, the ice flow rapidly increases towards Prydz Bay, reaching 1000 ma^{-1} plus at the ice front. The grounding point at the merging zone of the Scylla-Charybdis and Lambert Glacier does not appear to slow the rate of ice movement. There is a distortion of flow around this grounding point but this is dispersed over a relatively small area. The rapid slowing of the ice flow rate north east of Single Island coincides with a crevasse band that can be traced upstream on the Scylla/Charybdis Glacier into the Northern Prince Charles Mountains.

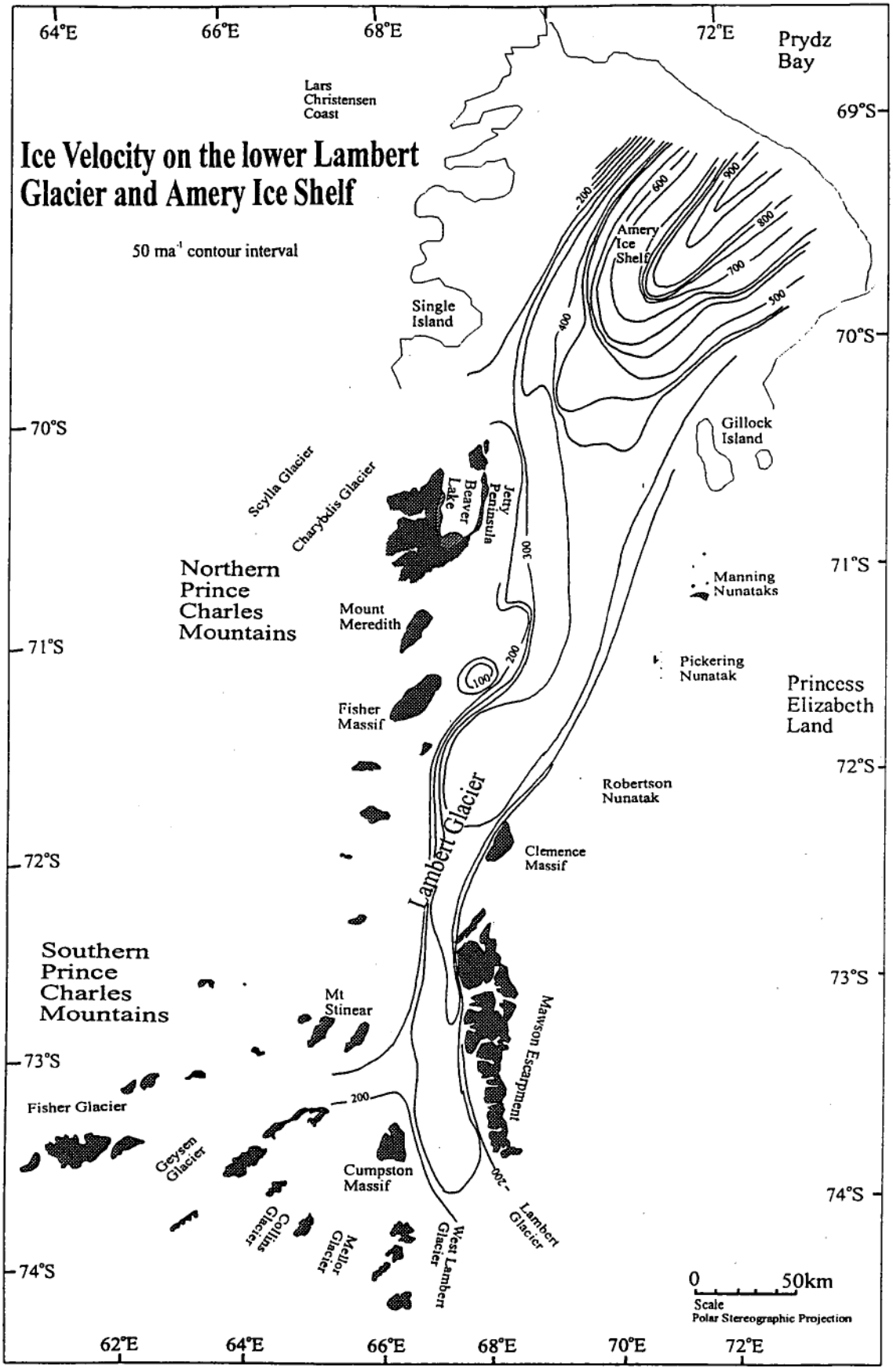

Figure 5.14 Surface ice velocity for the lower Lambert Glacier drainage system. The westerly grounded ice can be seen to influence velocity rates north east of Fisher Massif. The point of grounded ice between Single Island and Gillock Island does not appear to have a large impact on the surface ice velocity in the area.

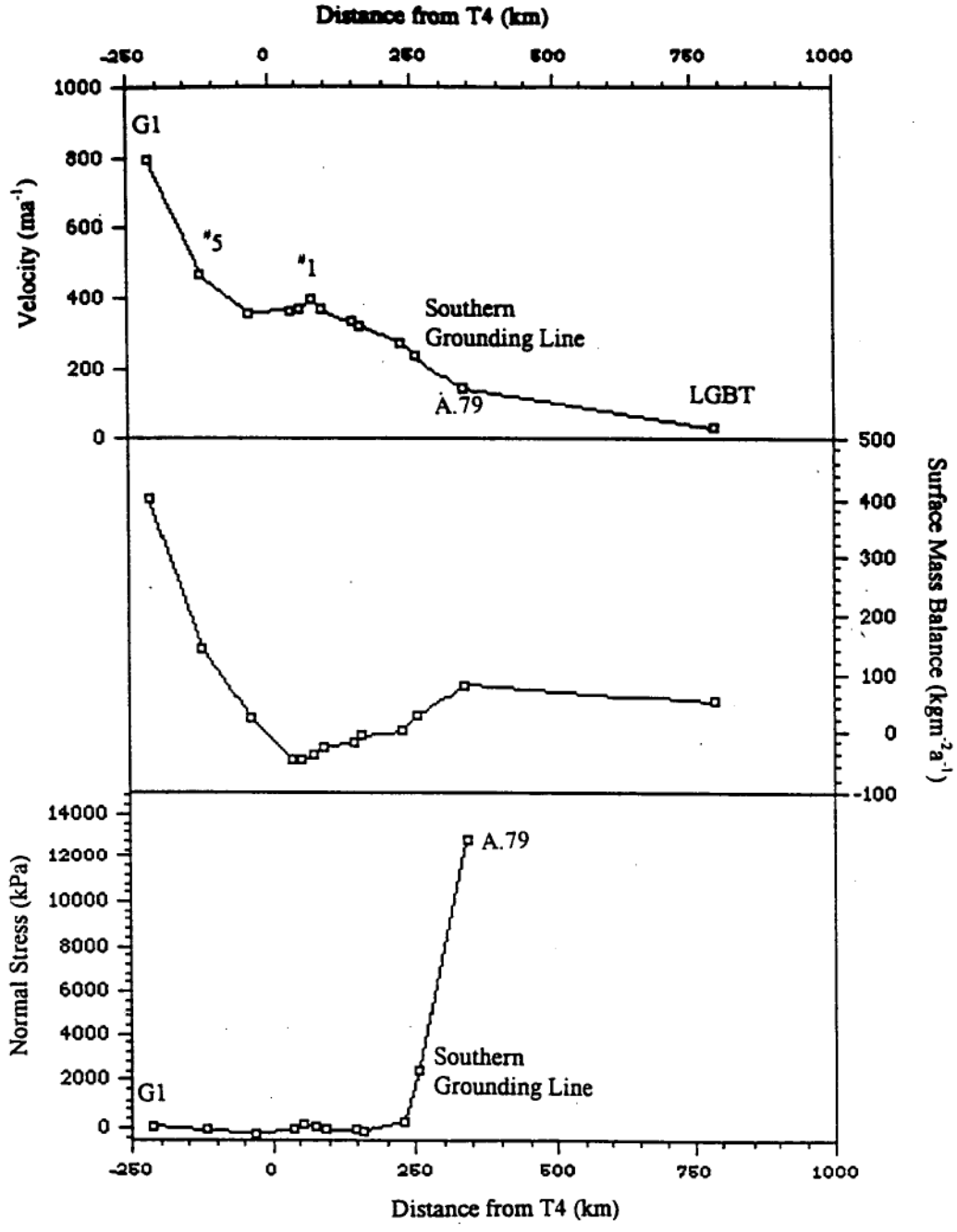

Figure 5.15. Three profiles comparing the drainage systems eastern side. Graph A is the average velocity across the Lambert Glacier as determined from the velocities of the Lambert and Mellor tributary glaciers in their flow lines from LGB (Higham, 1994) through the A.79 transects (after Allison, 1979) via the profiles by this author to G1 (Budd *et al.*, 1982). Graph B follows the same transect as A and represents accumulation rates with reference to the location of Profile #5. Graph C is the underlying normal stress from A.79 to G1. The area around the northern limits of the grounding zone contain more information than elsewhere along the profile. Given this, the observed trend along the study region is as expected with increasing velocity with an increasing rate of ice thinning and proximity to open water coinciding with this decrease in normal stress in the lower Lambert glacier ice stream.

5.3.4 Discussion

Figure 5.15 is a longitudinal profile summarising some of the information discussed already. Again, the points along the profiles of velocity, accumulation and driving stress pertain essentially to the eastern side of the Lambert Glacier. As could be expected with a drainage system such as the Lambert Glacier, the approach to low basal shear stress towards the ice shelf, is accompanied by a corresponding decrease in the ice normal stress. This is to be expected because no excess overburden above buoyancy exists on floating ice such as in this area. The grounding point at Profile #3 is reflected as a preliminary velocity decrease, and increase in driving stresses all within an ablation zone.

What follows in Chapter Six will be a discussion on the mass flux and mass budget of the study area within the lower Lambert Glacier and Amery Ice Shelf system. This will gain add to the definition of the grounding zone of this drainage system as determined from the morphology and dynamics of the system.

Chapter Six

Mass Flux

6.1 Introduction

This chapter is a discussion on the mass flux of the Lambert ice stream derived from the extrapolated and measured results of ice surface velocity, surface elevation and ice thickness. The error estimate for the calculations of mass budget vary from between 0.5 to 0.7 Gt a^{-1} over a range of fluxes within 8.5 - 10 Gt a^{-1} for each of the Lambert Glacier profiles. This error estimate is based on the difference between the mass fluxes of neighbouring profiles as well as the surface mass balance added from local accumulation and the volume change at the base through melt/freezing. An accumulation rate of 150 kgm^{-2} a^{-1} (Budd, 1966 Fig.7) north of G3 (between Profiles #3 and #4) was used for this calculation. This margin for calculated error can also be expressed as between 5-10 % due to a ± 20 m at an average thickness of 700 m and ± 5 ma^{-1} at an average surface velocity of 300 ma^{-1}.

6.2 Mass Budget

In Chapter Five the concept of mass flux along the lower Lambert Glacier was introduced and initial results were presented. Table 6.1 presents a summary of these results. Each of the profiles covers the region defined as the Lambert Glacier, comprising its six tributary sources, but they do not necessarily have spatial coverage of the same east and west tributary ice. This is reflected in Figure 6.1 in the relationship between the mass flux attributable to the Lambert ice stream in comparison to the mass flux of the entire profile. As the six tributary ice streams that form the Lambert Glacier flow north, the overall percentage contribution from these glaciers remains relatively constant. From Profile #1 to Profile #3 the mass flux appears to decrease. Beyond Profile #3 the mass flux increases due to a rise in surface mass

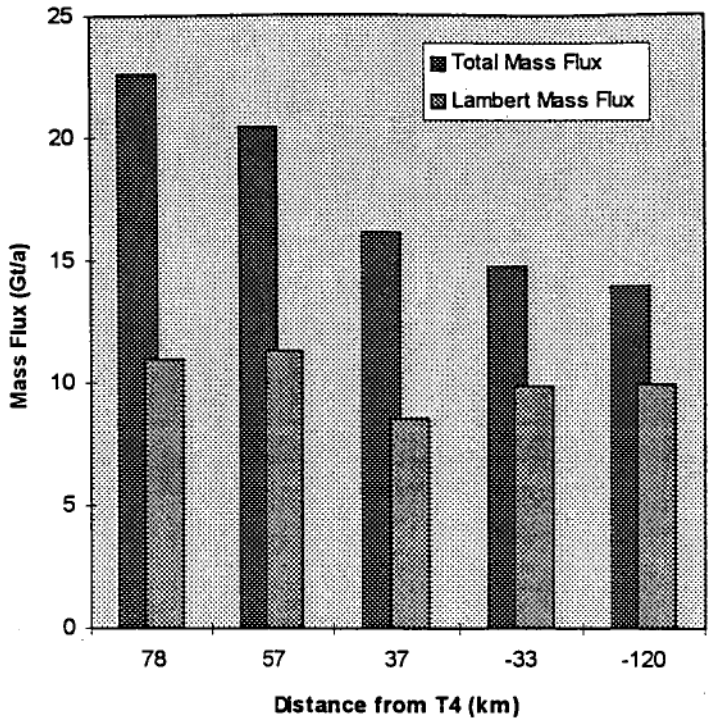

Figure 6.1. From Profiles #1 to #5 the contribution to the mass flux of the Lambert Glacier can be accounted for by its six tributary ice streams. These are, from east to west, The Lambert, West Lambert, Mellor, Collins, Geysen and Fisher Glaciers. In this figure the contribution of mass flux for the entire profile is compared to the mass flux originating from the Lambert ice stream. The left side of the graph represents south (Profile #1) and moving across the graph is travelling north and onto Profile #5 which is situated between Single Island and Gillock Island on the Amery Ice Shelf. The graph is viewed from south to north.

flux rate apparently from the accumulation of maritime precipitation (see Figure 5.13). Supporting the conclusion of the transition zones location, Figure 6.1 indicates a decreasing total mass flux of 2-3 Gta^{-1} per 20 km between Profiles #1 and #3 (~ 2-3 ma^{-1} net loss over an area 20 x 50 km). It is proposed that this is due to ocean circulation beneath the ice.

From Profile #5 in the north to Profile #1 towards the south, the contribution towards the mass flux of the Lambert ice stream can be accounted for by the total mass flux from the six tributary glaciers. When these glaciers flow as the Lambert Glacier, their percentage contribution to the total mass flux of the Lambert Basin remains constant between Profiles #1 to #5. From Chapters Four and Five, there is a change in the profiles of these tributary glaciers as they get wider and thinner the further north they

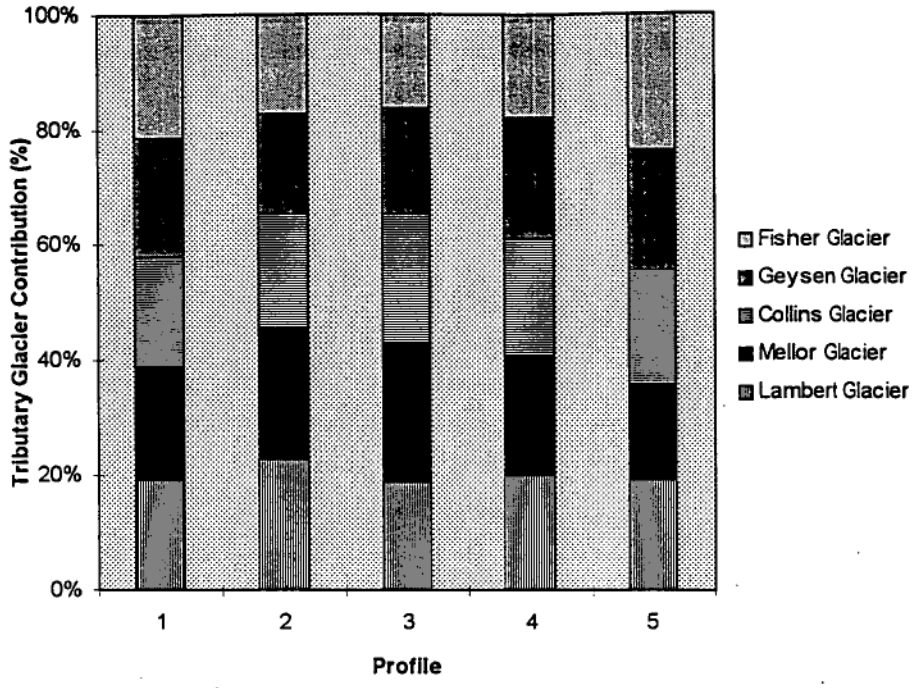

Figure 6.2. The Lambert Glacier ice stream is derived from the confluence of six tributary glaciers. Their contribution towards the mass flux of the Lambert Glacier, as measured between Profiles #1 to #5, is illustrated as a percentage of the overall mass flux of each transect.

flow. The average percentage contribution from these glaciers is: the Lambert Glacier, 41%; Mellor Glacier, 18%; Collins Glacier, 7%; and both the Geysen Glacier and Fisher Glacier each contributing an average 17% towards the total Lambert Glacier ice stream mass flux (Figure 6.2).

It has been calculated from LGBT data that the mass flux of the Lambert and Mellor Glaciers across the 2500 m surface contour elevation and into the Lambert graben is 38 Gta^{-1} (Allison, pers. com., 1995). By the surface elevation of 1500 m there is 17 Gta^{-1} passing through the A.79 transect which has its origin in the Lambert and Mellor Glaciers (Allison, 1979). Point D (z = 1700 m, ρ_i = 900 kgm^{-3}, v = 272 ma^{-1}, Y = 30 km and α = 1.3 $m^{-1}km$) the mass flux is 14 Gta^{-1}. The volume loss between the A.79

Profile	Distance from T4	Surface Elevation	av. Ice Thickness	Ice Stream Width	Surface Slope	Av. Velocity	Profile location from grounding line	Ice Density	Mass Flux of Ice Stream	Surface Mass Balance	Side Stress $\rho g \alpha Y$	Normal Stress above buoyancy	Basal Shear
	(km)	(m asl)	(m)	(km)	(mkm^{-1})	(ma^{-1})	(10^{-3} $years^{-1}$)	(kgm^{-3})	(Gta^{-1})	(kg^{-1} $m^{-2}a^{-1}$)	(kPa)	(kPa)	(kPa)
LGBT	790	2330	3000	-	17	26	-	916	38	50	-	-	458.3
A.79	340	1476	1700	-	20	138	-	-	17	80	-	12,799	299.9
Grounding Line	255	400	1500	30	4	233	7.7	-	15	23	-	2,450	52.9
Profile D	230	198	1700	30	1.3	272	9.1	900	14	0	171.9	274	19.5
Profile C	160	133	1500	30	0.2	321	10.7	900	12	-10	26.5	-167	2.6
Profile B	146	122	1300	40	0.4	331	8.3	900	12	-20	70.6	-78	4.6
Profile A	94	100	1100	40	0.08	367	9.2	900	10	-30	14.1	-98	0.8
Profile #1	78	96	900	40	0.12	399	10.0	900	11	-40	21.2	59	1.0
Profile #2	57	90	800	50	0.3	366	7.3	910	11.3	-50	66.9	98	2.1
Profile #3	37	75	775	48	0.26	364	7.6	890	8.5	-50	54.4	-100	1.8
Profile #4	-33	62	700	62	0.12	356	5.7	870	9.8	20	31.7	-284	0.7
Profile #5	-120	55	450	80	0.1	463	5.8	850	9.9	140	33.3	-123	0.4
G1 Profile	-215	64	380	120	0.18	800	6.7	854	15.8	400	90.4	83	0.6

Table 6.1. Summary of mass flux, ice thickness, surface mass balance, driving stresses and ice surface topography from LGBT to G1.

transect and Point D is due to several factors. Within this stretch of the glacier, a major topographic elevation drop of 1300 m over 110 km occurs. The area is heavily crevassed and has been visually interpreted as an ablation zone due to the appearance of a predominantly 'blue ice' surface. In the vicinity of Point D is also what has been interpreted by this author as basal melt lakes. As such basal melt and refreeze would have to be included in the equation of mass flux. If mass flux between A.79 and Profile #1 were recalculated assuming the glacier is in a state of equilibrium, then the mass flux at Point D would be approximately 13.7 Gt a^{-1}.

At Profile #1 the mass flux of the Lambert ice stream is 11 Gt a^{-1} ±5-10%. This is at a surface elevation of 80 m asl. By Profile #4, north of G3, the mass flux of the Lambert ice stream is 10 Gt a^{-1} ±5-10%. The relative continuity of the mass flux volume between these profiles could be attributable to the surface ablation and basal melt rates (Table 6.2) or a non-steady state change in ice thickness. The slight volume decrease of ice between these two profiles will change due to basal melt and refreeze under the ice shelf. As mentioned previously, the margin for error in these mass flux calculations is potentially in the order of ±0.5 - 0.7 Gt a^{-1}.

Profile	Area	Accumulation Rate	Flux In - Flux Out	∑ Surface Flux	Basal Mass Balance	Basal Melt Rate
	(km^2)	($kgm^{-2}a^{-1}$)	(Gt a^{-1})	(Gt a^{-1})	(Gt a^{-1})	($kgm^{-2}a^{-1}$)
#1 to #2	1827	-45	2.23	- 0.08	2.31	2310
#2 to #3	2400	-50	4.29	- 0.12	4.41	4410
#3 to #4	8400	-15	1.38	- 0.126	1.50	1510
#4 to #5	7569	80	0.85	+ 0.6	0.25	250

Table 6.2. Surface and basal mass balance across the entire profile. Accumulation values are from Figure 5.13. Area is measured between the referenced profiles. The basal melt rate (in meters per year) equates to the same figure as basal mass balance when considering this value as a change in elevation.

The decrease in the mass flux rate for the Lambert glacier ice stream is 8.5 Gt a^{-1} ±5-10% across Profile #3. This is a marked decrease in mass flux compared to the volume of ice passing through Profiles #2 and #1. This coincides with an area of ablation, surface velocity reduction and ice stream narrowing. In this area of Profile #3, there is evidence as suggested in Chapters Four and Five, that the ice is predominantly floating. Basal melting would reduce the volume of ice passing across the transect which also appears within an ablation zone. The increase in mass flux through Profiles #4 and #5 may be reflecting a surface mass gain that is marginally out-weighing the mass loss through basal processes which could involve exchange with the ocean.

Table 6.1 is a summary of the mass discharge characteristics by the Lambert Glacier and Amery Ice Shelf and of the ice dynamics from the Lambert Glacier Basin Traverse (after Higham, 1994) through to near the Amery ice front at G1 (after Budd *et al.*, 1982). Unless otherwise stated, all values relate to an average from the two main tributary glaciers; that is, the Lambert and Mellor Glaciers. Surface slope used in these calculations has been averaged over 50 km slope and the ice stream width used in determining mass flux has been derived from the average ice stream width from the Lambert and Mellor tributary Glaciers. These results pertain to the eastern side of the drainage system and are considered by this author to be the best reflection of the ice dynamics of the lower Lambert Glacier and Amery Ice Shelf system.

Figure 6.3 is an illustration of the mass flux per kilometre averaged from the Lambert and Mellor Glaciers. Compared with this is velocity, average ice stream width and ice thickness. About the Lambert Glacier Basin Traverse the ice mass is continental, flowing slowly and grounded to the bedrock, therefore flow is due to internal deformation. Between A.79 and Point D the steep surface topography suggests a similarly steep bedrock slope. This allows for a faster ice velocity under the now distinct ice stream. From Point D to Profile #1 the ice is undergoing a transition by not quite floating freely and not being entirely grounded. The basal sliding assists in this authors definition of the new grounding zone parameter. Except for some western grounding points, beyond Profile #1 the ice mass type is a floating one. These conclusions are based on information from Table 6.1.

6.3 Discussion

The mass flux of the Lambert Glacier, in its lower reaches, has been calculated by this author to be in the order of 11 Gta^{-1} ± 5-10% in the vicinity of Profile #1. At Profile #4 the mass flux is 10 Gta^{-1} ± 5-10%. This is comparable with the results of Budd *et al.* (1982) with 11 Gta^{-1} ± 15% across their G3 transect which covers a very similar site to Profile #4 between Jetty Peninsula and Manning Nunataks.

The mass budget calculations within the lower Lambert Glacier and Amery Ice Shelf system suggest the hypothesised location of the ablation zone and grounding zone proposed by this author from satellite image interpretation and RES extrapolation and interpretation can be identified in the mass budget trends of the Lambert Glacier in this study area.

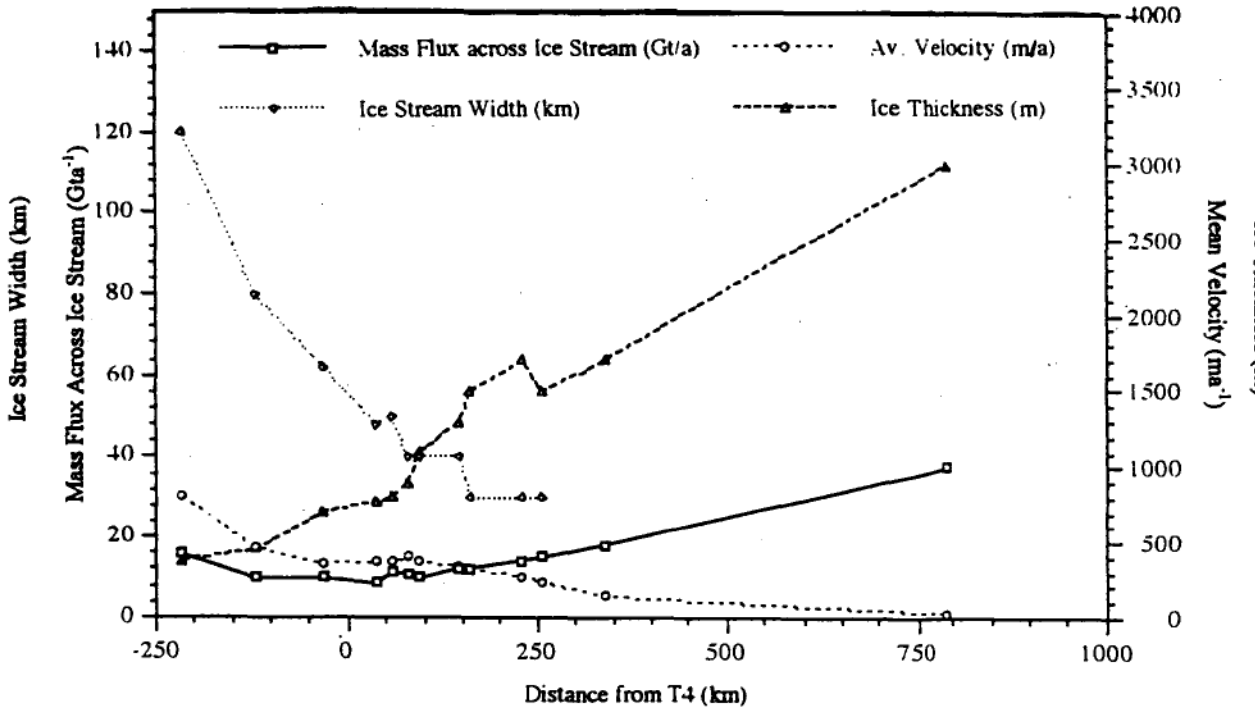

Figure 6.3. Some dynamic parameters for the eastern side of the Lambert Glacier ice stream between Profile #5 (north) and Point D (south). All results have been graphed with a weighted mean of three. Profiles #5 to #1 are observed and measured values. Points A to D have been interpolated from values at Profile #1 and the A.79 transect (after Allison, 1979). The graph is viewed north to south.

Chapter Seven

Conclusions

The Lambert Glacier stream lies within an area between 71° and 75° South and between 66° and 71° East. The average width of the ice stream is 35 km around the lower margins and 45-50 km within the Amery Ice Shelf. The grounding zone stretches between 72° to 73° 30' South (Figure 4.30). This conclusion has been based on extensive satellite image interpretation and analysis of Radio Echo Sounding data collected during the two austral summer seasons of 1988-89 and 1989-90.

This research has aimed to study and define the morphology and dynamics of the lower Lambert Glacier and Amery Ice Shelf system. Several conclusions have arisen from this work. Firstly, the Lambert Glacier is thicker on the western side of its lower drainage system. This leads to a greater portion of the Lambert Glacier ice stream to be grounded along this margin. The tributary from the grounded ice to the east is not funnelled through mountain ranges, as in the case of the Prince Charles Mountains in the west, and as such the drainage of the Princess Elizabeth Land is more moderated and allows for a gradual dispersion into the drainage system. Also, the larger area of grounded ice on the western side of the graben, in the vicinity of Fisher Massif, is an area of ablation. This has been deduced from surface mass balance and image interpretation. Dare (1995) also showed that the western side of the Lambert Glacier and Amery Ice Shelf drainage system is an area of stronger winds in comparison to the eastern side of the system. This adds to this authors interpretation of a steeper western tributary ice sheet in an area that is windier than the gentler slopes of the eastern side of the lower Lambert Glacier. This is because the winds from the eastern side of the drainage system are not being funnelled through a mountain range such as the Prince Charles Mountains to the west. This windswept zone coincides with an area of ablation. Within this vicinity, the ice is grounded and comparatively thicker than elsewhere.

The transition from ice that is grounded to the ice that is floating is often reflected as a change in the predominant stress pattern. Typically, this pattern change will be from high basal shear to low basal shear and greater longitudinal stresses or transverse shear. The low rate of change of velocity along the profile indicates that the

longitudinal stress gradients are not important. The spatial extent of this transition, or grounding zone, has often been thought of as extending over an area only a few ice thicknesses long where the ice sheet drains directly into the ice shelf (Paterson, 1994). The transition on the Lambert Glacier drainage system is however ~235km long.

The Lambert Glacier is not the only drainage system with an extended grounding zone. The ice streams on the Siple Coast also show relatively low surface slopes, low basal shear and extensive transition zones (Paterson, 1994). The grounding zone of the Lambert Glacier is ~10,575 km^2 connecting the inland ice in the upper catchment area to the Amery Ice Shelf. The Amery Ice Shelf can be considered as primarily having a single large tributary glacier entering into the relatively deep waters of Prydz Bay. At its deepest, the Lambert Glacier is over 2000 m thick when it initially flows into the southern reaches of the grounding zone, that is, at the Lambert Glacier hinge line near 73°19'S.

The parameters of the grounding zone have chiefly centred around the low driving stresses between the A.79 transect (after Allison, 1979) and the work at G1 (after Budd *et al.*, 1982). The five main cross sections used by this author were limited in their location by the availability of RES flight coverage. Future RES work in the area of the southern limits of the grounding zone will help confirm the results established by this author from data from only one flight. The grounding zone southern limit has been derived from radio echo sounding surveys that suggest the greatest ice thickness is in the confluence region between Mawson Escarpment and Mount Stinear. Further south and upstream, both the surface elevation and bedrock elevation rise rapidly into the Lambert Glacier Basin and the polar plateau beyond.

The ice types in this study have included the continental ice on the Lambert Glacier Basin Traverse route which is still grounded and flowing through internal deformation and basal sliding. By A.79, the flow lines of the Lambert ice stream become clearly discernible and contribute to the identification of the second ice type. This ice type is referred to as an ice stream or outlet glacier. The ice stream of the Lambert Glacier is essentially grounded north of the confluence (see the upper Lambert Glacier profile in Figure 4.25) but by Profile #1 the ice is predominantly floating. Profile #1 is approximately 80 km south of T4 which Budd *et al.* (1982) used as a definition for the Lambert Glacier grounding zone. The ice stream then flows on to a third ice mass, the Amery Ice Shelf. The area concentrated on in this research has been the Lambert

Glacier's transition from ice stream to ice shelf in the study of the grounding zone between Point D (230 km south of T4) and Profile #5 (120 km north of T4).

The Lambert Glacier has a positive mass budget of 29 to 32 Gt a^{-1} (Goodwin, 1995). The Amery Ice Shelf has a near ice front mass flux of 83 Gt a^{-1} (Bentley and Giovinetto, 1991). Thomas and Bentley (1978) point out that progressively larger zones of grounded ice and pinning points have the effect of reducing an outlet glaciers ability to drain its hinterland. This would have the effect of increasing the thickness of the ice which has been implied as a surface elevation rise on the Lambert Glacier by Allison (1979), Herzfeld *et al.* (1994) and Lingle *et al.* (1994). Some of this ice thickness may also be taken up in basal depressions as may be the case in the area identified as basal melt lakes.

Thirty eight Giga tonnes per annum of ice (Allison, pers. com., 1995) flows through the Mellor and Lambert Glaciers at the Lambert Glacier Basin Traverse line. By the A.79 transect of Allison (1979) the ice mass flux through the entire Lambert Glacier drainage system is 30 Gt a^{-1}. By Point D, 350 km south of Profile #5, approximately 18 Gt a^{-1} is discharging into the confluence zone from all the tributary ice streams. This implies a budget excess of 12 Gt a^{-1} within the upper basin from A.79 to Point D. The net surface loss (top and bottom) or thickness change rate is 3.6×10^{-3} Gt a^{-1} per km^2 (over an area approximately 110 km in length and across an average ice stream width of 30 km). Within this area the tributary ice narrows from a contribution width of over 400 km into a graben approximately 45 km across. Between Point D and Profile #1 the mass flux attributable to the Lambert ice stream reduces from 18 Gt a^{-1} to 10 Gt a^{-1}. This area has been defined as the Lambert Glacier grounding zone.

The mass flux continues to decrease until beyond Profile #3 where the effects of maritime precipitation increases accumulation. Within the Lambert Glacier grounding zone there is an implied mass budget excess of 8 Gt a^{-1}. The grounding zone region is an ablation zone and potentially overlays extensive basal melt lakes, basal marine environments and wide spread basal sliding. Hence the 8Gt a^{-1} may be lost by basal melt. The effects of the more pronounced grounding of the western side of the drainage system has a noticeable effect on the mass flux rate through the drainage system up to the vicinity of Profile #3.

The driving stresses along the study region show a marked reduction in basal shear and normal stress between A.79 and Point D. Within this area there is a steep ice surface elevation drop in the order of one hundred meters per kilometre and extensive surface crevassing. This demarcation has been defined as the southern limit for the Lambert Glacier grounding zone through the work of this author. Based primarily on the driving stresses and ice morphology, the northern limit of the Lambert Glacier grounding zone, at the centre flow line, has been identified as situated between Profile #1 and Point A. Here the ice thickness thins more rapidly than had occurred upstream and the basal profile takes on a predominantly smoother outline. In the region of the northern grounding zone limit, the transition from basally sliding to free floating occurs intermittently over considerable areas until north of Profile #3. The floating ice mass predominantly occupies the shallower eastern side of the drainage system.

The location of the profiles from the grounding line (Table 6.1) indicate that the average transverse strain rates to the edge of the stream are relatively uniform and comparable over the extensive grounding zone and are also similar to those over the northern part of the Amery Ice Shelf. This implies that the resistance to the flow and driving stress is taken primarily by the side shear rather than the basal shear over the transition zone. The near floating conditions over such an extensive floating-grounding zone results in very low basal shear stresses, normal stresses above buoyancy and driving stress over the large region of more than 200 km extent between the southern grounding line and Profile #3.

The redefined spatial extent of the Lambert Glacier, this drainage systems transition zone and inland extent of the Amery Ice Shelf has meant that the Lambert Glacier is probably no longer one of the worlds largest glaciers. From the Lambert Glacier basin to the Amery Ice Shelf front is still a vast distance, but the transition zone occupies a significant portion of it. With a decreasing mass flux rate from the LGBT to the ice shelf indicates a considereble positive balance and thickening of the ice sheet with possibly high basal melting rates beneath the extensive transition zone.

With a clearer definition of the Lambert Glacier's grounding zone, an opportunity now exists for more detailed modelling of the response Antarctica has to changing climate and sea level. No longer can the Lambert Glacier grounding zone be considered a line a few tens of kilometres wide. As demonstrated in this study, the grounding zone of

the Lambert Glacier is a large and complicated area to study being as it is one of the glaciers most sensitive regions to environmental change. With the grounding zone established, further radio echo sounding surveys and surface observations need to be made in the area of the southern reaches of the grounding zone for the Lambert Glacier. This is important in order to be able to monitor surface elevation change both at the ice surface and at the ice/rock interface.

Appendices

Appendix A:

Thematic Mapper (TM) satellite image over the Lambert Glacier confluence region. 146

Appendix B:

List of cartographic maps, satellite images and aerial photographs used in the research. 147

Appendix C:

Illustration of Profiles and Points created from RES surveys and used to determine the grounding zone of the Lambert Glacier. 149

Appendix D:

Selected velocity vectors and locations used and related to the study of the lower Lambert Glacier and Amery Ice shelf system. 150

Appendix A

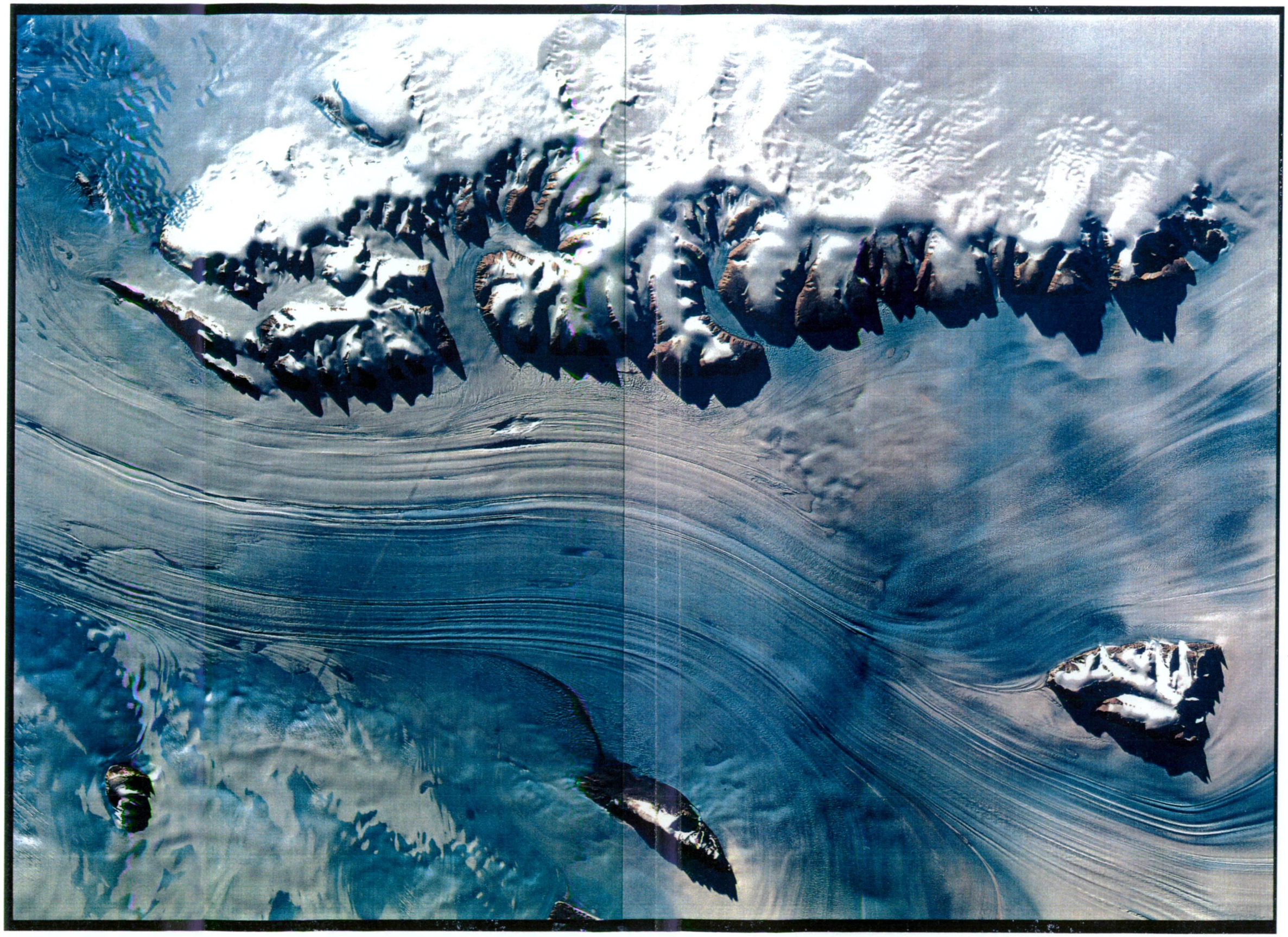

TITLE	SERIES NUMBER	SCALE	PUBLISHED
Topographic Maps			
Lambert Operations Area	AUSLIG	1:1,000,000	1994
Gory Sodruzestva	S-41-XVII, XVIII	1:200,000	1978
Massiv Nabl'udenu	S-42-XI, XII	1:200,000	1978
Campston Massif	S-42-XIII, XIV	1:200,000	1978
G. Udivitel'naja	S-42-XV	1:200,000	1978
Chr. Mezevoj	S-42-IX, X	1:200,000	1978
Skaly Roborovskogo	S-42-IX, X	1:200,000	1978
G. Iskristaja	S-42-III, IV	1:200,000	1978
G. Ploscadka	S-42- I, II	1:200,000	1978
MacKenzie Bay	R-42-XXXV, XXXVI	1:200,000	1978
Douglas Bay	R-42-XI, XII	1:200,000	1978
Foley Promontory	R-42-IX, X	1:200,000	1978
Lednik Buchtovyj	R-42-III, IV	1:200,000	1978
Mt. Kjerka	R-42-I, II	1:200,000	1978
Lednik Tekucij	R-42-XV, XIV, XVI	1:200,000	1978
Gr'ada Barjernaja	R-42-XXI, XXII	1:200,000	1978
G. Belaja Sapka	R-42-XIX, XX	1:200,000	1978
Gillock Island	R-42-XXIII, XXIV	1:200,000	1978
Gory Kosmonatov	R-42-XXV, XXVI	1:200,000	1978
Gr'ada Barjernaja	R-42-XXVII, XXVIII	1:200,000	1978
Manning Ntks	R-42-XXIX, XXX	1:200,000	1978
Fisher Massif	R-42-XXXI, XXXII	1:200,000	1978
Morena Dlinnaja	R-42-XXXIII, XXXIV	1:200,000	1978
Pickering Ntks	R-42-XXXV, XXXVI	1:200,000	1978
Reinbolt Hills	R-43-XIX, XX	1:200,000	1978
Ctatler Hills	R-43-XIII, XIV	1:200,000	1978
Prydz Bay	R-43-VII, VIII	1:200,000	1978
Princess Elizabeth Land	R-43-XXV	1:200,000	1978
Princess Elizabeth Land	R-43-XXXI	1:200,000	1978
Aerial Photographs			
	Negative # G153		1975

TITLE	SERIES NUMBER	SCALE	IMAGE DATE
Satellite Imagery			
Mawson Escarpment - North	TM 2B3G4R		4.5.1995
Mawson Escarpment - South	TM 2B3G4R		4.5.1995
EOSAT Landsat	E-42069-03215-4		15.3.1988
EOSAT Landsat	E-42069-03204-4		15.3.1988
EOSAT Landsat	E-42069-03155-4		8.3.1988
EOSAT Landsat	E-42051-03334-4		26.2.1988
DSTR - GEOMET Band 7	10148-03263		18.12.1972
DSTR - GEOMET Band 7	10236-03150		16.3.1973
DSTR - GEOMET Band 7	1236-031530		16.3.1973
AUSLIG Image Maps			**PUBLISHED**
Jetty Peninsula	SR 41-42a	1:500,000	1993
Lars Christensen Coast	SR 41-42b	1:500,000	1993
Charybdis Glacier	SR 41-42c	1:500,000	1993
Southern Prince Charles Mountains	SR 40-42b	1:500,000	1993

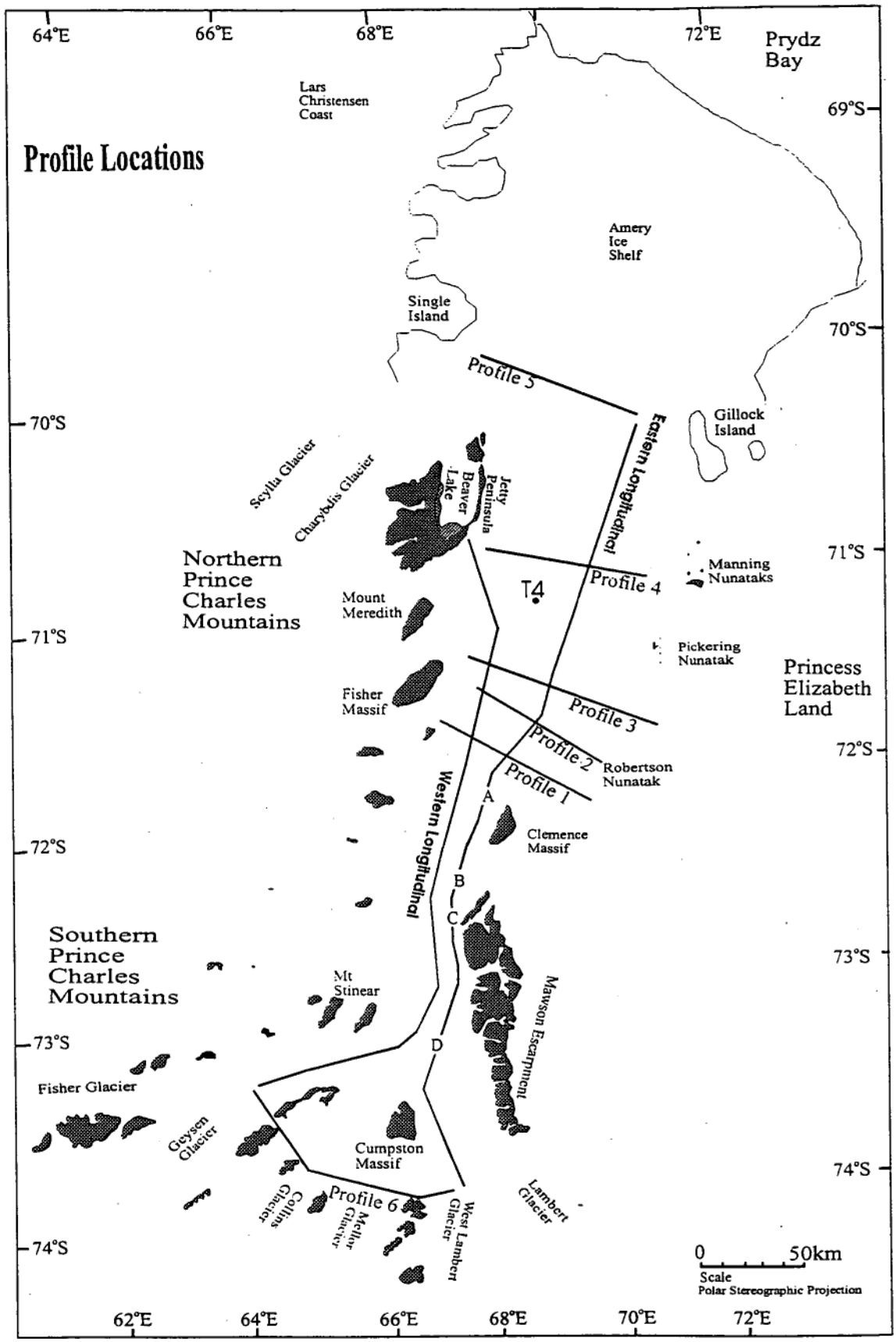

Appendix C: The location of all the transect profiles, longitudinal profiles and points A to D that are referred to in this study on the morphology and dynamics of the lower Lambert Glacier and Amery Ice Shelf.

Appendix D

Station	Latitude (degrees South)	Longitude (degrees East)	Velocity (ma^{-1})	Azimuth
LGB40	-75.857	68.202	9.3	9
LGB42	-75.858	69.298	18.6	18
LGB43	-76.068	63.910	46.5	29
LGB43	-75.857	68.750	26.6	26
LGB44	-75.855	70.401	32.7	32
LGB45	-75.854	70.950	29.8	29
LGB46	-75.853	71.500	29.0	28
LGB47	-75.768	57.061	33.3	31
LGB48	-75.662	72.269	45.2	42
LGB49	-75.566	72.650	56.3	53
LGB50	-75.471	73.030	30.4	325

STATION	YEAR	LATITUDE (degrees South)	LONGITUDE (degrees East)	HEIGHT (m asl)	VELOCITY (ma^{-1})
Blustery Bluff	1969	71.4238108	67.8857797		
	1970			1135	
A406 (T4)	1969	71.2265258	69.4726389		333.24
	1970	71.2234411	69.4756975	90.14	
A405	1969	71.1752167	69.5222344		336.31
	1970	71.1720856	69.5251339	86.35	
A404	1969	71.1523497	69.5547136		337.76
	1970	71.1491972	69.5575372	85.3	
A403	1969	71.1088258	69.6095775		340.07
	1970	71.1056639	69.6122697	84.26	

A402	1969	71.0457831	69.6856181		342.99
	1970	71.0425511	69.6881236	82.91	
A401	1969	70.9934117	69.7544008		345.76
	1970	70.9901408	69.7567606	83.8	
A129 G3	1969	70.9601411	69.7927881		347.28
	1970	70.9568486	69.7950561	85.06	
A131	1969	70.9740986	69.7767233		346.37
	1970	70.9708178	69.7790261	85.3	
A129 (G3)	1969	70.9601411	69.7927885		347.28
	1970	70.9568486	69505611	85.06	

STATION	**YEAR**	**LATITUDE** (degrees South)	**LONGITUDE** (degrees East)	**HEIGHT** (m asl)	**VELOCITY** (ma^{-1})
A131	1969	70.9740986	69.7767233		346.37
	1970	70.9780178	69.7790261		
A129 (G3)	1969	70.9601411	69.7927881		347.28
	1970	70.9568486	69.7950561	85.06	
A201	1969	70.9605164	69.8359192		348.53
	1970	70.9572111	69.8381817	90.18	
A202	1969	70.9693753	70.0708808		354.45
	1970	70.9660106	70.0731353	89.65	

A203	1969	70.9787528	70.3170181		360.83
	1970	70.9753242	70.3192653	87.52	
A204	1969	70.9819136	70.3919686		359.52
	1970	70.9784969	70.3942022	89.62	
A205	1969	70.9895481	70.5305503		350.68
	1970	70.9862172	70.5327578	89.35	
A206	1969	70.9951181	70.6148922		341.51
	1970	70.9918797	70.6171189	89	
A207 (T2)	1969	71.0042672	70.7478044		327.14
	1970	71.0011722	70.7500311	86.25	
NEW YR NTK	1969	71.0635464	71.5001706		

STATION	YEAR	LATITUDE (degrees South)	LONGITUDE (degrees East)	HEIGHT (m asl)	VELOCITY (ma^{-1})
A131	1968	70.9740986	69.7767233		346.37
	1970	70.9708178	69.7790261		346.37
A129 (G3)	1968	70.9601411	69.7927881	85.06	347.28
	1970	70.9568486	69.7950561		
A301	1968	70.9291431	69.6472939	90.37	345.34
	1970	70.9258689	69.6495397		
A302	1968	70.9145681	69.5752811	90.11	343.91

	1970	70.911305	69.5774889		
A303	1968	70.8788964	69.3902228	83.42	319.42
	1970	70.87586	69.3921897		
A304	1968	70.8656608	69.3174031	82.38	299.54
	1970	70.8628058	69.3191336		
A305	1968	70.8479017	69.2271406	75.33	252.17
	1970	70.8454883	69.2284328		
A306	1968	70.8201067	69.0909489	96.28	11.95
	1970	70.8200328	69.0912214		
A307	1968	70.8044497	69.0027508	178.09	12.86
	1970	70.8043658	69.0030325		
A308	1968	70.7910442	68.8940497	276.72	13.9
	1970	70.790945	68.8943283		

Reference List

Alley, R.B., Blankenship, D.D., Rooney, S.T. and Bentley, C.R. 1989 Water Pressure coupling of sliding and bed deformation: III. Application to Ice Stream B, Antarctica. *J. Glaciol.* 35 (119): 130-139.

Alley, R.B. and Whillans, I.M. 1991 Changes in the West Antarctic ice sheet. *Science* 254(5034): 959-963

Allison, I. 1979 The mass budget of the Lambert Glacier drainage basin, Antarctica. *J. Glaciol.*, 22 (87): 223-235

Allison, I., Young, N.W. and Medhurst, T. 1985 Letter to the Editor *J. Glaciol.* 31 (109): 378-381.

Allison, I., Wendler, G. and Radok, U. 1993 Climatology of the East Antarctic Ice Sheet (100°E to 140°E) derived from automatic weather stations. *J. Geophysical Research* 98 (D5) : 8815-8823.

Andrews, J.T. 1975 *Glacial Systems: An approach to glaciers and their environment* Duxberry Press, Massachusetts, 191pp.

AUSLIG 1995 Landsat TM image of Mawson Escarpment-North and Mawson Escarpment-South. Australian Centre for Remote Sensing

Bardin, V.I. 1977 Glacial geomorphology of the Lambert Glacier and its surrounding mountains. *Polar Geography* 1 (4): 251-269.

Bardin, V.I. 1986 Oasis in the ice-bound land. *Science in the USSR* July/August (4) 1986 : 86-95, 120.

Barrett, P.J. 1991 Antarctica and global climatic change- a geological perspective. *in* C.M. Harris and B. Stonehouse (Eds) *Antarctica and Global Climate Change*, Scott Polar Research Institute and Belhaven Press, Cambridge.

Bentley, C.R. 1985 Glaciological evidence: the Ross Sea sector. In *Glaciers, ice sheets, and sea level: effect of a CO^2 -induced climate change. Report of a workshop Seattle, 13-15 Sept. 1984 Washington*, National Academy Press, p. 178-196.

Bentley, C.R. 1987 Antarctic Ice Streams: A Review. *Journal of Geophysical Research* 9 (B9): 8843-8858.

Bentley, C.R., Clough, J.W., Jezek, K.C. and Shabtaie, S. 1979 Ice thickness patterns and the dynamics of the Ross Ice Shelf, Antarctica. *J. Glaciol.* 24(90):287-294

Bentley, C.R., Shabtaie, S., Blankenship, D.D., Rooney, S.T., Schultz, D.G., Anandakrishnan, S. and Alley, R.B. 1987 Remote Sensing of the Ross Ice Streams and adjacent Ross Ice Shelf, Antarctica. *Annals of Glaciol.* 9: 20-29.

Bentley, C.R. and Giovinetto, M.B. 1991 Mass balance of Antarctica and sea level change. In Weller *et al.* (eds.) *Proc. Int. Conf. of Polar Regions in Global Change, June 11-15, 1990* University of Alaska, :481-488.

Bohmer, W.J. and Herterich, K. 1990 A simplified three-dimensional ice-sheet model including ice shelves *Annals of Glaciol.* 14: 7-19.

Braithwaite, R.J. 1984 Can the Mass Balance of a glacier be estimated from its Equilibrium-Line Altitude? *J. Glaciol.* 30 (106): 364-368.

Budd, W.F. 1965 Glaciological survey of the Amery Ice Shelf *Antarctic* 4 (3): 158-159

Budd, W.F. 1966 The dynamics of the Amery Ice Shelf. *J. Glaciol.* 6 (45): 335-358

Budd, W.F. 1970 Ice flow over bedrock perturbations. *J. Glaciol.* 9(55): 29-48

Budd, W.F., Smith, I.L. and Wishart, E. 1967 The Amery Ice Shelf. *In* Oura, H. (ed) *Physics of Snow And Ice: International Conference on Low Temperature Science 1966 Proceedings* Vol. 1, Pt 1. [Sapporo], Hokkaido University. Institute of Low Temperature Science: 447-467.

Budd, W.F. and Allison, I.F. 1975 An empirical scheme for estimating the dynamics of unmeasured glaciers. *Snow and Ice-Symposium- Neiges et Glaces (Proceedings of the Moscow Symposium, August 1971*: IAHS-AISH Pub. No. 104.

Budd, W.F. and McInnes, B.J. 1979 Periodically surging of the Antarctic ice sheet - an assessment of modelling. *Hydrological Sciences Bulletin 24*(1): 95-105

Budd, W.F. and Smith, I.N. 1981 The growth and retreat of ice sheets in response to orbital radiation changes. *Sea Level, Ice and Climatic Change. Proc. Canberra Symp. 1979* Ed. I. Allison, pp 369-409 IAHS Pub. No. 131.

Budd, W.F., Corry, M.J. and Jacka, T.H. 1982 Results from the Amery Ice Shelf Project. *Annals of Glaciol.* 3: 36-41.

Budd, W.F. and Smith, I.N. 1982 Large-scale numerical modelling of the Antarctic ice sheet. *Annals of Glaciol.* 3: 42-49.

Budd, W.F., Jenssen, D. and Smith, I.N. 1984 A three-dimensional time-dependent model of the west Antarctic Ice Sheet. *Annals of Glaciol.* 5: 29-36.

Budd, W.F. and Jenssen, D. 1989 The dynamics of the Antarctic ice sheet. *Annals of Glaciol.* 12: 16-22.

Budd, W.F. and Rayner, P. 1990 Modelling global ice and climate changes through the ice ages. *Annals of Glaciol.* 14: 23-27.

Bull, C.B.B. 1971 Snow accumulation in Antarctica. *In* Quam L.O. (ed) *Research in the Antarctic. A Symposium presented at the Dallas meeting of the American Association for the Advancement of Science - December 1968.* Washington, DC, American Assoc. for the Advancement of Science: 367-421.

Chinn, T.J. 1980 Glacier balances in the Dry Valleys area, Victoria Land, Antarctica. *World Glacier Inventory, Proc. Riederalp Workshop, 1978*, IASH Publication 126: 237-247.

Chinn, T.J. 1991 Polar Glacier Margin and debris Features. *Memorie della Societa Geologica Italiana* Vol. XLVI: 25-44.

Clapperton, C.M.. and Sugden, D.E. 1990 Late Cenozoic glacial history of the Ross Embayment. *Antarctica Quaternary Science Reviews* 9: 253-272.

Colhoun, E.A., Mabin, M.C.G., Adamson, D.A. and Kirks, R.M. 1992 Antarctic ice volume and contribution to sea-level fall at 20,000 yr BP from raised beaches. *Nature* 358: 316-319.

Colbeck, S.C. (Ed) 1980 *Dynamics of snow and ice.* Academic Press (468 pp).

Crabtree, R.D. and Doake, C.S.M. 1982 Pine Island Glacier and its drainage basin: Results from radio echo-sounding. *Annals of Glaciol.* 3: 65-70.

Crary A.P. 1961 Glaciological regime at Little America Station, Antarctica. *J. Geophys. Res.* 66(3): 871-878.

Crary, A.P., Robinson, E.S., Bennett, H.F. and Boyd Jr., W.W. 1962 Glaciological studies of the Ross Ice Shelf, Antarctica, 1957-60 IGY. *Glaciological Report Series* (New York, IGY World Data Centre A Glaciology), No. 6.

Crary, A.P. and Chapman, W.H. 1963 Additional glaciological measurements at the abandoned Little America station, Antarctica. *J. Geophys. Res.* 68 (21): 6064-65.

Dare, R. 1995 *Mesoscale modelling of the Antarctic boundary layer*. PhD Thesis (unpublished) University of Tasmania.

Doake C.S.M. 1985 Antarctic mass balance: glaciological evidence from Antarctic Peninsula and Weddell Sea sector. (In *Glaciers, ice sheets, and sea level: effects of a CO^2 - induced climate change .Report of a workshop Seattle, 13-15 Sept. 1984 Washington*, National Academy Press, : 197-209.

Drewry, D.J., Jordan, S.R. and Jankowski, E. 1982 Measured properties of the Antarctic ice sheet: surface configurations, ice thickness, volume and bedrock characteristics. *Annals of Glaciol.* 3: 83-91.

Drewry, D.J. 1983 *Antarctica: glaciological and geophysical folio*. Cambridge, University of Cambridge. Scott Polar Research Institute.

Drewry, D.J. and McIntyre, N. 1986 referenced in Drewry, D.J. The response of the Antarctic ice sheet to climate change. In *Antarctica and global climate change* (ed) C.M. Harris and B. Stonehouse : 90 - 106 London: Belhaven Press 1991.

Echelmeyer, K.A. and Kamp, B. 1986 Stress gradient coupling in glacier flow: II. Longitudinal averaging in the flow response to small perturbations in ice thickness and surface slope. *J. Glaciol.* 32 (111): 285-298.

Frakes, L.A. 1978 Cenozoic climates: Antarctica and the Southern Ocean. *In Climatic Change and Variability: a Southern Perspective*. Eds. A.B. Pittock, L.A. Frakes, D. Jenssen, J.A. Peterson and J.W. Zillman, pp 53- 69. Cambridge University Press, Cambridge.

Frolich, R.M., Doake, C.S.M. 1988 Relative importance of lateral and vertical shear on Rutford Ice Stream, Antarctica. *Annals of Glaciol.* 11: 19-22.

Giovinetto, M.B. 1964 the Drainage systems of Antarctica: accumulation. In Mellor, M. (ed) *Antarctic snow and ice studies*. Washington, DC, American Geophysical Union: 127-155 (Antarctic Research Series 2).

Giovinetto, M.B. 1970 The Antarctic ice sheet and its probable bi-model response to climate. *Union Geodesique et Geophysique Internationale. Association Internationale d'Hydrologie Scientifique* [*International Council of Scientific Unions. Scientific Committee on Antarctic Research. International Association of Scientific Hydrology. Commission of Snow and Ice*] *International Symposium on Antarctic Glaciological Exploration (ISAGE), Hanover, New Hampshire, USA 3-7 September 1968* :347-358. [Publication No. 86 de l'Association Internationale d'Hydrologie Scientifique].

Giovinetto, M.B. and Bentley, C.R. 1985 Surface balance in ice drainage systems of Antarctica *Antarctic J. of the United States*, XX (4): 6-13.

Giovinetto, M.B. and Bull, C. 1987 Summary and analysis of surface mass balance compilations for Antarctica, 1960-1985. *Byrd Polar Research Centre Report* No. 1. Columbus, Ohio.

Giovinetto, M.B., Bromwich, D.H. and Wendler, G. 1992 Atmospheric net transport of water vapour and latent heat across 70°S. *J. Geophys. Res.* 97 (D1): 917-930.

Gjessing, Y.T. 1970 Mass transport of Jutulstraumen ice stream in Droning Maud Land. *Norsk Polarinstitutt - Arbok* 1970 : 227-232.

Gjessing, Y. and Wold, B. 1981 Absolute movements, mass balance and snow temperatures of the Riiser-Larsenisen, Antarctica. (abstract) *Annals of Glaciol.* 3:346

Gloersen, P.; Campbell, W.J.; Cavlieri, D.J.; Comiso, J.C.; Parkinson, C.L. and Zwally, H.J. 1992 *Arctic and Antarctic Sea Ice, 1978-87: Satellite Passive-Microwave Observations and Analysis* National Aeronautics and Space Administration, Washington, D.C.

Goodwin, I.D., Higham, M., Allison, I. and Jiawan, R. 1993 Accumulation variability in Eastern Kemp Land, Antarctica. *Fifth International Symposium on Antarctic Glaciology* (VISAG), Cambridge, UK, 5-10 September 1993.

Goodwin, I.D. 1995 *On the Antarctic Contribution to Holocene Sea-level.* PhD Thesis (unpublished), University of Tasmania.

Grigoryan, S.S., Buyanov, S.A., Krass, M.S. and Shumskiy, P.A. 1985 The mathematical model of ice sheets and the calculation of the evolution of the Greenland Ice Sheet. *J. Glaciol.* 31 (109),: 281-292.

Haeberli, W., Herren, E. and Hoelzle, M.(Eds) 1993 *Glacier Mass Balance Bulletin.* No.2 (1990-1991) IAHS.

Hambrey, M.J. 1991 Structure and dynamics of the Lambert Glacier-Amery Ice Shelf system Implications for the origin of Prydz Bay sediments. *Proc. Ocean Drill. Program Sci. Results* 119: 61-75

Hambrey, M.J. and Dowdeswell, J.A. 1993 Stability of the Lambert glacier system, Antarctica: structural evidence from satellite imagery. (abstract) *Fifth International Symposium on Antarctic Glaciology (VISAG), Cambridge, UK, 5-10 September 1993*

Hambrey, M.J. and Dowdeswell, J.A. 1994 Flow regime of the lambert Glacier-Amery Ice Shelf system, Antarctica: structural evidence from Landsat imagery. *Annals of Glaciol.* 20:401-406

Hamley, T.C., Smith, I.N. and Young, N.W. 1985 Mass-balance and ice-flow-law parameters for East Antarctica. *J. Glaciol.* 31 (109): 334-339.

Hatherton, T. (ed) 1990 *Antarctica: the Ross Sea region.* Wellington: DSIR Publishing. pp 287.

Hellmer, H.H. and Jacobs, S.S. 1992 Ocean interactions with the base of Amery Ice Shelf, Antarctica. *J. Geophys. Res.* 97(C12): 20,305-20,317

Herzfeld, U.C., Lingle, C. S. and Lee, L-H. 1993 Geostatistical evaluation of satellite radar altimetry for high resolution mapping of Lambert Glacier, Antarctica. *Annals of Glaciol.* 17: 77-85.

Herzfeld, U.C., Lingle, C. S. and Lee, L-H. 1994 Recent advance of the grounding line of Lambert Glacier, Antarctica, deduced from satellite-radar altimetry. *Annals of Glaciol.* 20: 43-47.

Higham, M. 1994 Surface mass balance and snow surface properties from the Lambert Glacier basin traverses, 1990-94. Submitted as *Antarctic CRC Research Note*, Australian Antarctic Division.

Hooke, R.L. 1981 Flow law for poly crystalline ice in glaciers: comparison of theoretical predictions, laboratory data, and field measurements. *Reviews of Geophysics and Space Physics* 9(4): 664-672.

Hooper, M. 1991 *A for Antarctica: Facts and stories from the frozen south.* Pan Books Ltd, England. pp145

Hughes, T. 1975 The West Antarctic ice sheet: instability, disintegration and initiation of ice ages. *Reviews of Geophysics and Space Physics* 13 (4) : 502-526.

Hughes, T. 1983 On the disintegration of ice shelves: The role of fracture. *J. Glaciol.* 29 (101): 98-111.

Hughes, T. 1992 On the pulling power of ice streams. *J. Glaciol.* 38 (128): 125-151.

Jacobs, S.S., Gorgon, A.L. and Ardair, Jr. J.L. 1979 Circulation and melting beneath the Ross Ice Shelf. *Science* 203 (4379): 439-443.

Jacobs, S.S., MacAyeal, D.R. and Ardai, Jr. J.L. 1986 The recent advance of the Ross Ice Shelf, Antarctica. *J. Glaciol.* 32, (112): 464-474.

Jacobs, S.S., Hellmer, H.H., Doake, C.S.M., Jenkins, A. and Frolich, R.M. 1992 Melting of ice shelves and the mass balance of Antarctica. *J. Glaciol.* 38 (130): 375-387.

Jacobs, S 1992 The voyage of Iceberg B9. *American Scientist* 80 (1): 32-42

Jenkins, A.; Jacobs, S.S. and Keys, H. 1994 Is this little PIG in hot water? *Antarctic Journal of the United States* 29 (5): 121-22

Kamp, B. 1986 Stress-gradient coupling in glacier flow: III Exact longitudinal equilibrium equation. *J. Glaciol*, 32 (112): 335-341.

Kamp, B. and Echelmeyer, K.A. 1986 Stress-gradient coupling in glacier flow: I. Longitudinal averaging of the influence of ice thickness and surface slope. *J. Glaciol.* 32 (111): 267-284.

Kapitsa, A.P., Ridley, J.K., Robin, G. de Q., Siegert, M.J. and Zotikov, I.A. 1996 A large deep freshwater lake beneath the ice of central East Antarctica. *Nature* Vol. 381: 684-686

Keys, J.R. 1990 The Ice Forms in T. Hatherton (ed.) *Antarctica the Ross Ice Shelf region.* DSIR Publishing, Wellington New Zealand pp 287.

Kohen, H. 1982 Glaciological investigations in the frontal zone of the Filchner and Ronne Ice Shelves. *Annals of Glaciol.* 3: 16-19.

Kotlyakov, V., Barkov, N.I., Loseva, I.A. and Petrov, V.N. 1974 Novaya karta pitaniya lednikovogo pokrova Antarktidy. [New map of the accumulation on the Antarctic ice sheet.] *Materialy Glyatsiologicheskikh Issledovaniy. Khronika. Obsuzhdeniya,* Vyp. 24: 248-255.

Krebs, K.A. 1992 *The distribution, activity and characteristics of alpine-type glaciers in the northern Prince Charles Mountains, East Antarctica.* Honours Thesis (unpublished) James Cook University of North Queensland.

Krebs, K.A. 1996 Distribution, classification and activity of alpine-type glaciers in the Northern Prince Charles Mountains, MacRobertson Land, East Antarctica. (abstract) *Prince Charles Mountains Workshop 2-3 October 1996 Abstracts Volume.* School of Earth Sciences, University of Melbourne.

Landon-Smith, I.H. 1964 Bericht über glaziologische Untersuchungen des Amery-Schelfeises in der Antarktis Polarforschung, Bd. 5, Jahrg. 33, Ht.1-2, 1963, p.190-91 In Budd, W.F. 1966 The dynamics of the Amery Ice Shelf. *J. Glaciol.* 6 (45): 335-358.

Lange, M.A. and Kohnen, H. 1985 Ice front fluctuations in the eastern and southern Weddell Sea. *Annals of Glaciol.* 6:187-191

Lange M. A. and MacAyeal D.R. 1986 Numerical models of the Filchner-Ronne Ice Shelf: an assessment of re-interpreted ice thickness distributions. *J. Geophys. Res.* 91 (B10): 10,457-10,462.

Law, P. 1966 Movement of the Amery Ice Shelf. *Polar Records* 13 (85): 439-441

Lingle, C.S. and Brown, T.J. 1987) A subglacial aquifer bed model and water pressure dependent basal sliding relationship for a west Antarctic ice stream. *in* C.J. van der Veen and J. Oerlemans (eds), *Dynamics of the West Antarctic Ice Sheet.*: 249-285.

Lingle, C.S., Lee, L-H., Zwally, H.J. and Seiss, T.C. 1993 Recent elevation increases on Lambert Glacier, Antarctica, from orbital cross-over analysis of satellite-radar altimetry. *Annals of Glaciol.* 20: 26-32.

Loewe, F. 1974 Considerations concerning the winds of Adelie Land. *Z. Gletscherk. Glazialgeol.* 10: 189-197.

Mabin, M.C.G. 1991 The glacial history of the Lambert Glacier - Prince Charles Mountains area and comparisons with the record from the TransAntarctic Mountains. *Quaternary Research in Australian Antarctica* (eds) D. Gillieson and S. Fitzsimmons, Special Publication No. 3

MacAyeal D.R. 1979 Transient temperature-depth profiles of the Ross Ice Shelf. [MSc. thesis, University of Maine at Orono, 1979] *in* MacAyeal, D.R., Thomas, R.H. 1986 *J. Glaciol.* 32 (110):72-86.

MacAyeal, D.R. and Thomas, R.H. 1986 The effects of basal melting on the present flow of the Ross Ice Shelf, Antarctica. *J. Glaciol.* 32 (110): 72-86.

MacAyeal, D.R., Shabtaie, S., Bentley, C.R. and King, S.E. 1986 Formation of ice sheet dynamic boundary conditions in terms of Coulomb rheology. *J. Geophys. Res.* 91 (B8) : 8177-8191.

MacAyeal, D.R. 1988 A tutorial on the use of control methods in ice sheet modelling. *J. Glaciol.* 39 (131): 91-98.

MacAyeal, D.R. and Barcilon, V. 1988 Ice-shelf response to ice-stream discharge fluctuations: I. Unconfined ice tongues. *J. Glaciol.* 34 (116): 121-127.

MacAyeal, D.R. 1989 Ice-shelf response to ice-stream discharge fluctuations: III. The effects of ice-stream imbalance on the Ross Ice Shelf, Antarctica. *J. Glaciol.* 35 (119): 38-42.

McDonald, J. and Whillans, I.M. 1992 Search for temporal changes in the velocity of Ice Stream B, West Antarctica. *J. Glaciol.* 38 (128): 157-161.

McInnes, B.J. and Budd, W.F. 1984 A cross-sectional model for west Antarctica. *Annals of Glaciol.* 5: 95-99.

McIntyre, N.F. 1985 A re-assessment of the mass balance of the Lambert Glacier drainage basin, Antarctica. *J. Glaciol.* 31 (107): 34-38 McIntyre, N.F. 1985 The Dynamics of Ice-Sheet Outlets. *J. Glaciol.* 31 (108): 99-107.

McIntyre, N. 1985 Letter to the editor. *J. Glaciol.* 31 (109): 381.

McLeod, I.R. 1967 Glaciological Observations in Enderby, Kemp, and Mac.Robertson Lands, Antarctica. *ANARE Interim Reports series A (IV)* Glaciology Pub. No. 90 Dept. External Affairs, Melbourne. pp 48.

Markov, K.K., Bardin, V.I., Lebedev, Orlov, A.I. and Suyetova, I.A. 1968 Geografiya Antarktidy. [The geography of Antarctica] Moskva, zdatel'stvo Mysl'. (*In* Jacobs *et al.* (1986) *J. Glaciol.* 32(112): 464-474.

Mellor, M. 1959 Mass balance studies in Antarctica. *J. Glaciol.* 3 (26): 522-533

Mellor, M. 1964 Remarks concerning the Antarctic mass balance. *Polarforschung*, Bd.5 Jarg.33 Ht.1-2:179-180

Mellor, M. 1967 Mass economy of Antarctica: Measurements at Mawson. *1957 ANARE Science Reports series A (IV)* Glaciology Pub. No. 97 Dept External Affairs, Melbourne.

Mellor, M. and McKinnon, G.W. 1960 The Amery Ice Shelf and its hinterland. *Polar Record* 10 (64): 30-34

Morgan, V.I. 1972 Oxygen isotope evidence for bottom freezing on the Amery Ice Shelf. *Nature* 238 (5364): 393-394.

Morgan, V.I. and Budd, W.F. 1975 Radio-echo sounding of the Lambert Glacier basin. *J. Glaciol.* 15 (73): 103-111.

Morgan, V.I., Jacka, T.H. and Akerman, G.J. 1982 Outlet glacier and mass- budget studies in Enderby, Kemp, and Mac. Robertson Lands, Antarctica. *Annals of Glaciol.* 3: 204-210.

Morland, L.W., Smith, G.D. and Boulton, G.S. 1984 Basal sliding relations deduced from ice-sheet data. *J. Glaciol.* 30, (105), 131-139.

Moller, D. and Ritter, B. 1988 Glacial Geodetic contributions to the mass balance and dynamics of ice shelves. *Annals of Glaciol.* 11: 89-94.

Myers, D.E. 1985 Co-kriging: Methods and Alternatives. *in* P. Glaeser (ed) *The Role of Data in Scientific Progress*, Elsevier Scientific Publishing, New York

Oerlemans, J. and Hoogendoorn, N.C. 1989 Mass-balance gradients and climate change. *J. Glaciol.* 35 (121): 399-405.

Paterson, W.S.B. 1994 *The Physics of Glaciers* (3rd edition) Elsevier Science Ltd, Oxford England

Parish, T.R. 1982 surface air flow over east Antarctica. *Mon. Weather Rev.* 10: 84-90

Partington, K.C., Cudlip, W., McIntyre, N.F. and King-Hele, S. 1987 Mapping of Amery Ice Shelf, Antarctica, surface features by surface altimetry. *Annals of Glaciol.* 9: 183-188.

Phillpot, H.R. 1985 Climate. *In* W.N. Bonner and D.W.H. Walton (eds) Key *Environments: Antarctica* Pergamon Press Ltd, England, 381 pp.

Pillsbury, R.D. and Jacobs, S.S. 1985 Preliminary observations from long-term current meter moorings near the Ross Ice Shelf, Antarctica. (*In* Jacobs, S.S. (ed) *Oceanography of the Antarctic continental shelf.* Washington DC. American Geophys. Union p. 87-107 (Ant. Res. Series Vol. 43)).

Pozdeev, V.S. 1991 Soviet RES data compiled for the Amery Ice Shelf and Mac.Robertson Land, 1:5000 000 maps. Unpublished

Radok, U., McInnes, B.J., Jenssen, D. and Budd, W.F. 1989 Model studies on ice-stream surging. *Annals of Glaciol.* 12: 132-137.

Ridley, J., Cudlip, W., McIntyre, N. and Rapley, C. 1989 The topography and surface characteristics of the Larsen Ice Shelf, Antarctica, using satellite altimetry. *J. Glaciol.* 35 (121): 299-310.

Robin, G. de Q. 1964 Glaciology. *Endeavour* XXIII (89): 102-107.

Robertson, F.B. 1993 *Amery Ice Shelf front mass budget.* BSc (Honours) thesis, University of Tasmania, unpublished.

Rott, H.; Skvarca, P and Nagler, T. 1996 Rapid collapse of northern Larsen Ice Shelf, Antarctica. *Science* 271 (5250): 788-792.

Seko, K., Wada, M. and Aoki, S. 1991 The characteristic variation of τ_b in the Antarctic region revealed by NOAA AVHRR channel 4 data Proc. NIPR Symp. *Polar Meteorol. Glaciol.* 4: 31-42.

Sanderson, T.J.O. 1979 Equilibrium profile of ice shelves. *J. Glaciol.* 22(88), 435-460.

Shabtaie, S. and C.R. Bentley 1987 West Antarctic ice streams draining into the Ross Ice Shelf: configuration and mass balance. *J. Geophys. Res.* 92 (B2) : 1311-1336.

Shabtaie, S. and Bentley, C.R. 1988 Ice-thickness map of the west Antarctic ice streams by radar sounding. *Annals of Glaciol.* 11: 26-36.

Shabtaie, S., Bentley, C.R., Bindschadler, R.A. and MacAyeal, D.R. 1988 Mass-balance studies of ice streams A, B, and C, west Antarctica, and possible surging behaviour of ice stream B *Annals of Glaciol*, 11:137-149.

Sharp, R.P. 1988 *Living Ice: Understanding glaciers and glaciation* Cambridge University Press 225 pp.

Shimizu, H., Watanabe, O., Kobayashi, S., Yamada, T., Naruse, R. and Ageta, Y. 1978 Geological aspects and mass budget of the ice sheet. *in* Mizuho *Plateau Memoirs of the National Institute of Polar Research.* Special Issue 7 : 264-274.

Simmons, D.A. 1986 Flow of the Brunt Ice Shelf, Antarctica, derived from Landsat images, 1974-85. *J. Glaciol.* 32 (111): 252-254.

Stephenson, S.N. and Doake, C.S.M. 1982 Dynamic behaviour of Rutford Ice Stream. *Annals of Glaciol.* 3: 295-299.

Sugden, D.E. and John, B.S. 1976 *Glaciers and Landscapes. A Geomorphological Approach*, Edward Arnold Publishing, Great Britain (1990 edition).

Swan, A.R.H. and Sandilands, M 1995 *Introduction to Geological Data Analysis*, Blackwell Science Ltd, Oxford

Swithinbank, C.W. 1963 Ice movement of valley glaciers flowing into the Ross Ice Shelf. *Antarctic Science* 141 (3580): 523-524.

Swithinbank, C.W.M. and Zumberge, J.H. 1965 The Ice Shelves (*In* Hatherton, T. (ed) *Antarctica : the Ross Sea region* Wellington DSIR Publishing 1990.

Swithinbank, C., Brunk, K. and Sievers, J. 1988 A glaciological map of Filchner-Ronne Ice Shelf, Antarctica. *Annals of Glaciol.* 11: 150-155.

Swithinbank, C. (Ed) 1988 Satellite Image Atlas of Glaciers of the World: *Antarctica United States Geological Survey Professional Paper* 1386-B: 62-73

Thiel, D.V. 1986 A preliminary assessment of glacial ice profiling using VLF surface-impedance measurements. *J. Glaciol.* 32 (112):76-82.

Thomas, R.H. 1979 The dynamics of marine ice sheets. *J. Glaciol.* 24 (90):167-177.

Thomas, R.H. and MacAyeal, D.R. 1982 Derived characteristics of the Ross Ice Shelf, Antarctica. *J. Glaciol.*, 28: 397-412.

Thomas, R.H., MacAyeal, D.R., Eilers, D.H. and Gaylord, D.R. 1984 Glaciological studies on the Ross Ice Shelf, Antarctica 1973- 1978 in Bentley, C.R. and Hayes, D.E. (eds) *The Ross Ice Shelf: Glaciology and geophysics.* Washington DC, American Geophys. Union : 21-53 (Antarctic Research Series Vol. 42).

Thomas, R.H., Stephenson, S.N., Bindschadler, R.A., Shabtaie, S. and Bentley, C.R. 1988 Thinning and grounding-line retreat on Ross Ice Shelf, Antarctica. *Annals of Glaciol.* 11: 165-172.

Thomas, R.H. and Bentley, C.R. 1978 A model for Holocene retreat of the West Antarctic Ice Sheet. *Quaternary Research*, 2: 150-170.

Thost, D.E., Leitchenkov, G., O'Brien, P.E., Tingey, R.J. and Wellman, P. 1995 Geoscience transect from the Southern Prince Charles Mountains to Prydz Bay, East Antarctica. *VII International Symposium on Antarctic Earth Science, 10-15 September 1995*, Siena (Italy), Abstract Vol. p376.

Thyssen F. 1986 The central part of the Filchner-Ronne Ice Shelf. *In* Kohnen H., comp. *Filchner-Ronne-Ice-Shelf-Programme. Report No. 3* Bremerhaven, Alfred-Wegener-Institute for Polar and Marine Research : 81-83.

Thyssen, F. 1988 Special aspects of the central part of Filchner-Ronne Ice Shelf, Antarctica. *Annals of Glaciol.* 11: 173-179.

Thyssen, F. and Grosfeld, K. 1988 Ekstrom Ice Shelf, Antarctica. *Annals of Glaciol.* 11: 180-183.

Tingey, R.J. 1991 Commentary on schematic geological map of Antarctica: Scale 1:10,000,000. *BMR Bulletin* 238, Aust. Govt. Pub. Serv., Canberra

Trail, D.S. 1964 The glacial geology of the Prince Charles Mountains, Antarctica. (*In* Craddock, C. ed. *Antarctic Geoscience. Proceedings of the third Symposium on Antarctic Geology and Geophysics, Madison, 22-27 August, 1977.* Madison, University of Wisconsin Press).

Uratsuka, S.; Nishio, F. and Mae, S. 1996 Internal and basal ice changes near the grounding line derived from radio echo sounding. *J. Glaciol.* 42 (140): 103-109

Vaughan, D. and Lachlan-Cope, T 1995 Recent retreat of ice shelves on the Antarctic Peninsula. *Weather* 50 (11): 374-76.

Vaughan, D.G. and Doake, C.S.M. 1996 Recent atmospheric warming and retreat of ice shelves on the Antarctic Peninsula. *Nature* 379 (6563): 328-331.

Veen, C.J. van der and Oerlemans, J (editors) 1987 *Dynamics of the West Antarctic ice sheet.* D. Reidel Publishing Co., Holland. pp 368.

Voronov, P.S. 1964 Tectonics and neotectonics of Antarctica. *Antarktika (Dokl. Komisii za 1963)* [*Antarctica (Reports of the Commission for 1963)*] Moscow, Nauka

Vornberger, P.L. and Whilans, I.M. 1990 Crevasse deformation and examples from Ice Stream B, Antarctica. *J. Glaciol.* 36 (122): 3-10.

Wakahama, G. and Budd, W.F. 1976 Formation of the three-layered structure of the Amery Ice Shelf, Antarctica. *J. Glaciol.* 16 (74): 295-297.

Walder, J.S. 1986 Hydraulics of subglacial cavities. *J. Glaciol.* 32 (112): 439-445.

Walton, D.W.H. (ed) 1987 *Antarctic Science* Cambridge University Press

Wellman, P., and Tingey, R.J. 1976 Gravity evidence for a major crustal fracture in eastern Antarctica. *BMR J. of Australian Geology and Geophysics* (Bureau of Mineral Resources, Geology and Geophysics), 1 (2): 105-108.

Wellman, P. 1982 Surging of Fisher Glacier, Eastern Antarctica: Evidence from geomorphology. *J. Glaciol.* 28 (98): 23-28.

Weertman, J. 1957 Deformation of floating ice shelves. *J. Glaciol.* 3 (21): 38-42.

Weertman, J. 1976 Glaciology's grand unsolved problem. *Nature* 260 (5549) : 284-286.

Weertman, J. and Birchfield, G.E. 1984 Ice-Sheet Modelling. *Annals of Glaciol.* 5: 180-184.

Whillans, I.M. and Bindschadler, R.A. 1988 Mass balance of Ice Stream B, West Antarctica. *Annals of Glaciol.* 11: 187-193.

Yuen, D.A., Saari, M.R. and Schubert, G. 1986 Explosive growth of shear-heating instabilities in the down-slope creep of ice sheets. *J. Glaciol.*, 32 (112): 314-320.

Zotikov, I.A., Ivanov, Yu, A. and Barbash, V.R. 1974 Antarctic continental ice discharge and the formation of Antarctic bottom waters. *Okeanologiya* 14(4): 607-13] *In* Jacobs *et al.* (1986) *J. Glaciol.* 32(112): 464-74.

Zwally, H.J., Cosimo, J.C., Parkinson, C.L., Campbell, W.J., Carsey, F.D. and Gloersen, P. 1983 *Antarctic sea-ice, 1973-1976: Satellite Passive- Microwave Observations*. NASA SP-459, Washington, 224 pp.